



# Vascular Discovery: From Genes to Medicine 2021

## Oral Abstracts

---

100

Mitochondrial Dynamics Directs Macrophage Polarization During Atherosclerosis: Implications For Disease Regression

**Leah I Susser**, My Anh Nguyen, UOHI, Ottawa, ON, Canada; Michele Geoffrion, Ottawa, ON, Canada; Mireille Khacho, Univ of Ottawa, Ottawa, ON, Canada; Katey J Rayner, UNIV OTTAWA HEART INST, Ottawa, ON, Canada

Coronary heart disease is caused by atherosclerosis, a cholesterol-driven inflammatory disease of the vessel wall. A hallmark of atherogenesis is the accumulation of pro-inflammatory (M1) macrophages within the vessel wall, which sustains the inflammatory environment of the atherosclerotic plaque. In contrast, during disease regression, macrophages adopt a pro-resolving, anti-inflammatory phenotype (M2). Macrophage subtypes also exhibit different metabolic programs, where M1 macrophages' preferentiality use glycolytic metabolism and are associated with high levels of reactive oxygen species (ROS), while M2 macrophages primarily use oxidative metabolism. Macrophages adapt to these different metabolic needs and protect from mitochondrial DNA damage by ROS by undergoing cycles of fission (fragmentation) & fusion (elongation), which have been demonstrated to direct differentiation and function in other cell types, including T-cells. We **hypothesize** that the balance of mitochondrial fusion & fission directs macrophage polarization and may influence macrophage plasticity during atherosclerosis progression and regression. We found that mouse bone marrow-derived macrophages polarized to an M1 phenotype have a more elongated mitochondrial network, whereas both resting (M0) and M2 macrophages have a more fragmented mitochondrial phenotype. We find that M1 macrophages are more active with a higher number of mitochondria undergoing either a fission or fusion event compared to both M0 and M2 cells. The M1-like elongated mitochondrial phenotype can also be seen under atherogenic lipid-loading conditions. Exciting preliminary data suggests inhibiting mitochondrial fission (i.e. by knocking down three critical proteins, Drp1, Mff & Fis1) or inhibiting mitochondrial fusion (i.e. by knocking down fusion proteins Opa1, Mfn1 & Mfn2) impacts macrophages ability to polarizing into M1 or M2 phenotypes. Together these data suggest that the changes in mitochondrial dynamics direct the polarization of these macrophages and thus could be targeted to promote regression. Regression is an untapped area of atherosclerosis research, and mitochondria dynamics may be a new target to direction macrophage polarization within a lesion.

**L.I.Susser:** None. **M.Nguyen:** n/a. **M.Geoffrion:** None. **M.Khacho:** n/a. **K.J.Rayner:** None.

---

101

B1b Cell Homeostasis Is Maintained By Cd40 In Atherosclerosis

**Myrthe E Reiche**, Amsterdam UMC, Amsterdam, Netherlands; Oom Pattarabajinard, Univ of Virginia, Charlottesville, VA; Aditi Upadhye, Univ of Virginia, Charlottesville, VA, Charlottesville, VA; Kikkie Poels, Amsterdam UMC - Location AMC, Amsterdam; Claudia van Tiel, Amsterdam UMC, Amsterdam, Netherlands; Stephen G Malin, Karolinska Instt, Stockholm, Sweden; Christoph J Binder, MEDICAL UNIVERSITY VIENNA, Vienna; Norbert Gerdes, Univ Hosp Duesseldorf, Duesseldorf; Christian Weber, KREISLAUFINSTITUT, Munich; Dorothee Atzler, KREISLAUFINSTITUT, Munich, Munich; Coleen A McNamara, UNIVERSITY VIRGINIA, Charlottesville, VA; Esther Lutgens, Amsterdam Univ Medical Ctr, Amsterdam

Background: The co-stimulatory CD40-CD40L dyad is an important driver of atherosclerosis. CD40 exerts divergent, cell-specific roles, which differentially impacts atherogenesis.

**Objectives:** We here investigate the role of the most prominent CD40-expressing cell type, the CD40<sup>+</sup> B cell, in atherosclerosis.

**Methods:** B cell subset specific CD40-expression of patients with mild and severe coronary artery disease (CAD) was determined by mass-cytometry and correlated to CAD severity. Underlying mechanisms were revealed using CD19-CD40<sup>fl/fl</sup>-ApoE<sup>-/-</sup>(CD40<sup>BKO</sup>) and CD40<sup>fl/fl</sup>-ApoE<sup>-/-</sup>(CD40<sup>BWT</sup>) mice.

**Results:** Patients with severe CAD had similar CD40 expression levels on most B cell subsets but showed a profound decrease in CD40 on B1 cells. This was associated with increased atherosclerotic plaque burden and decreased plaque fibrosis. Likewise, CD40<sup>BKO</sup> mice exhibited an increased plaque area and a more advanced stage of atherosclerosis. Absence of B cell CD40 caused a decrease in immunoglobulin (Ig) producing cells, including germinal center-, plasma-, but especially B1 cells, thereby reducing levels of (anti-ox/MDA-LDL) IgM and (anti-ox/MDA-LDL) IgG. Interestingly, transcriptomics analysis revealed that the absence of CD40 on B1b cells in particular, caused altered gene expression pathways related to lipid uptake (*Cd36*, *Ldlr*), cellular stress and metabolism (*Nr4a1*, *Hif1a*), and cell death (*Naip5/6*, *Top1*).

Indeed, *in vitro* analysis showed that B1b<sup>CD40<sup>BKO</sup></sup> cells took up excessive amounts of ac/oxLDL, exhibited defective BCR signaling, and were prone to apoptosis, especially in hyperlipidemic conditions.

Finally, transfer of wild-type B1b cells into CD40<sup>BKO</sup> mice prevented the increase in atherosclerosis.

**Conclusions:** We here show that CD40 is a critical modulator of B1 cell protective function in hypercholesterolemia and atherosclerosis.

**M.E.Reiche:** None. **D.Atzler:** None. **C.A.Mcnamara:** None. **E.Lutgens:** None. **O.Pattarabajinard:** n/a. **A.Upadhye:** None. **K.Poels:** None. **C.Van tiel:** None. **S.G.Malin:** n/a. **C.J.Binder:** Honoraria; Modest; Amgen, Novartis, Daiichi Sankyo, Ownership Interest; Modest; Technoclone. **N.Gerdes:** None. **C.Weber:** n/a.

---

102

Apolipoprotein E Receptor 2 In Endothelium Affords Protection From Both Atherosclerosis And Insulin Resistance

**Anastasia Sacharidou,** UT Southwestern Medical Ctr, Dallas, TX; Linzhang Huang, Inst of Material Medica, Beijing, China; Keiji Tanigaki, Chieko Mineo, Philip W Shaul, UT Southwestern Medical Ctr, Dallas, TX

**Introduction:** Apolipoprotein E Receptor 2 (ApoER2) is an LDL receptor family member that mediates the actions of apolipoprotein E (apoE) and other ligands. The LRP8 gene that encodes ApoER2 is a major gene locus for premature atherosclerosis and myocardial infarction. Studies were designed to determine how ApoER2 in endothelial cells impacts cardiovascular and metabolic health. **Hypothesis:** Based on prior cell culture studies, the hypothesis was that endothelial ApoER2 is atheroprotective. How endothelial ApoER2 impacts adiposity or glucose homeostasis is more difficult to predict. **Methods:** In vivo studies were done in control ApoER2 floxed mice (ApoER2<sup>fl/fl</sup>) and mice deficient in ApoER2 in endothelial cells (ApoER2<sup>ΔEC</sup>). Studies of endothelial cell insulin uptake and transcytosis were performed in human aortic and skeletal muscle endothelial cells (HAEC and HSMEC). **Results:** Atherosclerotic lesion severity on LDLR<sup>-/-</sup> background was increased in ApoER2<sup>ΔEC</sup> mice compared to ApoER2<sup>fl/fl</sup>, and this was not related to differences in circulating lipids. Intravital microscopy revealed that leukocyte-endothelial cell adhesion is increased in ApoER2<sup>ΔEC</sup>, and vascular TNFα and IL-1β expression was exaggerated. There was no impact of endothelial ApoER2 silencing on adiposity. However, standard chow-fed ApoER2<sup>ΔEC</sup> mice displayed marked glucose intolerance and insulin resistance. Both pancreatic insulin secretion and hepatic insulin sensitivity were normal. Alternatively, in ApoER2<sup>ΔEC</sup> mice skeletal muscle glucose disposal was decreased by 41%, and this was due to a 55% fall in insulin delivery to muscle. Using human apoE3 ex vivo, apoE stimulated a 279% increase in insulin uptake in HAEC, and the finding was confirmed in HSMEC. Insulin transcytosis rose 209% with apoE, and apoE enhancement of insulin transport was fully ApoER2-dependent. **Conclusions:** Endothelial ApoER2 affords atheroprotection by decreasing leukocyte-endothelial cell adhesion and inflammatory gene expression in the vessel wall. Endothelial ApoER2 also has antidiabetic action, and this is due to the promotion of endothelial insulin transport to skeletal muscle. Targeting of the related mechanisms may provide protection from both cardiovascular and metabolic disease.

**A.Sacharidou:** None. **L.Huang:** n/a. **K.Tanigaki:** None. **C.Mineo:** None. **P.W.Shaul:** None.

## Smooth Muscle Cell Specific Overexpression Of Adamts7 Drives Atherosclerosis Development Through The Remodeling Of The Extracellular Matrix

**Allen Chung**, Columbia Univ Irving Medical Ctr, New York, NY; **Hyun-kyung Chang**, Rajesh Soni, Columbia Univ, New York, NY; **Muredach P Reilly**, COLUMBIA UNIVERSITY MEDICAL CENTER, New York, NY; **Robert C Bauer**, COLUMBIA UNIVERSITY, New York, NY

Genome-wide association studies in humans link ADAMTS7 with coronary artery disease. Subsequent studies in mice showed ADAMTS7 to be proatherogenic, as whole-body knockout (KO) reduced atherosclerosis independent of lipid-lowering. Further studies show that Adamts7 expression is temporarily induced in response to vascular injury, and Adamts7 KO reduces primary smooth muscle cell (SMC) migration ex vivo. However, both the mechanism through which ADAMTS7 influences atherosclerosis progression and the responsible cell type remain unclear.

As ADAMTS7 is secreted, we sought to determine its cleavage targets. We generated an immortalized human SMC line with doxycycline-inducible expression of GFP or ADAMTS7. We analyzed conditioned media from these cells via terminal amine isotopic labeling of substrates (TAILS) proteomics. This method labels new protein N termini, enabling the identification of cleavage products. Overexpression of Adamts7 enriched extracellular matrix (ECM) peptides such as Col1a1, Col1a2, Col4a2, and fibronectin. Furthermore, KEGG analysis identified ECM receptor interaction and focal adhesion formation as highly enriched pathways in the dataset. These results suggest ADAMTS7 alters SMCs by modulating signaling between cell and ECM.

To examine the cell type that confers the proatherogenic effects of Adamts7, we generated a conditional transgenic ADAMTS7 mouse on the Ldlr knockout background. Given previously described roles for ADAMTS7 in SMC migration and vascular reendothelialization, we crossed these mice to either the Tie2-Cre or Myh11-CreERT2 to overexpress ADAMTS7 in endothelial and SMCs respectively. We found >3-fold increase ( $p = 0.0002$ ) in plaque burden by en face staining in overexpression of Adamts7 in SMCs compared to controls. In contrast, transgenic overexpression of Adamts7 in endothelial cells is embryonic or perinatally lethal (Chi-squared = 0.0018).

In summary, our transgenic study affirms the proatherogenic effect of increased Adamts7 expression in SMCs in vivo. Furthermore, our TAILS data suggests a dynamic role of ADAMTS7 in cleaving ECM. These studies fill critical knowledge gaps in our understanding of ADAMTS7 biology and help inform potential therapeutic avenues to targeting this enzyme.

**A.Chung:** None. **H.Chang:** None. **R.Soni:** None. **M.P.Reilly:** None. **R.C.Bauer:** None.

## Massively Parallel Validation Of Genetic Variants With Inflammatory-specific Effects In Human Endothelial Cells

**Lindsey K Stolze**, The Univ of Arizona, Tucson, AZ; **Anu Toropainen**, Tiit Ord, Univ of Eastern Finland, Kuopio, Finland; **Michael B Whalen**, The Univ of Arizona, Tucson, AZ; **Minna Kaikkonen**, Univ of Eastern Finland, Kuopio, Finland; **Casey E Romanoski**, Univ of Arizona, Tucson, AZ

Genome-wide association studies have linked thousands of genetic variants with complex diseases and traits. However, most genetic variants identified reside in non-coding regions of the genome, including variants associated with a myriad of vascular phenotypes, including coronary artery disease, pulse pressure, and stroke. In a prior study, we performed Quantitative Trait Locus (QTL) analysis for expression, transcription factor binding, chromatin accessibility, and histone H3 acetylation on the 27<sup>th</sup> residue (H3K27ac) across 53 primary Human Aortic Endothelial Cell (HAEC) samples. This analysis was performed in untreated and pro-inflammatory cytokine Interleukin 1 Beta (IL1B) treated conditions. This resource allowed us to fine-map non-coding functional variants within HAECs in both simulated healthy and diseased conditions. To this, we now add results from massively parallel reporter assay for >16,000 regions that were prioritized from our QTL study. Using Self-Transcribing Active Regulatory Region sequencing (STARR-seq) for these regions in the immortalized HAEC cell line (teloHAECs), we identified 5,592 common variants with allele specific effects. These variants are enriched for endothelial cell specific transcription factor ERG binding QTLs as well as HAEC chromatin accessible sites, but not enriched for accessible regions from other cell types. This suggests cell-type specificity of the allele specific signals detected. We

performed STARR-seq in untreated and two time points of IL1B-treated conditions. We found that the variants with significant allelic effects were enriched for inflammatory master regulator NF-kB binding QTLs regardless of the treatment condition in which STARR-seq was performed, highlighting the importance of the healthy cell regulatory landscape in determining inflammation response. Additionally, of the 3,459 loci with allele specific signals and QTL evidence, 219 were associated with a complex disease or trait via the GWAS catalog. These data together allow us to elucidate the functional variants within disease associated loci and link them to epigenetic traits and gene expression providing potential pathways through which genetic variation modifies endothelial cell biology and vascular health.

**L.K.Stolze:** None. **A.Toropainen:** n/a. **T.Ord:** None. **M.B.Whalen:** None. **M.Kaikkonen:** n/a. **C.E.Romanoski:** None.

---

105

## Chronic Stress Primes Innate Immune Responses In Mice And Humans

**Tessa J Barrett,** NYU SCHOOL OF MEDICINE, New York, NY; Emma Corr, Cabinteely; Coen Solingen, NYUMC LANGONE MEDICAL CENTER, New York, NY; Florencia Schlamp, Emily J Brown, NYU SCHOOL OF MEDICINE, New York, NY; Graeme J KOELWYN, New York, NY; Angela Lee, NEW YORK UNIVERSITY, New York, NY; Lianne Shanley, Trinity Coll Dublin, Dublin; Tanya Spruill, Fazli Bozal, Annika De Jong, NYU SCHOOL OF MEDICINE, New York, NY; Alexandra Newman, New York Univ, New York, NY; Kamelia Drenkova, New York Univ, New York, NY, New York, NY; Michele Silvestro, NYU Sch of Med, New York, NY; Bhama Rhamkhelawon, NYU SCHOOL OF MEDICINE, New York, NY; Harmony Reynolds, NYU SCHOOL OF MEDICINE, New York, NY; Judith S Hochman, Matthias Nahrendorf, NYU SCHOOL OF MEDICINE, New York, NY; Filip K Swirski, MASSACHUSETTS GENERAL HOSP, Boston, MA; Edward A A Fisher, NYU LANGONE MEDICAL CENTER, New York, NY; Jeffrey S Berger, NEW YORK UNIVERSITY SCHOOL OF MEDICINE, New York, NY; Kathryn J Moore, NEW YORK UNIV MEDICAL CTR, New York, NY

Psychological stress is associated with elevated circulating markers of inflammation, including inflammatory cytokines and acute phase reactants that accelerate progression of chronic inflammatory diseases (e.g., atherosclerosis, metabolic syndrome, autoimmune diseases and cancer). However, the mechanisms underlying inflammatory reactivity to stress and how it confers future health risk are poorly understood. Monocyte-derived macrophages play key roles in sustaining tissue inflammation, and recent studies show that they can maintain epigenetic memory of pathogen or sterile inflammatory insults, leading to a heightened inflammatory state upon secondary stimulation. We show herein that psychological stress induces transcriptomic and epigenomic reprogramming of monocytes which primes them for a heightened inflammatory immune response following challenge. Monocytes isolated from stressed mice or humans with high reported levels of psychological stress exhibit a common signature of heightened inflammatory gene expression and produce increased levels of proinflammatory cytokines upon ex vivo stimulation with Toll-like receptor ligands. RNA and ATAC sequencing studies revealed that monocytes from stressed mice and humans exhibit activation of cellular metabolic pathways, including mTOR and PI3Kinase pathways, and reduced chromatin accessibility at loci associated with mitochondrial respiration. Taken together, our findings suggest that psychological stress primes the reprogramming of innate immune cells resulting in a hyperresponsive inflammatory state, which may explain its deleterious association with inflammatory disease risk.

**T.J.Barrett:** None. **F.Bozal:** n/a. **A.De Jong:** n/a. **A.Newman:** None. **K.Drenkova:** None. **M.Silvestro:** None. **B.Rhamkhelawon:** n/a. **H.Reynolds:** Other; Modest; Abbott Vascular, Siemens, BioTelemetry. **J.S.Hochman:** Employment; Significant; NYUSOM, Other; Significant; Amgen, Inc, Espero BioPharma, Medtronic, Inc., Abbott Vascular, Inc (formerly St. Jude Medical, Inc), Royal Philips NV (formerly Volcano Corporation), Merck Sharp & Dohme Corp, Omron Healthcare, Inc, Sunovion Pharmaceuticals, Inc, Other Research Support; Significant; AstraZeneca; Pharmaceuticals, LP; , Arbor Pharmaceuticals, LLC, Research Grant; Significant; NIH/NHLBI grant support for ISCHEMIA Trial. **M.Nahrendorf:** n/a. **F.K.Swirski:** Other; Significant; Verseau Therapeutics. **E.Corr:** None. **E.A.A fisher:** Expert Witness; Significant; Amgen, DOAR. **J.S.Berger:** Honoraria; Modest; Amgen, Other Research Support; Significant; Jannssen, Research Grant; Significant; NIH, AHA, Astra Zeneca. **K.J.Moore:** Stock Shareholder; Significant; Merck Research Laboratories. **C.Solingen:** None. **F.Schlamp:** n/a. **E.J.Brown:** None. **G.J.Koelwyn:** None. **A.Lee:** None. **L.Shanley:** None. **T.Spruill:** Research Grant; Significant; American Heart Association, Centers for Disease Control and Prevention, National Institutes of Health.

## Novel Nanoparticle-mediated Robust Genome Editing Targeting The Vascular Endothelium Of Postnatal And Adult Mice

Xianming Zhang, Xiaojia Huang, Hua Jin, Birendra Chaurasiya, Daoyin Dong, **Youyang Zhao**, Northwestern U-Lurie Children's Hosp of Chicago, Chicago, IL

Current viral and non-viral delivery of transgene after i.v. administration is mainly enriched in the liver. To target the vascular endothelium for robust genome editing in adults, we developed a novel nanoparticle system. A single i.v. administration of the mixture of nanoparticles and all-in-one plasmid DNA expressing Cas9 controlled by *CDH5* promoter and guide RNA by *U6* promoter induced highly efficient genome editing in endothelial cells of the vasculatures including lung, heart, aorta, and the peripheral vessels in adult mice in as quick as 5 days. Western blotting and immunofluorescent staining demonstrated an 80% decrease of protein expression selectively in endothelial cells, resulting in a phenotype similar to that of genetic knockout mice. This nanoparticle /plasmid delivery system could also deliver a transgene targeting the vascular endothelium simultaneously and/or multiple gRNAs to knockout multiple genes at the same time. The nanoparticle/plasmid DNA delivery system could also achieve robust gene-correction through a base editor in the vascular endothelium in adult mice. These data demonstrate that nanoparticle delivery of plasmid DNA expressing a genome editing system (e.g., CRISPR/Cas9, or base editor, etc.) and/or a transgene is a simple powerful tool to rapidly and efficiently alter expression of gene(s) in vascular endothelium. This provides a significant advance in cardiovascular research and a potential novel gene therapy strategy for cardiovascular diseases.

**X.Zhang:** n/a. **X.Huang:** n/a. **H.Jin:** n/a. **B.Chaurasiya:** n/a. **D.Dong:** None. **Y.Zhao:** n/a.

## PKM2 Promotes Neutrophil Activation And Cerebral Thrombo-inflammation: Therapeutic Implications For Ischemic Stroke

**Nirav Dhanesha**, Rakeshkumar Patel, Univ of Iowa, Iowa City, IA; Manish Jain, university of Iowa, Iowa City, IA; Mariia Kumskova, Univ of Iowa, Iowa City, IA; Daniel Thedens, Univ Iowa, Iowa City, IA; Heena M Olalde, Univ of Iowa Hosp, Iowa City, IA; Manasa Nayak, Prakash Doddapattar, Enrique C. C Leira, Anil K Chauhan, Univ of Iowa, Iowa City, IA

In recent years compelling evidence has emerged that implicates role of metabolic reprogramming in the modulation of thrombosis and inflammation. The dimeric form of the metabolic enzyme pyruvate kinase muscle 2 (PKM2) enters nucleus and exerts protein kinase activity. We found that nuclear PKM2 levels were upregulated in neutrophils after the onset of ischemic stroke both in humans and in mice. Therefore, we evaluated the role of PKM2 in promoting thrombo-inflammation and ischemic brain injury. We generated novel myeloid cell-specific *PKM2*<sup>-/-</sup> mice on wild-type (*PKM2*<sup>fl/fl</sup>*LysMCre*<sup>+</sup>) and hyperlipidemic background (*PKM2*<sup>fl/fl</sup>*LysMCre*<sup>+</sup>*Apoe*<sup>-/-</sup>). We observed that genetic deletion of PKM2 in myeloid cells limited inflammatory response in peripheral neutrophils and reduced neutrophil extracellular traps following cerebral ischemia/reperfusion. In the filament and autologous clot/rtPA stroke models, irrespective of sex, deletion of PKM2 in myeloid cells either in wild-type or hyperlipidemic mice reduced infarcts and enhanced long-term sensorimotor recovery. Laser speckle imaging revealed improved regional cerebral blood flow in myeloid cell-specific PKM2-deficient mice that was concomitant with reduced post-ischemic cerebral thrombo-inflammation (intracerebral fibrin(ogen), platelet (CD41- positive) deposition, neutrophil infiltration, and inflammatory cytokines). Mechanistically, PKM2 regulates post-ischemic inflammation in peripheral neutrophils by promoting STAT3 phosphorylation. Utilizing small molecule inhibitor (ML265) that inhibits PKM2 dimerization, we evaluated ex vivo thrombosis using human whole blood in a microfluidic flow chamber system. We observed a fivefold reduction in the thrombus growth rate in ML265-treated group. Similarly, ML265 treatment in mice resulted into significantly reduced poststroke neutrophil hyperactivation and improved short-term and long-term functional outcomes following stroke. Collectively, these findings identify PKM2 as a novel therapeutic target to improve brain salvage and recovery following reperfusion.

**N.Dhanesha:** n/a. **A.K.Chauhan:** None. **R.Patel:** n/a. **M.Jain:** None. **M.Kumskova:** n/a. **D.Thedens:** n/a. **H.M.O lalde:** n/a. **M.Nayak:** None. **P.Doddapattar:** None. **E.C.Leira:** Research Grant; Significant; NIH-NINDS.

## Quantitative Phosphoproteomics And Causal Analysis Reveal Distinct And Combinatorial Signaling Mechanisms In Protease-Activated Receptor PAR1 And PAR4 Platelet Activation Programs

Stephanie Reitsma, OHSU, Portland, OR; John Klimek, Iván Parra-Izquierdo, Oregon Health & Science Univ, Portland, OR; Ozgun Babur, Univ of Massachusetts Boston, Boston, MA; Alexander Melrose, Tony Zheng, Jiaqing Pang, Oregon Health & Science Univ, Portland, OR; Owen J McCarty, OREGON HEALTH SCIENCE UNIVERSITY, Portland, OR; Jessica Minnier, Oregon Health & Science Univ, Portland, OR; Phillip Wilmarth, OHSU, Portland, OR; Emek Demir, Ashok Reddy, Oregon Health & Science Univ, Portland, OR; Larry David, **Joseph Aslan**, Oregon Health & Science Univ, Portland, OR

Intracellular signaling pathways downstream of platelet protease-activated receptors (PARs) mediate hemostasis - and, also contribute to thrombosis in vascular diseases - through mechanisms that remain unspecified. Here, we assess the hypothesis that platelet PAR1 and PAR4 each activate specific, as well as overlapping signaling systems to drive platelet responses underlying hemostasis and thrombosis. Our systems biology approach incorporates state-of-the-art mass spectrometry, computational and cell physiological tools to measure and map phosphorylation events in platelet PAR responses. Following isolation from n=4 healthy human donors, washed platelets were treated with PAR1 agonist (TRAP6), PAR4 agonist (AYPGFK), thrombin, or vehicle, prior to lysis, digestion, phosphopeptide enrichment and 16plex tandem mass tag (TMT) labeling. Relative to resting platelets, we measured >1,000 significant phosphorylation events in response to PAR agonists (fold-change >1.5; false discovery rate <0.01), including >600 phosphorylation events common to TRAP6, AYPGFK and thrombin stimulation. These included phosphorylation of well-established mediators (GSK3 $\alpha$ , PAK2) and more novel and emerging effectors in platelet activation pathways (BIN2, NKX3-2). Specific PAR1 and PAR4 agonist responses of mechanistic and translational interest were also noted, including phosphorylation of PAR1 T410 or PAR4 S369; thrombin uniquely activated tyrosine kinase Fer Y714 phosphorylation, in a manner that may integrate PAR1 and PAR4 signaling. CausalPath analysis identified >100 signaling relations among site-specific phosphorylation changes downstream of PARs, around MAPK, PI3K/Akt, mTOR/S6K and other pathways. Finally, physiological assays of platelet adhesion, secretion and aggregation, as well as biochemical assays of platelet signaling validated roles for several effectors and pathways in platelet PAR responses. In conclusion, we provide a quantitative omics study and causal analysis of platelet PAR signaling, including specific PAR1 and PAR4 agonist responses. Ultimately, this work will help to specify essential effectors, as well as biomarkers and therapeutic targets in platelet dysregulation, hyperactivity and thrombotic diseases.

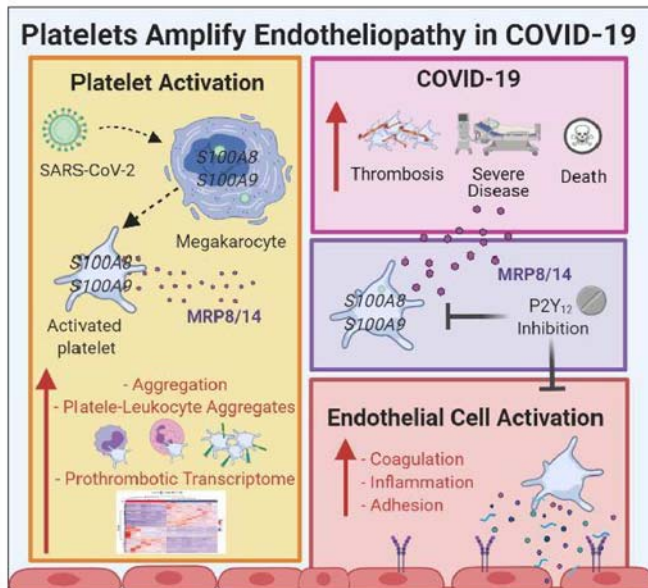
**S. Reitsma:** None. **J. Klimek:** None. **I. Parra-Izquierdo:** None. **O. Babur:** None. **A. Melrose:** Employment; Significant; Oregon Health Science University. **T. Zheng:** None. **O.J. McCarty:** None. **J. Minnier:** None. **P. Wilmarth:** None. **E. Demir:** None. **A. Reddy:** None. **L. David:** None.

## Platelets Amplify Endotheliopathy In Covid-19

**Tessa J Barrett**, NYU SCHOOL OF MEDICINE, New York, NY; MacIntosh Cornwell, NYU Sch of Med, New York, NY; Khrystyna Myndzar, NYU Sch of Med, New York, NY, Brooklyn, NY; Christina Rolling, NYU SCHOOL OF MEDICINE, New York, NY; Yuhe Xia, NYU Langone Health, New York, NY; Kamelia Drenkova, NYU Langone Health, New York, NY, New York, NY; Antoine Biebuyck, NYU SCHOOL OF MEDICINE, New York, NY; Alexander Fields, Univ of California, San Francisco, CA; Michael Tawil, NYU Sch of Med, New York, NY; Elliot Luttrell-Williams, NYU Langone, New York, NY; Eugene Yuriditsky, NYU, New York, NY; Grace Smith, Paolo Cotzia, Natl Cancer Inst, Bethesda, MD; Matthew D Neal, MD, Sewickley, TX; Lucy Kornblith, Stefania Pittaluga, Sewickley, TX, San Francisco, CA; Amy Rapkiewicz, mineola, NY; Hannah Burgess, Ian Mohr, mineola, NY, new york, NY; Kenneth Stapleford, New York, NY; Deepak Voora, DUKE UNIVERSITY, Durham, NC; Kelly Ruggles, Judith Hochman, DUKE UNIVERSITY, Durham, NC, New York, NY; Jeffrey S Berger, NEW YORK UNIVERSITY SCHOOL MEDICINE, New York, NY

In addition to their pivotal role in thrombosis and hemostasis, platelets participate in inflammatory responses and endothelial cell activation - hallmarks in the pathogenesis of coronavirus disease 2019 (COVID-19). Given the evidence for a hyperactive platelet phenotype in COVID-19, we investigated effector cell properties of COVID-19 platelets on endothelial cells (ECs). To explore this interaction, ECs were treated

with platelet releasate from patients with and without COVID-19, and EC mRNA sequencing performed. We demonstrate that platelet released factors in COVID-19 promote an inflammatory hypercoagulable endotheliopathy. Investigation of the COVID-19 platelet transcriptome identified pathways related to organelle/granule release, metabolism, and immune effector function in addition to upregulation of *S100A8* and *S100A9* mRNA. Incubation of primary megakaryocytes with severe acute respiratory syndrome coronavirus 2 (SARS-CoV-2) also induced upregulation of *S100A8* and *S100A9* mRNA. Consistent with increased gene expression, the heterodimer protein product of *S100A8/A9*, myeloid-related protein (MRP)8/14, was released to a greater extent by platelets from COVID-19 patients relative to controls. We demonstrate that platelet-derived MRP8/14 activates microvascular endothelial cells, promotes an inflammatory hypercoagulable phenotype, and is a significant contributor to thromboinflammation and poor clinical outcomes in COVID-19 patients. Finally, we present evidence that therapeutic targeting of platelet P2Y<sub>12</sub> represents a promising candidate to reduce proinflammatory and prothrombotic platelet-endothelial interactions. Altogether, these findings demonstrate a previously unappreciated role for platelets and their activation-induced endotheliopathy in COVID-19.



**T.J.Barrett:** None. **E.Luttrell-williams:** None. **E.Yuriditsky:** None. **G.Smith:** n/a. **P.Cotzia:** None. **M.D.Neal, md:** Honoraria; Modest; Haemonetics, Other Research Support; Modest; Janssen Pharmaceuticals, Research Grant; Modest; Instrumentation Laboratories, Noveome, Stock Shareholder; Modest; Haima Therapeutics. **L.Kornblith:** Other; Modest; Cerus. **S.Pittaluga:** n/a. **A.Rapkiewicz:** None. **H.Burgess:** None. **I.Mohr:** None. **M.Cornwell:** n/a. **K.Stapleford:** None. **D.Voora:** Other; Significant; UnitedHealthGroup. **K.Ruggles:** n/a. **J.Hochman:** n/a. **J.S.Berger:** Honoraria; Modest; Amgen, Other Research Support; Significant; Jannssen, Research Grant; Significant; NIH, AHA, Astra Zeneca. **K.Myndzar:** None. **C.Rolling:** None. **Y.Xia:** None. **K.Drenkova:** None. **A.Biebuyck:** None. **A.Fields:** None. **M.Tawil:** None.

#### C1 Esterase Inhibitor Functions As An Anticoagulant In Human And Murine Venous Thrombosis

**Steven P Grover,** UNIVERSITY OF NORTH CAROLINA CH, Chapel Hill, NC; Kristian Hindberg, Univ of Tromso, Tromso, Norway; Alisa S Wolberg, UNIV OF NORTH CAROLINA, Chapel Hill, NC; Sigrid Braekkan, Univ of Tromso, Tromso, Norway; Nigel Mackman, Univ of Chapel Hill, Chapel Hill, NC; John-bjarne Hansen, Univ of Tromso, Tromso, Norway

Factor (F) XII and FXI play a central role in venous thrombus formation in preclinical disease models and contributes to venous thromboembolism (VTE) in humans. Agents targeting FXIa have been developed and effectively prevent VTE in humans. C1 esterase inhibitor (C1INH) is a serine protease inhibitor that inhibits several proteases, including FXII and FXI. In this study, we investigated the anticoagulant activity of C1INH in humans and mice. First, plasma C1INH levels were determined in a population-based nested case-control study consisting of 405 VTE patients and 829 age- and sex-matched controls derived from the

Tromsø Study. Participants with plasma C1INH levels in the highest quartile had a significantly lower risk of VTE (odds ratio [OR] of 0.68, confidence interval 0.49–0.96,  $P<0.05$ ), unprovoked VTE (OR 0.59, confidence interval 0.39–0.89) and pulmonary embolism (OR 0.57, confidence interval 0.34–0.92) compared to participants with C1INH levels in the lowest quartile after adjustment for age and sex. Secondly, plasma-based thrombin generation studies were conducted to assess the anticoagulant function of C1INH. Supplementation of normal human pooled plasma with exogenous human purified C1INH (0.2 and 0.4mg/ml) significantly inhibited thrombin generation initiated with silica ( $P<0.05$ ) and significantly prolonged the activated partial thromboplastin assay clotting time ( $P<0.001$ ). Thirdly, administration of a clinically approved human purified C1INH product to mice significantly reduced thrombus weight ( $P<0.05$ ) in the murine inferior vena cava stenosis model of venous thrombosis. Studies with C1 inhibitor deficient mice and substrate selective C1INH variants are currently ongoing. Our results indicate that C1INH serves as an endogenous anticoagulant with higher plasma levels of C1INH associated with a decreased future risk of VTE. Further, exogenous C1INH effectively inhibits thrombin generation in vitro and venous thrombus formation in a mouse model. Our findings suggest that C1INH may prevent thrombosis caused by activation of the intrinsic coagulation pathway.

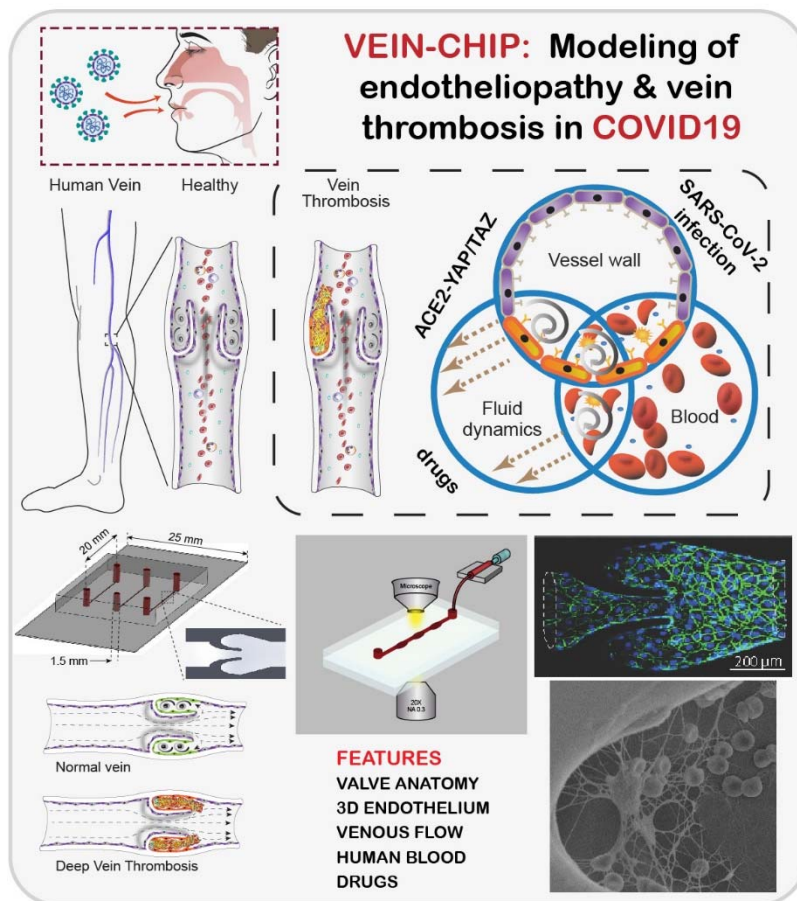
**S.P.Grover:** None. **K.Hindberg:** None. **A.S.Wolberg:** Research Grant; Significant; Takeda, Bristol Myers Squibb. **S.Braekkan:** None. **N.Mackman:** None. **J.Hansen:** None.

#### Vein-Chip Is A New Experimental Model To Predict Pathophysiology Of SARS-CoV-2 Induced Thrombosis

Navaneeth Krishna Rajeeva Pandian, TAMU, College Station, TX; John H. Connor, Boston Univ, Boston, MA; John P Cooke, HOUSTON METHODIST RESEARCH INS, Houston, TX; **Abhishek Jain**, Texas AnM Univ, College Station, TX

There is a serious limitation of experimental models that can improve our limited knowledge of the mechanisms that regulate endotheliopathy and venous thrombosis (VT) clinically observed frequently amongst the most severe COVID-19 patients. Also, while observation and study of VT in humans are difficult due to the deep-lying nature of the deep veins in which VT develops, lab animal models do not include the venous valves, which are the sites for thrombus development in humans. We develop a Vein-chip microfluidic platform that includes venous valve architecture, endothelial cells (ECs), and whole blood flow, which can include the three factors of Virchow's triad - endothelial inflammation, stasis of blood flow, and coagulable nature of blood. Our *in silico* and *in vitro* observations with Vein-Chip reveal that incompetent valves and thrombosis changes the blood flow pattern in and around the venous valves. We show that healthy endothelium at the venous valve cusps adapt to the complex flow patterns and have an anti-thrombotic phenotype compared to the venous lumen. But exposure of the lumen to living and replicating SARS-CoV-2 virus and inflammatory cytokines found in COVID-19 patient samples inflames the lumen and the valve endothelium becomes pro-thrombotic. Interestingly, when we directed our investigation to analyze the ACE2 expression on these cells, as ACE2 is the functional receptor of the SARS-CoV-2 virus, we found that ACE2 expression was poor under a static culture, but increased dramatically when venous ECs were exposed to shear stress within the vein-chip. This data supports our hypothesis that ACE2 expression (and therefore, SARS-CoV-2 entry into the endothelium) is dependent on venous hemodynamics and the Vein-Chip model is a highly dissectible platform that will help us to unravel the molecular mechanisms that lead to VT and its treatment strategies for COVID-19 and beyond.





**N.Rajeeva pandian:** None. **J.H.Connor:** n/a. **J.P.Cooke:** Other; Modest; Humann, Fibralign, Stock Shareholder; Significant; Cooke Consulting. **A.Jain:** None.

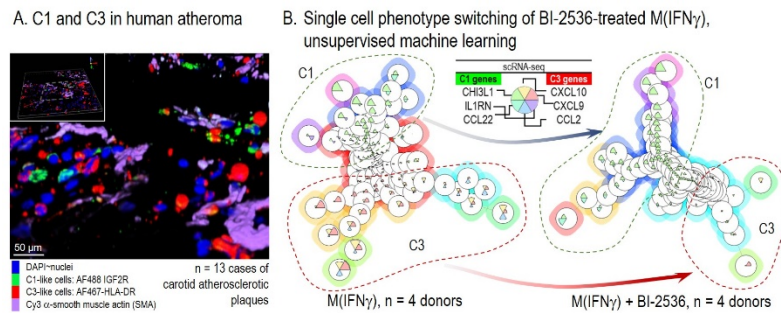
112

Examining The Heterogeneity Of Primary Human Macrophages And Pharmacogenomic Networks To Identify Novel Targets For Precision Medicine For Vascular Inflammation

**Julius Decano,** Enrico Maiorino, Joan T. Matamalas, Sarvesh Chelvanambi, Bart Tiemeijer, Edwin D'Souza, Shin Mukai, Yoshihiro Yanagihara, Mary Whelan, Takaharu Asano, Sasha A Singh, Amitabh Sharma, Elena Aikawa, Masanori Aikawa, BWH and Harvard Medical Sch, Boston, MA

**Background:** We hypothesize that macrophage heterogeneity is an unexploited source of therapeutic targets for vascular inflammation. Interferon-gamma (IFN $\gamma$ ) stimulated primary human macrophages M(IFN $\gamma$ ) is a widely used *in vitro* model for proinflammatory macrophages. However, typical activation-induced transcript profiling assumes a homogenous macrophage population. Our goal is to evaluate the extent of heterogeneity of activated macrophages to devise a strategy for precision medicine for inflammatory vascular disease. **Methods:** Using unbiased single-cell RNA sequencing (scRNA-seq), systems biology, and machine learning, we examined inter-subgroup differences of human primary M(IFN $\gamma$ ) (4 donors). Network analysis, kinetic proteomics, and *in vitro* assays (n=3-6) characterized the clusters, followed by validation in human carotid atherosclerotic plaques (n=13). scRNAseq data analysis in the L1000 CDS<sup>2</sup> drug-gene network computationally identified drugs that may potentiate or suppress each cluster. **Results:** The scRNA-seq demonstrated 3 distinct subpopulations: Clusters 1, 2, and 3 (C1, 2, and 3). C3 showed increased proinflammatory chemokine production, protein synthesis, and glycolysis. C1 was more efferocytotic/phagocytic, chemotactic, and less inflammatory. C2 is intermediate between C1 and C3. Histological analysis localized C1 and C3-like macrophages in different areas of the plaques (**Fig. 1A**). In addition, we used targeted scRNAseq (n=4) to analyze M(IFN $\gamma$ ) treated with an L1000-derived drug BI-2536 (Polo-like kinase inhibitor). As predicted, BI-2536 shifted the phenotypic heterogeneity of M(IFN $\gamma$ ) towards less inflammatory characteristics (**Fig. 1B**) which were further validated with bulk qPCR & ELISA

(n=8). **Conclusion:** Our study presents a novel strategy for precision medicine that leverages single-cell data and gene interaction networks to identify modulators of macrophage heterogeneity as new anti-inflammatory therapies.



**J.Decano:** None. **T.Asano:** Employment; Significant; Kowa. **S.A.Singh:** None. **A.Sharma:** n/a. **E.Aikawa:** None. **M.Aikawa:** Research Grant; Significant; Kowa, Sanofi, Pfizer. **E.Maiorino:** None. **J.Matamalas:** None. **S.Chelvanambi:** None. **B.Tiemeijer:** None. **E.D'souza:** n/a. **S.Mukai:** None. **Y.Yanagihara:** Employment; Significant; Kowa Company, Ltd.. **M.Whelan:** None.

113

## Cell-specific Chromatin Landscape Of Human Coronary Artery Resolves Mechanisms Of Disease Risk

Adam W Turner, Sheng-en Hu, Jose E. Verdezoto Mosquera, Wei Feng Ma, Chani J Hodonsky, Doris Wong, Gaelle E Auguste, Katia Sol-Church, Emily Farber, Univ of Virginia, Charlottesville, VA; Soumya Kundu, Anshul B. Kundaje, Nicolas G. Lopez, Stanford Univ, Stanford, CA; Lijiang Ma, Icahn Sch of Med at Mount Sinai, New York, NY; Saikat Ghosh, CVPPath Inst, Gaithersburg, MD; Suna Onengut-Gumuscu, Univ of Virginia, Charlottesville, VA; Euan A Ashley, STANFORD UNIVERSITY, Stanford, CA; Thomas Quertermous, Stanford Univ, Stanford, CA; Alope Finn, CVPPath Inst, Gaithersburg, MD; Nick J Leeper, STANFORD UNIVERSITY, Stanford, CA; Jason C. Kovacic, ST VINCENTS, Bronte Nsw, Australia; Johan L.M. Björkegren, Icahn Sch of medicine, New York, NY; Chongzhi Zang, **Clint L Miller**, Univ of Virginia, Charlottesville, VA

Coronary artery disease (CAD) is a complex inflammatory disease involving genetic influences across several cell types. Genome-wide association studies (GWAS) have identified over 170 loci associated with CAD, where the majority of risk variants reside in noncoding DNA sequences impacting *cis*-regulatory elements (CREs). Here, we applied single-cell ATAC-seq to profile 28,316 cells across coronary artery segments from 41 patients with varying stages of CAD, which revealed 14 distinct cellular clusters. We mapped over 320,000 accessible sites across all cells, identified cell type-specific elements, transcription factors, and prioritized functional CAD risk variants via quantitative trait locus and sequence-based predictive modeling. Using differential peak analyses we identified a number of candidate mechanisms for smooth muscle cell transition states (e.g. fibromyocytes). By integrating these profiles with GWAS meta-analysis summary data we resolved cell type-specific putative binding sites for the majority of CAD risk variants. In particular, we prioritized functional variants predicted to alter MEF2 binding in smooth muscle cells at the *MRAS* locus. We also identify variants predicted to alter macrophage-specific regulation of *LIPA*. We further employed DNA to gene linkage to nominate disease-associated key driver transcription factors such as *PRDM16* and *TBX2*. Together, this single cell atlas provides a critical step towards interpreting *cis*-regulatory mechanisms in the vessel wall across the continuum of CAD risk.

**A.W.Turner:** None. **S.Kundu:** None. **A.B.Kundaje:** Other; Modest; PatchBio Inc., RavelBio Inc, SerImmune Inc., Stock Shareholder; Modest; Deep Genomics, Freenome Inc, ImmuneAI Inc.. **N.G.Lopez:** n/a. **L.Ma:** None. **S.Ghosh:** None. **S.Onengut-gumuscu:** n/a. **E.A.Ashley:** Honoraria; Significant; Apple, Other; Significant; AstraZeneca, Ownership Interest; Modest; SequenceBio, Deepcell, Silicon Valley Exercise Analytics, Ownership Interest; Significant; Personalis. **T.Quertermous:** None. **A.Finn:** n/a. **N.J.Leeper:** None. **S.Hu:** n/a. **J.C.Kovacic:** n/a. **J.L.Björkegren:** None. **C.Zang:** None. **C.L.Miller:** None. **J.E.Verdezoto mosquera:** n/a. **W.Ma:** None. **C.J.Hodonsky:** n/a. **D.Wong:** None. **G.E.Auguste:** None. **K.Sol-church:** None. **E.Farber:** None.

## Single-cell and Spatial Transcriptomics Reveal An IL-1 $\beta$ Mediated VSMC Phenotypic Switch During Vasculitis and Cardiovascular Inflammation

**Rebecca A Porritt**, Cedars Sinai Medical Ctr, Los Angeles, CA; David Zemmour, Harvard Medical Sch, Boston, CA; Masanori Abe, Youngho Lee, Angela Gomez, Shuang Chen, Timothy R Crother, Kenichi Shimada, Moshe Arditi, Magali Noval Rivas, Cedars Sinai Medical Ctr, Los Angeles, CA

NLRP3 activation and IL-1 $\beta$  production are implicated in Kawasaki Disease (KD) pathogenesis, however a detailed description of the molecular networks and cellular subsets involved in this process is lacking. Here, we used single-cell RNA sequencing and spatial transcriptomics to characterize the cellular landscape of vascular tissues in a murine model of KD vasculitis. We observed infiltrations of innate and adaptive immune cells associated with increased expression of *Nlrp3*, *Il1b* and *Il18*. Monocytes, macrophages and dendritic cells were the main sources of IL-1 $\beta$ . Fibroblasts and vascular smooth muscle cells (VSMCs) expressed high levels of IL-1 receptor, while lymphocytes expressed high levels of IL-18 receptor. VSMCs in vasculitis lesions underwent a phenotypic switch, with upregulation of inflammatory mediators and fibroblast markers, and a downregulation of genes involved in contractile functions. Genetic inhibition of IL-1 $\beta$  signalling on VSMCs efficiently attenuated the phenotypic switch of VSMCs and the development of cardiovascular lesions during murine KD. In addition, pharmacological inhibition of NLRP3 prevented the development of cardiovascular inflammation. Our results unravel the cellular diversity involved in IL-1 $\beta$  production and signalling in KD cardiovascular lesions and demonstrate that therapeutic strategies targeting NLRP3 might be beneficial for human KD.

**R.A.Porritt:** None. **M.Noval rivas:** None. **D.Zemmour:** Other; Significant; Nference. **M.Abe:** None. **Y.Lee:** None. **A.Gomez:** None. **S.Chen:** None. **T.R.Crother:** None. **K.Shimada:** None. **M.Arditi:** None.

## Microskeletal Stiffness Promotes Aortic Aneurysm By Sustaining Pathological Vascular Smooth Muscle Cell Mechanosensation Via Piezo1

Tarik Hadi, NYU Langone Medical Ctr, New York, NY; Cristobal Felipe Rivera, NYU MEDICAL CENTER, New York, NY; Michele Silvestro, NYU Sch of Med, New York, NY; Thomas Maldonado, **Bhama Ramkhelawon**, NYU MEDICAL CENTER, New York, NY

Mechanical overload of the vascular wall is a pathological hallmark of life-threatening abdominal aortic aneurysms (AAA). However, how this mechanical stress resonates at the unicellular level of vascular smooth muscle cells (VSMC) in AAA is undefined. Here, we combined novel ultrasound tweezers-based micromechanical system and single-cell RNA sequencing to map defective mechano-phenotype signature of VSMC niched in AAA. In the presence of AAA-promoting signal, Netrin-1, VSMC gradually adopted a mechanically solid-like state by upregulating cytoskeleton (CSK) crosslinker,  $\alpha$ -actinin2, thereby directly powering the activity of mechanosensory ion channel Piezo1. Theoretical modelling predicted that CSK alterations fueled cell membrane tension thereby modulating mechanoallostatic responses of VSMC which were validated by single-cell measurements. Stimulation of VSMC with recombinant Netrin-1 dose-dependently increased the expression of  $\alpha$ -actinin2 and Piezo1. Treatment with  $\alpha$ -actinin2 inhibitor in these conditions repressed Piezo1 expression. Atomic force microscopy analysis of AAA sections revealed increased stiffness in aortic segments of mice with AAA compared to controls. Notably, regions of increased stiffness coincident with  $\alpha$ -actinin2 and Piezo1 expression in aneurysmal tissues. In contrast, mice with deletion of Netrin-1 demonstrated reduced stiffened regions consistent with reduced  $\alpha$ -actinin2 and Piezo1 expression and were protected from AAA development. Immunostaining of human AAA sections confirmed elevated expression of mechanosensitive ion channel Piezo1 in VSMC compared to non-aneurysmal tissue collected from brain-dead organ donors. Conditional deletion of Piezo1 in VSMC and inhibition of Piezo1 in angiotensin II and elastase AAA experimental models prevented mice from developing AAA by alleviating pathological vascular remodeling imposed by exaggerated mechanical tension. Our findings demonstrate that deviations of mechanosensation behaviors of VSMC is detrimental for AAA and identifies Piezo1 as a novel culprit of mechanically fatigued aorta in AAA.

**T.Hadi:** None. **C.F.Rivera:** n/a. **M.Silvestro:** None. **T.Maldonado:** n/a. **B.Ramkhelawon:** None.

## Platelet-Induced Neutrophil Extracellular Traps Drive Ischemic Stroke Brain Injury

**Frederik Denorme**, Irina Portier, Mark J Cody, Univ of Utah, Salt Lake City, UT; Matthew D Neal, MD, Univ of Pittsburgh, Pittsburgh, PA; Matthew T Rondina, Jennifer J Majersik, Christian C Yost, Robert A Campbell, Univ of Utah, Salt Lake City, UT

Ischemic stroke prompts a strong inflammatory response which is associated with exacerbated stroke outcomes. However, classic anti-inflammatory strategies have been unsuccessful in stroke patients implying other unknown mechanisms contribute to injurious inflammation in stroke. Increasing evidence suggests immunothrombosis, a process involving coagulation, neutrophil and platelet activation, and neutrophil extracellular trap (NET) formation, is an important contributor to cardiovascular diseases. However, mechanistic regulators of immunothrombosis and their role in ischemic stroke remain unclear. We examined markers of immunothrombosis in ischemic stroke patients and matched healthy donors. Stroke patients had significantly increased levels of D-Dimers, platelet factor 4, neutrophil calprotectin, citrullinated histone H3 (H3cit) and MPO-DNA complexes, markers of NET formation. In particular, H3cit and MPO-DNA complexes positively correlated with long-term stroke outcomes. Mechanistically, we observed increased plasma and platelet HMGB1 in stroke patients, which significantly correlated with plasma NETs, indicating a role for platelet HMGB1 in NET formation. To directly examine the role of platelet HMGB1, we employed a transient ischemic stroke mouse model. Depleting platelets significantly reduced plasma HMGB1 levels, inhibited NET formation and improved stroke outcomes. Correspondingly, administering a HMGB1 inhibitor reduced NET formation and improved stroke outcomes, implying a causative role for platelet HMGB1 in mediating NET formation after stroke. As NETs appeared detrimental in ischemic stroke, we investigated the therapeutic potential of an endogenous NET inhibitory factor (NIF), recently discovered in neonates. Mice pretreated with NIF had reduced brain injury, improved neurological and motor function and enhanced survival after stroke. Importantly, NIF specifically blocked NET formation after stroke without affecting brain neutrophil recruitment. Critically, NIF still improved stroke outcomes when administered after stroke onset.

These results support a pathological role for NETs in stroke brain injury and indicate the use of NIF as a therapeutic strategy to target immunothrombosis in stroke.

**I. Portier:** None. **M.D. Neal, MD:** Stock Shareholder; Modest; Haima Therapeutics. Other Research Support; Modest; Janssen Pharmaceuticals. Honoraria; Modest; Haemonetics. Research Grant; Modest; Instrumentation Laboratories, Noveome. **M.T. Rondina:** Other; Modest; Acticor. Other Research Support; Modest; Novartis. **J.J. Majersik:** Research Grant; Significant; NIH/NINDS. **R.A. Campbell:** None.

## Effect Of Home-Based Leg Heat Therapy On Walking Performance In Symptomatic Peripheral Artery Disease: A Pilot Randomized Clinical Trial

Jacob Monroe, PURDUE UNIVERSITY, W Lafayette, IN; Susan Perkins, Yan Han, Raghunandan Motaganahalli, Indiana Univ Sch of Med, Indianapolis, IN; **Bruno Roseguini**, PURDUE UNIVERSITY, W Lafayette, IN

**Introduction:** Few non-invasive therapies currently exist to improve functional performance and restore quality of life in people with lower extremity peripheral artery disease (PAD). We previously demonstrated that supervised leg heat therapy using tube-lined trousers perfused with warm water elicited a clinically meaningful improvement in perceived physical functioning in patients with PAD. **Hypothesis:** We tested the hypothesis that unsupervised, home-based leg HT is safe and well-tolerated and improves walking performance in patients with symptomatic PAD. **Methods:** Thirty-four participants with an ankle-brachial index (ABI) values < 0.90 and a history of claudication were randomized into one of two groups: those receiving leg HT (n=18) or those receiving a sham treatment (n=16). Patients in both groups were provided with identical water-circulating trousers and a portable heating pump and were asked to apply the therapy daily (7 days/week, 90 min per session) for 8 consecutive weeks. The pump given to participants in the HT group circulated water at 43°C through the trousers, while in the sham group the pump circulated water at 33°C. The primary study outcome was the change in 6-min walk distance from baseline to 8 weeks. **Results:** Among the thirty-four patients enrolled in the study, 3 were excluded for failing to comply with study procedures and 1 voluntarily withdrew. One patient in the sham-treated group could not

complete the 8-week assessment due to the COVID-19 pandemic. Overall, participants completed 96±4% of the required treatment sessions (Control: 97±4%, HT:96±3%). Further, no serious adverse reactions to treatment were observed. Changes in 6-minute walk distance between baseline and the 8-week follow-up were compared between groups using the Wilcoxon rank sum test, since the data distribution was non-normal. The change in 6-minute walk distance was significantly higher ( $p=0.029$ ) in the group exposed to HT ( $n=15$ ; median: 21.3; 25%,75% percentiles: 10.0,42.3) as compared to the control group ( $n=14$ ; median: -0.91; 25%,75% percentiles: -5.7,14.3). **Conclusions:** These preliminary results suggest that home-based leg HT for 8 weeks promotes clinically meaningful changes in 6-minute walk distance in patients with symptomatic PAD.

**J.Monroe:** None. **S.Perkins:** None. **Y.Han:** None. **R.Motaganahalli:** None. **B.Roseguini:** None.

---

118

#### Methamphetamine Causes Endothelial Dysfunction Via Reduction Of Cystathionine Gamma Lyase And Hydrogen Sulfide Bioavailability

**Gopi Krishna K Kolluru,** John D Glawe, Sibile Pardue, Ahmad Kasabali, LSU HEALTH SCIENCES CENTER, Shreveport, LA; Saranya RAJENDRAN, Indiana Univ, Bloomington, IN; Allison L Cannon, Chowdhury S Abdullah, James G Traylor, Rodney Shackelford, Matthew D Woolard, Paari Dominic, Shenuarin Bhuiyan, Wayne W Orr, Nicholas E Goeders, LSU HEALTH SCIENCES CENTER, Shreveport, LA; Chris Kevil, LSU HEALTH SHREVEPORT, Shreveport, LA

**Background:** Methamphetamine (METH) is an addictive illicit drug used worldwide that can elicit significant damage on blood vessels resulting in increased inflammation and cardiovascular dysfunction. Recent studies highlight increased prevalence of cardiovascular disease (CVD) and associated complications including hypertension, vasospasm, left ventricular hypertrophy, and coronary artery disease in younger populations due to METH use making cardiovascular complications the second leading cause of death in METH substance users. The purpose of this study is to understand the underlying molecular mechanisms of METH-related cardiovascular injury. **Methods and Results:** Here we report that METH administration in a mouse model of 'binge and crash' decreases vascular function through a CSE/H<sub>2</sub>S/NO-dependent pathway. METH significantly reduced H<sub>2</sub>S and NO bioavailability in plasma and skeletal muscle tissues co-incident with a significant reduction in flow-mediated vasodilation (FMD) and blood flow velocity highlighting endothelial dysfunction. METH administration also reduced cardiac ejection fraction (EF) and fractional shortening (FS) indicating pump dysfunction. Interestingly, METH treatment selectively decreased CSE expression co-incident with reduced eNOS phosphorylation. Importantly, either exogenous H<sub>2</sub>S therapy or endothelial CSE transgenic overexpression corrected endothelial dysfunction and associated pathological responses due to METH toxicity. **Conclusions:** Our results uniquely demonstrate that METH mediates reduction of CSE expression and activity in endothelial cells, and subsequent attenuation of H<sub>2</sub>S/NO bioavailability directly leading to impaired cardiac and vascular function. Exogenous sulfide therapy or endothelial CSE transgenic overexpression rescues METH-induced vascular dysfunction.

**G.K.Kolluru:** None. **M.D.Woolard:** Research Grant; Significant; NIH NHLBI. **P.Dominic:** None. **S.Bhuiyan:** None. **W.W.Orr:** None. **N.E.Goeders:** None. **C.Kevil:** Ownership Interest; Significant; Innolyzer LLC. **J.D.Glawe:** n/a. **S.Pardue:** None. **A.Kasabali:** n/a. **S.Rajendran:** n/a. **A.L.Cannon:** None. **C.S.Abdullah:** None. **J.G.Traylor:** n/a. **R.Shackelford:** n/a.

---

119

#### Mitochondrial Redox Mechanisms Leading To Sustained Radiation-induced Endothelial Injury

**Karima Ait-Aissa,** Univ of Iowa, Iowa City, IA; Olha Koval, Iowa City, IA; Nathaniel R Lindsey, Kimberly Broadhurst, Univ of Iowa, Iowa City, IA; Isabella M Grumbach, CARVER COLLEGE OF MEDICINE, Iowa City, IA

**Rationale:** Radiation therapy strongly increases the risk of developing atherosclerotic vascular disease, such as coronary and carotid artery disease. Recently, we found that *in vitro* inhibition of the mitochondrial Ca<sup>2+</sup> uniporter (MCU) protects from endothelial barrier breakdown following

irradiation. **Objective:** To determine the mechanisms by which irradiation initiates vascular wall injury and test potential mitigators. **Methods and Results:** At 24 and 240 h After head and neck irradiation with 12 Gy x-ray, decreased endothelium-dependent vasodilation was seen in carotid arteries of C57Bl/6 mice. This was prevented by pre-infusion of the mitochondrial superoxide scavenger mitoTEMPO. Altered dilation correlated with increased mitochondrial ROS, loss of NO production and mitochondrial, but not nuclear DNA damage in human coronary endothelial cells *in vitro*. Enhancing mitochondrial in contrast to nuclear base excision repair by overexpression of subcellular targeted 8-Oxoguanine glycosylase blocked mitochondrial ROS and maintained NO production at all time points. Similarly, treatment with pravastatin, knockdown of MCU or its pharmacologic inhibition blocked irradiation-induced mitochondrial DNA damage and excess oxidative stress while maintaining NO production. These findings were recapitulated *in vivo* in a transgenic model of endothelial MCU knockout and in mice pretreated with pravastatin at 24 and 240 h after irradiation. Irradiation hyperpolarized the mitochondrial membrane potential ( $\alpha\psi_{\text{mito}}$ ) and increased baseline matrix  $\text{Ca}^{2+}$  levels ( $[\text{Ca}^{2+}]_{\text{m}}$ ) as well as  $\text{Ca}^{2+}$  transients. MCU knockdown decreased  $\alpha\psi_{\text{mito}}$ ,  $[\text{Ca}^{2+}]_{\text{m}}$  and  $\text{Ca}^{2+}$  transients as did mitoTEMPO, whereas pravastatin pretreatment hyperpolarized  $\alpha\psi_{\text{mito}}$  despite lowering  $[\text{Ca}^{2+}]_{\text{m}}$ . **Conclusion:** These findings demonstrate that mitochondrial DNA damage after irradiation drives a feed-forward circuit with ROS production and is sufficient to maintain endothelial dysfunction. Irradiation hyperpolarizes  $\alpha\psi_{\text{mito}}$  and blocking this or its sequela, increased  $[\text{Ca}^{2+}]_{\text{m}}$ , prevents irradiation-induced endothelial injury. These findings also suggest additional mechanisms of statins in mitochondria and MCU as a new approach to mitigate irradiation-induced vascular disease.

K.Ait-aissa: None. O.Koval: None. N.R.Lindsey: n/a. K.Broadhurst: n/a. I.M.Grumbach: None.

---

120

#### Genetic And Physiological Role For Hepatic C/EBP $\alpha$ In Plasma Lipid Metabolism

Krista Y Hu, Columbia Univ Irving Medical Ctr, New York, NY; Kavita Jadhav, Columbia Univ, New York, NY; Noel M Walsh, Columbia Univ Irving Medical Ctr, New York, NY; Elizabeth E Ha, Columbia Univ, New York, NY; Gabriella Quartuccia, Binghamton Univ, Binghamton, NY; Robert C Bauer, COLUMBIA UNIVERSITY, New York, NY

CCAAT/enhancer-binding protein alpha (C/EBP $\alpha$ ) is a transcription factor known to mediate glucose and lipid metabolism. Hepatic protein levels of C/EBP $\alpha$  are controlled by the pseudokinase Tribbles-1 (*TRIB1*), a gene which has repeatedly been linked to plasma lipids and coronary artery disease by human genome-wide association studies. Previous work has shown that genetic perturbation of hepatic Trib1 in mice alters plasma lipids. However, it is unknown if C/EBP $\alpha$  governs the relationship between Trib1 and plasma lipids. To investigate this, we first reasoned that if C/EBP $\alpha$  does govern this relationship, then human *CEBPA* should also be a GWAS hit for plasma lipids in existing data. Indeed, there is a GWAS locus for HDL cholesterol and triglycerides (TGs) at Chr19q13.11, with the lead SNP located 80kb downstream of *CEBPA* in an intron of the annotated gene *PEPD*. To see if this GWAS locus is identifying C/EBP $\alpha$ , we performed CRISPR deletion and CRISPR interference (CRISPRi) of the SNP locus in human hepatocytes and found that doing so reduced *CEBPA* gene expression (CRISPR: -85.5%,  $p < 0.01$ ; CRISPRi: -29.7%,  $p < 0.005$ ), confirming that the 19q13 GWAS locus regulates *CEBPA* gene expression. We next sought to determine how hepatic C/EBP $\alpha$  regulates lipids by performing hepatic knockout of *Cebpa* via AAV-Cre treatment in adult mice. Hepatic knockout of C/EBP $\alpha$  significantly reduced plasma lipids (-21%,  $p < 0.005$ ). RNA-seq analysis of livers from these mice identified changes in expression of known regulators of plasma lipids, including reduced *Pcsk9* expression (-60.5%,  $p < 0.005$ ). Subsequent ELISA analysis confirmed that mice lacking hepatic C/EBP $\alpha$  have reduced circulating PCSK9 (-54%,  $p < 0.005$ ). Crossing these mice to a transgenic mouse expressing human apoB confirmed that these mice have reduced non-HDL cholesterol (-49.7%,  $p < 0.01$ ). Ongoing studies seek to confirm the PCSK9 phenotype in human hepatoma cells, while also investigating how C/EBP $\alpha$  may regulate plasma TGs and HDL cholesterol. In summary, we demonstrate here that human *CEBPA* is likely a causal gene at the 19q13 plasma lipid GWAS locus, and that in mice, *Cebpa* is a novel regulator of plasma PCSK9 and non-HDL cholesterol. These data illustrate the translational relevance of targeting hepatic C/EBP $\alpha$  in adult animals.

K.Y.Hu: None. K.Jadhav: None. N.M.Walsh: None. E.E.Ha: None. G.Quartuccia: None. R.C.Bauer: None.

---

121

## Exploiting Natural Genetic Variation In The Human Triglyceride Regulator APOA5 To Understand Its Function

**Sylvia Stankov**, Cecilia Vitali, Univ of Pennsylvania, Philadelphia, PA; Joseph Park, Perelman Sch of Med at the, Philadelphia, PA; David Nguyen, S. Walter Englander, Univ of Pennsylvania, Philadelphia, PA; Michael C Phillips, UNIVERSITY OF PENNSYLVANIA, Glenside, PA; Nicholas J Hand, UPenn SOM, Philadelphia, PA; Daniel J Rader, Univ of Pennsylvania, Philadelphia, PA

Plasma triglycerides (TGs) are an independent predictor of the risk for CAD, the leading cause of death worldwide. TGs are also positively associated with risk and severity of hyperTG-induced acute pancreatitis (HTG-AP). Current therapies are often insufficient in reducing extremely elevated TGs. We believe that apolipoprotein A-V (apoA-V, encoded by APOA5) can fill this unmet medical need. ApoA-V is a potent modulator of TG metabolism; it enhances lipoprotein lipase TG hydrolysis. We hypothesize that naturally occurring human APOA5 variants can inform ApoA-V function and identify novel ApoA-V based therapeutic axes.

We used the Penn Medicine Biobank (PMBB) to identify and measure plasma TGs of carriers of APOA5 variants predicted to change ApoA-V structure-function. Then, we used hydrogen-deuterium exchange mass spectroscopy to determine the secondary structure of ApoA-V, thereby identifying putative functional domains onto which we mapped our variants of interest. Finally, we characterized the plasma lipid effects of these mutants using adeno-associated viral (AAV) vectors in apoA5 knockout (KO) mice. We identified APOA5 variants associated with changes in plasma TGs. These variants primarily fall near the central heparin binding domain or C-terminal lipid binding domain. We selected APOA5 Q275X, which removes the entire lipid binding domain, for further interrogation. ApoA5 KO mice that received APOA5 Q275X AAV had higher plasma TGs than mice treated with WT APOA5 AAV. While WT ApoA-V protein associated with VLDL and HDL particles, Q275X ApoA-V protein appeared in lipoprotein free fractions. We have identified APOA5 variants associated with plasma TG phenotypes in humans, and mapped them to an experimentally determined ApoA-V secondary structure to identify the functional domains likely impacted. We have identified APOA5 Q275X as a loss of function variant that fails to bind lipoprotein particles and is associated with elevated plasma TGs. Continued study of this and other interesting naturally occurring variants will provide insight into the function of ApoA-V in TG metabolism. These insights can help us to therapeutically enhance ApoA-V to rapidly reduce TG levels during acute HTG-AP and to help prevent recurrent HTG-AP.

**S.Stankov:** None. **C.Vitali:** None. **J.Park:** None. **D.Nguyen:** n/a. **S.Englander:** n/a. **M.C.Phillips:** None. **N.J.Hand:** None. **D.J.Rader:** Honoraria; Modest; Verve, Honoraria; Significant; Alnylam, Novartis, Pfizer, Stock Shareholder; Significant; VascularStrategies.

---

122

## The Anti-Oxidant Function Of Apolipoprotein A-I Rescues Pancreatic $\beta$ -Cells From Cholesterol-Induced Mitochondrial Dysfunction

**Bikash Manandhar**, UNSW, Sydney, Australia; Elvis Pandzic, Sydney, Australia; Nandan Deshpande, Sing-Young Chen, Valerie C. Wasinger, UNSW, Sydney, Australia; Maaie Kockx, ANZAC Res Inst, Concord, Australia; Elias Glaros, UNSW, Sydney, Australia; Kwok Leung Ong, Univ of New South Wales, Kensington, Australia; Shane Thomas, Univ of New South Wales, Sydney, Australia; Marc Wilkins, Renee Whan, UNSW, Sydney, Australia; Blake J Cochran, UNSW Sydney, Unsw Sydney, Australia; Kerry Anne Rye, Univ of New South Wales, Sydney, Australia

**Introduction:** Apolipoprotein (apo) A-I, the main apolipoprotein constituent of high-density lipoproteins, increases glucose-stimulated insulin secretion (GSIS) and is internalised by  $\beta$ -cells. Cholesterol accumulation in  $\beta$ -cells causes oxidative stress, reduces islet mass and decreases GSIS. ApoA-I increases GSIS in  $\beta$ -cells with high cholesterol levels, but it is not known if this is dependent on apoA-I internalisation. **Hypothesis:** Internalised apoA-I increases GSIS in  $\beta$ -cells with high cholesterol levels by lowering oxidative stress. **Methods:** Cholesterol-loaded Ins-1E insulinoma cells were incubated with unlabelled and/or Alexa Fluor488-labelled apoA-I. Alexa488-labelled apoA-I internalisation was quantified by flow cytometry and its intracellular location was determined by confocal microscopy and western blotting. ApoA-I binding partners on the Ins-1E surface were identified by mass spectroscopy. Generation of reactive oxygen species (ROS) in mitochondria was measured using MitoSOX. **Results:** ApoA-I was internalised by 43.4 $\pm$ 3.6% of the Ins-1E cells (apoA-I<sup>+</sup> cells) in a dose-, time-, temperature- and cholesterol-dependent manner. ApoA-I internalisation was comparable under basal (2.8 mM) and high (25

mM) glucose conditions and mediated by an F<sub>1</sub>-ATPase  $\beta$ -subunit on the Ins-1E cell surface. Cell surface F<sub>1</sub>-ATPase  $\beta$ -subunit and cholesterol levels in apoA-I<sup>+</sup> Ins-1E cells were 1.7 $\pm$ 0.3- and 1.3 $\pm$ 0.1-fold higher, respectively, than in Ins-1E cells without internalised apoA-I (apoA-I<sup>-</sup> cells). Differentially expressed genes in the apoA-I<sup>+</sup> and apoA-I<sup>-</sup> Ins-1E cells were related to protein synthesis, the ER stress-related unfolded protein response, insulin secretion and mitochondrial function. Internalised apoA-I localised to mitochondria, lowered the cholesterol-mediated increase in ROS levels, and improved insulin secretion in cholesterol-loaded Ins-1E cells. The ATPase inhibitory factor 1, IF<sub>1</sub>, inhibited apoA-I internalisation and attenuated the apoA-I-mediated decrease of ROS levels in Ins-1E cells and isolated mouse islets. **Conclusions:** These results establish that internalised apoA-I restores insulin secretion in  $\beta$ -cells with high cholesterol levels by improving mitochondrial redox balance.

**B.Manandhar:** None. **M.Wilkins:** n/a. **R.Whan:** None. **B.J.Cochran:** None. **K.Rye:** Honoraria; Significant; The Journal of Lipid Research. **E.Pandzic:** None. **N.Deshpande:** None. **S.Chen:** None. **V.C.Wasinger:** None. **M.Kockx:** None. **E.Glaros:** None. **K.Ong:** None. **S.Thomas:** None.

---

123

#### Investigating the Role of the Mevalonate Pathway in Intestinal Lipid Absorption

**Alexandria M. Doerfler**, Baylor Coll of Med, Houston, TX; Jun Han, Univ of Victoria, Victoria, BC, Canada; Li Tang, Marco De Giorgi, Baylor Coll of Med, Houston, TX; Kelsey E Jarrett, UCLA, Los Angeles, CA; Ayrea Hurley, Baylor Coll of Med, Houston, TX; Ang Li, Rice Univ, Houston, TX; Marcel Chuecos, Baylor Coll of Med, Houston, TX; Pauline Morand, Univ of California Los Angeles, Los Angeles, CA; Claudia Ayala, James F Martin, Baylor Coll of Med, Houston, TX; David R. Goodlett, Univ of Victoria, Victoria, BC, Canada; Thomas A Vallim, UCLA, Los Angeles, CA; Noah Shroyer, William R Lagor, Baylor Coll of Med, Houston, TX

While the intestine is the critical interface between cholesterol absorption and excretion, surprisingly little is known about the role of *de novo* cholesterol synthesis in this organ and how it affects whole body cholesterol homeostasis. The mevalonate pathway is most well-known for the production of cholesterol, but it is also required for the production of essential non-sterol isoprenoids. 3-hydroxy-3-methylglutaryl-coenzyme A reductase (HMGCR), the rate-limiting enzyme in the mevalonate pathway, is regulated by a three-protein complex made up of INSIG, SCAP, and SREBP2. Intestine specific knockouts of *Scap* and *Srebp2* both result in severe enteropathy and reduced mouse survival. Here, we assessed the hypothesis that *Hmgcr* is required for enterocyte viability. Mice harboring floxed alleles for *Hmgcr* were bred with the *Villin-Cre* transgene to specifically knock out this enzyme in the villus and crypt epithelial cells of the small intestine (i-KO). The i-KO mice are viable through adulthood and fertile. *Hmgcr* is efficiently deleted based on analysis via drop digital PCR and qPCR. RNA sequencing shows reduction in all SREBP2 target genes throughout the mevalonate pathway in intestinal epithelial cells. Lipidomics confirms substantial reductions in abundance of all sterol and non-sterol isoprenoids, except 7-dehydrocholesterol and cholesterol. Cholesterol is likely maintained through reabsorption of biliary cholesterol or increased uptake from the circulation. Circulating cholesterol levels and cholesterol absorption are not altered in i-KO mice, but triglyceride absorption is increased through compensatory changes in bile acid composition and intestinal growth. At the cellular level, the intestine rapidly compensates for loss of *Hmgcr* via dramatic expansion of the stem cell compartment within the crypts. In conclusion, the mechanisms by which the intestine compensates for genetic loss of *Hmgcr* include altered triglyceride absorption, bile acid composition, increased absorptive surface area, and expansion of the resident stem cell compartment. Together these studies provide insight into the effects of HMGCR knockout in intestinal development and lipid metabolism.

**A.M. Doerfler:** None. **J. Han:** None. **L. Tang:** None. **M. De Giorgi:** None. **K.E. Jarrett:** None. **A. Hurley:** None. **A. Li:** None. **M. Chuecos:** None. **P. Morand:** None. **C. Ayala:** None. **J.F. Martin:** Ownership Interest; Modest; Yap Therapeutics. **T.A. Vallim:** None. **N. Shroyer:** None. **W.R. Lagor:** None.

---

124

#### The Immunometabolic Role Of Platelets In Uncomplicated Malaria Infection

**Sara K Blick-Nitko**, Univ of Rochester, Rochester, NY; Craig Morrell, UNIVERISTY ROCHESTER, Rochester, NY; Alison C Livada, Preeti Maurya, Sara Ture, Joshua Munger, Xenia Schafer, Univ of Rochester, Rochester, NY



The malaria causing *Plasmodium* parasite is a major public health threat. *Plasmodium vivax* (*P. vivax*) is the cause of uncomplicated malaria (UCM). Platelets are the cellular mediators of thrombosis and are also the most numerous immune cells in the blood, and a first responder to infections. Thrombocytopenia is a frequent complication of malaria, and a decrease in platelet count is a negative predictor of disease outcome. Malaria infection elicits a strong interferon gamma (IFN $\gamma$ ) response. IFN $\gamma$  is a potent inducer of indoleamine 2,3-dioxygenase (IDO1) the rate-limiting enzyme that catalyzes the first step in Tryptophan (Trp) metabolism in the kynurenine (Kyn) pathway, shunting Trp away from serotonin production. Trp metabolism may be altered in malaria infection as a means to regulate immunometabolic responses, but the mechanisms remain unknown. Our platelet RNA-sequencing data from *P. vivax* infected humans and from *P. yoelii* infected mice showed increased expression of genes related to Trp metabolism, including *IDO1*. The role for platelets in metabolic pathway regulation is poorly explored in general, but particularly in infectious diseases. We introduce a novel idea that platelets participate in immunometabolism to infection. Using complementary experimental approaches such as liquid chromatography-mass spectrometry, ELISA, PCR, western blot, and flow cytometry, we test the hypothesis that platelets are a source of IDO1 in UCM malaria, and thrombocytopenia results in IDO1 depletion and immune dysregulation. We have discovered a role for platelets in Trp metabolic pathway regulation and that platelet regulated immune responses to malaria infection are in part dependent on the Trp metabolic pathways. During *P. yoelii* infection there is a depletion of Trp, and increased Kyn metabolites, as well as decreased plasma serotonin. Platelet transfusions to infected mice can increase Kyn. Understanding the interplay between platelets and immunometabolic pathways may provide a better understanding of the impact of thrombocytopenia in diseases beyond malaria, and provide a means to improve malaria infection responses as well as improved platelet-directed therapeutics in many hematological, metabolic, and immune diseases.

**S.K.Blick-**

**nitko:** None. **C.Morrell:** None. **A.C.Livada:** None. **P.Maurya:** None. **S.Ture:** None. **J.Munger:** n/a. **X.Schafer:** None.

---

125

## Trans-ancestry Genome-wide Association Study Of Varicose Veins In >1 Million Individuals Reveals Circulating Effectors Of Venous Disease

**Michael Levin**, Univ of Pennsylvania, Philadelphia, PA; Jennifer Huffman, Anurag Verma, Alexis Rodriguez, Argonne Natl Lab, Chicago, IL; Alexander G Bick, Massachusetts General Hosp, Boston, MA; Ravi Madduri, Argonne Natl Lab, Chicago, IL; Scott Damrauer, Argonne Natl Lab, Chicago, IL, Bryn Mawr, PA

**Background:** Varicose veins (VV) represent a common cause of cardiovascular morbidity and healthcare expenditures, with limited available medical therapies. The molecular and genetic basis of VV remains uncertain.

**Methods:** We identified individuals of diverse ancestry with and without diagnosis of VV in the VA Million Veteran Program (MVP). Genome-wide association studies (GWAS) were performed using logistic regression adjusted for age, sex, and population structure. Trans-ancestry meta-analysis was then performed with 6 additional VV GWAS among participants of UK Biobank (UKB), FinnGen, eMERGE, and Biobank Japan. Downstream fine-mapping, phenome-wide association (pheWAS), colocalization, and Mendelian randomization (MR) analyses were performed to identify putative causal genetic variants, clinical traits, and circulating proteins that share associations with VV.

**Results:** GWAS meta-analysis included 49,765 VV cases and 1,334,301 controls, identifying 151 independent genetic loci ( $p < 5 \times 10^{-8}$ ) associated with VV. Fine-mapping revealed 11 loci where a single causal variant was prioritized with high confidence (posterior probability  $> 0.7$ ). PheWAS of lead variants revealed associations at 101 unique loci with 90 circulating proteins and 992 clinical traits/measurements assessed in UKB. Colocalization identified shared genetic signals (posterior probability  $> 0.7$ ) between VV and clusters of proteins (eg. a cluster of vascular proteins at the ABO locus including vascular proteins like VEGFR2/3, and ICAM1/4/5, among others), and clusters of clinical traits (eg. a cluster of anthropometric associations at the *DLC1* locus). To separate shared genetics from causal associations we performed proteome-wide MR across 738 circulating proteins. We found significant causal associations ( $p < 0.05/738$ ) between 15 proteins and VV, including vasoactive proteins like ADM; extracellular matrix and connective proteins like MFAP2, POSTN, ASPN, ECM1; and hormone-proteins like SHBG.

**Conclusions:** We assembled the largest trans-ancestry GWAS of diagnosed VV to date. These results highlight shared associations between VV and anthropometric traits, and identify causal circulating proteins that may represent biomarkers or therapeutic targets.

**M. Levin:** None. **A. Rodriguez:** None. **A.G. Bick:** None. **R. Madduri:** Ownership Interest; Modest; Navipoint Genomics, LLC. **S. Damrauer:** Other; Modest; US Patent. Research Grant; Significant; RenalytixAI. Other; Modest; Calcio Labs.

---

126

#### Exposure To Thirdhand Hookah Smoke Elevates The Risk Of Thrombogenesis By Enhancing Platelet Function

Ahmed Alarabi, Texas A&M Univ, Kingsville, TX; Zubair Karim, The Univ of Texas at El Paso, El Paso, TX; Patricia Lozano, Fadi T Khasawneh, **Fatima Z Alshbool**, Texas A&M Univ, Kingsville, TX

While the rate of smoking has been on the decline, the popularity of other forms of tobacco, including hookah/waterpipe continues to rise. While hookahs are thought to be safe, our recent studies have documented that exposure to waterpipe smoke (WPS) produces detrimental cardiovascular health effects, including thrombotic events; similar to what was observed with traditional cigarette smoking. In this connection, we have also documented that the new risk, termed thirdhand smoke (THS)-which is the residual tobacco smoke contaminant that remains after a cigarette is extinguished- increases the risk of thrombosis, much like both active/first hand smoke (FHS) and passive/second hand smoke (SHS) exposure. However, whether Thirdhand Hookah Smoke (THHS) exposure produces similar negative health effects remains to be determined. By employing a novel exposure protocol, mice were exposed to THHS starting at 10 weeks of age for three months, as per the gold standard Beirut protocol, which is as follows: one-hour session of 171 puffs of 530 mL volume, each puff is 2.6 s duration, and there are a 17 s interpuff interval. Our data shows that THHS exposed platelets exhibited enhanced agonist-induced aggregation, as well as dense and alpha granules secretion responses. Moreover, we also found that integrin activation, and phosphatidylserine exposure are increased as a result of THHS exposure. Consistent with these findings, we also obtained biochemical evidence of enhanced platelet reactivity, namely increased activation/phosphorylation of Akt. Notably, we observed high levels of the tobacco marker cotinine in the urine of the THHS mice, but not from the controls. Finally, and in terms of its *in vivo* impact, we observed that THHS enhances hemostasis and increases the risk of thrombosis in comparison to controls as documented by the shortened bleeding and occlusion times. Our results demonstrate, for the first time, that exposure to THHS results in a prothrombotic phenotype, which is attributed, at least in part, to a potentiated state of platelet reactivity. Thus, the negative health consequences of THHS should not be underestimated, and warrant further investigation. These findings should also guide policy development for regulating exposure to this form of tobacco.

**A.Alarabi:** None. **Z.Karim:** None. **P.Lozano:** None. **F.T.Khasawneh:** None. **F.Z.Alshbool:** None.

---

127

#### Aspirin Resistant Biomechanical Platelet Activation In Fibromuscular Dysplasia: Novel Mechanisms Of Platelet Activation & Stroke

**Rohan Bhandari**, Cleveland Clinic Fndn, Cleveland, OH; Anu Aggarwal, Cleveland, OH; Matthew Godwin, Crystal Pascual, Cleveland Clinic Fndn, Cleveland, OH; Sharon Shim, Park Ridge, IL; Natalia Fendrikova-Mahlay, Cleveland Clinic Fndn, Cleveland, OH; Stanley L Hazen, CLEVELAND CLINIC FOUNDATION, Cleveland, OH; Ayman Elbadawi, Universtiy of Texas Medical Branch, Galveston, TX; Joseph E Aslan, Oregon Health and Science Universit, Portland, OR; Scott J CAMERON, Cleveland Clinic Fndn, Solon, OH

**Background:** Fibromuscular dysplasia (FMD) is a non-atherosclerotic, non-inflammatory disorder characterized by abnormal arterial morphology and turbulent blood flow. In regions of disturbed blood flow, circulating platelets may become activated. Cerebrovascular FMD is common and increases the risk of stroke in affected patients. Most FMD patients are treated with antiplatelet agents, however these medications target biochemical and not biomechanical pathways of platelet activation.

**Methods:** Thrombotic outcomes were determined by multivariate regression analysis of 105,887 patients with FMD. Platelets were isolated from humans and activation was assessed by FACS and aggregometry following exposure to *ex vivo* steady laminar and disturbed flow (SF and DF, respectively) conditions using a cone and flow system. Single-cell phenotyping of control and FMD platelets with transcriptomics (RNAseq) and proteomics were performed. Cellular bioenergetics were evaluated by real-time metabolic analyses.

**Results:** In patients with FMD, long-term aspirin therapy is paradoxically an independent risk factor for acute ischemic stroke (OR 1.64, 95% CI 1.29-1.94) but seems to protect against acute hemorrhagic stroke (OR 0.47, 95% CI 0.24-0.89). FMD platelet activation and aggregation were hyporeactive to biochemical agonists, but hyperreactive to ex vivo mechanical, disturbed blood flow conditions compared to age/gender-matched controls. FMD platelet activation in DF was attenuated by the mechanosensitive channel inhibitor, GsMTx4. Principle component analyses of RNAseq and proteomics identified markedly different platelet phenotypes with key differences in mitochondrial function/fission. Platelet imaging and metabolic analyses revealed abnormal mitochondrial architecture and respiration in FMD.

**Conclusions:** FMD platelets display a divergent, dysregulated platelet phenotype with attenuated biochemical but augmented biomechanical activation. DF exposure of platelets in irregularly shaped arteries in FMD may alter the platelet phenotype and metabolic function. Therapeutics targeting biomechanical pathways of platelet activation may provide a superior mechanism for stroke prevention without unintended bleeding consequences.

**R.Bhandari:** None. **S.J.Cameron:** None. **A.Aggarwal:** None. **M.Godwin:** None. **C.Pascual:** n/a. **S.Shim:** None. **N.Fendrikova-mahlay:** n/a. **S.L.Hazen:** Other; Modest; Procter & Gamble, Other; Significant; Procter & Gamble, Cleveland Heart Lab/Quest Diagnostics, Research Grant; Significant; Procter & Gamble. **A.Elbadawi:** None. **J.E.Aslan:** None.

---

128

#### Nicotine Transgenerationally Alters Gene Methylation And Abdominal Aortic Aneurysm Risk

Joscha Udo Nikolaus Mulorz, Dept of Vascular and Endovascular Surgery Univ Hosp, Düsseldorf, Germany; Pireyatharsheny Mulorz, YaeHyun Rhee, Stanford Cardiovascular Inst - Stanford Univ, Stanford, CA; Markus Wagenhaeuser, Heinrich-Heine-Univ, Düsseldorf; Philip S Tsao, VAPAHCS - Stanford Univ, Palo Alto, CA; **Joshua M. Spin**, Stanford Cardiovascular Inst - Stanford Univ, Stanford, CA

**Significance:** Both smoking and family history are major risk factors for abdominal aortic aneurysm (AAA). Smoking is a powerful modulator of DNA methylation, and nicotine alone can cause heritable epigenetic alterations in animal models and humans. Nicotine also increases aortic stiffness, predisposing towards AAA. We investigated the effects of parental nicotine exposure in mice on their offspring's risk for experimental AAA and on transgenerational DNA methylation. **Methods:** Male and female Apo E-/- mice (F0) were exposed to subcutaneous nicotine (25 mg/kg/day) or saline infusion for 28 days. After treatment completion, mice were mated to untreated controls. F1 generation offspring underwent Angiotensin II infusion (1µg/kg/min) to induce AAA at age 10-weeks. Aneurysm growth was tracked via ultrasound over 28 days. Subgroups of F1 mice underwent ex-vivo pressure myography assessment of the abdominal aorta. Germ and aortic tissue from both F0 and F1 were evaluated using RRBS-Seq genome-wide DNA methylation analysis. **Results:** Parental nicotine augments model AAA formation, incidence, and rupture rates in their offspring. This effect was most significant in male offspring of nicotine-exposed females (vs. saline). Maternal nicotine exposure also increased F1 aortic stiffness. F0 nicotine exposure altered DNA methylation in multiple tissues, and led to numerous significant differentially methylated regions (DMRs) in their F1 offspring, many precisely conserved. Nicotine caused global DNA hypermethylation, altered maternally imprinted genes in F0 females, and had variable patterns depending on gender. Nicotine altered aortic methylation patterns in genes known to relate to AAA development, including lncRNAs/miRNAs. DMR pathway analysis revealed enrichment for transcription factors, suggesting that nicotine transgenerationally influences numerous genes through expression modulation. **Conclusion:** Nicotine exposure can augment experimental AAA growth and aortic stiffness across generations. These effects are accompanied by widespread epigenetic changes in germ tissue and aorta, including several key AAA modulator genes, with enrichment in transcription factors, including many targeting known AAA-related genes.

**J.U.Mulorz:** None. **P.Mulorz:** None. **Y.Rhee:** None. **M.Wagenhaeuser:** None. **P.S.Tsao:** None. **J.M.Spin:** None.

## BAF60c Prevents Abdominal Aortic Aneurysm Formation Through Maintaining Vascular Smooth Muscle Cell Homeostasis

**Guizhen Zhao**, Univ of Michigan, Ann Arbor, MI; Jifeng Zhang, UNIV MICH, Ann Arbor, MI; Eugene Chen, UNIV OF MICHIGAN MEDICAL CTR, Ann Arbor, MI; Yang Zhao, UNIV OF MICHIGAN MEDICAL CTR, Ann Arbor, MI, Ann Arbor, MI; Haocheng Lu, Univ of Michigan, Ann Arbor, MI; tianqing zhu, Univ of Michigan, Ann Arbor, MI, Ann Arbor, MI; Ziji Chang, Univ of Michigan, Ann Arbor, MI, Ann Arbor, MI, Changsha

**Background:** Abdominal aortic aneurysm (AAA) is a common and life-threatening vascular disease. Vascular smooth muscle cell (VSMC) dysfunction is involved in the dilatation and eventual rupture of AAA, with the precise epigenetic control of this process less studied. BAF60c, a unique subunit of SWI/SNF chromatin remodeling complex, serves as a core modulator of physiological and pathological processes, yet little is known about its function in the vasculature and pathogenesis of AAA. **Methods and results:** BAF60c is downregulated in AAAs from humans and mice with primary staining to the aortic VSMC, confirmed by single cell RNA sequencing. In vivo studies revealed that VSMC-specific knockout Baf60c markedly aggravated both AngII- and elastase-induced murine AAA formation, with significant increases of elastin degradation, inflammatory cell accumulation, VSMC phenotype switching, and apoptosis. In vitro studies showed that knockdown of BAF60c in human aortic smooth muscle cells resulted in the loss of contractile phenotype while upregulation of inflammatory genes and increased apoptosis. Chromatin immunoprecipitation followed by sequencing and qPCR, as well as CoIP assays showed that BAF60c maintained VSMC contractile phenotype by enhancing serum response factor association with its co-activator p300 and SWI/SNF complex, suppressed VSMC inflammation via precise control of the repressive state of NF- $\kappa$ B-target genes, as well as prevented VSMC apoptosis through transcriptional activation of KLF5-dependent BCL2 expression. **Conclusions:** Our study indicates that BAF60c is essential for SWI/SNF complex recruitment to chromatin and interaction with diverse transcription factors to precise epigenetic control of VSMC homeostasis and prevention of AAA formation.

**G.Zhao:** None. **J.Zhang:** None. **E.Chen:** None. **Y.Zhao:** None. **H.Lu:** None. **T.Zhu:** n/a. **Z.Chang:** None.

## Wnt16 Deficiency Worsens Angiotensin II - Induced Aneurysmal Remodeling Of Ascending Thoracic Aorta

Abraham Samuel Behrmann, UT Southwestern, Dallas, TX; Dalian Zhong, Dallas, TX; Li Li, Parastoo Sabaeifard, UTSW, Dallas, TX; Mohammad Goodarzi, Andrew Lemoff, Dallas, TX; **Dwight A Towler**, UT SOUTHWESTERN MEDICAL CENTER, Dallas, TX

Wnt16 controls bone strength via paracrine osteoblast-osteoclast remodeling interactions. *Wnt16* mRNA is highly expressed in both aorta & bone, & immunofluorescence (IF) localized Wnt16 to vascular smooth muscle (VSM). Paracrine VSM - monocyte/macrophage (M/MAC) interactions control arterial remodeling, resembling osteoblast-osteoclast interactions in bone. We assessed the impact of Wnt16 deficiency on aneurysmal remodeling (6-7/group). Angiotensin II infusion for 4 weeks increased ascending thoracic aorta diameter by 60% (Holm-Sidak  $p = 1.5E-4$ , ANOVA  $p = 2.7E-6$ ) in male LDLR<sup>-/-</sup> mice. Wnt16<sup>-/-</sup>;LDLR<sup>-/-</sup> cohorts exhibited worsened ascending aorta dilatation (by 20%; Holm-Sidak  $p = 0.03$ ), indicating a protective role for Wnt16. Mass spectrometry of thoracic aorta proteins from Wnt16<sup>-/-</sup>;LDLR<sup>-/-</sup> vs. LDLR<sup>-/-</sup> mice revealed a 9-fold increase in MMP12 ( $p = 0.008$ ;  $n=3$ /group) — a M/MAC protease key to aneurysmal remodeling. IF confirmed enhanced adventitial MMP12 in aortas of Wnt16-null mice. Treatment of M/MACs with Wnt16 (8 nM) down-regulated *Mmp12* mRNA (78%;  $p < 0.001$ ), with increased *IL10* (2-fold;  $p < 0.05$ ) & *Arg1* (6-fold;  $p = 0.001$ ). Hypomorphic alleles encoding contractile proteins predispose to hereditary thoracic aortic aneurysm; thus, we studied the impact of Wnt16 deficiency on the contractile phenotype. VSM from Wnt16-null thoracic aorta exhibited reductions in *Myh11* (down 60%;  $p < 0.05$ ), *Acta2* (by 35%,  $p < 0.05$ ), & the VSM transcriptional co-activator *Myocardin* (by 65%;  $p = 0.0002$ ), while *Axin2* was increased 1.7-fold ( $p = 0.01$ ). Acute siRNA-mediated knockdown of *Wnt16* in VSM - M/MAC admixtures (95% VSM, 5% M/MAC) also downregulated contractile genes & upregulated *Mmp12*. This was phenocopied by siRNA targeting *Taz/Wwtr1* — a transcriptional collaborator of Myocd we identified as exhibiting impaired nuclear localization in Wnt16-null VSM. In vivo dosing with Wnt16 (0.25 mg/kg/day, 2 days) upregulated aortic contractile gene expression 1.6- to 1.8-fold, with *Mmp12* reduced 50% ( $p < 0.05$ ), as consistent with the reciprocal changes upon Wnt16 deficiency. Wnt16 limits thoracic aortic remodeling, preserves the VSM

contractile phenotype, & reduces Mmp12. Strategies that augment Wnt16 signaling may mitigate enlargement of thoracic aortic aneurysms.

**A.S.Behrmann:** None. **D.Zhong:** None. **L.Li:** None. **P.Sabaeifard:** None. **M.Goodarzi:** None. **A.Lemoff:** None. **D.A.Towler:** Other; Modest; Former Radius Health, Research Grant; Significant; National Institutes of Health, American Diabetes Association, Burroughs Wellcome Fund.

---

131

#### *Gata4* Ablation In Smooth Muscle Cells Reduces Aortic Root Dilation In A Murine Model Of Loeys-Dietz Syndrome

**Emily E. Bramel,** Muzna Saqib, Johns Hopkins Sch of Med, Baltimore, MD; Tyler J Creamer, Elena Gallo MacFarlane, Johns Hopkins Univ, Baltimore, MD

Loeys-Dietz syndrome (LDS) is a connective tissue disorder characterized by predisposition to aneurysm. Although dilation can develop in all segments of the arterial tree, the aortic root is especially prone to disease. This aortic region is primarily composed of vascular smooth muscle cells (VSMCs) derived from secondary heart field (SHF) progenitors, while VSMCs derived from the cardiac neural crest (CNC) predominate in the more distal ascending aorta. Although intrinsic differences have been found between these two types of VSMCs, it remains unclear how these may contribute to localized risk. To identify transcripts associated with the vulnerability of the aortic root in LDS, we performed single cell transcriptomic analysis on proximal aortas from 16-week-old control and *Tgfb1*<sup>M318R/+</sup> LDS mice, which carry a kinase-inactivating mutation in TGF- $\beta$  Receptor 1. We identified four major VSMC clusters regardless of genotype, with two clusters being defined by CNC-enriched transcripts and two clusters by SHF-enriched transcripts. The latter were defined by expression of *Gata4*, which codes for a transcription factor required for development of SHF-derived vascular structures, as well as by higher expression of transcripts previously involved in aneurysm pathogenesis such as *Thbs1*, *Tgfb1*, and *Tgfb3*. In situ RNA hybridization confirmed that *Gata4*-expressing VSMCs were enriched in the aortic root and proximal ascending aorta, with almost no expression in the more distal ascending aorta, suggesting that this transcript defined the aortic region most susceptible to the effects of the *Tgfb1*<sup>M318R/+</sup> mutation. GATA4 protein levels were also upregulated in the aortic root of LDS mice. To test if excessive GATA4 expression or activity in VSMCs contributed to aortic root dilation in LDS, we generated LDS mice in which *Gata4* was specifically deleted in VSMCs by tamoxifen administration at 6 weeks of age. We found that this intervention significantly reduced aortic root growth from 8 to 20 weeks of age. Although the mechanisms remain under investigation, these data suggest that expression of *Gata4* might sensitize specific subsets of aortic VSMCs to the effects of an LDS mutation, rendering the aortic root more susceptible to disease.

**E.E.Bramel:** None. **M.Saqib:** None. **T.J.Creamer:** None. **E.Gallo macfarlane:** None.

## Moderated Posters

---

MP01

### Retinoic Acid Receptor Alpha (Rar $\alpha$ ) In Macrophages Protects From Diet-induced Atherosclerosis In Mice

**Fathima Nafrisha Cassim Bawa**, Yingdong Zhu, Kent State Univ, Kent, OH; Raja Gopoju, Yanyong Xu, shuwei hu, Northeast Ohio Medical Univ, Rootstown, OH; Kavita Jadhav, Kent State Univ, Kent, OH; Yanqiao Zhang, NORTHEAST OHIO MEDICAL UNIVERS, Rootstown, OH

Atherosclerosis is a chronic vascular disease caused by inflammation and accumulation of lipids in the blood vessels. Macrophages in atherosclerotic lesions participate in lipid accumulation giving rise to formation of foam cells and production of mediating inflammatory cytokines. This makes them an attractive target for therapy. Previous studies have shown that retinoid signaling plays a broader role in modulating macrophage lipid metabolism and its inflammatory phenotype. Our preliminary results showed that when macrophages (RAW267.4 cells and mouse peritoneal macrophages) were treated with all-trans retinoic acid or retinoic acid receptor alpha (Rar $\alpha$ )-specific agonist, cholesterol efflux genes like *Abca1* And *Abcg1* and anti-inflammatory gene like *Arg-1* were significantly increased. We hypothesized that retinoic acid receptor alpha (Rar $\alpha$ ) may play a role in macrophages to protect against diet-induced atherosclerosis. To test this hypothesis, we conducted in-vivo studies using macrophage-specific Rar $\alpha$  knockout mice. Rar $\alpha$  floxed mice were crossed with lysozyme-cre transgenic mice to generate macrophage specific knockout mice (m-Rar $\alpha$ <sup>-/-</sup>). Rar $\alpha$ <sup>fl/fl</sup> (control) and m-Rar $\alpha$ <sup>-/-</sup> were given high fat/high cholesterol (HFHC) diet for 16 weeks. Intracellular triglyceride and cholesterol levels were significantly increased in peritoneal macrophages of m-Rar $\alpha$ <sup>-/-</sup> compared to the control. Analysis of macrophage gene expression showed increase in the expression of pro-inflammatory genes (*Il-1 $\beta$* , *Tnf $\alpha$*  and *Tgm-2*) with decrease in genes involved in cholesterol efflux (*Abca1* and *Abcg1*) and anti-inflammation (*Arg-1* and *Mrc-1*) in m-Rar $\alpha$ <sup>-/-</sup> macrophages. This implies that loss of Rar $\alpha$  in macrophages can aggravate atherosclerosis. To test this hypothesis, we generated mice deficient in macrophage Rar $\alpha$  and low-density lipoprotein receptor and their control mice. These mice were then fed an HFHC diet for 16 weeks. The Oil Red O staining of aortas showed that mice lacking macrophage Rar had a significant increase in atherosclerotic plaques compared to the control mice. Our data demonstrate that Rar $\alpha$  in macrophages is protective from atherosclerosis.

**F.Cassim bawa:** None. **Y.Zhu:** None. **R.Gopoju:** n/a. **Y.Xu:** None. **S.Hu:** None. **K.Jadhav:** n/a. **Y.Zhang:** None.

---

MP02

### Proprotein Convertase Subtilisin/kexin Type 6 (PCSK6) Is Involved In Regulation Of Vasculogenesis

**Melody Chemaly**, Karolinska Instt, Solna, Sweden; Bianca Esmee Suur, Karolinska Inst, Stockholm, Sweden; Hong Jin, Karolinska Instt, Stockholm, Sweden; Anders Malarstig, Ljubica Matic, Karolinska Instt, Solna, Sweden

**Background** PCSK6 cleaves and activates growth factors involved in cell differentiation and *Pcsk6*<sup>-/-</sup> mice exhibit 25% embryonic lethality, while surviving offspring have blindness and cyclopia. We have shown that PCSK6 localizes to vascular smooth muscle cells of intra-plaque neovessels. **Hypothesis** We hypothesize that a) the processes of vasculogenesis, atherosclerosis and plaque neovascularisation share common molecular regulators and b) that PCSK6 plays a common role in vascular remodeling. **Methods** Association between SNPs near the PCSK6 gene and levels of 90 plasma proteins was tested using data from 30,931 individuals in the SCALLOP consortium. Data from the FinnGen consortium (Release 3) were queried to explore the PCSK6 SNPs associated with specific disease phenotypes. Morpholino technology was used for *Pcsk6* knockdown in zebrafish, coupled with vascular phenotype studies. *Pcsk6*<sup>-/-</sup> mice were used to study the expression of vasculogenesis related genes as well as vascular morphology. **Results** Rs7178801 and rs11639051 in the *PCSK6* gene were found to relate to plasma PDGFB and VEGFD levels, while rs45482895 associated with diabetic retinopathy and disorders of the choroid and retina in humans. Gross phenotypic and histological examination of zebrafish embryos with ablated PCSK6 showed improper peripheral vascular patterning of intersegmental vessels, cerebral and myocardial haemorrhage, atrial dilatation and pericardial oedema. Gene expression levels of vasculogenesis related genes, i.e. *Vegfa*, *Vegfb*, *Angpt1* and *Tgfb2* were altered in the heart, liver and adipose tissue in *Pcsk6*<sup>-/-</sup> mice. In the retinas of *Pcsk6*<sup>-/-</sup> mice, *Pdgfb* was significantly downregulated

compared to controls. Staining of the retinal vasculature showed that superficial retinal vasculature had a lower number of branching points and vessel width, while deep retinal vasculature covered a significantly smaller area in *Pcsk6*<sup>-/-</sup> **Conclusions** Here, we show that variants in the *PCSK6* gene associate with growth factors implicated in vasculogenesis and retinopathy. Lack of *Pcsk6* in mice and zebrafish led to vascular patterning defects. Further studies will aim to elucidate the mechanisms by which PCSK6 regulates vasculogenesis in homeostatic and pathological conditions

**M.Chemaly:** None. **B.E.Suur:** None. **H.Jin:** None. **A.Malarstig:** Employment; Significant; Pfizer. **L.Matic:** None.

---

MP03

#### Histone-mediated Platelet Activation And Microvesicle-induced Thrombin Generation In COVID-19

**Alicia S. Eustes,** Jagadish Swamy, melissa jensen, Katina M Wilson, Univ of Iowa, Iowa City, IA; Shibani M Kudchadkar, Des Moines, IA; Usha Perepu, Univ of Iowa, Iowa City, IA; Francis J Miller Jr., Duke University, Durham, NC; Steven R Lentz, UNIVERSITY OF IOWA, Iowa City, IA; Sanjana Dayal, UNIVERSITY IOWA HEALTH CARE, Iowa City, IA

**Background:** Severe COVID-19 leads to inflammation and coagulopathy with progression to multiple organ failure. Several prothrombotic mechanisms have been proposed, including NETosis with release of citrullinated histones, platelet hyperactivation, and generation of procoagulant microvesicles. **Aims:** We hypothesized that histones derived from NETosis promote platelet activation and release of microvesicles that mechanistically contribute to thrombin generation and thrombosis in COVID-19. **Methods:** Platelet poor plasma (PPP) was prepared from 136 COVID-19 patients enrolled in a multicenter randomized clinical trial comparing standard prophylactic dose to intermediate dose enoxaparin in hospitalized patients with COVID-19 (NCT04360824). We also prepared PPP and washed platelets from 53 healthy subjects. We measured citrullinated histone H3 (H3Cit) by ELISA, microvesicles by flow cytometry, and thrombin generation using the Calibrated Automated Thrombogram. *Ex vivo* platelet adhesion and thrombus growth on collagen was measured in a microfluidic chamber. **Results:** Compared to healthy subjects, COVID-19 patients had elevated plasma levels of H3Cit and platelet-derived microvesicles. When PPP was triggered with exogenous tissue factor and phospholipids, higher endogenous thrombin potential, peak thrombin, and velocity index were observed in COVID-19 patients compared to healthy subjects. Increased thrombin generation with COVID-19 PPP was evident even when triggered without added phospholipids, suggesting the presence of procoagulant microvesicles in COVID-19 plasma. Enhanced thrombin generation also was observed after transfer of microvesicles isolated from COVID-19 patient plasma to control PPP. Incubation of control platelets with PPP from COVID-19 patients but not healthy subjects caused increased platelet-dependent thrombin generation and larger platelet-thrombi under venous shear stress. These effects of COVID-19 plasma on platelet-dependent thrombin generation and platelet-thrombi formation were inhibited by a histone aptamer. **Conclusions:** We conclude that histone-mediated platelet activation promotes thrombosis in COVID-19 in part via increased thrombin generation driven by microvesicles.

**A.S.Eustes:** Employment; Significant; University of Iowa. **J.Swamy:** n/a. **M.Jensen:** n/a. **K.M.Wilson:** n/a. **S.M.Kudchadkar:** n/a. **U.Perepu:** n/a. **F.J.Miller:** None. **S.R.Lentz:** Other; Modest; Opko, Other; Significant; Novo Nordisk, Research Grant; Significant; Novo Nordisk, Apellis. **S.Dayal:** None.

---

MP04

#### Single Cell Profiling Identifies IgM To MDA-LDL Producing Human B Cells And Atheroprotective Role Of CD24

**Tanyaporn Pattarabanjird,** Univ of Virginia, Charlottesville, VA; Anh Nguyen, Duke, Durham, NC; Chantel McSkimming, Univ of Virginia, Charlottesville, VA; Huy Dinh, Univ of Wisconsin, Madison, WI; Melissa Marshall, Univ of Virginia, Charlottesville, VA; Yanal Ghosheh, La Jolla Inst for Immunology, La Jolla, CA; Christopher Durant, La Jolla Inst of Immunology, La Jolla, CA; Jenifer Vallejo, Rishab Gulati, La Jolla Inst for Immunology, San Diego, CA; Ryosuke Saigusa, La Jolla Inst, La Jolla, CA; Fabrizio Drago, Univ of Virginia, Charlottesville, VA; Angela Taylor, Univ of Virginia, Charlottesville, VA; Ayelet Gonen, UCSD, La Jolla, CA; Sotirios Tsimikas, Yury I Miller, UNIV CALIFORNIA SAN DIEGO, La Jolla, CA; Klaus F Ley II, La Jolla Inst, La

Jolla, CA; Catherine C Hedrick, La Jolla Inst for Allergy and, La Jolla, CA; Coleen A McNamara, UNIVERSITY VIRGINIA, Charlottesville, VA

Murine B-1 cells produce IgMs that inactivate oxidation-specific epitopes and protect against atherosclerosis. Despite compelling data that IgM to MDA-LDL (IgM<sup>MDA-LDL</sup>) is inversely associated with coronary artery disease (CAD) and cardiovascular (CV) events in human, the human B cell subtype that produces IgM<sup>MDA-LDL</sup> is unknown. Here, we utilized mass cytometry to identify the 11 circulating human B cell subtypes and discovered that only the frequency of CD20<sup>+</sup>CD27<sup>+</sup>IgM<sup>+</sup> cells was associated with IgM<sup>MDA-LDL</sup> levels. Notably, high expression of CD24, a GPI-anchored sialoglycoprotein, was associated with IgM<sup>MDA-LDL</sup> ( $r = 0.57$ ,  $p = 0.002$ ) and inversely associated with CAD severity ( $r = -0.58$ ,  $p = 0.001$ ). Adoptive transfer (AT) of sorted CD20<sup>+</sup>CD27<sup>+</sup>IgM<sup>+</sup>CD24<sup>hi</sup> (B<sup>27+IgM+CD24hi</sup>) and CD24<sup>lo/-</sup> (B<sup>27+IgM+CD24lo/-</sup>) human B cells into humanized mice demonstrated that CD24 is critical for trafficking to the spleen and IgM production. Bulk RNAseq coupled with pathway analysis of B<sup>27+IgM+CD24hi</sup> and B<sup>27+IgM+CD24lo/-</sup> cells revealed enhanced BCR and CCR6 signaling in B<sup>27+IgM+CD24hi</sup>. Imaging flow cytometry indicated colocalization between CD24 and CCR6 which was abrogated by CD24 blocking antibody (CD24mAb). Trans-well migration and internalization assays demonstrated that CD24 blockade increased CCL20-induced CCR6 internalization ( $p < 0.05$ ,  $n = 4$ ), and reduced CCL20-induced migration of B<sup>27+IgM+CD24hi</sup> cells ( $p < 0.05$ ,  $n = 4$ ). CD24mAb treatment of B<sup>27+IgM+CD24hi</sup> cells prior to AT into humanized mice also reduced the amount of surface CCR6 on B<sup>27+IgM+CD24hi</sup> cells *in vivo* ( $p < 0.05$ ,  $n = 4$ ). Both CCR6 knockout and CD24 inhibition of B<sup>27+IgM+CD24hi</sup> cells reduced migration to the spleen ( $p < 0.05$ ,  $n = 4$ ), and plasma level of human IgM ( $p = 0.057$ ,  $n = 4$ ). Lastly, single cell multi-omics sequencing of PBMCs from 60 CAD subjects revealed elevated CCR6 and IgM signaling in B<sup>27+IgM+CD24hi</sup> cells in subjects with less severe CAD. Results provide the first evidence for a role for CD24 in regulating CCR6-mediated B cell homing to the spleen, IgM production and CAD in humans. Findings may have important implications for the new CD24 immunotherapy entering clinical trials and raise the possibility that augmenting CD24 and/or CCR6 on B<sup>27+IgM+</sup> cells may be an effective atheroprotective strategy.

**T.Pattarabanjird:** None. **R.Saigusa:** None. **F.Drago:** None. **A.Taylor:** None. **A.Gonen:** n/a. **S.Tsimikas:** Employment; Significant; Ionis Pharma, Ownership Interest; Modest; Kleanthi Diagnostics, Ownership Interest; Significant; Oxitope, Inc. **Y.I.Miller:** n/a. **K.F.Ley:** None. **C.C.Hedrick:** None. **C.A.Mcnamara:** None. **A.Nguyen:** n/a. **C.Mcskimming:** None. **H.Dinh:** n/a. **M.Marshall:** None. **Y.Ghosheh:** None. **C.Durant:** n/a. **J.Vallejo:** None. **R.Gulati:** n/a.

---

MP05

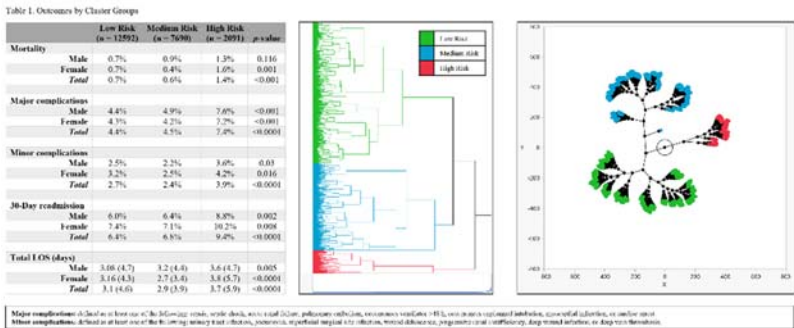
Sex Differences In Mortality And 30-day All Cause Readmission Following Carotid Endarterectomy Following Acute Ischemic Stroke: A Nsqip Study (2014 - 2017)

**Mariana M Suarez,** Massachusetts Inst of Technology, Cambridge, MA; Anshul Saxena, Venkataraghavan Ramamoorthy, Muni Rubens, Peter McGranaghan, Emir Veledar, Baptist Health South Florida, Coral Gables, FL; Mahdi O Garelnabi, UMass Lowell, Lowell, MA

**Background:** Studies report that acute ischemic stroke (AIS) affects males and females differently. For example, the treatment outcomes of intra-arterial thrombolysis differ between males and females. In this study, we examined mortality and 30-day readmission differences by sex among AIS patients who had carotid endarterectomy (CEA). **Methods:** We used data from National Surgical Quality Improvement Program (NSQIP) registry (2014-2017). Patients  $\geq 18$  years of age, with CEA for AIS were included. AIS and CEA were identified using ICD-9 and ICD-10 diagnosis, and CPT codes, respectively. Using machine learning methods such as Hierarchical clustering, we grouped patients (low, medium, and high-risk clusters) based on their demographics, past medical history, and preoperative variables. Differences in means, and differences in proportions were calculated. Logistic regression was conducted for 30-day readmission and survival analysis for mortality, accounting for cluster groups and sex. **Results:** There were a total of 22,373 AIS patients who received CEA treatment. Mean (SD) age of the sample was 70.7 (9.4) years, and 61% were males while 39% were females. Mortality rates were 0.8% and 0.7% for men and women ( $p = 0.113$ ), respectively. Thirty-day readmission rates were 6.3% and 7.6% for men and women ( $p < 0.0001$ ), respectively. There were 56.3%, 34.4%, and 9.3% patients in Low, Medium, and High-Risk clusters, respectively. Females were 1.2 times (OR 95% CI: 1.1 - 1.3) as likely to be readmitted compared to males. Survival analysis showed that there was no significant difference in mortality between males and females (HR: 0.8; 95% CI: 0.6 - 1.2;  $p = 0.28$ ). **Conclusion:** Our study found sex related disparities in short-term readmissions as it was higher among females. This could be because of underlying sex specific



pathophysiology of AIS. Healthcare providers should consider sex-specific management to improve post-stroke recovery for women and reduce their excess burden.



M.M.Suarez: None. A.Saxena: None. V.Ramamoorthy: n/a. M.Rubens: n/a. P.Mcgranaghan: None. E.Veledar: None. M.O.Garelnabi: None.

MP06

The Signaling Roles Of The Adaptor Protein Nck1 In Atherosclerosis

Mabruka Alfaidi, Milla Reddick, LSU Health Sciences Ctr-Shreveport, Shreveport, LA; Xinggui Shen, LSU HEALTH - SHREVEPORT, Shreveport, LA; Wayne Orr, LSU Health Sciences Ctr-Shreveport, Shreveport, LA

**Rational:** Alterations in hemodynamic shear stress (SS) at atherosclerosis-prone sites promotes endothelial activation, characterized by nuclear factor- $\kappa$ B (NF- $\kappa$ B)-driven expression of cell adhesion molecules that mediate leukocyte homing. In addition, proinflammatory cytokines (e.g. IL-1 $\beta$ ) promote NF- $\kappa$ B-dependent endothelial activation. While the recent CANTOS trial using an IL-1 $\beta$  antagonist highlights the potential for treating atherogenic inflammation beyond lipid lowering therapies alone, our understanding of how endothelial activation contributes to this effect remains limited.

**Methodology & Results:** We identified the signaling adaptor Nck1 as a critical regulator of atherogenic endothelial activation. Endothelial cells deficient in Nck1 lack SS-induced NF- $\kappa$ B activation and proinflammatory gene expression. Additionally, we demonstrated an interaction between Nck1 and IL-1 $\beta$  signaling in response to SS, showing that SS activates the IL-1 $\beta$  receptor (IL1R1) signaling partner IRAK-1 in a Nck1-dependent manner both *in vitro* and *in vivo*. Mechanistically, point mutation analysis suggest a critical role for the Nck1 SH2 domain (phosphotyrosine binding domain) in mediating these effects. Nck1 affinity pulling down and mass spectrometry identified multiple downstream effectors of IL-1 pathway. In vivo, Global Nck1 knockout mice show reduced atherosclerosis characterized by diminished macrophage and smooth muscle incorporation and bone marrow chimeras suggest non-hematopoietic Nck1 mediates this response.

**Conclusions:** A recent GWAS analysis linked Nck1 to coronary artery disease, underscoring its importance to human disease. Therefore, our data suggest that Nck1 mediates the formation of IL-1-related signaling complexes to induce atherogenic endothelial activation, and selective inhibition of Nck1 or its critical domains will allow efficient inhibition of atherosclerosis in humans.

M.Alfaidi: None. M.Reddick: None. X.Shen: None. W.Orr: None.

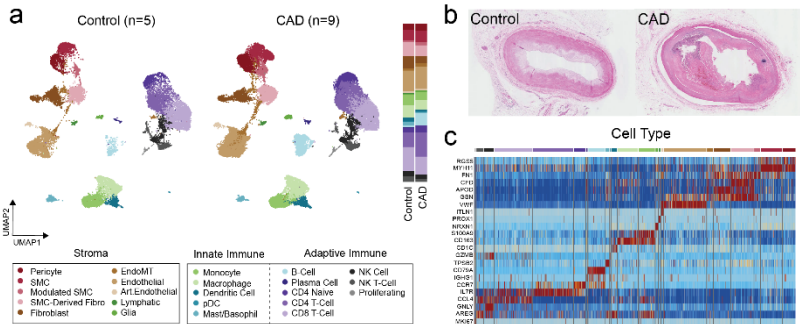
MP07

Multi Omic Atlas Of Human Coronary Artery Disease

Junedh M Amrute, Andrea Bredemeyer, Washington Univ Sch of Med in St. Louis, Saint Louis, MO; Xin Luo, Tracy Yamawaki, Amgen Inc, South San Francisco, CA; Andrew Koenig, Cameran Jones, Washington Univ Sch of Med in St. Louis, Saint Louis, MO; Simon Jackson, Milena B Furtado, Sally Shi, Chi-Ming Li, Brandon Ason, Amgen Inc, South San Francisco, CA; Nathan O Stitzel\*, Kory J Lavine, Washington Univ Sch of Med in St. Louis, Saint Louis, MO

Previous human genetic studies have provided insight into the genes and pathways involved in atherosclerotic CAD, however, there remains an incomplete understanding of the precise cell types that

drive disease pathogenesis. To generate a cellular atlas for CAD, we performed CITE-seq on left human coronary arteries with obstructive CAD (n=5), CAD with coronary stenting (n=4), or controls without CAD (n=5); single-nuclei RNA sequencing was performed on a subset (n=4) of these samples. Standard histopathology was used to assess the degree of atherosclerotic plaque burden and annotate disease status (Fig b). Sequencing yielded 65,437 cells with 23 distinct cell types (Fig a) and canonical marker genes (Fig c). Within the stroma we found prominent transcriptional changes in endothelial cells and fibroblasts along with the emergence of a modulated smooth muscle cell (SMC) state in CAD tissue. The modulated SMC cells were enriched with fibroblast activator protein surface expression. Additionally, we noted the emergence of a proliferative SMC population in stented arteries. Two distinct fibroblast populations were present: one was specific to coronary arteries in GTex and this population was enriched for SVEP1 expression in the CAD samples. Furthermore, pseudotime analysis and integration of published single-cell SMC lineage tracing data in atherosclerotic mice show that this population is SMC-derived. Within the immune cells, we find expansion of B- and T-cell populations with transcriptional changes within myeloid subsets. We found 4 distinct macrophage populations: inflammatory, TREM2, HLA-II high, and resident-like macrophages. CAD macrophages had enriched inflammatory and foam-cell like signatures compared to controls. Furthermore, foam cell genes were localized to the inflammatory and TREM2 macrophages. Together, our results provide the first multi-omic single cell atlas of human coronary artery tissue with insights into disease pathogenesis.



**J.M.Amrute:** n/a. **C.Li:** Employment; Significant; Amgen Inc. **B.Ason:** Employment; Significant; Amgen, Inc. **N.O.Stitzel\*:** Research Grant; Significant; Regeneron Pharmaceuticals. **K.J.Lavine:** Other; Modest; Medtronic , Research Grant; Significant; Amgen. **A.Bredemeyer:** None. **X.Luo:** Employment; Significant; Amgen Inc. **T.Yamawaki:** Employment; Significant; Amgen, Inc., Stock Shareholder; Significant; Amgen, Inc.. **A.Koenig:** None. **C.Jones:** None. **S.Jackson:** Employment; Significant; Amgen Inc.. **M.B.Furtado:** n/a. **S.Shi:** Employment; Significant; Amgen Inc..

MP08

Telomerase Reverse Transcriptase Mediates Osteogenesis In Calcific Aortic Valve Disease

**Rolando A Cuevas,** Univ of Pittsburgh, Pittsburgh, PA; **Luis Hortells,** Cincinnati Children's Hosp, Cincinnati, OH; **Camille Boufford,** Cincinnati Children's Hosp, Cincinnati, OH, Vermillion, SD; **Cailyn Regan,** VMI St. Hilaire Lab, Pittsburgh, PA; **Ryan Wong,** Alexander Crane, Univ of Pittsburgh, Pittsburgh, PA; **Claire Chu,** Pittsburgh, PA; **William Moorhead,** Angela Lee, Univ of Pittsburgh, Pittsburgh, PA; **Michael Bashline,** Univ of Pittsburgh Medical Ce, Pittsburgh, PA; **Aditi Gurkar,** Aging Inst, Univ of Pitt, Pittsburgh, PA; **Dennis Bruemmer,** Aging Inst, Univ of Pitt, Pittsburgh, PA, Pittsburgh, PA; **mauricio rojas,** Univ of Pittsburgh, Pittsburgh, PA; **Thomas G Gleason,** Univ of Maryland, Baltimore, MD; **Marie Billaud,** Ibrahim Sultan, Cynthia St Hilaire, Univ of Pittsburgh, Pittsburgh, PA

Calcific aortic valve disease (CAVD) is the leading heart valve disorder in the US. It is characterized by an active accumulation of calcium nodules on the aortic valve leaflets which lead to stiffening and remodeling of the valve leaflets causing valve dysfunction, cardiac failure and increased stroke risk. Inflammation and mechanical stresses contribute to CAVD pathogenesis. However, the mechanisms driving the fibrocalcific remodeling of the aortic valve are currently ill-defined. Multiple studies have revealed that the catalytic subunit of telomerase reverse transcriptase (TERT) can induce gene transcription and its overexpression primes mesenchymal stem cells to differentiate into osteoblasts, suggesting that TERT has a role in the activation of osteogenic transcriptional programs. We hypothesized that TERT contributes to early events leading to calcification of the valve leaflet. In human calcified valve

tissue, we found that TERT protein is highly expressed in areas of calcification compared to control valve tissue, with no effect on telomere length. Alpha-SMA, a VIC activation marker, and RUNX2, a key transcription factor involved in the osteogenic differentiation of osteoblast, were also elevated in CAVD tissue. Under osteogenic differentiation conditions, human valve interstitial cells (VICs) upregulated TERT, RUNX2, and alpha-SMA protein levels and calcified, while CAVD VICs calcified de novo. Inflammatory stimuli intensified in vitro calcification, and induced TERT, RUNX2, and alpha-SMA protein expression. PLA and ChIP analysis showed that TERT interacts with Signal Transducer and Activator of Transcription 5A/B (STAT5) and together bind to *RUNX2* promoter, respectively. shRNA-mediated TERT downregulation reduced expression of RUNX2 and alpha-SMA and genetic deletion of *Tert* in murine mesenchymal stem cells and vascular smooth muscle cells prevented calcification. These data provide evidence that TERT is required for calcification, regulates the transition of quiescent VICs into calcifying VICs, and that STAT5 functions as a TERT-interacting partner for DNA binding.

**R.A. Cuevas:** None. **L. Hortells:** None. **C. Boufford:** None. **C. Regan:** None. **R. Wong:** None. **C. Chu:** None. **W. Moorhead:** None. **A. Gurkar:** None. **M. rojas:** None. **T.G. Gleason:** Research Grant; Modest; Medtronic. Other Research Support; Modest; Boston Scientific. Other; Modest; Abbott. Other Research Support; Modest; Cytosorb. **I. Sultan:** None. **C. St Hilaire:** Research Grant; Significant; NIH. Honoraria; Modest; AHA - CircRes EB.

---

MP09

MLKL (Mixed Lineage Kinase Domain-like Protein) Is A Novel Regulator Of The Splenic Microenvironment That Restricts Hematopoiesis During Atherosclerosis

**Adil Rasheed,** Hailey Wyatt, Ottawa Heart Inst, Ottawa, ON, Canada; Taylor Dennison, uOttawa Heart Inst, Ottawa, ON, Canada; My-anh Nguyen, UOTTAWA HEART INSTITUTE, Ottawa, ON, Canada; Sabrina Robichaud, Ottawa Heart Inst, Ottawa, ON, Canada; Michele Geoffrion, Ottawa Heart Inst, Ottawa, ON, Canada, Ottawa, ON, Canada; Adir Baxi, Ottawa Heart Inst, Ottawa, ON, Canada; Richard Lee, Ionis Pharmaceuticals, Carlsbad, CA; Mireille I Ouimet, Univ of Ottawa, Ottawa, ON, Canada; Katey J Rayner, UNIV OTTAWA HEART INST, Ottawa, ON, Canada

During atherosclerosis, macrophages within the aorta undergo necroptosis, a mode of pro-inflammatory cell death that is triggered by the phosphorylation of RIPK1 & RIPK3 and leads to the activation of the mixed lineage kinase domain-like protein (MLKL) and cell lysis. Our previous work demonstrated that while inhibition of MLKL decreased necroptosis and necrotic core in the plaque, unlike RIPK1 & RIPK3 this inhibition did not lead to overall decrease in plaque area, suggesting that MLKL may in fact participate in other processes that drive atherosclerotic plaque development. Because circulating leukocytes are recruited and contribute to the growing atheroma, and these leukocytes are derived from hematopoietic stem and progenitor cells (HSPCs) found in both the bone marrow (BM) and the spleen, we investigated whether these hematopoietic reservoirs became dysregulated upon loss of MLKL during atherogenesis. To induce atherogenesis, *Apoe*-knockout mice (*Apoe*<sup>-/-</sup>) were fed a high fat-high cholesterol diet for 16 weeks while receiving weekly subcutaneous administration of antisense oligonucleotides (ASOs) to knockdown MLKL expression. In the *Apoe*<sup>-/-</sup> mice receiving MLKL ASO we observed a 3.1-fold increase in splenomegaly compared to the control ASO, specifically with an expansion of the splenic red pulp, the area of splenic hematopoiesis. Furthermore, flow cytometry revealed a significant increase in myeloid HSPCs and mature myeloid populations in the spleen, but not the BM, after MLKL knockdown. However, no changes were observed in these hematopoietic measures after transplantation of *Ldlr*-knockout mice with MLKL-knockout BM, indicating that MLKL restricts hematopoiesis through its regulation of non-hematopoietic cells of the splenic niche. Indeed, upon MLKL knockdown in the *Apoe*<sup>-/-</sup> mice we observed a >50% reduction in splenic endothelial cells, which are required to promote HSPC quiescence and repress hematopoiesis. These data therefore demonstrate a novel role for MLKL on preserving splenic endothelial cells to limit immune cell development during atherosclerosis, and more generally, highlight the importance of the dysregulation of the splenic microenvironment to contributing to the inflammatory processes that drive atherosclerosis.

**A.Rasheed:** None. **K.J.Rayner:** None. **H.Wyatt:** n/a. **T.Dennison:** None. **M.Nguyen:** None. **S.Robichaud:** None. **M.Geoffrion:** None. **A.Baxi:** None. **R.Lee:** n/a. **M.I.Ouimet:** None.

## The Long Non-coding RNA LINC02502 Modulates Vascular Smooth Muscle Cell Phenotypes

**Elisabeth Haag**, Tan Dang, Deutsches Herzzentrum Muenchen, Munich, Germany; Jana Wobst, German Heart Ctr Munich, Munich; Carolin Hoehne, Louise Hegge, Deutsches Herzzentrum Muenchen, Munich, Germany; Hanna Winter, Klinikum rechts der Isar der TUM, Muenchen; Lars Maegdefessel, Klinikum rechts der Isar der TUM, Muenchen, Munich; Heribert Schunkert, German Heart Ctr, Munich; Thorsten Kessler, GERMAN HEART CENTRE MUNICH, Munich

**Background:** Genome-wide association studies led to the identification of several genomic loci associated with coronary artery disease risk. One such locus is chromosome 4q27 which harbors the long non-coding RNA (lncRNA) *LINC02502* and the *PDE5A* gene. *PDE5A* encodes phosphodiesterase 5a, the enzyme that degrades the second messenger cyclic guanosine monophosphate. We previously showed that differential *PDE5A* expression is mediated via *LINC02502*-mediated scaffolding of the transcription factor REST. **Methods and Results:** In a screening of vascular cell types, we identified vascular smooth muscle cells (VSMC) to express both *PDE5A* and *LINC02502*. Using RNA interference, we studied the ability of VSMC to migrate in the presence or absence of *LINC02502* in *in vitro* scratch wound healing assays. Knockdown of *LINC02502* led to a significant reduction of VSMC migration. VSMC proliferation was determined using BrdU incorporation assays. After knockdown of *LINC02502*, VSMC proliferation was decreased. To investigate whether *LINC02502* influences inflammatory phenotypes, we ectopically overexpressed the lncRNA in VSMC and analyzed a panel of inflammatory transcripts using quantitative PCR. In general, overexpression of *LINC02502* rendered VSMC more inflammatory. Particularly, *LINC02502* increased the expression of interleukin-1 $\beta$ , chemokine (C-X-C motif) ligand 1, and fractalkine. Importantly, we did not make these observations secondary to overexpression of *PDE5A*, suggesting that *LINC02502* regulates these transcripts in an independent manner. *In silico* analysis, however, revealed that *LINC02502*-regulated targets were enriched for predicted targets of REST. **Conclusion:** The lncRNA *LINC02502* is a candidate for mediating the risk of coronary artery disease at the chromosome 4q27 locus via regulating *PDE5A*. Independent of *PDE5A* regulation, *LINC02502* promotes pro-atherosclerotic phenotypes in VSMC, i.e., migration, proliferation, and expression of inflammatory transcripts. Modulating *LINC02502* might be a novel approach to prevent and treat coronary atherosclerosis via multiple pathways.

**E.Haag:** None. **T.Dang:** None. **J.Wobst:** None. **C.Hoehne:** None. **L.Hegge:** None. **H.Winter:** None. **L.Maegdefessel:** None. **H.Schunkert:** None. **T.Kessler:** None.

## Histone Methyl Transferase (Suv39h1): Function In Smooth Muscle Cell Phenotypic Plasticity

**Payel Chatterjee**, Yale Univ, New Haven, CT; Raja Chakraborty, Yi Xie, YALE UNIVERSITY, New Haven, CT; Ashley Sizer, Yale Univ, New Haven, CT; John Hwa, YALE SCHOOL MEDICINE, New Haven, CT; Kathleen A Martin, YALE SCHOOL OF MEDICINE, New Haven, CT

**Introduction** The phenotypic plasticity of vascular smooth muscle cells (VSMCs) is central to growth and remodeling processes, but also contributes to cardiovascular disease. This unique ability of VSMCs to reversibly differentiate and de-differentiate is incompletely understood. SUV39H1 is a histone methyltransferase that specifically trimethylates Lysine-9 of histone H3 (H3K9me3), resulting in transcriptional repression through epigenetic gene silencing. **Hypothesis** We hypothesized that SUV39H1 may play a role in SMC phenotypic switch. **Methods** Using *in vitro* and *in vivo* approaches including knockdown, qPCR, western, and chromatin immunoprecipitation (ChIP) assays to determine role of SUV39H1 in SMC plasticity. **Results** A qPCR array screen of epigenetic regulators in VSMCs identified SUV39H1 mRNA as upregulated with PDGF induced dedifferentiation and downregulated with rapamycin induced differentiation. This was confirmed at the protein level. SUV39H1 knockdown significantly increased VSMC contractile protein mRNA, protein levels and decreased dedifferentiation associated gene expression, and also decreased PDGF-induced VSMC migration (n=4). Interestingly, we found that expression of KLF4, the master transcriptional regulator of dedifferentiation in SMCs, was dramatically decreased after SUV39H1 knockdown (n=5). We further noted that SUV39H1 knockdown decreased KLF4 mRNA stability (n=3). Mechanistically, SUV39H1 knockdown increased miRNA143, a well-known repressor of KLF4. ChIP assays at contractile gene promoters showed a significant decrease in H3K9me3 mark and an increase in H3K27 acetylation, an activation mark (n=4). Carotid artery ligation induced intimal

hyperplastic lesions in wild type C57BL/6 mice, showed a significant increase in SUV39H1 and H3K9me3 expression compared to uninjured vessels. **Conclusion** We identify SUV39H1 an epigenetic regulator of VSMC phenotype whose expression and activity increase with dedifferentiation *in vitro* and *in vivo*. Mechanistically, SUV39H1 influences VSMC chromatin marks and KLF4 expression to repress contractile phenotype. Understanding the role of SUV39H1 and its targets may have implications for developing new therapeutic strategies for treating vascular diseases.

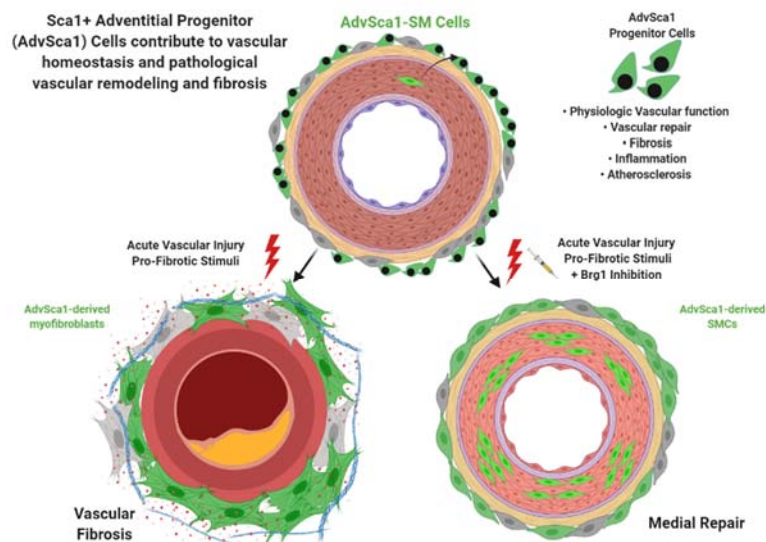
**P.Chatterjee:** None. **R.Chakraborty:** None. **Y.Xie:** None. **A.Sizer:** n/a. **J.Hwa:** None. **K.A.Martin:** None.

MP12

## The Epigenetic Remodeling Protein Brg1 Is Implicated In Vascular Progenitor Cell Contribution To Pathological Vascular Remodeling And Fibrosis

**Austin Jolly,** Sizhao Lu, Allison Dubner, Keith Strand, Marie Mutryn, Karen Moulton, Raphael Nemenoff, Mary Weiser-Evans, Univ of Colorado Anschutz, Aurora, CO

Vascular fibrosis is an irreversible consequence of vascular remodeling that ensues in many cardiovascular diseases. Currently, no treatments are available to target chronic vascular fibrosis. We identified a unique population of multipotent smooth muscle-derived Sca1<sup>+</sup> progenitor cells that reside in the vascular adventitia (AdvSca1-SM cells). While AdvSca1-SM cells can differentiate into mature smooth muscle cells (SMCs) and repair the vessel wall, AdvSca1-SM cells also have the potential to differentiate into myofibroblasts and greatly contribute to vascular fibrosis after acute vascular injury. The epigenetic remodeling protein Brg1 is upregulated in AdvSca1-SM cells in the setting of vascular injury, but how Brg1 influences AdvSca1-SM differentiation is unknown. Using *in vitro* and *in vivo* approaches, our goal was to define the role of Brg1 in AdvSca1-SM cells. We hypothesized that Brg1 regulates chromatin density around genetic loci associated with fibrosis to preferentially drive AdvSca1-SM cell differentiation towards pathologic myofibroblasts. Further, we hypothesized that pharmacologic inhibition of Brg1 will disrupt AdvSca1-SM differentiation into myofibroblasts and attenuate vascular fibrosis. Mice subjected to carotid ligation and treated with the highly specific Brg1 inhibitor, PFI-3, exhibited decreased vascular fibrosis, reduced neointima, and decreased adventitial expansion of AdvSca1-SM cells as compared to mice that received vehicle control. This *in vivo* data was complemented by *in vitro* studies where cultured AdvSca1-SM cells stimulated with TGF- $\beta$  expressed myofibroblast genes including  $\alpha$ SMA and periostin, and co-treatment with PFI-3 blocked TGF- $\beta$ -induced myofibroblast marker expression at the mRNA and protein level. In conclusion, these results support the hypothesis that Brg1 is a major regulator of AdvSca1-SM myofibroblast differentiation and may represent a novel targetable protein to treat vascular fibrosis.



**A.Jolly:** None. **S.Lu:** None. **A.Dubner:** Research Grant; Significant; CCTSI grant TL1TR002533--Predoctoral Fellowship. **K.Strand:** None. **M.Mutryn:** None. **K.Moulton:** None. **R.Nemenoff:** None. **M.Weiser-evans:** n/a.

### Small RNA Profiling Identifies Mir-200b As A Repressor Of Vascular Smooth Muscle Cell Migration And Proliferation

**Mingyuan Du**, Cristina Espinosa-Diez, Univ of Pittsburgh, pittsburgh, PA; Mingjun Liu, Sidney Mahan, Delphine Gomez, Univ of Pittsburgh, Pittsburgh, PA

**Background and Objectives:** A large body of research has identified miRNA as pivotal regulators of smooth muscle cell (SMC) fate in various vascular diseases. However, global changes of miRNA expression profile during SMC phenotypic modulation have not been well characterized. As the targetome of a given miRNA is highly dependent on the cell type and context, comparative analysis of mRNA and miRNA expression profiles can provide decisive information for assessing the versatility in miRNA functions and discovering novel miRNA modulating SMC phenotype. Our goal is to define the miRNA signatures in differentiated and de-differentiated SMC, the miRNA overall contribution to the transcriptome, and novel functionally relevant miRNA. **Methods:** By performing RNAseq and small RNAseq, we defined the mRNA/miRNA expression profiles in aortic SMC cultured in differentiation or de-differentiation media with Platelet Derived Growth Factor-BB (PDGF-BB) and performed functional studies on differentially expressed miRNAs (DEmiR). **Results:** We found that PDGF-BB-induced SMC de-differentiation generated 48 significant DEmiRs, including 15 downregulated and 33 upregulated DEmiRs. Integrative analysis predicted that nearly 40% (1335 of 3523) of differentially expressed transcripts were direct targets of DEmiRs. The miR-200 cluster (miR-200a, miR-200b and miR-429) was found potentially downregulated after PDGF-BB treatment, as well as Tet2 and Myocardin knockdown, while its expression increased in rapamycin treated SMC. We found that miR-200b overexpression prevented PDGF-BB-induced SMC migration and proliferation, while miR-200b inhibition had an opposite effect. Finally, we identified Quaking, a potent inducer of SMC phenotypic switching, as a primary target of miR-200b. **Conclusion:** Our study predicted a marked contribution of miRNA in regulating SMC transcriptomic profile. miR-200b was identified as a novel pro-differentiation miRNA in SMC through inhibition of phenotypic switching.

**M.Du:** None. **C.Espinosa-diez:** None. **M.Liu:** None. **S.Mahan:** None. **D.Gomez:** None.

### The Profibrotic Transition Of Vascular Smooth Muscle Cells-derived Resident Vascular Adventitial Progenitor Cells Contributes To Angiotensin II-induced Cardiac Fibrosis.

**Sizhao Lu**, Keith Strand, Austin Jolly, Allison Dubner, Marie Mutryn, Raphael A Nemenoff, Karen Moulton, Timothy A McKinsey, Mary CM Weiser-Evans, Univ of Colorado-Anschutz, Aurora, CO

Cardiovascular fibrosis is an important end-stage pathology that characterizes most cardiovascular diseases. Activated cardiac myofibroblasts (MFs) are the major contributors to ECM deposition in pathological fibrosis. However, due to potential heterogeneity of MFs, the origin of these cells remains controversial. Using highly specific smooth muscle cell lineage-tracing mouse models, we discovered the smooth muscle cell origin of a subpopulation of resident vascular adventitial progenitor cells, defined by the expression of the stem cell marker Sca1 (AdvSca1-SM cells), which rapidly proliferate and adopt a myofibroblast phenotype in response to acute vascular injury. Further, we identified a specific gene signature of active hedgehog/Wnt/ $\beta$ -catenin/Klf4 signaling in AdvSca1-SM cells and validated a Gli1-CreERT2-ROSA26-YFP (Gli1) reporter mouse model to be a faithful lineage tracing system for AdvSca1-SM cells. However, the function of AdvSca1-SM cells in cardiac fibrosis is unknown. Using immunofluorescent staining and label-free second harmonic generation (SHG) imaging, we observed the expansion and migration of AdvSca1-SM cells in close association with perivascular and interstitial cardiac fibrosis in a model of Angiotensin II (AngII)-induced cardiac fibrosis in Gli1 reporter mice. We performed single cell RNA sequencing (scRNA-seq) to examine the phenotype of AdvSca1-SM cells in this model. Our data showed that, upon AngII challenge, AdvSca1-SM cells differentiate along a profibrotic trajectory, which is characterized by loss of expression of *Klf4*, the lncRNA, *Meg3*, and stemness genes and up-regulation of myofibroblast genes. Importantly, AngII-induced profibrotic transcriptomic changes of AdvSca1-SM cells were recapitulated in human ventricular tissues exhibiting a gene signature of cardiac hypertrophy, emphasizing the translational significance of this phenotypic transition. Connectivity map analysis of the scRNA-seq data identified statins as potential candidates for inhibition of the profibrotic transition of

AdvSca1-SM cells. In agreement, simvastatin induced the expression of stemness genes and inhibited TGF $\beta$ -induced up-regulation of  $\alpha$ SMA and down-regulation of Klf4 in cultured AdvSca1-SM cells.

**S.Lu:** None. **K.Strand:** None. **A.Jolly:** None. **A.Dubner:** Research Grant; Significant; CCTSI grant TL1TR002533--Predoctoral Fellowship. **M.Mutryn:** None. **R.A.Nemenoff:** None. **K.Moulton:** None. **T.A.Mckinsey:** Other Research Support; Modest; Italfarmaco. **M.C.Weiser-evans:** n/a.

---

MP15

Structural Vs. Acute Load Dependent Mechanisms For Carotid Artery Stiffening With Aging: The Multi-ethnic Study Of Atherosclerosis (MESA)

**Ryan Pewowaruk**, Univ of Wisconsin - Madison, Madison, WI; Yacob Tedla, Vanderbilt Univ Medical Cente, Nashville, TN; Claudia E Korcarz, UNIVERSITY OF WISCONSIN, Madison, WI; Matthew C Tattersall, UNIVERSITY OF WISCONSIN HOSPITAL, Madison, TX; James H Stein, UNIV WISCONSIN MED SCH, Madison, WI; Naomi C Chesler, Adam Gepner, Univ of California, Irvine, Irvine, CA

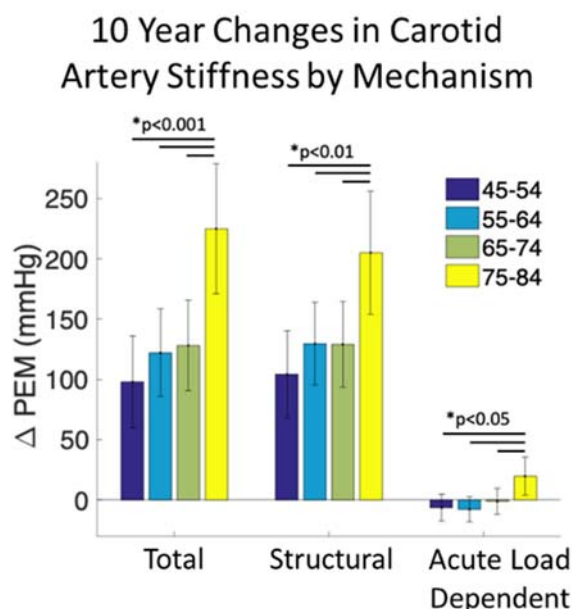
**Introduction:** Aging stiffens arteries, increasing cardiovascular disease (CVD) risk. Elastic arteries stiffen via two main mechanisms: 1) acute load dependent stiffening from higher blood pressure (BP), and 2) structural stiffening such as collagen accumulation. AHA's arterial stiffness scientific statement highlights differentiating structural vs acute load dependent stiffening with aging as a crucial, unanswered question.

**Hypothesis:** Longitudinal rates of structural and acute load dependent arterial stiffening will differ based on age.

**Methods:** MESA participants with B-mode carotid ultrasound and brachial BP at Exam 1 and Exam 5 (year 10) were included in this study (n=2604). Peterson's and Young's elastic moduli (PEM and YEM) were calculated to represent total stiffness. Structural stiffness was calculated by adjusting PEM and YEM to a standard BP of 120/80 mmHg with participant-specific models. Acute load dependent stiffness was the difference of total and structural stiffness. Changes in carotid artery stiffness mechanisms over 10 years were compared by age groups with ANCOVA models adjusted for baseline CVD risk factors.

**Results:** The 75-84 age group had the greatest rate of total ( $p<0.001$ ), structural ( $p<0.01$ ), and acute load dependent stiffening ( $p<0.05$ ) compared to younger groups. Only age was predictive of structural stiffening, but age, race/ethnicity, education, BP, cholesterol, and medications were predictive of increased acute load dependent stiffening. On average, structural stiffening accounted for the vast majority (>99%) of total stiffening, but 37% of participants had more acute load dependent than structural stiffening.

**Conclusions:** Rates of structural and acute load dependent carotid artery stiffening increased with age. Structural stiffening was consistently observed, and acute load dependent stiffening was highly variable. The heterogeneity in arterial stiffening mechanisms with aging may influence CVD development.





**R.Pewowaruk:** None. **Y.Tedla:** None. **C.E.Korcarz:** None. **M.C.Tattersall:** None. **J.H.Stein:** Other; Significant; Eli Lilly and Co.. **N.C.Chesler:** Other; Modest; Mivi Neuroscience, Other Research Support; Modest; Endotronix, Inc., Other Research Support; Significant; Mivi Neuroscience, Inari Medical. **A.Gepner:** n/a.

---

MP16

## Multi-trait Gwas Of Atherosclerosis Detects Novel Loci And Potential Therapeutic Targets

**William P Bone**, Univ of Pennsylvania, Philadelphia, PA; **Tiffany Bellomo**, Philadelphia, PA; **Brian Y Chen**, Katerina A Gawronski, David Zhang, Univ of Pennsylvania, Philadelphia, PA; **Joseph Park**, Perelman Sch of Med at the, Philadelphia, PA; **Michael Levin**, Noah Tsao, Univ of Pennsylvania, Philadelphia, PA; **Derek Klarin**, Massachusetts General Hosp, Boston, MA; **Julie Lynch**, VA Salt Lake City, Bedford, MA; **Themistocles L Assimes**, STANFORD UNIVERSITY, Palo Alto, CA; **Michael Gaziano**, Peter Wilson, STANFORD UNIVERSITY, Palo Alto, CA, Boston, MA; **Kelly Cho**, VA Boston Healthcare System, Boston, MA; **Marijana Vujkovic**, Univ of Pennsylvania, Philadelphia, PA; the VA Million Veteran Program; **Chris J O'Donnell**, VA Boston Healthcare System, Boston, MA; **Kyong-Mi Chang**, Corporal Michael J. Crescenz VA Medical Ctr, Philadelphia, PA; **Philip S Tsao**, VAPAHCS - Stanford Univ, Palo Alto, CA; **Daniel J Rader**, Marylyn Ritchie, Univ of Pennsylvania, Philadelphia, PA; **Scott Damrauer**, Bryn Mawr, PA; **Benjamin F Voight**, Corporal Michael J. Crescenz VA Medical Ctr, Philadelphia, PA

Atherosclerosis, which is the narrowing of the arterial walls via accumulation of cholesterol-rich arterial plaques, is the leading cause of vascular disease worldwide, including myocardial infarction and ischemic stroke. Although atherosclerosis affects arteries throughout the body, previous genome-wide association studies (GWAS) have been performed on specific atherosclerotic phenotypes such as coronary artery disease (CAD) and peripheral artery disease (PAD). There is substantial evidence to suggest that these more specific atherosclerosis phenotypes share a common genetic etiology. We performed a series of multi-trait GWAS using combinations of two atherosclerosis traits and seven atherosclerosis risk factor traits and detected 31 novel pleiotropic loci. We performed these multi-trait GWAS using the N-GWAMA multi-trait GWAS method and summary statistics for CAD (van der Harst et al. 2018), PAD (Klarin et al. 2019), body mass index (Pulit et al. 2019), type II diabetes (Vujkovic et al. 2020), smoking initiation (Wootton et al. 2020), and lipid traits (Klarin et al. 2019). We identified candidate causal genes for 14 of these loci through colocalization analysis with GTEx expression quantitative trait locus (eQTL) data. *VDAC2* and *PCSK6* are two candidate causal genes that our results and previous literature suggest are potential therapeutic targets. *VDAC2* eQTLs in aorta and tibial artery colocalized with a multi-trait GWAS signal detected in the CAD PAD multi-trait GWAS. Previous work has shown that *VDAC2* regulates apoptosis, and our results suggest increased *VDAC2* expression in smooth muscle cells could increase smooth muscle cell accumulation in atherosclerotic plaques. A sQTL (splicing QTL) for *PCSK6* in liver colocalized with a multi-trait GWAS signal between PAD and LDL. Further analysis of the sQTL signal suggested that the effect allele correlates with a more active isoform of *PCSK6*, which could increase lipid fractions and risk of atherosclerosis. These results show that joint analysis of atherosclerotic disease traits and their risk factors allows for identification of unified biology that may offer the opportunity for therapeutic manipulation.

**W.P.Bone:** None. **J.Lynch:** None. **T.L.Assimes:** None. **M.Gaziano:** n/a. **P.Wilson:** n/a. **K.Cho:** n/a. **M.Vujkovic:** None. **The va million veteran program:** n/a. **C.J.O'donnell:** n/a. **K.Chang:** n/a. **P.S.Tsao:** None. **T.Bellomo:** None. **D.J.Rader:** Honoraria; Modest; Verve, Honoraria; Significant; Alnylam, Novartis, Pfizer, Stock Shareholder; Significant; VascularStrategies. **M.Ritchie:** Other; Modest; CIPHEROME, Regeneron Genetics Center. **S.Damrauer:** Other; Modest; US Patent, Calcio Labs, Research Grant; Significant; RenalytixAI. **B.F.Voight:** n/a. **B.Y.Chen:** None. **K.A.B.Gawronski:** None. **D.Zhang:** None. **J.Park:** None. **M.Levin:** None. **N.Tsao:** None. **D.Klarin:** None.



## TLR4 May Play A Role In Accelerated Atherosclerosis In Beta Thalassemia

**Julian Hurtado**, Hassan Sellak, Emory Univ, Atlanta, GA; David Robert Archer, W. Robert R Taylor, EMORY UNIVERSITY SCHOOL OF MEDICINE, Atlanta, GA

Beta Thalassemia (BT) is an autosomal recessive hemoglobinopathy that affects 80 million people worldwide. Children with BT display an increase in carotid-intima media thickness, an early sign suggestive of premature atherosclerosis. However, it is unknown if there is a direct relationship between BT and atherosclerotic disease. BT has increased free heme leading to ROS generation directly or via Toll Like Receptor (TLR4) activation, but the role of heme in disease progression in BT is poorly characterized. The aim of this study is to evaluate the progression of atherosclerosis in BT mice and the potential role of TLR4. Atherosclerosis was induced by implementing short (ST) and long term (LT) models. In our ST model, both BT (*Hbb<sup>th-3</sup>*) and wild type (b6) male/female littermates (n=5) were fed a Paigen high fat diet (PD) for 8 weeks. On week 2, mice were injected with AAV8-PCSK9 to knockdown the LDL receptor. On weeks 4-8, mice were treated with Angiotensin II via subcutaneous osmotic pumps implantation. The LT model was performed by placing mice on 3 months of PD with PCSK9 overexpression. Atherosclerosis was evaluated by atherosclerotic plaque lesion area of the descending aorta via *en face* analysis, histology of the aortic roots, and RT-qPCR of inflammatory markers. In addition, to evaluate the possible contribution of TLR4 in atherosclerosis, bone marrow transplants were performed by grafting WT and BT bone marrow (n=2-4) to both b6 and TLR4<sup>-/-</sup> mice, and atherosclerosis was performed as described in our LT model. In our ST model, aortic *en face* analysis revealed elevated plaque accumulation in BT mice (WT: 22 ± 4% plaque area vs. Thal: 45 ± 11% plaque area, p = .024). Aortic root (H&E) analysis did not display a significant difference in our ST model, but it was significantly increased in the LT model. Gene expression profiling indicated a significant increase in both IL-6 and CD-68 (p<0.041) in BT mice. In our BMT experiments, we saw a significant decrease in aortic root plaque in TLR4<sup>-/-</sup> mice with Thal BM (.24 ± .06 mm<sup>2</sup>) compared to wild type mice with Thal BM (.39 ± .07 mm<sup>2</sup>). Our data demonstrate for the first time that the underlying pathophysiology of BT clearly leads to accelerated atherosclerosis and suggest TLR4 is playing a role in atherosclerotic development in BT.

**J.Hurtado:** None. **H.Sellak:** None. **D.R.Archer:** Other; Modest; Global Blood Therapeutics, Research Grant; Significant; Global Blood Therapeutics. **W.R.Taylor:** n/a.

## Mitochondrial Inducing Factor 1 Affects Stabilization Of Advanced Atherosclerotic Lesions In Carotid Artery Disease

**Lukas Bischoff**, Technische Univ München, München, Germany; Jessica Pauli, NONE, 80802 Munich; Valentina Paloschi, TECHNICAL UNIVERSITY MUNICH, Munich; Lars Maegdefessel, TECHNICAL UNIVERSITY MUNICH, Munich, Munich

Whereas cerebrovascular diseases, most and foremost ischemic events, being the second most deadliest disease as of today in the western world the process behind carotid artery plaque (CAP) vulnerability remains understood insufficiently. Through proteomic analysis of blood serum from patients treated for atherosclerotic lesions in carotid arteries we were able to determine proteins of potential relevance to CAP stability. One of the identified targets is mitochondrial apoptosis inducing factor 1 (AIFM1), which we found upregulated in serum profiles from patients with vulnerable atherosclerotic lesions. The study were conducted with human vascular tissue and blood samples from the 'Munich Vascular Biobank'. Proteomic profiling of serum was performed using the platform OLink (Uppsala, Sweden) taken from patients with either stable (n=53) or unstable (n=53) CAPs. Furthermore, gene expression of AIFM1 in stable (n=5) and unstable (n=3) CAPs was assessed via RT-qPCR. Via Immunostaining the regions showing higher expression of AIFM1 within the plaques (n=10) were determined and put in perspective with markers of cell types predominantly accumulated in those regions. In addition, blood monocyte-derived macrophages were stimulated with different factors and changes in expression of AIFM1 was assessed. With the proteomic sequencing of blood sera, higher levels of AIFM1 in patients with unstable versus stable CAP were determined. This trend was also seen assessing the gene expression of AIFM1 in the human vascular tissue. A significant enrichment of staining of AIFM1 positivity was observed in regions where apoptosis occurred, such as the necrotic core and the shoulder regions of the advanced CAP. Furthermore, AIFM1 enriched

regions were identified as areas infiltrated by immune cells, especially macrophages. Monocytes of healthy donors showed an increased expression of AIFM1 when developed into macrophages. In conclusion AIFM1 was identified as a potential novel marker for advanced, unstable lesions in CAPs. Future studies (in vitro and in vivo) will reveal which role AIFM1 might play during processes that trigger CAP destabilization. Of further importance will be cell type expression patterns that we are also assessing in currently ongoing studies.

**L.Bischoff:** None. **J.Pauli:** None. **V.Paloschi:** None. **L.Maegdefessel:** None.

---

#### MP19

New Insight Into The Optimal Duration Of DAPT Following PCI In High-risk Twilight-like Patients With Acute Coronary Syndrome

**Haoyu Wang,** Kefei Dou, Fuwai Hosp, Chinese Acad of Medical Sciences & Peking Union Medical Coll, Beijing, China

**Introduction:** Recent emphasis on shorter DAPT regimen after PCI irrespective of indication for PCI may fail to account for the substantial residual risk of recurrent atherothrombotic events in ACS patients. We aim to determine the association of extended-term (>12-month) vs. short-term dual antiplatelet therapy (DAPT) with ischemic and hemorrhagic events in high-risk "TWILIGHT-like" patients undergoing PCI for ACS in clinical practice.

**Methods:** All consecutive patients fulfilling the "TWILIGHT-like" criteria undergoing PCI were identified from the prospective Fuwai PCI Registry. High-risk patients (n=5,404) were defined by at least 1 clinical and 1 angiographic feature based on TWILIGHT trial selection criteria. The primary ischemic endpoint was major adverse cardiac and cerebrovascular events at 30 months, composed of all-cause mortality, myocardial infarction, or stroke while BARC type 2, 3, or 5 bleeding was key secondary outcome.

**Results:** The proportion of patients with 1-3, 4-5, or 6-9 risk factors was 19.7%, 58.6%, and 21.6%, respectively. Cessation of DAPT was less frequent in patients with ACS at 12 months (31.6% versus 68.4%), with 22.7% of ACS patients still on DAPT beyond 24 months. Of 4,875 high-risk ACS patients who remained event-free at 12 months after PCI, DAPT>12-month compared with shorter DAPT reduced the primary ischemic endpoint by 63% (1.5% vs. 3.8%; HRadj: 0.374, 95% CI: 0.256 to 0.548; HRmatched: 0.361, 95% CI: 0.221-0.590). The HR for cardiovascular death was 0.049 (0.007 to 0.362) and that for MI 0.45 (0.153 to 1.320) and definite/probable stent thrombosis 0.296 (0.080-1.095) in propensity-matched analyses. Rates of BARC type 2, 3, or 5 bleeding (0.9% vs. 1.3%; HRadj: 0.668 [0.379 to 1.178]; HRmatched: 0.721 [0.369-1.410]) did not differ significantly between two groups.

**Conclusions:** Among high-risk ACS patients undergoing PCI, long-term DAPT, compared with shorter DAPT, reduced ischemic events without a concomitant increase in clinically meaning bleeding events, suggesting that long-term DAPT can be considered in patients with ACS following PCI who are carefully assessed to be at low bleeding risk and heightened ischemic risk, and have tolerated antiplatelet therapy without a major bleeding during 1 year of DAPT.

**H.Wang:** None. **K.Dou:** n/a.

---

#### MP20

Pd-1 Pathway Upregulation By Orchiectomy Attenuates The Aldosterone And High Salt Induced Aortic Aneurysms In Male Mice

**Xufang Mu,** Univ of Kentucky, Lexington, KY; Shu Liu, UNIV OF KENTUCKY, Lexington, KY; Timothy McClintock, Arnold Stromberg, Alejandro Villasante-Tezanos, Ming C Gong, Univ of Kentucky, Lexington, KY; Zhenheng Guo, UNIV OF KENTUCKY, Lexington, KY

**Ø Objective** - Male sex is a well-established risk factor for abdominal aortic aneurysms (AAA) but the underlying mechanisms remain to be fully understood. Using an aldosterone and high salt (Aldo/salt) induced AAA mouse model, we have demonstrated that androgen and its receptor mediate the high susceptibility to Aldo/salt induced AAA. The current study further investigates the mechanisms downstream of androgen. **Ø Approaches and Results** - To dissect the mechanisms connecting androgen and AAA, aortas were collected for RNA sequencing from 3 groups of 10-month-old wild-type mice #1 intact mice; #2 orchiectomized mice; and #3 orchiectomized mice plus DHT. All mice were given Aldo/salt

for 7 days. Differentially expressed genes were analyzed using DESeq2 in R. We filtered genes that were upregulated in group #2 compared to group #1 and the up-regulation was reversed in group #3 by the DHT, or vice versa (fold change >1.5 and padj <0.05). Selected genes were run for gene ontology analysis in Enrichr (database Bioplane 2019). Many pathways related to T cell activity were significantly enriched, particularly PD-1 signaling was one of the top pathways upregulated in orchietomy group #2. PD-1 is known for its role as an immune checkpoint, and inflammation is a major hallmark for AAA development. Therefore to explore the role of PD-1, we first confirmed the PD-1 mRNA changes in aorta by qPCR. Secondly, IHC staining also showed PD-1 protein was significantly increased in the spleen of orchietomized mice compared to intact controls. Finally, to investigate the potential causal role of PD-1 in the androgen-mediated aortic aneurysms formation, we injected  $\alpha$ PD-1 antibody or control IgG antibody to orchietomized mice 3 days before and during the 8 weeks of Aldo/salt administration. Results showed that 5 out of 12  $\alpha$ PD-1 mice, while none of the 8 control mice developed aortic aneurysms ( $p < 0.05$ ).  
**Ø Conclusions** - PD-1 pathway is involved in the androgen associated high susceptibility of Aldo/salt induced aortic aneurysms in mice.

**X. Mu:** None. **S. Liu:** None. **Z. Guo:** None.

---

MP21

Transcriptomic Modulation Of Second Heart Field-derived Smooth Muscle Cells In Angiotensin II-infused Mice Promotes Aortopathy

**Hisashi Sawada**, Univ of Kentucky, Lexington, KY; Chen Zhang, Yanming Li, Baylor Coll of Med, Houston, TX; Yuriko Katsumata, Univ of Kentucky, Lexington, KY; Ying H Shen, Scott A Lemaire, BAYLOR COLLEGE MEDICINE, Houston, TX; Hong S Lu, UNIVERSITY KENTUCKY, Lexington, KY; Alan Daugherty, UNIVERSITY OF KENTUCKY, Lexington, KY

**Objective:** Smooth muscle cells (SMCs) in the ascending aorta are derived from both the cardiac neural crest and second heart field (SHF). The importance of cardiac neural crest-derived SMCs on development of thoracic aortic aneurysms has been reported, while functional roles of SHF-derived SMCs are controversial. The aim of this study was to profile the transcriptome of SHF-derived SMCs in ascending aortas of angiotensin II (AngII)-infused mice by single cell RNA sequencing.

**Methods and Results:** Female ROSA26 mT/mG mice were bred to male mice expressing Cre under the control of the Mef2c promoter (Mef2c Cre). Angiotensin II (AngII, 1,000 ng/kg/day) was infused subcutaneously into Mef2c Cre +/- mice and ascending aortas were harvested at day 3 of AngII infusion ( $n=5$ ). Ascending aortas without AngII infusion were harvested as control ( $n=4$ ). SHF-derived cells were sorted based on mGFP signal by FACS and single cell sequencing was performed using SHF-derived cells. Single cell RNA sequencing detected mRNA in multiple cell types, and AngII altered mRNA abundance of 3,658 genes in the SMC cluster. Several SMC contractile-related genes, such as *Acta2*, *Tagln* and *Cnn1*, were increased by AngII compared to control SHF-derived SMCs. Conversely, *Klf4*, a proliferative gene, was decreased in SHF-derived SMCs of AngII-infused mice. In addition, AngII increased multiple extracellular matrix component genes, including fibrillin1 and elastin. AngII also upregulated *Serpine1* and  *that are important for extracellular matrix organization. Thus, AngII led to transcriptomic modulations in SHF-derived SMCs. Of note, AngII infusion decreased mRNA abundance of *Tgfb2* and *Lrp1*, key regulators of extracellular matrix maturation, in SHF-derived SMCs. To further investigate the importance of SHF-derived SMCs, we deleted either *Tgfb2* or *Lrp1* in SHF-derived cells. SHF-specific *Tgfb2* deletion was embryonic lethal with peritoneal hemorrhage and outflow tract dilatation. SHF-specific *Lrp1* deletion augmented AngII-induced thoracic aortic rupture and dilatations.*

**Conclusion:** SHF-derived SMCs play an important role in maintaining aortic integrity, and exhibit transcriptomic modulations by AngII infusion that may contribute to aortopathies.

**H. Sawada:** None. **C. Zhang:** None. **Y. Li:** None. **Y. Katsumata:** None. **Y.H. Shen:** None. **S.A. Lemaire:** Other; Modest; Biom'up, Acer Therapeutics, Terumo Aortic. Other Research Support; Modest; Terumo Aortic, CytoSorbants, W.L. Gore & Associates. **H.S. Lu:** None. **A. Daugherty:** None.

## Effect Of Nanoparticle Size And Dose On Detection Of Aortic Injury Using Nanoparticle Contrast-enhanced Computed Tomography

**Laxman Devkota**, Chen Zhang, Prajwal Bhandari, Baylor Coll of Med, Houston, TX; Zbigniew Starosolski, Texas Children's Hosp, Houston, TX; Ying H Shen, Scott A Lemaire, Ketan Ghaghada, Baylor Coll of Med, Houston, TX

**Background:** Early detection and prediction of disease progression are critical for improving outcomes in patients with aortic aneurysms and dissections (AAD). Recently, we reported that nanoparticle contrast-enhanced computed tomography (n-CECT) enables early detection of aortic injury before vessel enlargement is evident on CT angiography. In this work, we investigated the effect of nanoparticle contrast agent (NPCA) size and dose on detection of aortic injury. Additionally, we performed a longitudinal study to examine long-term fate of intramural NPCA. **Methods:** In a mouse model of sporadic AAD, mice (n=8/group) were challenged with high fat diet for 5 weeks and angiotensin-II infusion during the last week. Animals were intravenously administered one of three NPCA size variants (80, 150 and 250 nm). For dose effect study, 150 nm NPCA variant was tested at 3 dose levels: 300, 600 and 1200 mg I/kg. *In vivo* n-CECT was performed after 4 days. *Ex vivo* n-CECT and gross examination were performed on excised aortas. To study intramural fate of NPCA, a subset of animals underwent longitudinal CT imaging for up to 6 months. **Results:** All NPCA size variants showed a higher incidence of n-CECT findings compared to gross aortic examination: absolute improvements in detection rates were 12% for 80 nm, 28% for 150 nm, and 8% for 250 nm. NPCA dose analysis showed that sensitivity of n-CECT for detection of aortic injury improved with increasing dose level (33% for 300 mg I/kg, 44% for 600 mg/kg, and 62% for 1200 mg I/kg) (Figure 1). Longitudinal imaging demonstrated clearance of a majority of intramural NPCA that accumulated at sites of aortic pathology by 4 months. Furthermore, n-CECT imaging enabled monitoring of vascular permeability changes at sites of aortic injury. **Conclusion:** Regardless of NPCA size, n-CECT imaging showed higher sensitivity for early detection of aortic degeneration compared to gross aortic examination. Detection of aortic injury improved with increasing NPCA dose.

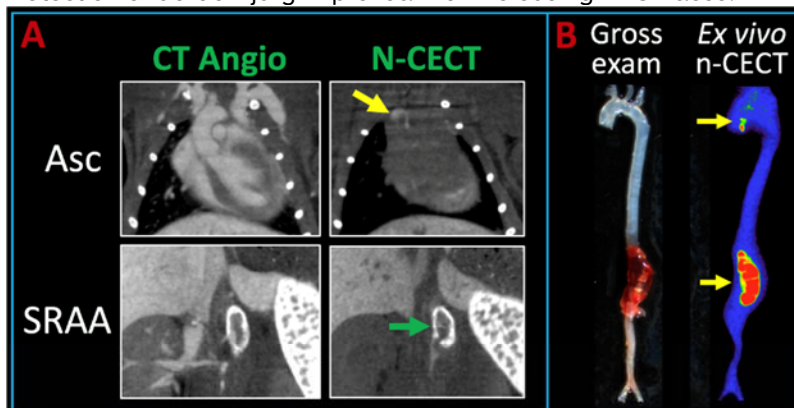


**Figure 1. N-CECT imaging of aortic injury.** (A) *In vivo* n-CECT shows mild signal enhancement (yellow arrow) in ascending aorta (Asc) that appears normal on CT angiography. High signal enhancement (green arrow) is seen in suprarenal abdominal aorta (SRAA) in n-CECT imaging, indicative of severe aortic disease. (B) Gross exam shows no findings in ascending aorta; however, *ex vivo* n-CECT of excised aorta confirms signal enhancement, indicative of mild aortic injury. Gross aortic exam shows severe disease in SRAA that correlates with high signal intensity in n-CECT imaging. N-CECT images were acquired using a 150 nm NPCA size variant and 1200 mg I/kg dose.

**L.Devkota:** None. **C.Zhang:** None. **P.Bhandari:** None. **Z.Starosolski:** Other; Modest; InContext.ai, Stock Shareholder; Modest; Alzeca Biosciences, Inc.. **Y.H.Shen:** None. **S.A.Lemaire:** Other; Modest; Biom'up, Acer Therapeutics, Terumo Aortic, Other Research Support; Modest; Terumo Aortic, CytoSorbants, W.L. Gore & Associates. **K.Ghaghada:** Other; Significant; Alzeca Biosciences Inc..

Knockout Of Pgc1 $\alpha$  In Endothelial Cells Augments Abdominal Aortic Aneurysm Formation

Timothy F Fernandez, Hassan Sellak, Bernard P Lassegue, William R Taylor, Emory Univ, Atlanta, GA

**Introduction:** It is well described that changes in the aortic media are crucial in the development of Abdominal Aortic Aneurysms (AAA), however the involvement of the endothelium is not as clear. The endothelium is the first vascular layer exposed to blood flow and aneurysms preferentially form in areas of disturbed flow. The regulatory mechanisms as to why aneurysms form at these sites remains unclear. Here we propose that the transcription coactivator peroxisome proliferator-activated receptor gamma coactivator 1- $\alpha$  (PGC1 $\alpha$ ) plays a pivotal role in the endothelium's response to AAA formation in a shear responsive manner. **Methods:** 10-12 week old male mice deficient in endothelial specific PGC1 $\alpha$  (KO) and their corresponding wild type background mice (WT) were treated with 0.75 mg/kg/day of Ang II. Our primary endpoints were measurement of the maximal width of the suprarenal aortas, frequency, and complexity based on the Daugherty classification. To determine the effects of shear, HAECs exposed to steady flow (15 dyn/cm<sup>2</sup>) and disturbed flow (0 $\pm$ 6 dyn/cm<sup>2</sup> at 1 Hz) for 12 hours were compared to determine if mRNA expression were different for PGC1 $\alpha$  and SIRT1. **Results:** AAA incidence and severity were increased in ANG II-infused KO compared to the WT mice (100% vs. 20%, respectively). Measurements of excised aortas showed that KO mice exhibited larger AAA fold-increase compared to WT (2.00  $\pm$  0.11 fold increase vs. 0.43  $\pm$  0.19 fold increase, p-value 0.0002). The KO male mice also exhibited a more complex phenotype. HAECs that underwent disturbed flow had a significant decrease in expression of SIRT1 (p = 0.02) and trended towards a decrease in expression of PGC1 $\alpha$  (p = 0.06). **Conclusions:** Our data strongly suggests that knockout of endothelial specific PGC1 $\alpha$  leads to more frequent, complex and larger AAAs primarily in the suprarenal aorta, which is an area of disturbed flow. Interestingly, the addition of ANG II alone was able to induce AAA formation in our model. Additionally, we show that PGC1 $\alpha$  and SIRT1 are regulated in a shear responsive manner. Taken together, endothelial PGC1 $\alpha$  likely plays a regulatory role in AAA formation through shear-related mechanisms.

**T.F.Fernandez:** None. **H.Sellak:** None. **B.P.Lassegue:** Research Grant; Significant; NIH. **W.R.Taylor:** Research Grant; Significant; NIH.

## Disruption Of Actin Remodeling Intensifies Aneurysm-promoting Signals In Smooth Muscle Cells

Zhihua Jiang, Fen Wang, Univ of Florida, Gainesville, FL; Gilbert R Upchurch Jr., Univ of FL Dept of Surgery, Gainesville, FL

Mutations within proteins coding for extracellular matrix assembly or those in the transforming growth factor beta (TGF $\beta$ ) signaling pathway lead to aneurysm formation in patients and mice. As the SMC cytoskeletal network is intricately linked to TGF $\beta$  and ECM signaling, we sought to determine if disruption of the cytoskeletal filaments would alter how SMCs respond to angiotensin II, an important mediator of aneurysm formation.

C57BL/6 mice lacking *Tgbr1* in SMCs (SMC- *Tgbr1*<sup>iko</sup>) generated by Jiang et al. have been shown to develop rapid and severe aortic aneurysm degeneration with 100% penetrance. Analysis was conducted on aneurysm and control mouse and human aortic tissue sections. We observed that SMC- *Tgbr1*<sup>iko</sup> mice had reduced expression of filamentous (f-) and  $\alpha$ -actin protein in the aortic media than control mice.

Primary *Tgbr1*<sup>iko</sup> SMCs also had higher levels of pRelA expression, less  $\alpha$ -actin mRNA, and less f-actin than control SMCs. Tissue sections from aneurysm patients had reduced f-actin staining relative to controls. Disruption of f-actin with the destabilizer latrunculin A *in vitro* led to increased RelA and ERK activation in the presence of AngII, which was further augmented in the presence of a neutralizing antibody for TGF $\beta$ . In contrast, jasplakinolide—an f-actin stabilizer—prevented TGF $\beta$  blockade induced pRelA expression, suggesting that altered/inhibited TGF $\beta$  signaling modulates NF $\kappa$ B through actin depolymerization. While stabilization and disruption of microtubules led to RelA activation, no effect was observed on TGF $\beta$  blockade-induced pRelA expression. The phosphoantibody array revealed that f-actin disruption in the presence of AngII activated the CREB, AKT1/2/3, ERK1/2, and STAT3 pathways in mouse aortic SMCs. SMC- *Tgbr1*<sup>iko</sup> mice treated with cytochalasin B suffered significantly greater mortality and had increased aortic growth over a 30-day follow-up period.

Aortic aneurysms are coincident with reduced f-actin expression in murine and human aortic SMCs.

Chemical deconstruction of actin filaments promotes an inflammatory phenotype in mouse SMCs *in vitro*, and aggravates aneurysm formation *in vivo*. Aberrant or inhibited TGFβ signaling potentiates NFκB activation in SMCs, which may be dependent on f-actin disassembly.

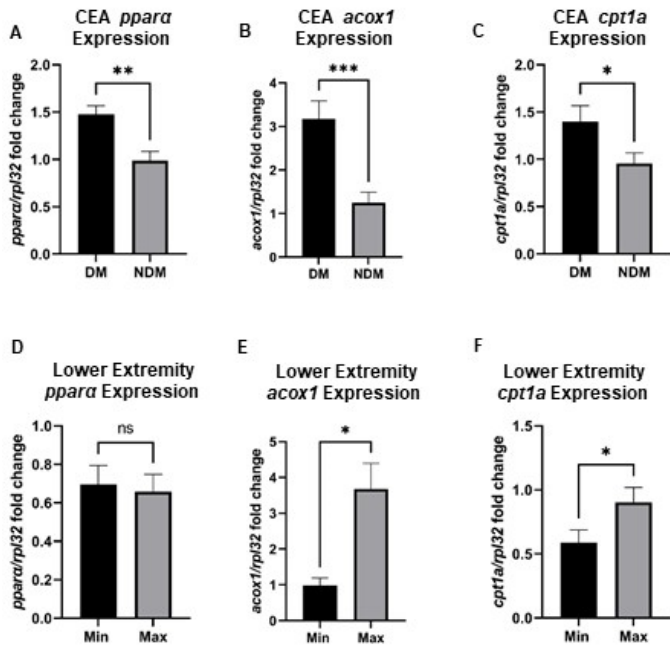
**Z.Jiang:** None. **F.Wang:** None. **G.R.Upchurch:** None.

MP25

Differential Expression Of Ppara In Peripheral Arterial Segments Of Patients With Advanced Atherosclerosis

**connor engel**, Washington Univ in St. Louis, St. Louis, MO; Nikolai Harroun, Amanda Penrose, Mehreen Shafqat, Rodrigo Meade, Xiaohua Jin, Gayan DeSilva, Washington Univ in St. Louis, St. Louis, MO; Clay F Semenkovich, WASHINGTON UNIVERSITY, Saint Louis, MO; Mohamed Zayed, Washington Univ in St. Louis, St. Louis, MO

Peripheral atherosclerosis manifests in both the extracranial carotid and lower extremity arteries and can lead to significant morbidity and mortality. However, atherosclerotic disease progression is often not homogenous and is accelerated by diabetes. We previously observed altered phospholipidomic profiles between minimally (MIN) and maximally (MAX) diseased peripheral arterial segments. Since Peroxisome Proliferator-Activated Receptor alpha (*ppara*) is a key regulator of lipid metabolism, we hypothesized that it may have variable content and signaling in MIN and MAX diseased arterial segments. To test our hypothesis, 12 patients who underwent carotid endarterectomy (CEA), and 19 patients who underwent major lower extremity amputation were recruited. MIN and MAX disease segments were obtained in real time from the operating room from CEA plaque and arterial segments from amputated lower extremities. mRNA was isolated from all specimens and relative content of *ppara*, Acyl-CoA Oxidase 1 (*acox1*), and Carnitine Palmitoyltransferase 1A (*cpt1a*) were evaluated. We observed significantly higher *ppara* expression in CEA segments in patients with diabetes ( $p < 0.01$ ), as well as higher *acox1* ( $p < 0.001$ ) and *cpt1a* ( $p < 0.05$ ) expression (A-C). Hemoglobin A1C had a significant correlation with *ppara* gene expression. There was no significant difference in gene expression between MAX and MIN diseased CEA plaque segments. Interestingly, we observed that in lower extremity arterial segments there was no difference in *ppara*, *acox1*, and *cpt1a* in patients with and without diabetes, but downstream genes were significantly increased in MAX diseased arterial segments (D-F). This study demonstrates the variable expression pattern of *ppara* and its downstream genes in human peripheral arteries. Our findings suggest variable gene expression in different peripheral arterial beds, which may have an impact on mechanisms of disease progression and pharmacologic targeting.



**C.Engel:** None. **N.Harroun:** n/a. **A.Penrose:** None. **M.Shafqat:** None. **R.Meade:** None. **X.Jin:** None. **G.Desilva:** n/a. **C.F.Semenkovich:** None. **M.Zayed:** n/a.

### Activating P2Y<sub>1</sub> Receptors Improves Function In Arteries With Repressed Autophagy

**Jae Cho**, Seul-Ki Park, Univ of Utah, Salt Lake Cty, UT; Oh Sung Kwon, Univ of Connecticut, Storrs, CT; D. Taylor La Salle, James Cerbie, Caitlin C. Fermoye, David Morgan, Ashley Nelson, Amber Bledsoe, Leena P Bharath, Megan Tandar, Univ of Utah, Salt Lake Cty, UT; Satya P Kunapuli, TEMPLE UNIVERSITY SCHOOL MEDIC, Philadelphia, PA; Russ Richardson, Univ of Utah, Salt Lake City, UT; Pon Velayutham Anandh Babu, Sohom Mookherjee, Univ of Utah, Salt Lake Cty, UT; Bellamkonda K Kishore, VA Medical Ctr, Salt Lake City, UT; Fei Wang, Univ of Utah, Salt Lake City, UT; Tianxin Yang, UNIVERSITY UTAH, Salt Lake City, UT; Sihem Boudina, Joel D Trinity, J David D Symons, Univ of Utah, Salt Lake Cty, UT

**Objective.** The importance of endothelial cell (EC) autophagy to vascular homeostasis is evolving. Earlier we reported that purinergic P2Y<sub>1</sub> receptor (P2Y<sub>1</sub>-R) activation rejuvenates shear-stress induced nitric oxide (NO) generation in bovine aortic endothelial cells that is otherwise compromised after pharmacological and genetic autophagy repression. Here we determined the translational and functional relevance of these findings. **Approach and Results.** First we assessed translational relevance using older humans and mice that exhibit blunted EC autophagy at rest together with impaired arterial function vs. appropriate controls. Rhythmic handgrip exercise elevated radial artery shear rate similarly in adult and older males for 60-min. Compared to baseline, autophagy initiation, p-eNOS<sup>S1177</sup> activation, and NO generation, occurred in radial artery ECs from adult but not older subjects. Regarding mice, indexes of autophagy and p-eNOS<sup>S1177</sup> activation were robust in ECs from adult but not older mice in response to 60-min treadmill-running. Next we questioned whether an inability to initiate EC autophagy precipitates arterial dysfunction. Age-associated reductions in intraluminal flow-mediated vasodilation observed in older vs. adult mice were recapitulated in arteries from adult mice by : (i) NO synthase inhibition; (ii) autophagy impairment using 3-methyladenine (3-MA); (iii) EC Atg3 depletion (iecAtg3KO mice); (iv) P2Y<sub>1</sub>-R blockade; and (v) germline depletion of P2Y<sub>1</sub>-Rs. Importantly, P2Y<sub>1</sub>-R activation using 2-methylthio-ADP (2-Me-ADP) improved vasodilatory capacity in arteries from : (i) adult mice treated with 3-MA; (ii) adult iecAtg3KO mice; and (iii) older animals with repressed EC autophagy. **Conclusions.** Arterial dysfunction concurrent with pharmacological, genetic, and age-associated EC autophagy compromise is improved by activating P2Y<sub>1</sub>-Rs.

**J.Cho:** n/a. **L.P.bharath:** n/a. **M.Tandar:** n/a. **S.P.Kunapuli:** n/a. **R.Richardson:** n/a. **P.Anandh babu:** n/a. **S.Mookherjee:** n/a. **B.K.Kishore:** n/a. **F.Wang:** n/a. **T.Yang:** None. **S.Boudina:** n/a. **S.Park:** n/a. **J.Trinity:** n/a. **J.D.Symons:** None. **O.Kwon:** None. **D.La salle:** n/a. **J.Cerbie:** n/a. **C.Fermoye:** n/a. **D.Morgan:** n/a. **A.Nelson:** n/a. **A.Bledsoe:** n/a.

### Endothelial Nogo-B Modulates Ischemia Induced Collateral Artery Remodeling

Cheng Zhang, Temple Univ, Philadelphia, PA; Yuanyuan Zhang, Jennifer Lucitti, Yale Univ Sch of Med,, New Haven, CT; Andrea Palos-Jasso, TEMPLE UNIVERSITY Lewis Katz Sch of Med, Philadelphia, PA; Sebastian Albinsson, Yuan Gao, Yale Univ Sch of Med, New Haven, CT; Yaru Cui, TEMPLE UNIVERSITY Lewis Katz Sch of Med, Philadelphia, PA; Takahisa Murata, Yale Univ Sch of Med, New Haven, CT; James E Faber, UNIVERSITY NORTH CAROLINA, Chapel Hill, NC; William C Sessa, YALE UNIVERSITY SCHOOL MEDICINE, New Haven, CT; **Jun Yu**, TEMPLE UNIVERSITY Lewis Katz Sch of Med, Philadelphia, PA

Nogo-B, a member of the reticulon 4 family of proteins, is the dominant isoform expressed in endothelial cells (EC). We have shown that Nogo-B is necessary for blood flow recovery in ischemia. Mice lacking Nogo-B exhibit reduced arteriogenesis and angiogenesis that are linked to a decrease in macrophage infiltration and inflammatory gene expression in vivo. However, whether endothelial Nogo-B regulates arteriogenesis and/or angiogenesis is unknown. We generated an inducible EC-specific mouse overexpressing Nogo-B (Ng<sup>ECtg</sup>) and investigated the arteriogenesis and angiogenesis in limb ischemia. Ischemia increased endothelial and serum Nogo-B expression. Blood flow recovery was markedly diminished after femoral artery ligation (FAL) in Ng<sup>ECtg</sup> compared to WT mice, in association with lower collateral density accessed by micro-CT arteriography. There was no reduction in capillary density or decrease in smooth muscle/pericyte and macrophage recruitment in Ng<sup>ECtg</sup> mice, suggesting EC Nogo-B overexpression regulates arteriogenesis but not angiogenesis. While Ng<sup>ECtg</sup> mice have normal number of native collateral artery, the early remodeling of the collateral artery was impaired after

ischemia. Furthermore, in line with impaired remodeling, Ng<sup>ECtg</sup> mice have decreased functional (exercise) hyperemia response in the non-ischemic limb in vivo, and resistant arteries from Ng<sup>ECtg</sup> have diminished flow induced vasodilatation ex vivo compared to WT mice. Moreover, endothelial reconstitution of Nogo-B in global Nogo knockout background (NogoKO<sup>ECrc</sup>) restored blood flow recovery after ischemia in vivo, further suggesting the EC specific function of Nogo-B in arteriogenesis. Mechanistically, we have shown that EC isolated from Ng<sup>ECtg</sup> mice have decreased nitric oxide release. Nogo-B overexpression negatively regulates eNOS phosphorylation, expression and golgi localization in EC. Future parabiosis study is warranted to elucidate the contribution of paracrine or EC intrinsic Nogo-B in modulating arteriogenesis and angiogenesis. In conclusion, our data showed for the first time that endothelial Nogo-B plays important roles in regulating collateral artery remodeling and blood flow through, at least in part, regulating NO bioavailability.

**C. Zhang:** None. **A. Palos-Jasso:** None. **W.C. Sessa:** None. **J. Yu:** None.

---

MP28

The Bet Bromodomain Inhibitor, (+)-JQ1, Inhibits Neointima Formation Following Acute Vascular Injury Via Pten Upregulation

**Keith Strand**, Univ of Colorado-Anschutz, Aurora, CO; Sizhao Lu, UNIVERSITY OF COLORADO DENVER, Aurora, CO; Marie Mutryn, Univ of Colorado Anschutz, Aurora, CO; Allison Dubner, Univ of Colorado, Aurora, CO; Austin Jolly, Univ of Colorado Anschutz, Aurora, CO; Raphael Nemenoff, Univ of Colorado Anschutz, Aurora, CO, Aurora, CO; Maria A Cavasin, Univ of Colorado, Aurora, CO; Timothy A McKinsey, UNIVERSITY OF COLORADO DENVER, Aurora, CO; Mary C Weiser Evans, UNIV COLORADO ANSCHUTZ MEDICAL CAMP, Aurora, CO

The primary aim of this work was to identify compounds that upregulate phosphatase and tensin homolog (PTEN) expression in smooth muscle cells (SMCs), with the expectation that PTEN upregulation would inhibit pathological vascular remodeling by promoting SMC homeostasis. Our recent work demonstrated that PTEN is an important regulator of SMC phenotype. SMC-specific PTEN deletion promotes spontaneous vascular remodeling and PTEN loss correlates with increased atherosclerotic lesion severity in human coronary arteries. In mice, PTEN overexpression reduces plaque area and preserves SMC contractile protein expression in atherosclerosis and blunts Angiotensin-II-induced pathological vascular remodeling, suggesting that pharmacologic PTEN upregulation could be a novel therapeutic approach to treat vascular disease. Currently, there are few known pharmacologic inducers of PTEN, however, we have shown that (+)-JQ1, which targets the epigenetic reader protein, Brd4, directly activates the PTEN promoter to drive PTEN expression. Mechanistically, our findings suggest that Brd4 inhibition results in p300-mediated hyper-acetylation of the PTEN promoter to increase PTEN transcriptional activity. Administration of (+)-JQ1 or SMC-specific Brd4 deletion inhibited neointima formation following acute carotid artery injury in mice. Using SMC-specific PTEN depletion both in vitro and in vivo, we showed that the observed anti-remodeling, anti-inflammatory effects were PTEN-dependent. Furthermore, we tested the effects of (+)-JQ1 on macrophage polarization, as systemic drug delivery could potentially modulate the phenotype of other resident vascular cells, including macrophages. We found that (+)-JQ1 inhibited bone marrow-derived macrophage polarization towards a pro-inflammatory phenotype, which is notable because vascular inflammation driven by SMC-macrophage cross-talk is known to promote neointima development. Importantly, our findings may hold direct clinical relevance, as BET bromodomain inhibitors related to (+)-JQ1 are currently undergoing clinical trials. These results are significant because they indicate that targeting PTEN upregulation in SMCs is a completely novel approach to inhibit vascular remodeling.

**K.Strand:** None. **S.Lu:** None. **M.Mutryn:** None. **A.Dubner:** Research Grant; Significant; CCTSI grant TL1TR002533--Predoctoral Fellowship. **A.Jolly:** None. **R.Nemenoff:** None. **M.A.Cavasin:** None. **T.A.Mckinsey:** Other Research Support; Modest; Italfarmaco. **M.C.Weiser evans:** None.



### Skeletal Muscle Satellite Cells Enhance Vascular Growth Through Paracrine Signaling

Giji Joseph, Emory Univ, Atlanta, GA; Tao Yu, Sophia Mavris, EMORY UNIVERSITY, Atlanta, GA; W. Robert R Taylor, EMORY UNIVERSITY SCHOOL OF MEDICINE, Atlanta, GA; **Laura M Hansen**, EMORY UNIVERSITY, Atlanta, GA

Peripheral arterial disease (PAD) is a major health problem that affects over 200 million people worldwide. Decreased blood flow to the limb muscles leads to ischemia that results in pain, decreased quality of life, and in severe cases amputation. Despite the prevalence and severity of the disease, effective treatment options are still limited. One factor correlated with improved prognosis is the generation of a more robust collateral vessel network. This study hypothesized that skeletal muscle satellite cells, which play a key role in skeletal muscle regeneration, also contribute to vascular regeneration in the setting of ischemia. Specifically, satellite cells are proposed to generate cytokine and growth factors which modulate vascular growth via paracrine signaling. Satellite cells were isolated and cultured for vasculogenic assays include migration co-cultures. Satellite cells encapsulated in alginate were delivered to a hindlimb ischemia model of vascular growth to assess their therapeutic potential in vivo. Gene expression of satellite cells from ischemic tissue was assessed using a microarray. The migration assays demonstrated that satellite cells produce chemokines which increased smooth muscle migration (3.5 fold) and endothelial cell migration (2.8 fold) over control conditions ( $n = 4$ ,  $p < 0.05$ ). In the hind limb ischemia model, alginate encapsulated satellite cells increased perfusion 17% closer to baseline (68% vs 51%,  $n = 11$ ,  $p < 0.05$ ) measured via Laser Doppler imaging. Capillary density as measured by Lectin staining increased 1.6 fold and smooth muscle positive vessels increase more than 2 fold ( $n = 6$ ,  $p < 0.05$ ). Finally, Ingenuity pathway analysis of the gene array data suggested that vasculogenic and cell migration pathways were increased. Taken together, these findings demonstrate that satellite cells produce a number of factors that can serve as chemokines in vitro and increase vascular growth in vivo. Further work will explore the mechanisms by which satellite cells exhibit their effects and develop a therapeutic application of satellite cells as a novel treatment for patients with peripheral artery disease.

**G.Joseph:** None. **T.Yu:** None. **S.Mavris:** None. **W.R.Taylor:** n/a. **L.M.Hansen:** n/a.

### Excess HDL Free Cholesterol Bioavailability Drives Free Cholesterol Accretion Into Macrophages And Erythrocytes In Scarb1<sup>-/-</sup> Mice

Jing Liu, **Baiba K Gillard**, Houston Methodist Res Inst, Houston, TX; Dedipya Yelamanchili, Houston Methodist Res Inst, HOUSTON, TX; Ziyi Wang, Houston Methodist Res Inst, Houston, TX; Antonio M Gotto Jr, Weill Cornell Med, New York, NY; Corina Rosales, Henry J Pownall, Houston Methodist Res Inst, Houston, TX

**Aim:** In humans, very high plasma HDL-cholesterol concentrations are associated with increased all cause- and atherosclerotic cardiovascular disease (ASCVD)-mortality. The HDL receptor-deficient mouse (Scarb1<sup>-/-</sup>), a robust model of this phenotype, is characterized by high free cholesterol (FC) bioavailability due to too many HDL particles that are FC-rich. Clinically, plasma LDL and HDL are quantified according to total cholesterol content, the sum of FC and esterified cholesterol, which likely contribute to ASCVD pathophysiology differently. A Western diet induces ASCVD in Scarb1<sup>-/-</sup> mice, despite an attendant increase in HDL. We tested the hypothesis that high HDL-FC bioavailability contributes to ASCVD in Scarb1<sup>-/-</sup> mice by increasing FC flux into macrophage cells, erythrocytes and other major tissues. **Methods:** Influx of HDL-FC and efflux of macrophage FC were determined between WT and Scarb1<sup>-/-</sup> HDL and J774 macrophage cells. HDL of both genotypes were radiolabelled with [<sup>3</sup>H]FC, injected into autologous mice, and the rates of plasma clearance and erythrocyte uptake were determined. **Results:** The magnitude of FC transfer from Scarb1<sup>-/-</sup> HDL to LDL is greater than that from WT HDL; APOB-containing lipoproteins from Scarb1<sup>-/-</sup> vs. WT mice are FC-enriched due likely to greater HDL-FC transfer. While macrophage efflux to HDL of Scarb1<sup>-/-</sup> vs. WT HDL was not different, FC influx from Scarb1<sup>-/-</sup> vs. WT HDL to macrophages was three-fold greater, a net effect that increased the FC burden of macrophages. In vivo studies showed that compared to WT mice, in Scarb1<sup>-/-</sup> mice, autologous HDL-FC cleared more slowly and more FC transferred to erythrocytes. We compared the FC, CE, PL, and TG contents of all major tissues and determined that FC accretion by some tissues is higher among Scarb1<sup>-/-</sup> vs. WT mice whereas in other tissues FC homeostasis is maintained. Lastly, we determined that the tissue compositions and plasma FC clearance kinetics varied

according to sex, particularly among *Scarb1*<sup>-/-</sup> mice. **Conclusions:** These findings are relevant to pathologies specific to *Scarb1*<sup>-/-</sup> mice and to the evolving model of the role of HDL-FC in RCT. They provide a rationale for human studies to determine the utility of HDL-FC bioavailability as a risk factor for ASCVD and other pathologies.

**J.Liu:** None. **B.K.Gillard:** n/a. **D.Yelamanchili:** None. **Z.Wang:** None. **A.M.Gotto:** Other; Modest; Esperion Therapeutics, Kowa Pharmaceuticals, Akcea Pharmaceuticals, Amarin. **C.Rosales:** None. **H.J.Pownall:** None.

---

MP31

#### Bmal1 Regulates Production Of Larger Lipoproteins By Modulating Crebh And Apolipoprotein A 4

**Xiaoyue Pan,** NYU Long Island Sch of Med, Mineola, NY; **M Mahmood Hussain,** NYU Long Island Sch of Med, Mineola, NY

High plasma lipid and lipoprotein levels are risk factors for various metabolic diseases, such as diabetes, obesity, metabolic syndrome, and atherosclerosis. We previously showed that circadian rhythms regulate plasma lipids, and deregulation of these rhythms cause hyperlipidemia and atherosclerosis in mice. Here, we show that global and liver-specific *Bmal1*-deficient mice maintained on a chow or a Western diet developed hyperlipidemia, which was denoted by the presence of higher amounts of triglyceride- and apoAIV-rich larger chylomicron and very-low-density lipoprotein, due to overproduction. *Bmal1* deficiency decreased *Shp* and increased *MTP*, a key protein that facilitates primordial lipoprotein assembly and secretion. Moreover, we show that *Bmal1* regulates *Crebh* to modulate apoAIV expression and the assembly of larger lipoproteins. This is supported by the observation that *Crebh*- and apoAIV-deficient mice, along with *Bmal1*-deficient mice with knockdown of *Crebh*, had smaller lipoproteins. Further, overexpression of *Bmal1* in *Crebh*-deficient mice had no effect on apoAIV expression and lipoprotein size. These studies indicate that regulation of apoAIV and assembly of larger lipoproteins by *Bmal1* requires *Crebh*. Mechanistic studies showed that *Bmal1* regulates *Crebh* expression by two mechanisms. First, *Bmal1* interacts with the *Crebh* promoter to control circadian regulation. Second, *Bmal1* increases *Rev-erba* expression, and *Rev-erba* interacts with the *Crebh* promoter to repress expression. In short, *Bmal1* modulates both the synthesis of primordial lipoproteins and their subsequent expansion into larger lipoproteins by regulating two different proteins, *MTP* and apoAIV, via two different transcription factors, *Shp* and *Crebh*. It is likely that disruptions in circadian mechanisms contribute to hyperlipidemia, and synchronization of circadian rhythms may limit/prevent hyperlipidemia and atherosclerosis.

**X. Pan:** None. **M.M. Hussain:** None.

---

MP32

#### Diaphanous 1 Regulates Actin Polymerization In Adipocytes: Potential Mechanism Regulating Obesity In Mice

**Henry H Ruiz,** NYU Langone Grossman Sch of Med, New York, NY; **Ann Marie Schmidt,** NY, NY

The underlying pathophysiological mechanisms of obesity, a hallmark of metabolic and cardiovascular diseases, are not fully elucidated. Adipocyte hypertrophy contributes to insulin resistance, and is coupled to meaningful alterations in actin dynamics that favor actin polymerization. Diaphanous 1 (*Diaph1*) is a formin protein that associates with the fast-growing/banded end of actin filaments to regulate actin dynamics. We hypothesized that deletion of *Diaph1* or pharmacological regulation of actin polymerization in the context of lipid surplus would prevent obesity, decrease adipocyte lipid load and protect from obesity-associated metabolic disease. We modeled obesity by feeding wild type (Wt) mice and mice globally or with adipocyte-specific deletion of *Diaph1* a high fat diet (60%kcal from fat). Body composition was assessed by Dual-energy X-ray absorptiometry (DEXA) and dynamic glucose and insulin tolerance testing was performed to assess metabolic state. *In-vitro* studies were carried out in adipocytes differentiated from primary pre-adipocytes or 3T3-L1 fibroblasts. Lipid overload was modeled using a mixture of palmitate/oleate (P/O). Actin manipulations were achieved by pharmacologically preventing (Latrunculin B [LatB]) or promoting (Jasplakinolide [Jasp]) F-actin polymerization. Mice globally devoid of, or with adipocyte specific *Diaph1* deletion were protected from obesity, glucose intolerance and insulin resistance. Wt adipocytes treated with P/O exhibited pronounced accumulation of triglycerides (Tg) which was absent in adipocytes differentiated from *Diaph1* knock out mice. Pharmacological studies in 3T3-L1-

derived adipocytes confirmed the P/O-induced Tg accumulation which was prevented by LatB and exacerbated by Jasp. We present the novel finding that adipocyte DIAPH1 is a major player in the pathophysiology of obesity and associated metabolic sequelae which results, at least in part, from regulation of adipocyte hypertrophy by preventing actin polymerization. Thus, we propose that actin remodeling is an underlying mechanism for adipocyte hypertrophy in obesity and inhibition of DIAPH1 may represent a potential therapeutic target for the treatment of obesity and related metabolic and cardiovascular disorders.

**H.H.Ruiz:** None. **A.Schmidt:** n/a.

---

MP33

#### Coordination Of Metabolic Functions By SR-BI And PCPE2 In Adipocytes

**Darcy A Knaack**, Medical Coll of Wisconsin, Milwaukee, WI; **Mary G Sorci Thomas**, MEDICAL COLLEGE OF WISCONSIN, Milwaukee, WI; **Michael J Thomas**, MEDICAL COLLEGE WISCONSIN, Milwaukee, WI; **Yiliang Chen**, Medical Coll of Wisconsin, Milwaukee, WI; **Daisy Sahoo**, MEDICAL COLLEGE OF WISCONSIN, Milwaukee, WI

Obesity continues to be an epidemic in the United States, placing individuals at a higher risk of developing other comorbidities such as type 2 diabetes and cardiovascular disease. Adipocytes accumulate excess triglycerides and undergo hypertrophic expansion as a protective mechanism to avoid lipotoxicity. Adipocytes are also highly dynamic cells that perform many key metabolic processes including lipid and glucose metabolism. Recent collaborative studies demonstrated that SR-BI function may require the extracellular matrix protein procollagen C-endopeptidase enhancer 2 (PCPE2) in to regulate cholesterol transport in hepatocytes and adipocytes. However, the roles of SR-BI and PCPE2 in other adipocyte metabolic processes remain unclear. This knowledge gap prompted our novel hypothesis that PCPE2 facilitates SR-BI's ability to regulate metabolic processes in adipocytes. To test our hypothesis, we have optimized an adipocyte model system where mesenchymal stem cells isolated from the outer ears of wild-type (WT), SR-BI knockout (SR-BI<sup>-/-</sup>), and PCPE2<sup>-/-</sup> mice were differentiated into adipocyte-like cells. We validated our adipocyte model system by demonstrating increased Oil Red O staining, mRNA expression of adipogenesis markers, and adiponectin secretion over a 9-day post-differentiation period for all three genotypes. This model system was then used to test the roles of SR-BI and PCPE2 on various metabolic functions. Preliminary data suggests that absence of SR-BI or PCPE2 slightly impairs fatty acid uptake into adipocytes despite elevated gene expression of fatty acid transporters (FABP4, CD36) compared to WT. These data further suggest that SR-BI may rely on PCPE2 to aid in transport of fatty acids. Adipocytes lacking SR-BI or PCPE2 also displayed higher levels of mitochondrial reactive oxygen species, indicating that SR-BI and PCPE2 may be important for maintaining healthy mitochondria in adipocytes. These changes in function do not appear to depend on SR-BI oligomerization, as BS<sup>3</sup> crosslinking studies demonstrated the presence of SR-BI oligomers in adipocytes despite the loss of PCPE2. Altogether, these data suggest that SR-BI and PCPE2 may be reliant on each other and are important for mediating metabolic processes in adipocytes.

**D.A.Knaack:** None. **M.G.Sorci thomas:** None. **M.J.Thomas:** n/a. **Y.Chen:** None. **D.Sahoo:** None.

---

MP35

#### Single-cell Analysis Uncovers Multiple Adventitial Fibroblast Populations With Expression Of CAD GWAS Genes In Murine Atherosclerosis

**Hyun-kyung Chang**, Columbia Univ, New York, NY; **Eunyoung Kim**, Fort Lee, NJ; **Muredach P Reilly**, COLUMBIA UNIVERSITY MEDICAL CENTER, New York, NY; **Robert C Bauer**, COLUMBIA UNIVERSITY, New York, NY

The arterial adventitia is a layer of cells outside the external lamina of blood vessels that contribute to the progression of coronary artery disease (CAD) like atherosclerosis. Adventitial fibroblasts are known regulators of vascular remodeling through their deposition of collagen fibrils around vessels during atherosclerotic lesion development. However, the molecular identity and function of the participating fibroblasts have not been well studied. We used single cell RNA sequencing (scRNA-seq) to characterize the transcriptome of adventitial fibroblasts and other cell types at multiple timepoints during atherogenesis in

hyperlipidemic Ldlr knockout mice. Specifically, scRNA-seq was applied to Ldlr KO aortic adventitia after 0, 9, and 16 weeks of western diet (WD) feeding. Unbiased clustering analysis uncovered 9 different cell clusters, including 5 different fibroblast populations (Fibro1-5), and a single cluster each of macrophages, T cells, SMCs, and ECs. We observed that, as atherosclerosis progressed from 9 to 16 weeks of feedings, the proportion of total cells that were Fibro1, 3, and 4 decreased (33, 40, and 13%), while populations of Fibro2 and 5 slightly increased (13 and 18%). All of non-fibroblast populations (Macrophage, T cells, SMCs and ECs) increased from 9-16wks of diet. Next, we asked whether genes associated with coronary artery disease by human genome-wide association studies (GWAS) are expressed in different adventitial fibroblast clusters. We determined the expression of 266 genes implicated in CAD by GWAS and found 201 genes (76%) were expressed in adventitial cells at either/both 9 or 16wks. 34 genes displayed large changes in expression from 9 to 16wks. We identified five genes that were highly expressed in the adventitial Fibro5 cluster specifically, and additional other CAD GWAS genes specifically expressed in adventitial macrophages, SMCs, and ECs. In summary, we present here a cell atlas defined by scRNA-seq that reveals the heterogeneity amongst the fibroblasts in adventitial cells during atherogenesis. Additionally, we find that many CAD GWAS genes are expressed in adventitial cell populations, raising the intriguing possibility that CAD GWAS are identifying adventitial mechanisms that contribute to CAD.

**H. Chang:** None. **E. Kim:** None. **M.P. Reilly:** None. **R.C. Bauer:** None.

---

MP37

Effect Of Sex Dimorphism And Pregnancy On Innate Lymphoid Cells Expressing Elabela

**Evila Da Silva Lopes Salle,** Hesam Khodadadi, Liezl Domingo, Augusta Univ, Augusta, GA; Bruno Zavan, Federal Univ of Alfenas, Alfenas, Brazil; Jack Yu, Babak Baban, Augusta Univ, Augusta, GA

Elabela is an endogenous secreted peptide and its role has been investigated in heart and preeclampsia development. Endogenous peptides are usually known for their potential role as regulators of the innate immune function. In this study, we evaluated the expression of Elabela by the three different types of Innate Lymphoid Cells (ILCs): ILC1s, ILC2s, and ILC3s. ILCs are a family of immune cells that mirror the phenotypes and functions of T cells and promptly response to signals from injured tissues. We hypothesized that ILCs may regulate the immune response by expressing Elabela (ILCsEla+). Since heart and the uterine decidua have been the focus of studies about Elabela, we collected both tissues from ICR males (n=3), virgins (n=3), and pregnant females on the 6<sup>th</sup> (n=3), 10<sup>th</sup> (n=3), and 14<sup>th</sup> (n=3) gestation days. The collected tissues were prepared for further flow cytometric analysis. Also, part of the decidua from 10<sup>th</sup> gestation day was used to perform Mixed Lymphocyte Reaction (MLR) *in vitro*. Our findings showed that ILCs in both heart and decidua express Elabela. The analysis showed that the number of ILC3sEla+ (10.7 ± 1.2) was higher in virgin female comparing to males (3.3 ± 0.8) (p=0.0032). In pregnant females, the total number of ILCsEla+ increased during the period of 6<sup>th</sup> to 14<sup>th</sup> gestation days in both heart {6<sup>th</sup> (27 ± 1.1); 14<sup>th</sup> (42 ± 1.5) (p=0.0104)} and decidua {6<sup>th</sup> (26.6 ± 0.5); 14<sup>th</sup> (47 ± 12) (p= 0.0273)}. The analysis of the MLR showed that Elabela was able to decrease the total number of active T cells. In conclusion, our study showed that Elabela as part of the innate immune system is expressed by ILCs. Also, there is a sex difference in the number of ILCsEla+ in the heart. These findings highlight the importance of exploring the role of Elabela as an immunomodulator in different cardiovascular disease models.

**E.Da Silva Lopes Salle:** None. **H.Khodadadi:** n/a. **L.Domingo:** n/a. **B.Zavan:** n/a. **J.Yu:** n/a. **B.Baban:** None.

---

MP38

Functional Investigation Of A Novel Adipose Long Intergenic Non-coding RNA, Linc- ADAIN, During Obesity

**Marcella E O'Reilly,** Columbia Univ Medical Ctr, New York, NY; Chenyi Xue, Columbia Univ, New York, NY; Esther Cynn, Columbia Univ Medical Ctr, New York, NY; Wen Liu, Columbia Univ Medical Ctr, NY, NY; Lucie Zhu, Columbia Univ Medical Ctr, New York, NY; Muredach P Reilly, COLUMBIA UNIVERSITY MEDICAL CENTER, New York, NY

**Background:** Long intergenic non-coding RNAs (lincRNAs) are important emerging regulators of cellular functions. Dysfunctional adipose tissue, characterized by increased inflammation and insulin resistance, plays a central role in the development of type 2 diabetes (T2DM) and atherosclerotic cardiovascular diseases. Deep RNA-sequencing of human adipose during low-dose endotoxemia, identified novel

lincRNAs shown to be regulated by inflammation and were validated in an independent human cohort, before and after bariatric surgery. LincADAIN was identified as a top candidate that is 1) abundantly expressed in adipose tissue 2) reduced in both obesity-induced chronic and LPS-induced acute inflammation (-77% and -53%,  $p < 0.05$ ). **Methods:** Knock down (KD) of lincRNAs was carried out via lentiviral expression of shRNA and antisense oligonucleotides (ASOs) in human adipose stromal cells (ASCs)-adipocytes. Subcellular location of LincADAIN was identified through qPCR after cellular fractionation. Biotinylated lincRNA pulldown assay was used to identify interacting proteins by Mass Spectrometry (MS). **Results:** Human LincADAIN expression negatively correlates to BMI in obese ( $p < 0.001$ ,  $r^2 = 0.3042$ ) but not lean individuals. PPAR $\gamma$  antagonist treatment showed reduced expression of LincADAIN and PPAR $\gamma$  ChIP-seq peaks indicate that PPAR $\gamma$  may be a transcriptional activator. KD via shRNA of LincADAIN in ASC-adipocytes, increased protein but not mRNA levels of inflammatory cytokines in adipocytes such as IL-8 and MCP-1. Cellular fractionation experiments indicate that LincADAIN is mainly located in the nucleus. MS analysis of biotinylated LincADAIN pulldown proteins revealed many central nuclear and ribosomal proteins as potential interactors, which may be involved in the post-transcriptional mechanism of LincADAIN regulating inflammatory cytokines. **Conclusion:** These results suggest that LincADAIN is a novel lincRNA with roles in regulating adipose inflammation through nuclear and cytoplasmic actions including modulation of RNA translation. Functional investigations of lincRNAs, such as these are warranted, as recent genomic studies suggest that lincRNAs are likely the causal element driving human disease at some GWAS loci.

**M.E.Oreilly:** None. **C.Xue:** None. **E.Cynn:** None. **W.Liu:** None. **L.Zhu:** None. **M.P.Reilly:** None.

---

MP39

*FHL5*, A Novel Cofactor Associated With Coronary Artery Disease, Regulates Smooth Muscle Cell Function Through A Transcriptional Network Linking Multiple Risk Loci

**Doris Wong**, Univ of Virginia, Charlottesville, VA; Adam Turner, Charlottesville, VA; Mohammad Daud Khan, Univ of Virginia, Charlottesville, VA; Meredith Palmore, Univ of Virginia, Charlottesville, VA, Warrenton, VA; Noah Perry, maniselvan kuppasamy, Univ of Virginia, Charlottesville, VA; Matteo Ottolini, Charlottesville, VA; Ljubica Matic, Charlottesville, VA, Solna, Stockholm, Sweden; Ulf Hedin, KAROLINSKA INSTITUTE, Stockholm, Sweden; Lijiang Ma, KAROLINSKA INSTITUTE, Stockholm, Sweden, New York, NY; Swapnil K Sonkusare, KAROLINSKA INSTITUTE, Stockholm, Sweden, New York, NY, Charlottesville, VA; Mete Civelek, UNIVERSITY VIRGINIA, Charlottesville, VA; Jason C Kovacic, VCCRI, Randwick, Australia; Johan Björkegren, Icahn Sch of medicine, New York, NY; Clint L Miller, Univ Of Virginia, Charlottesville, VA

**Introduction:** Coronary artery disease (CAD) is the leading cause of death worldwide with an estimated heritability of ~50%. The most recent genome wide association study (GWAS) for CAD and myocardial infarction (MI) identified over 200 loci. One such novel CAD/MI locus, *UFL1-FHL5* ( $P = 1.1E-8$ ), is associated with additional vascular pathologies, including hypertension, migraines, and coronary calcification. We previously showed through statistical fine-mapping that *FHL5* is the top candidate causal gene underlying each of these vascular trait associations and highly enriched in the contractile mural cell populations in the artery. These preliminary studies motivate our hypothesis that *FHL5* functions as a transcriptional regulator of SMC contractility to affect vascular disease risk. **Methods and Results:** Given the reported role of *FHL5* as a cofactor, we mapped 17,201 candidate *FHL5* binding sites in coronary artery SMCs using the Cleavage Under Targets and Release Using Nuclease (CUT&RUN) method. Binding sites were enriched for AP-1 family motifs and strongly overlapped CREB binding sites and H3K27ac enhancer marks. *FHL5* target genes were functionally enriched in well characterized CAD pathways, such as extracellular matrix organization ( $P = 5.2E-15$ ,  $OR = 2.1$ ) and TGF-beta signaling ( $P = 8.0E-5$ ,  $OR = 2.0$ ). Interestingly, *FHL5* binding sites were also enriched for CAD ( $P = 1.8E-7$ ,  $OR = 2.3$ ) and blood pressure (BP) risk variants ( $P = 0.04$ ,  $OR = 1.2$ ), thereby linking *FHL5* with the regulation of multiple downstream CAD/BP loci. Weighted gene co-expression network and key driver analyses of human coronary artery transcriptomic data further support this regulatory role. Lastly, we validated these findings by performing confocal based calcium imaging and collagen gel contraction assays. Consistent with our functional genomic analyses, overexpression of *FHL5* elevated intracellular calcium levels 2.5X and increased SMC contractility by ~45%. **Conclusion:** Taken together, our results provide evidence that *FHL5* may impact CAD risk by regulating a network of disease-associated genes mediating SMC functions. These findings further contribute to our understanding of the heritable risk for multiple vascular diseases.

**D.Wong:** n/a. **L.Ma:** None. **S.K.Sonkusare:** None. **M.Civelek:** None. **J.C.Kovacik:** None. **J.Bjorkegren:** None. **C.L. Miller:** None. **A.Turner:** None. **M.Khan:** Employment; Significant; University of virginia  
**M.Palmore:** None. **N.Perry:** n/a. **M.Kuppusamy:** n/a. **M.Ottolini:** None. **L.Matic:** None. **U.Hedin:** None.

---

MP40

Breakpoint Cluster Region Protein Function As A Kinase Mediates The Atheroprotective Actions Of Hdl In Vascular Endothelium

**Anastasia Sacharidou,** UT SOUTHWESTERN MEDICAL CENTER, Dallas, TX; Ken Chambliss, UT Soutwestern Medical Ctr, Dallas, TX; Haiyan Chu, UTSW, Dallas, TX; Wan-Ru Lee, UTSW, Dallas, TX, Coppell, TX; Lin Xu, Philip W Shaul, UT SOUTHWESTERN MEDICAL CENTER, Dallas, TX; Chieko Mineo, UNIV TX SOUTHWESTERN MED CTR, Dallas, TX

**Introduction:** HDL has direct atheroprotective actions on endothelial cells (EC) that include the attenuation of vascular inflammation and promotion of endothelial monolayer integrity. These processes are mediated by scavenger receptor class B, type 1 (SR-BI) and its adaptor protein PDZK1. We have identified the breakpoint cluster region protein (BCR) as a PDZK1 interacting protein in EC. Best known as a gene in the BCR-ABL complex associated with the Philadelphia chromosome, BCR structure predicts both adaptor protein and kinase functions. **Hypothesis:** Via interaction with PDZK1 and kinase activity, BCR mediates the atheroprotective actions of HDL on EC. **Methods:** Newly-developed kinase assays that employ time-resolved Forster resonance energy transfer were used to detect kinase activity and identify kinase substrates. In vivo studies were done in ApoAI<sup>-/-</sup> versus ApoAI<sup>-/-</sup>;BCR<sup>-/-</sup> mice administered control AAV or AAV-ApoAI. Leukocyte-EC interaction and carotid artery reendothelialization were evaluated by intravital microscopy and thermal injury, respectively. Atherosclerosis was invoked using AAV8-PCSK9. BCR expression was compared in human atherosclerotic and normal arteries in two independent publicly available patient cohorts. **Results:** In cultured EC, HDL activation of eNOS, blunting of EC-monocyte adhesion, and promotion of EC migration all required BCR, and reconstitution studies with BCR mutants revealed requirements for both BCR-PDZK1 interaction and kinase activity. In response to HDL, BCR directly phosphorylated Akt-Ser473 and it provoked Akt-Thr308 phosphorylation by PDK1. ApoAI restoration in vivo in ApoAI<sup>-/-</sup> mice prompted SR-BI-PDZK1-BCR protein complex formation and BCR phosphorylation of Akt-Ser473 in mouse aorta. It also blunted leukocyte-endothelial cell adhesion and enhanced carotid artery reendothelialization in BCR<sup>+/+</sup>, but not in BCR<sup>-/-</sup> mice. Furthermore, the atheroprotective effect of ApoAI restoration was demonstrable in BCR<sup>+/+</sup>, but not in BCR<sup>-/-</sup> mice. In both human cohorts BCR expression was decreased in atherosclerotic versus normal arteries. **Conclusion:** BCR function as a novel direct and indirect kinase of Akt mediates the atheroprotective actions of HDL in vascular endothelium.

**A.Sacharidou:** None. **K.Chambliss:** None. **H.Chu:** None. **W.Lee:** n/a. **L.Xu:** None. **P.W.Shaul:** None. **C.Mineo:** None.

---

MP41

Myeloid Ccn3 Protects Against Aortic Valve Calcification

**Peinan Tu,** Emory, Atlanta, GA; Zhiyong Lin, Emory Univ, Atlanta, GA; xianming zhou, Emory, Atlanta, GA; Hanjoong Jo, EMORY UNIVERSITY, Atlanta, GA; Nicolas Villa-roel, EMORY UNIVERSITY, Atlanta, GA, Atlanta, GA; Sandeep Kumar, Emory Univ, Atlanta, GA; Caiwen Ou, Emory, Atlanta, GA; Nianguo Dong, Emory, Atlanta, GA, Wuhan

**Objective —** CCN3, an inhibitor in osteoblast differentiation, can modulate calcium signaling, yet, whether CCN3 can regulate valvular calcification is unknown. While it has been suggested that macrophages are important in the regulation of valvular calcification, the molecular and cellular mechanisms of this process remain poorly understood. In the present study, we investigated the specific role that macrophage-derived CCN3 plays during the progression of calcific aortic valve disease (CAVD). **Methods and Results —** Myeloid-specific knockout of CCN3 (Myc-CCN3-KO) and control mice were subjected to a single injection of AAV encoding mutant mPCSK9 (rAAV8/D377Y-mPCSK9) to induce hyperlipidemia. AAV-injected mice were then fed a high fat diet (HFD) for 40 weeks. At the conclusion of HFD feeding, tissues were harvested for subsequent histological and pathological analysis. Echocardiography revealed that both male and female myc-CCN3-KO animals displayed compromised aortic valvular function accompanied by exacerbated valve thickness and cardiac dysfunction. Histologically, alizarin red and OsteoSense staining

revealed a marked increase of aortic valve calcification in mye-CCN3-KO animals when compared to controls. In vitro, CCN3 deficiency augmented bmp2 production and secretion from bone marrow derived macrophages (BMDMs). Further, human valvular interstitial cells (VICs) cocultured with conditional media from CCN3-deficient BMDMs resulted in exaggerated pro-calcifying gene expression and the attendant calcification as revealed by alizarin red staining. **Conclusions** — Our data uncovered a novel role of myeloid CCN3 in the regulation of aortic valve calcification. Modulation of bmp2 production and secretion in macrophages might serve as a key mechanism for CCN3's anti-calcification function in the development of CAVD.

**P. Tu:** None. **Z. Lin:** None. **H. Jo:** Ownership Interest; Modest; FloKines Pharma. **N. Villa-roel:** None. **S. Kumar:** None.

---

MP42

#### Macrophage Chromatin Remodeling Complex Subunit Baf60a In Atherosclerosis

**Yang Zhao**, Dept of pharmacology, Univ of Michigan, Ann Arbor, MI; Yuhao Liu, Guizhen Zhao, Haocheng Lu, Ziyi Chang, Chao Xue, Eugene Chen, Jifeng Zhang, Univ of Michigan Medical Ctr, Ann Arbor, MI

**Abstract Objectives:** Atherosclerosis is a primary medical concern due to the increasing prevalence and lack of effective treatment that reverses the disease progression. While multiple genetic mutations/variants have been associated with atherosclerotic risk, the development of atherosclerosis in response to risk factors is also contributed by factors at the epigenetic and chromatin level. The SWI/SNF chromatin remodeling complex alters DNA accessibility and chromatin structure to modulate gene expression in response to external and internal cellular environments, potentially serving as an underexplored compartment of CVD and atherosclerosis development. **Approach and Results:** In an effort to identify key chromatin remodeling compartments involved in atherosclerotic foam cell formation, primary bone marrow-derived macrophages (BMDMs) were exposed to a pro-atherogenic environment, specifically to oxidized Low-density lipoprotein (oxLDL). We observed drastically and time-dependent decrease in the protein abundance of BAF60a, a transcription factor interacting subunit of the SWI/SNF chromatin remodeling complex. Macrophage-specific Baf60a deletion in ApoE deficient mice showed over 30% increase in aortic plaque formation after 16-weeks of western diet feeding (N=12, p=0.0097). Integrated analysis of RNA-seq and ATAC-seq regulatory network in oxLDL treated BAF60a deficient BMDMs identified a shift of chromatin accessibility, transcription factor footprint, and a reshape in gene expression patterns that regulate extracellular matrix organization, focal adhesion, integrin signaling, inflammation, and lead to foam cell formation which ultimately contribute to the atherosclerotic plaque build-up. **Conclusions:** Our data demonstrated the role of macrophage BAF60a in atherogenesis and suggested a potential therapeutic target to treat atherosclerosis, presumably by compensating for the loss of Baf60a.

**Y. Zhao:** None. **Y. Liu:** None. **G. Zhao:** None. **H. Lu:** None. **Z. Chang:** None. **C. Xue:** None. **E. Chen:** None. **J. Zhang:** None.

---

MP43

#### Liposome-human ACE2 Complex As An Engineered Decoy To Abrogate SARS-CoV-2-induced Inflammatory Responses In Macrophages

Sandro Satta, UCLA, Los Angeles, CA; Zhaojie Meng, **Rebecca Hernandez**, UNIVERSITY OF CALIFORNIA, RIVERSIDE, Riverside, CA; Susana Cavallero, UCLA, Los Angeles, CA; Tong Zhou, Univ of Nevada, Reno, NV; Tzung K Hsiai, UCLA SCH OF MED CARDIOLOGY DIV, Los Angeles, CA; Changcheng Zhou, UNIVERSITY OF CALIFORNIA, RIVERSIDE, Riverside, CA

**Introduction:** Innate immune cells such as macrophages have been implicated in pathological inflammation in COVID-19 patients. As many immune cells express low levels of human angiotensin-converting enzyme 2 (hACE2), the mechanisms underlying SARS-CoV-2-mediated macrophage inflammatory responses remain elusive. Further, neutralizing SARS-CoV-2 prior to their binding to the host cells was proposed as a therapeutic approach to ameliorate SARS-CoV-2-stimulated inflammation. This study aims to investigate whether an engineered decoy receptor can affect SARS-CoV-2-induced macrophage inflammation.

**Hypothesis:** Liposome-based hACE2 complex acts as a molecular decoy to abrogate SARS-CoV-2-induced

macrophage inflammation.

**Methods:** Rhodamine encapsulated liposome-based nanoparticles were used to generate Liposome-human ACE2 complex (Liposome-hACE2). Liposome-hACE2 was used as a decoy receptor or competitive inhibitor to inhibit SARS-CoV-2 or Spike protein-induced macrophage inflammation in vitro and in vivo.

**Results and Conclusions:** SARS-CoV-2 or Spike protein induces strong inflammatory responses in murine macrophages in a hACE2-independent manner. Liposome-hACE2 can efficiently abrogate SARS-CoV-2 or Spike protein-induced inflammatory responses in murine macrophages in vitro and in vivo.

Mechanistically, Spike protein stimulated macrophage inflammation by activating canonical IKK $\beta$ /NF- $\kappa$ B signaling, and deficiency of IKK $\beta$  abolished Spike protein-elicited inflammatory responses in macrophages.

The use of Liposome-hACE2 as a molecular decoy was further recapitulated in human macrophages.

SARS-CoV-2 or Spike protein-induced inflammatory responses in human peripheral blood mononuclear cells and differentiated THP-1 macrophages were also abolished by Liposome-hACE2 treatment. These results suggest that neutralizing SARS-CoV-2 by liposomes may present an innovative therapeutic strategy treating COVID-19.

**S.Satta:** None. **Z.Meng:** None. **R.Hernandez:** n/a. **S.Cavallero:** n/a. **T.Zhou:** n/a. **T.K.Hsiai:** None. **C.Zhou:** n/a

---

MP45

The Roles Of Telomeric Repeat Binding Factor 2-interacting Protein (TERF2IP) K240 SUMOylation In Endothelial Cells On Atherogenesis

**Masaki Imanishi,** UT MD Anderson Cancer Ctr, Houston, TX; **Loka reddy Velatooru,** Houston Methodist Res Inst, Houston, TX; **Kyung ae Ko,** MD Anderson Cancer Ctr, Houston, TX; **Kyung-Sun Heo,** CHUNGNAM NATIONAL UNIVERSITY, Daejeon; **Tamlyn Thomas,** MD Anderson Cancer Ctr, Houston, TX; **YOUNG JIN GI,** MD ANDERSON CANCER CENTER, HOUSTON, TX; **Keigi Fujiwara,** U. of Texas MD Anderson Cancer Cent, Houston, TX; **Nhat Tu Le,** Houston Methodist Res Inst., Houston, TX; **Sivareddy Kotla,** Houston Methodist Res Inst., Houston, TX; **Junichi Abe,** Univ of Texas MD Anderson Can, Houston, TX

**Background and Objectives:** It is not yet clear how the pro-atherogenic signaling events in endothelial cells (ECs) such as those that lead to EC senescence, apoptosis and activation are interconnected and promote atherosclerotic plaque formation in the area exposed to disturbed blood flow (d-flow). TERF2IP, a member of the shelterin complex of the telomere, regulates all three pathological events. We investigated the role of TERF2IP K240 SUMOylation in the process of d-flow-induced atherosclerotic plaque formation. **Methods and Results:** We found that d-flow increased TERF2IP K240 SUMOylation in ECs and that it was suppressed by a p90RSK specific inhibitor, FMK-MEA. This SUMOylation was independent of TERF2IP S205 phosphorylation. The d-flow-induced senescence, DNA damage, and apoptosis were inhibited in ECs with TERF2IP depletion or point-mutated phosphorylation (S205A) and SUMOylation (K240R) sites. NF- $\kappa$ B activation induced by d-flow or overexpression of p90RSK was also significantly inhibited in ECs overexpressing the TERF2IP S205A phosphorylation mutant. However, cells overexpressing the TERF2IP K240R SUMOylation mutant showed no effect on the d-flow or p90RSK-mediated NF- $\kappa$ B activation. To determine the biological function of TERF2IP K240 SUMOylation, we generated TERF2IP K240R knock-in (KI) mice and examined d-flow-induced atherosclerotic plaque formation using partial left carotid ligation model mice fed a high-fat diet after AAV8-PCSK9 injection. We found no differences in body weights and cholesterol levels between TERF2IP K240R KI and wild type control (WT) mice, but plaque formation was significantly inhibited in the KI mice compared to WT animals (Oil Red O positive area (%): 19.0 +/- 12.5 (KI mice, n=8) vs 61.2 +/- 24.3 (WT mice, n=7), p = 0.0008). Bone marrow from WT mice were transplanted into KI and WT mice, which were then injected with AAV8-PCSK9 virus and fed a high-fat diet for 16 weeks, but we still found that plaque formation was inhibited in the KI mice. **Conclusion:** TERF2IP SUMOylation plays a role in EC senescence but not in activation. The significant inhibition of plaque formation in the TERF2IP K240R KI mice is due to downregulation of TERF2IP SUMOylation in ECs not in myeloid cells.

**M.Imanishi:** None. **J.Abe:** Research Grant; Significant; NIH, CPRIT. **L.Velatooru:** None. **K.Ko:** None. **K.Heo:** None. **T.Thomas:** None. **Y.Gi:** None. **K.Fujiwara:** None. **N.T.Le:** None. **S.Kotla:** None.



## Assessment Of Atherosclerosis In A Novel Transgenic Mouse Expressing Pathogenic Levels Of Human Lipoprotein(a)

**Julia Assini**, Chuce Xing, Justin Clark, Tasnim Reza, Robert Gros, ROBERTS RESEARCH INSTITUTE, London, ON, Canada; Michael Boffa, The Univ of Western Ontario, London, ON, Canada; Marlys L Koschinsky, Western Univ, London, ON, Canada

Studying the role of elevated plasma levels of lipoprotein(a) (Lp(a)) in atherogenesis is challenging given that the *LPA* gene encoding apo(a) is absent in typical animal models. As such we created a novel transgenic mouse line expressing both human apolipoprotein(a) (apo(a)) and human apoB100 (*Tg(LPA<sup>+/0</sup>;APOB<sup>+/0</sup>)*). The *LPA* transgene, assembled in the pLIV vector, produces a physiologically relevant 12-kringle apo(a) isoform. The *APOB* transgene contains the entire human *APOB* gene with a mutation preventing *APOB* editing. In our atherosclerosis model, male and female mice were injected weekly with an antisense oligonucleotide targeting the mouse LDL receptor (IONIS Pharmaceuticals), and fed a high-fat, high-cholesterol diet for 12 weeks. High plasma Lp(a) levels were observed in both male and female *Tg(LPA<sup>+/0</sup>;APOB<sup>+/0</sup>)* mice (219.0±11.9 and 133.7±12.1 mg/dL, respectively; n=12/group). Importantly, high levels of Lp(a) in plasma did not result in metabolic alterations, including differences in weight gain, energy expenditure, activity, RER, VO<sub>2</sub>/VCO<sub>2</sub> consumption/output, and glucose tolerance compared to *Tg(APOB<sup>+/0</sup>)* control mice. Both male and female *Tg(LPA<sup>+/0</sup>;APOB<sup>+/0</sup>)* and *Tg(APOB<sup>+/0</sup>)* mice exhibited enhanced proatherogenic lipoprotein profiles with the majority of the cholesterol and TG present in the VLDL and LDL fractions. Complex lesions developed in all transgenic mice, including large, lipid-rich necrotic cores, with overlying fibrous caps and intimal calcium deposition. Immunohistochemistry with a monoclonal apo(a) antibody revealed the presence of Lp(a) in the plaques of *Tg(LPA<sup>+/0</sup>;APOB<sup>+/0</sup>)* mice. Analysis of aortic sinus lesions revealed a 23% increase in total plaque area in female *Tg(LPA<sup>+/0</sup>;APOB<sup>+/0</sup>)* mice compared to female *Tg(APOB<sup>+/0</sup>)* mice (p=0.0836). Moreover, atherosclerotic plaques in female *Tg(LPA<sup>+/0</sup>;APOB<sup>+/0</sup>)* mice contained significantly more calcium deposition than female *Tg(APOB<sup>+/0</sup>)* mice (1.79±0.4% vs. 2.96±0.3% of total plaque area (p<0.05)). No differences in plaque area or calcium were observed in male mice. In this ongoing study, detailed analyses of atherosclerotic plaque components in *Tg(LPA<sup>+/0</sup>;APOB<sup>+/0</sup>)* mice will be required to uncover the unique contribution of Lp(a) to atherogenesis.

**J.Assini:** None. **C.Xing:** n/a. **J.Clark:** n/a. **T.Reza:** n/a. **R.Gros:** n/a. **M.Boffa:** Other Research Support; Modest; Ionis, Research Grant; Significant; Canadian Institutes of Health Research, Natural Sciences and Engineering Research Council of Canada. **M.L.Koschinsky:** Honoraria; Modest; Eli Lilly, Other; Modest; Sanofi, Amgen, Other Research Support; Modest; Sanofi, Ionis, Eli Lilly, Abcentra, Research Grant; Significant; Canadian Institutes of Health Research, Heart and Stroke Foundation of Canada, Natural Sciences and Engineering Research Council of Canada, Pfizer, Speaker/Speaker's Bureau; Modest; Amgen, Regeneron.

## Smooth Muscle Cell-Specific Deletion Of O-GlcNAc Transferase Impedes Atherosclerotic Lesion Formation In Western Diet-fed ApoE<sup>-/-</sup> Mice

**Saugat Khanal**, Amy Mathias, Jason Lallo, Neha Bhavnani, Shreya Gupta, NorthEast Ohio Medical Univ, Rootstown, OH; Priya Raman, NEOMED - IMS, Rootstown, OH

Attachment of O-linked N-acetylglucosamine (O-GlcNAc) to nucleocytoplasmic proteins or 'O-GlcNAcylation' is a ubiquitous post-translational modification affecting numerous cellular processes. We and others have previously reported that augmented protein O-GlcNAcylation mediates upregulation of numerous genes associated with atherosclerosis. Recent studies suggest the role of O-GlcNAc transferase (OGT), a key regulator of O-GlcNAc signaling, in diabetic vascular calcification and wound healing. However, the role of OGT in the etiology of atherosclerosis is elusive. The goal of the current study was to interrogate whether OGT plays a direct role in the development of atherosclerosis. For this, we crossed tamoxifen-inducible male Myh11-CreERT2;OGT<sup>fl/y</sup>;ApoE<sup>-/-</sup> mice with female OGT<sup>fl/+</sup>;ApoE<sup>-/-</sup> to generate SMC-specific OGT knockout on ApoE<sup>-/-</sup> background. To induce Cre recombinase activity, mice genotypes were injected i.p. with 60mg/Kg/day tamoxifen (peanut oil-vehicle control) once daily for 5 consecutive days beginning at 6 wks age. This was followed by a Western diet feeding regimen for additional 6-7 wks.

Mice were harvested at 14 wks age after overnight fasting; plasma, aorta, and heart were collected for biochemical, molecular, and lesion studies. Immunoblotting confirmed loss of OGT expression in aortic vessels of tamoxifen-treated Cre<sup>tg</sup>;OGT<sup>fl/y</sup>;ApoE<sup>-/-</sup> mice (smOGT<sup>KO</sup>;ApoE<sup>-/-</sup>) vs. age-matched tamoxifen-treated Cre<sup>tg</sup>;OGT<sup>+/y</sup>;ApoE<sup>-/-</sup> littermates (smOGT<sup>WT</sup>;ApoE<sup>-/-</sup>, with intact OGT). Aortic root morphometry revealed a significant reduction (2.5-fold) in lesion lipid burden in smOGT<sup>KO</sup>;ApoE<sup>-/-</sup> mice compared with smOGT<sup>WT</sup>;ApoE<sup>-/-</sup>. This was accompanied by attenuated PCNA (proliferation marker), osteopontin (SM synthetic marker), pERK (SM signaling regulator), YY1 (transcriptional repressor of SM contractile genes), and SRF (transcriptional regulator of SMC proliferation) expression in smOGT<sup>KO</sup>;ApoE<sup>-/-</sup> vs. smOGT<sup>WT</sup>;ApoE<sup>-/-</sup> aortic lysates, shown via immunoblotting. Interestingly, SMC-specific OGT deletion had no effect on plasma total cholesterol and total triglyceride levels. Taken together, these results demonstrate a protective role of SMC-specific loss of OGT on atherosclerotic lesion formation.

**S.Khanal:** n/a. **A.Mathias:** None. **J.Lallo:** n/a. **N.Bhavani:** None. **S.Gupta:** None. **P.Raman:** None.

---

MP49

#### Macrophage-mediated Extracellular Digestive Exophagy Of Aggregated LDL Is Responsible For The Formation Of Cholesterol Crystals In Atherosclerotic Plaques

**Cheng-I Jonathan J. Ma,** Weill Cornell Medical Coll, New York, NY; Valeria Barbosa Lorenzi, Weill Cornell Med, New York, NY; Frederick R Maxfield, WEILL CORNELL MEDICAL COLLEGE, New York, NY

Atherosclerosis is a disease that develops overtime through dyslipidemia and chronic inflammation. Formation of cholesterol crystals in the atherosclerotic plaques is a major contributor to the inflammatory response. However, how these crystals form in the atherosclerotic plaques remained poorly understood. We have observed that macrophage-mediated extracellular digestive exophagy of aggregated LDL releases a large amount of free cholesterol in the extracellular space. Therefore, we hypothesized that this release of cholesterol may play a major role in formation of cholesterol crystals in plaques. We have shown previously that TLR4 knockout in macrophages compromises digestive exophagy of aggregated LDL. Thus, to evaluate the role of digestive exophagy in cholesterol crystal formation, we examined cryosections of aortic plaques from *Ldlr*<sup>-/-</sup> mice that were gamma-irradiated and reconstituted with WT or *Tlr4*<sup>-/-</sup> bone marrows. Interestingly, TLR4 KO in macrophages reduce both free cholesterol and cholesterol crystal in plaques compared to WT macrophages, suggesting a role of digestive exophagy in cholesterol crystal formation. To investigate whether digestive exophagy of aggregated LDL results in inflammatory response, we cultured bone-marrow derived macrophages expressing the inflammasome marker ASC-citrine with aggregated LDL over time. We observed a gradual increase in number of inflammasomes over a 24 h time period. We also observed extracellular cholesterol crystal formation as early as 2 h after the addition of aggregated LDL. Moreover, treating bone marrow-derived macrophages with acetylated LDL did not result in the formation of extracellular cholesterol crystals, suggesting this process is specific to a subset of modified LDL in the vessel wall. Overall, our data provide evidence that macrophage-mediated digestive exophagy of aggregated LDL is a major contributor to the formation of extracellular cholesterol crystal found in atherosclerotic lesions.

**C.J.Ma:** None. **V.Barbosa lorenzi:** None. **F.R.Maxfield:** Research Grant; Significant; NIHHLBI.

## Poster Abstracts

---

P101

### Suppression Of Serum Amyloid A Limits Progression Of Obesity Associated Abdominal Aortic Aneurysms

Andrea Trumbauer, UNIVERSITY OF KENTUCKY, Lexington, KY; Victoria Noffsinger, Ailing Ji, UNIVERSITY KENTUCKY, Lexington, KY; Frederick C DEBEER, UNIVERSITY OF KENTUCKY, Lexington, KY; Adam Dugan, Univ of Kentucky, Lexington, KY; Adam E Mullick, Ionis Pharmaceuticals, Inc., Carlsbad, CA; Nancy R Webb, UNIVERSITY KENTUCKY, Lexington, KY; **Preetha Shridas**, Lisa R Tannock, UNIVERSITY OF KENTUCKY, Lexington, KY

Obesity increases the risk for abdominal aortic aneurysms (AAA) in humans, and enhances angiotensin II (AngII)-induced AAA formation in C57BL/6 mice. Obesity is also associated with increases in serum amyloid A (SAA). We previously reported that deficiency of SAA significantly reduces AngII-induced inflammation and AAA in apoE-deficient mice. In this study we investigated whether SAA plays a role in progression of an established AAA in obese C57BL/6 mice. Approach and results: Male C57BL/6 mice were fed a high fat diet (60% kcal as fat) throughout the study. After 4 months of diet the mice were infused with angiotensin II (AngII) at 1000ng/kg/min until the end of the study. Ultrasound (US) was performed in all mice before and after 28 days of AngII infusion, and mice that had at least a 25% increase in the luminal diameter of the abdominal aorta were stratified by luminal diameter into 3 groups. Group 1 was killed to establish baseline AAA. Groups 2 and 3 continued to receive AngII for a further 8 weeks along with an antisense oligonucleotide (ASO) that suppresses all 3 acute phase SAA isoforms (SAA-ASO), or a control ASO (5 mg/kg/wk). US was repeated at study end to assess AAA progression. Plasma SAA at the end of the experiment was  $89.2 \pm 83.2$  mg/L in the control ASO group, and  $18.6 \pm 0.7$  mg/L in the SAA-ASO group (mean $\pm$ SD,  $p=0.008$ ). There was no impact of SAA suppression on body weight, body fat, or blood pressure. After the first 4 weeks of AngII infusion, the average luminal diameter in all mice was  $1.81 \pm 0.40$  mm (mean $\pm$ SD). Mice that received the control ASO had continued aortic dilation (average luminal aortic diameter  $2.06 \pm 0.42$  mm), whereas the mice that received the SAA-ASO had a significant reduction in progression of aortic dilation (average luminal diameter  $1.64 \pm 0.43$  mm,  $p=0.0015$  for interaction between time and group). Conclusions: We demonstrate for the first time that suppression of SAA protects obese C57BL/6 mice from progression of AngII-induced AAA. Suppression of SAA may be a therapeutic approach to limit AAA progression.

**A.Trumbauer:** None. **V.Noffsinger:** None. **A.Ji:** None. **F.C.Debeer:** None. **A.Dugan:** None. **A.E.Mullick:** Employment; Significant; Ionis Pharmaceuticals, Inc, Stock Shareholder; Significant; Ionis Pharmaceuticals, Inc. **N.R.Webb:** None. **P.Shridas:** None. **L.R.Tannock:** None.

---

P102

### False Lumen Volume Is A Predictor Of Successful Thoracic Endovascular Aortic Repair

**Kameel Khabaz**, Seth Sankary, Ross Milner, Luka Pocivavsek, Univ of Chicago, Chicago, IL

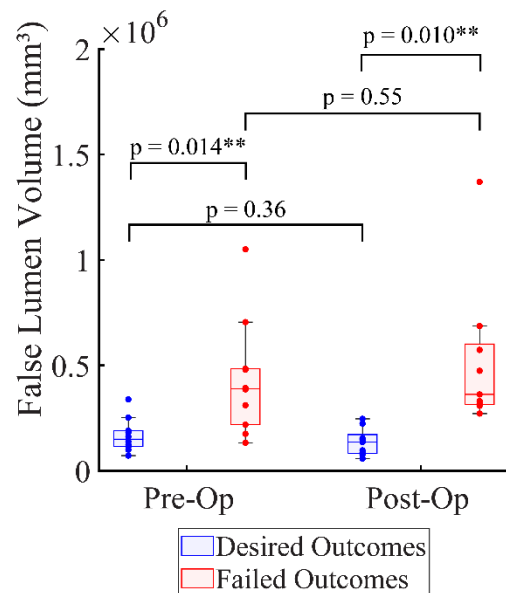
**Objectives:** Thoracic endovascular aortic repair (TEVAR) is becoming the treatment modality of choice for type B aortic dissection (TBAD). Using CTA imaging, clinicians track dissection evolution; however, clinical imaging analysis is limited to linearized measurements of maximum diameter that poorly predict post-operative outcomes. Achieving post-operative thrombosis of the false lumen is a desired characteristic that is thought to prevent aneurysmal degeneration, complication, and reintervention. We hypothesize that decrease in false lumen volume can be used to accurately predict successful TEVAR, as defined by lack of reintervention.

**Methods:** We studied 20 TBAD patients that underwent TEVAR, 10 with desired outcomes, defined by the absence of post-operative reintervention, and 10 with failed outcomes, defined by the presence of reintervention. Utilizing CTA imaging, we performed pre- and post-operative segmentations of the false lumen for each patient. We calculated the volume of the false lumen of each scan. We performed two-sample t-tests on the null hypothesis that false lumen volume does not change post-TEVAR. We also tested the null hypothesis that patients with desired outcomes and poor outcomes have equal false lumen volumes.

**Results:** We found a statistically significant difference in the pre-operative false lumen volume of patients

with desired outcomes post-TEVAR versus patients with failed outcomes ( $p=0.014$ ). However, we found no statistically significant change in false lumen volume of patients with successful or failed TEVAR.

**Conclusions:** Pre-operative false lumen volume distinguishes desired versus failed post-TEVAR outcomes. While our initial hypothesis was not proven, our results identify that pre-operative false lumen volume is a viable predictor of TEVAR success. The clinical implication of our finding is that patients with a large false lumen volume may not be ideal candidates for an endovascular approach to TBAD repair.



**K. Khabaz:** None. **R. Milner:** Honoraria; Modest; Medtronic, WL Gore, Endospan.

P103

#### Molecular Imaging Analysis Of Integrin $\alpha\beta3$ Expression With Gallium-68-labeled Arg-gly-asp In A Murine Model Of Thoracic Aortic Aneurysms

**Javier E. Anaya-Ayala,** Insto Nacional de Ciencias Medicas y Nutricion Salvador Zubiran, Univ Nacional Autonoma de Mexico, Mexico, Mexico; **Luis A. Medina,** Univ Nacional Autonoma de Mexico, Insto Nacional de Cancerologia, Mexico City, Mexico; **Ana T. Verduzco-Vazquez,** Insto Nacional de Ciencias Medicas y Nutrición Salvador Zubiran, Mexico, Mexico; **Carlos Bravo-Reyna,** Ricardo Martinez-Martinez, Insto Nacional de Ciencias Medicas y Nutricion Salvador Zubiran, Mexico, Mexico; **Carlos A. Hinojosa,** Insto Nacional de Ciencias Medicas y Nutricion Salvador Zubiran, Univ Nacional Autonoma de Mexico, Mexico, Mexico

**Background/Objective:** Angiogenesis is a complex process. Studies in aneurysmal aortic wall in human tissue and animal models have demonstrated an increased mural neovascularization, and Integrin  $\alpha\beta3$  is a molecular indicator of angiogenesis. We aim to study and characterize Integrin  $\alpha\beta3$  expression with Gallium-68( $^{68}\text{Ga}$ )-labeled Arg-Gly-Asp (RGD) as a potential radiotracer using micro Positron Emission Tomography (PET) in a Murine model of Thoracic Aortic Aneurysms (TAA). **Methods:** Eight specimens of Wistar rat with Calcium Chloride ( $\text{CaCl}_2$ ) TAA-induced were evaluated. The equipment utilized was an Albira microPET/CT unit (Bruker, Spain), access was obtained in one of the caudal veins for the radiolabeled  $^{68}\text{Ga}$ -RGD infusion. The PET uptake and activity were expressed as median value with interquartile range and the Mann-Whitney U test was employed to analyze and compare the chemically induced-site (Aneurysm) and intact aortic tissue (Control) in the same specimens. Statistical analysis was performed with GraphPad Prism 8.0 software. **Results:** All specimens tolerated well the procedures through a left thoracotomy (Upper panel figure A, B), and underwent imaging studies. A focal increased uptake was observed in the thoracic aortic lesions compared to control regions. The median standard uptake value (SUV) of  $^{68}\text{Ga}$ -RGD in the chemically induced-injury site (aneurysm) was 0.0125, while the uptake in the intact site (control) was 0.0003 ( $P$  value=0.0117) during a mean follow up period of 32 days (Lower panel figure A-C). **Conclusion:** We found significant differences of Integrin  $\alpha\beta3$  expression uptake with microPET imaging in chemically induced aneurysms and the intact aortic tissue within 5 weeks of vessel injury. Longitudinal studies with this imaging modality may assist in the molecular characterization of angiogenesis and aneurysmal progression in animal models, and its potential translation in clinical

research studies in human patients with aortic aneurysm.

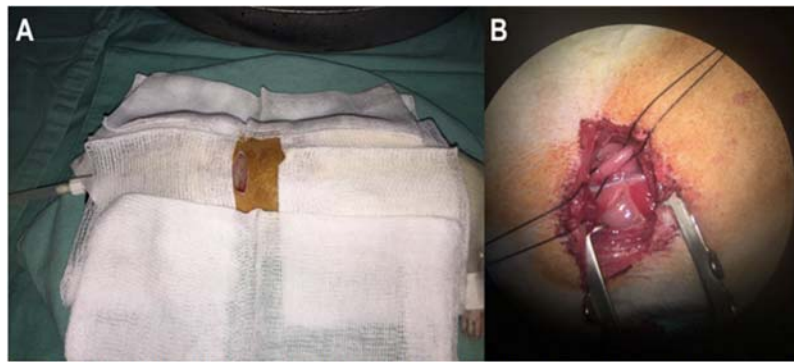


**Figure A, B.** Wistar Rat model undergoes a left thoracotomy under general endotracheal anesthesia (A). The descending thoracic aorta is isolated and controlled for chemical induction of the aneurysm (B).

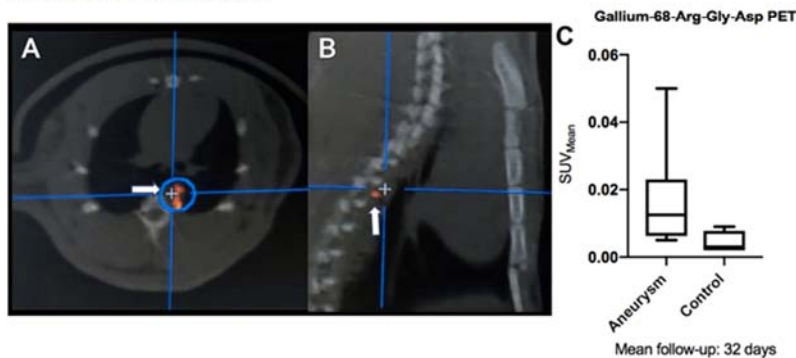


**Figure 2 A-C.** 68Ga-RGD PET scan, axial (A) and lateral (B) views. The white arrows indicate the area of higher uptakes. Statistical differences are observed in the graph between the aneurysm and control sites at 32 days of follow up (C).

J.E.Anaya-ayala: None. L.A.Medina: None. A.T.Verduzco-vazquez: n/a. C.Bravo-reyna: n/a. R.Martinez-martinez: None. C.A.Hinojosa: n/a.

P104

## The Transcription Factor Erg Governs Chromatin Accessibility And Gene Expression Programs Underlying Vascular Dysfunction In Aortic Endothelial Cells

**Steven R Botts**, Nadiya Khyzha, Rathnakumar Kumaragurubaran, Ruilin Wu, Sneha Raju, Kamalben Prajapati, Kathryn L Howe, Jason E Fish, Univ Health Network, Toronto, ON, Canada

**Aims:** The transcription factor ERG has emerged as an important regulator of vascular function through its ability to repress inflammation in endothelial cells (ECs) and ERG dysregulation is associated with chronic inflammation in atherosclerosis and aortic aneurysms. To characterize the cellular mechanisms that underlie this regulation, we deleted *ERG* in human aortic ECs and assessed genome-wide chromatin accessibility and gene expression to identify dysregulated pathways. Furthermore, we have begun to investigate ERG expression in mouse atherosclerotic plaque.

**Methods:** CRISPR/Cas9 was used to delete *ERG* exon 6 in immortalized human aortic ECs. Wildtype or  $\Delta$ ERG ECs were profiled with ATAC-seq and RNA-seq (n=2-4). GREAT and clusterProfiler were used to identify enriched pathways ( $\log_2FC > |1|$ ; FDR < 0.05). Regulatory regions were defined as 5kb upstream and 1kb downstream of transcription start sites with  $\leq 1$ Mb nearest gene extension. To determine if ERG expression is altered during atherosclerosis, 8-week-old *Ldlr*<sup>-/-</sup> mice were fed a 12-week high-cholesterol diet (1.25%) before sacrifice. Ascending aortic sections were stained with anti-CD68 and anti-ERG (n=2). Images were obtained using a Leica SP8 confocal microscope.

**Results:** Pathway analysis of >21,000 differentially accessible chromatin regions identified 67 enriched processes in  $\Delta$ ERG ECs. Of these, the top 20% included disrupted wound healing, abnormal aorta morphology, and aneurysm, which were driven by association with proatherogenic and proaneurysmal genes including *PDGFRB* and *TGFBR1*. Gene expression analysis revealed that loss of ERG contributes to endothelial to mesenchymal transition (increased *KLF4* and *SNAI2*), inflammation (increased *IL18*), and

dysregulated extracellular matrix and cell adhesion (increased *FBLN2* and *VCAN*). In the mouse aorta, preliminary data suggest that ERG expression may be elevated in EC nuclei overlying plaque compared to non-atherosclerotic regions.

**Conclusions:** The loss of ERG has a broad impact on chromatin accessibility and gene expression in aortic ECs, with enrichment of vascular dysfunction pathways. Further investigation will establish how altered ERG expression contributes to *in vivo* models of atherosclerosis and aortic aneurysms.

**S.R.Botts:** None. **N.Khyzha:** None. **R.Kumaragurubaran:** None. **R.Wu:** None. **S.Raju:** None. **K.Prajapati:** None. **K.L.Howe:** None. **J.E.Fish:** None.

---

P105

Inducible Deletion Of Fibrillin-1 In Smooth Muscle Cells Has Modest Effects On Thoracic Aortic Dilatation In Adult Mice

**Sohei Ito,** Satoko Ohno, Michael Franklin, Univ of Kentucky, Lexington, KY; Jessica J Moorlegghen, UNIVERSITY OF KENTUCKY, Lexington, KY; Deborah A Howatt, UNIVERSITY OF KENTUCKY, KY; Hisashi Sawada, Univ of Kentucky, Lexington, KY; Hong S Lu, UNIVERSITY KENTUCKY, Lexington, KY; Alan Daugherty, UNIVERSITY OF KENTUCKY, Lexington, KY

**Introduction:** Fibrillin-1 (*Fbn1*) mutations are associated with thoracic aortic aneurysms (TAAs) in patients with Marfan syndrome. Constitutive deletion of *Fbn1* leads to neonatal death due to aortic rupture in mice. However, the role of *Fbn1* in maintaining aortic integrity during the adult phase remains unclear. Since smooth muscle cell (SMC) is a major constituent of the aortic media, this study examined whether deletion of *Fbn1* in SMCs of adult mice leads to compromise of aortic integrity.

**Methods and Results:** *Fbn1* floxed mice were generated that included insertion of tdTomato as a reporter for gene deletion. Female *Fbn1* floxed mice were bred with male *Fbn1* floxed mice expressing CreER<sup>T2</sup> driven by an *Acta2* promotor. Tamoxifen was injected intraperitoneally for 5 days into male *Fbn1* floxed littermate mice that were either Cre negative or positive (n=6-8/genotype, 5-week-old) to create sm*Fbn1*<sup>+/+</sup> and -/- mice, respectively. Gene recombination was confirmed by the presence of tdTomato in sm*Fbn1*<sup>-/-</sup> mice using PCR and confocal microscopy. To investigate the impact of SMC-specific *Fbn1* deletion, male sm*Fbn1*<sup>+/+</sup> and -/- littermates terminated at two intervals, 5 and 36 weeks after completion of tamoxifen injections. In situ aortic images were captured, and aortic diameters were measured at ascending, arch, and descending thoracic aortas. Five weeks after tamoxifen injection, aortic diameters of sm*Fbn1*<sup>+/+</sup> and -/- mice were not different. Despite the long-term deletion of *Fbn1* in SMCs, aortic dilatation was not observed in any regions of aortas in sm*Fbn1*<sup>-/-</sup> mice compared to wild type littermates 36 weeks after tamoxifen injection. Next, we investigated whether *Fbn1* deletion in SMCs augmented angiotensin II (AngII)-induced aortic dilatation. AngII was infused subcutaneously into male sm*Fbn1*<sup>+/+</sup> and -/- littermates for 12 weeks (n=11-12/genotype), started 2 weeks after completion of tamoxifen injections. AngII-induced aortic dilatations were augmented modestly by SMC-specific *Fbn1* deletion (+/+ 1.7±0.0, -/- 1.9±0.1 mm, P=0.047).

**Conclusion:** Deletion of *Fbn1* in SMCs did not cause spontaneous TAA formation and had modest effects on AngII-induced TAAs in adult mice. *Fbn1* in SMCs does not exert a critical role in mice after the aortic structure has formed.

**S.Ito:** n/a. **S.Ohno:** None. **M.Franklin:** None. **J.J.Moorlegghen:** None. **D.A.Howatt:** None. **H.Sawada:** None. **H.S.Lu:** None. **A.Daugherty:** None.

---

P106

Sustained Inhibition Of High Mobility Group Box 1 Mrna By Antisense Oligonucleotides Demonstrated A Protracted Half-life Of The Protein

**Shayan Mohammadmoradi,** Hisashi Sawada, Univ of Kentucky, Lexington, KY; Sohei Ito, Lexington, KY; Dien Ye, Univ of Kentucky, Lexington, KY; Adam E Mullick, Ionis Pharmaceuticals, Inc., Carlsbad, CA; Deborah A Howatt, UNIVERSITY OF KENTUCKY, KY; Michael Franklin, Univ of Kentucky, Lexington, KY; Hong S Lu, UNIVERSITY KENTUCKY, Lexington, KY; Alan Daugherty, UNIVERSITY OF KENTUCKY, Lexington, KY

**Background and Objectives:** High-mobility group box 1 (HMGB1) is a highly conserved nonhistone DNA-binding nuclear protein which is present in almost all eukaryotic cells. HMGB1 is proposed to exert effects

on several forms of vascular disease including atherosclerosis, pulmonary hypertension, and abdominal aortic aneurysm. However, the lack of a viable whole-body genetic deletion has increased interest in pharmacological approaches to sufficiently inhibit HMGB1 to investigate its role in pathological conditions. In the current study, we assessed the efficacy of a novel antisense oligonucleotides (ASOs) approach to deplete HMGB1 in mice. **Methods and Results:** Either ASOs (25 mg/kg/day) or phosphate-buffered saline (PBS) were injected intraperitoneally into male C57BL/6J mice (8-10-week-old). ASOs were injected at day 0 and day 3 in the initial week and once a week for the duration of the study. Mice were terminated at either 2, 4, or 12 weeks after the initial injection of ASOs (N = 5/group). Since HMGB1 is highly abundant in kidney and liver, mRNA and protein abundance of HMGB1 were examined subsequently in these organs by qPCR and Western blot analyses. ASO administration resulted in 90% decrease of *Hmgb1* mRNA abundance in kidney and liver by 2 weeks of ASO injection. The decreased *Hmgb1* mRNA abundance was observed consistently at both week 4 and 12. Surprisingly, ASOs failed to deplete HMGB1 protein abundance in kidney and liver at 2- and 4-week time intervals. However, HMGB1 protein abundance was markedly reduced to less than 20% in kidney and liver tissues at week 12, indicating an extended protein half-life. **Conclusion:** These findings reveal the protracted interval need to deplete HMGB1 protein depletion after mRNA inhibition.

**S.Mohammadmoradi:** None. **H.Sawada:** None. **S.Ito:** None. **D.Ye:** None. **A.E.Mullick:** Employment; Significant; Ionis Pharmaceuticals, Inc, Stock Shareholder; Significant; Ionis Pharmaceuticals, Inc. **D.A.Howatt:** None. **M.Franklin:** None. **H.S.Lu:** None. **A.Daugherty:** None.

---

P107

Celastrol Supplementation Profoundly Activates Aortic Mmp-9 And Abolishes Sexual Dimorphism Of Abdominal Aortic Aneurysm In Mice.

**Aida Javidan,** UNIVERSITY OF KENTUCKY, Lexington, KY; Weihua Jiang, Lihua Yang, Univ of Kentucky, Lexington, KY; Venkateswaran Subramanian, UNIVERSITY OF KENTUCKY, Lexington, KY

**Background and Objective:** Abdominal Aortic Aneurysms (AAAs) are permanent dilations of the abdominal aorta with greater than 80% mortality after rupture. AAA prevalence is 4-5 times greater in males than females. AAA formation involves a complex process of destruction of aortic media through degradation of extracellular matrix proteins, elastin and collagen. Angiotensin II (AngII) infusion model of AAA in mice recapitulates major features of human AAA mainly male gender specificity. Celastrol, a pentacyclic triterpene from the root extracts of Thunder God Vine (*Tripterygium wilfordii*), strongly suppressed AngII-induced cardiovascular complications in mice. The purpose of this study is to test the effect of Celastrol supplementation on AngII-induced AAAs in mice. **Methods and Results:** Male and female LDL receptor -/- mice (8 weeks old; n= 12 per group) were fed a fat-enriched diet (21% wt/wt fat; 0.15% wt/wt cholesterol) supplemented with or without Celastrol (10mg/kg/day) for 5 weeks. After 1 week of diet feeding, mice were infused with AngII (500 or 1000 ng/kg/min) for 28 days by osmotic minipumps. Dietary supplementation of celastrol significantly promoted AngII-induced abdominal aortic luminal dilation (Con =  $1.25 \pm 0.05$  versus Celas =  $1.55 \pm 0.09$  mm,  $P < 0.05$ ) and external aortic width (Con =  $1.01 \pm 0.09$  versus Celas =  $1.62 \pm 0.14$  mm,  $P < 0.05$ ) in male mice as measured by ultra-sonography and ex vivo measurement, with 90% incidence (10/11) compared to 36% (4/11) in control group. Interestingly, celastrol supplementation to AAA female mice, resulted in a significant increase in AngII-induced aortic luminal dilation (Con =  $1.17 \pm 0.30$  versus Celas =  $1.57 \pm 0.21$  mm,  $P < 0.001$ ) and AAA formation (Con =  $0.94 \pm 0.03$  versus Celas =  $1.36 \pm 0.25$  mm,  $P < 0.05$ ) mice with 80% incidence (12/15) compared to 6% (1/15) in control group. Celastrol supplementation dramatically increased AngII-induced aortic leukocyte accumulation, MMP-9 activity and medial elastin degradation in both male and female mice compared to saline and AngII controls. **Conclusion:** These findings demonstrate that celastrol supplementation to LDLR -/- mice ablates sexual dimorphism and promotes AngII-induced AAA formation, which is associated with increased leukocytic infiltration and MMP-9 activation.

**A.Javidan:** n/a. **W.Jiang:** None. **L.Yang:** None. **V.Subramanian:** None.

## Inflammatory Factors And Metalloproteinases Levels Are Elevated In Aorta Of Patients With Abdominal Aortic Aneurysm

**Jessyca Michelin Barbosa** 1, Carlos A Corsi 1, Fabíola L Mestriner 1, Carolina D Mesquita 1, Ariel E Couto 1, Lígia C Campos 1, Vinícius F Dugaich 1, Faculty of Med of Ribeirão Preto - Univ of São Paulo, Ribeirão Preto, Brazil; Maria Cecília Jordani 1, Edwaldo E Joviliano 1, Faculty of Med of Ribeirão Preto - Univ of São Paulo, string:BEBEDOURO, Brazil; Paulo Roberto B Évora 1, Faculty of Med of Ribeirão Preto - Univ of São Paulo, Ribeirão Preto, Brazil; Katarzyna Polonis 2, Clínica Mayo, Rochester, MN, Brazil; Maurício S Ribeiro 1, Christiane Becari 1, Faculty of Med of Ribeirão Preto - Univ of São Paulo, Ribeirão Preto, Brazil

**Introduction:** The pathophysiology of abdominal aortic aneurysm (AAA) remains poorly understood. The identification of the mechanisms involved in growth, progression, and the risk of aortic rupture could bring a novel treatment perspective and improve patient outcomes. Inflammatory mediators and metalloproteinases (MMPs) 2 and 9 have been shown to contribute to the pathophysiology of AAA in humans. It is widely recognized that these mediators produce both local (tissue) and systemic (circulation) responses. Therefore, in this study, we sought to characterize the inflammatory and MMP-2 and MMP-9 profiles in the aorta and plasma in patients with AAA. **Methodology:** Plasma and aorta tissue from AAA patients (n=31) were obtained during conventional AAA correction surgeries at Ribeirão Preto Medical School Hospital-University of São Paulo. The control samples were obtained from organ donors without AAA (n=15). The levels of inflammatory markers (IL-6, IL-8, TGFbeta) and MMPs were measured by radioimmunoassay and zymography, respectively, in plasma and aorta. **Results:** Levels of IL-6 (p=0.001), IL-8 (p=0.01) and TGF beta (p=0.05) were significantly elevated in the aorta of AAA patients, but not in plasma, when compared to control group. Interestingly, levels of IL-6 (p=0.05) and IL-8 (p=0.02) were lower both in the aorta and plasma of controls. MMP-2 and MMP-9 levels were upregulated in plasma (p=0.02 and p=0.0007, respectively) and in aorta (p=0.017 and p=0.03, respectively) of AAA patients when compared to controls. The tissular levels of MMP-2 and MMP-9 were upregulated in the aorta in both AAA patients (p=0.001 and p=0.0001, respectively) and controls (p=0.008 and p=0.001, respectively) when compared to plasmatic levels of respective groups. **Conclusion:** Our data show that a profile of AAA patients is characterized by locally elevated inflammation factors and MMPs, and systemically elevated MMPs levels. This might suggest that the local response in aortas is an important pathway in the pathophysiology of AAA development.

**J. Michelin barbosa:** Research Grant; Significant; The São Paulo Research Foundation, FAPESP. **P.B. Évora:** n/a. **K. Polonis:** n/a. **M.S. Ribeiro:** n/a. **C. Becari ribeiro:** n/a. **C.A.C. Corsi:** n/a. **F.L.M. Mestriner:** None. **C.D.M. Mesquita:** n/a. **A.E.C. Couto:** n/a. **L.C.B. Campos:** n/a. **V.F.D. Dugaich:** n/a. **M. Jordani:** n/a. **E.E. Joviliano:** None.

## Angiotensin 1-7 Attenuates Angiotensin II-induced Aortic Aneurysm In A Preclinical Murine Model

**Anshul Jadli**, Univ of Calgary, Calgary, AB, Canada; Karina Gomes, Noura Ballasy, Vaibhav B Patel, Univ of Calgary, Calgary, AB, Canada

**Background:** Aortic aneurysm (AA) is a vascular disease that involves extracellular matrix degeneration of the aorta wall leading to dilatation and eventually aorta wall rupture. Aortic aneurysms contribute significantly to global morbidity and mortality due to vascular diseases. Elusive pathophysiology of initiation and progression of aortic aneurysm led to the absence of clinically relevant therapeutic interventions against aortic aneurysm. Though the role of AngII in the development and progression of AA is widely studied, the effect of Ang 1-7 on hallmarks of AA i.e. SMCs apoptosis, aorta matrix remodeling, and inflammation are poorly understood. **Methods and Results:** In the present study, we have investigated Ang 1-7-mediated protective effect on the AngII-infused murine model. AngII-infused ApoEKO murine model showed aortic dilatation in the thoracic and abdominal region with matrix remodeling. Infusion of Ang 1-7 rescued the phenotype evident by echocardiography. While histology staining showed excessive matrix remodeling i.e. collagen deposition in thoracic aorta and immunofluorescence showed VSMCs cell death in the abdominal aorta, suggesting different mechanisms underlying the development of TAA and AAA. The inflammatory markers, MMP2, MMP9, and TNF- $\alpha$  were significantly reduced in the thoracic aorta post-infusion of Ang 1-7. The Ang 1-7 treatment led to a reduced phenotypic switch in abdominal VSMCs



evident by increased expression of ACTA2, MyH11, Calponin and reduced expressions of MMP2, MMP9, Collagen I, and collagen III. The apoptosis assay using flow cytometry showed attenuation of cell death of abdominal VSMCs after infusion of Ang 1-7 in a murine model of AA. The analysis of apoptosis-associated proteins, Caspase 3 and 8, showed reduced expression in the abdominal aorta. **Conclusion:** The study showed mitigation of AngII-mediated AA by Ang 1-7 infusion. Ang 1-7 treatment attenuated AngII-induced TAA by suppressing aortic matrix remodeling and AAA by inhibiting VSMCs apoptosis and vascular inflammation. Ang 1-7 can be a potential therapeutic alternative for the treatment of AA.

**A.Jadli:** None. **K.Gomes:** None. **N.Ballasy:** None. **V.B.Patel:** None.

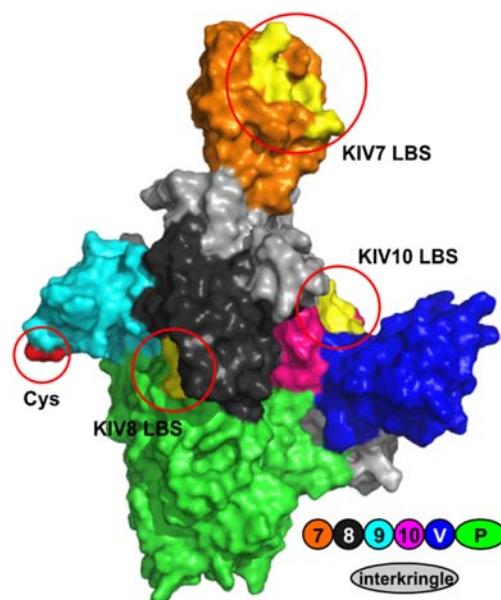
---

P110

# Molecular Modeling Of Apolipoprotein(a): Insight Into The Orientation Of Key Functional Domains Mediating Lipoprotein(a) Assembly And Ligand Binding

Luke G Daichendt, Robert Szabla, Murray S Junop, Marlys L Koschinsky, **Michael B Boffa**, The Univ of Western Ontario, London, ON, Canada

The apo(a) component of Lp(a) plays a major role in mediating the pathological effects of Lp(a) in vascular disease. Apo(a) is composed of repeating kringle (K) domains, of which 10 types are unique (KIV1; KIV3-KIV10; KV) and one (KIV2) is present in variable numbers. KIV7 and KIV8 contain weak lysine binding sites (LBS) that play a role in Lp(a) assembly and KIV10 contains a strong LBS important for binding of Lp(a) to biological substrates and the attachment of pro-inflammatory oxidized phospholipids. Following the kringle domains is an inactive protease domain. While the structures of individual kringles have been solved, no structural information exists on intact apo(a). We therefore performed *in silico* molecular modeling of apo(a) KIV7-protease. This region contains the key functional domains of apo(a) and has a similar topology to plasminogen. The structures of human, rhesus monkey (lacking the KIV10 strong LBS) and baboon (lacking KV) apo(a) were modeled with Swiss-Model using the crystal structure of the closed conformation of full-length plasminogen (pdb: 4A5T) as the template, followed by energy minimization using Rosetta Relax. The lowest energy human apo(a) model represented a compact, plasminogen-like, tertiary structure that promoted high solvent exposure of the KIV7 LBS and the KIV9 unpaired cysteine, moderate exposure of the KIV10 LBS, and low exposure of the KIV8 LBS. Interestingly, there was substantial variability in the energy minimized models; of the 10 lowest energy models from Rosetta Relax, two showed notable translation of the protease domain resulting in increased solvent exposure of KIV8 at the expense of KIV10. The rhesus and baboon models were highly similar to human but showed much less variability in energy minimized models. Our findings show that not all key sites in apo(a) are highly solvent exposed, but the flexibility of human apo(a) structure suggests the possibility of conformational changes that could alter their accessibility.



**L.G.Daichendt:** None. **R.Szabla:** n/a. **M.S.Junop:** None. **M.L.Koschinsky:** Honoraria; Modest; Eli Lilly, Other; Modest; Sanofi, Amgen, Other Research Support; Modest; Sanofi, Ionis, Eli Lilly, Abcentra, Research Grant; Significant; Canadian Institutes of Health Research, Heart and Stroke Foundation of Canada, Natural Sciences and Engineering Research Council of Canada, Pfizer, Speaker/Speaker's Bureau; Modest; Amgen, Regeneron. **M.B.Boffa:** Other Research Support; Modest; Ionis, Research Grant; Significant; Canadian Institutes of Health Research, Natural Sciences and Engineering Research Council of Canada.

---

P111

#### Effects Of Magnetic Field On Abca1-mediated Cellular Lipid Release And Adult Brain Cell Generation In Mice

**Maki Tsujita,** Hiroshi Takase, Natsuko Kumamoto, Shinya Ugawa, NAGOYA CITY UNIV GRADUATE SCH, Nagoya, Japan; Yoshito Furuie, Motonari Tsubaki, Kobe Univ Graduate Sch of Science and Technology, Kobe, Japan

**Aim:** This project aims to explore a novel magnetic field (MF) health care based on the cholesterol metabolism. **Methods:** Mouse peritoneal macrophages foam cells were incubated in CO<sub>2</sub>-independent culture medium containing apoA-I and were exposed in a MF (0.4 T) using the electromagnet of EPR spectrometer. C57BL/6N mice (8 week-old) were peritoneally injected F-ara-EdU (133µg/g mouse body weight) then exposed to MF under the identical condition. Mouse plasma, cerebrospinal fluid, liver and brain were harvested on the 28<sup>th</sup> day. Lipoprotein profiles were examined enzymatic detection followed by a gel-permeable-HPLC (Skylight Biotech Inc.). Amyloid β40 and β42 levels were determined by WAKO ELISA kit. Fixed mouse brain sections (40µm) were prepared by Leica CM1900 cryostat. Alexa fluor® 488 conjugates were link to F-ara-EdU by a click chemistry method and fluor positive nucleus images were captured by a confocal super resolution SpinSR10 (Olympus, Inc.). **Results:** ABCA1-apoA-I mediated cellular cholesterol release was not affected or reduced by the exposure in the MF of 0.4 T. The *Pcsk9* expression showed significant reduction in the hepatocytes. Reduction of *Abca1* expression and increase of *Scarb1* were obtained non significantly. The newly generated hippocampal dentate gyrus cells in the control mice group and the MF exposed group were 1.6±1.17, and 0.47±0.62 cells per dentate gyrus section, respectively (P=0.003) despite bulk of new cells in olfactory bulbs in the both groups. **Discussions:** No substantial increase in cellular cholesterol export was observed by MF irradiation of mouse peritoneal macrophage cells. In addition, the lipoprotein profile showed a decrease in HDL cholesterol even after 28 days. As a result of gene expression in the liver, a decrease in ABCA1 expression and an increase in SR-BI expression inferred reduction of HDL. The number of new cells detected in the granular zone and the subgranular zone in the dentate gyrus of the hippocampus was significantly reduced in the mice subjected to the MF treatment. In the future, it is necessary to investigate in detail whether these newborn cells are neuron or glial cells.

**M.Tsujita:** None. **H.Takase:** n/a. **N.Kumamoto:** n/a. **S.Ugawa:** n/a. **Y.Furuie:** n/a. **M.Tsubaki:** n/a.

---

P112

#### A Simple, Rapid, And Sensitive Fluorescence-based Method To Assess Triacylglycerol Hydrolase Activities

**Sujith Rajan,** Hazel C De Guzman, NYU Long Island Sch of Med, Mineola, NY; Thomas Palaia, NYU Winthrop Hosp, Mineola, NY; Ira J Goldberg, NYU Langone Health, New York, NY; Mahmood Hussain, NYU Long Island Sch of Med, Mineola, NY

**Introduction:** Lipases constitute an important class of water-soluble enzymes that catalyze the hydrolysis of hydrophobic triacylglycerol (TAG). Their activity is usually measured after isolation and quantification of the hydrolyzed free fatty acids. We have used NBD-labeled lipids previously to develop TAG, cholesteryl ester, and phospholipid transfer assays for microsomal triglyceride transfer protein. To date, however, NBD-labeled TAG (NBD-TAG) has not been used to assess the enzymatic activities of different lipases. **Methods:** We developed methods to measure lipase activities using adipose triglyceride lipase (ATGL), lipoprotein lipase (LpL), and pancreatic triglyceride lipase (PNLIP) as model lipases. In these assays, we incubated a source of ATGL, LpL, or PNLIP with substrate emulsions containing nitrobenzoxadiazole (NBD)-labeled TAG in phosphatidylcholine (PC) and phosphatidylinositol (PI), measured increases in NBD fluorescence with time, and calculated enzyme activities. **Results:** Incorporation of NBD-TAG into PC vesicles resulted in some hydrolysis; but required

product isolation step to measure NBD fluorescence. However, incorporation of PI into these NBD-TAG/PC vesicles significantly increased substrate hydrolysis in time, protein, and substrate concentration dependent manner negating the need to isolate products to measure lipase activities. Further, increasing the ratio of NBD-TAG to PC enhanced substrate hydrolysis. Next, we tested specific lipase inhibitors and found that orlistat inhibits all three enzymes indicating that it is a pan-lipase inhibitor. **Conclusions:** We describe a simple, rapid fluorescence-based TAG hydrolysis assay to assess three major TAG hydrolases: ATGL localized intracellularly, LpL localized at the extracellular endothelium, and PNLIP produced and secreted from the pancreas into the intestinal lumen. The major advantages of this method are its speed, simplicity, and avoidance of a product isolation step. This assay is potentially applicable to a wide range of lipases and is amenable to high-throughput screening to discover novel modulators of triacylglycerol hydrolases, and in the diagnosis of diseases associated with increases in plasma lipase activities.

**S.Rajan:** None. **H.De guzman:** None. **T.Palaia:** None. **I.Goldberg:** n/a. **M.Hussain:** n/a.

---

P113

Multi Omics Analysis Identified Fndc1 And Mxra5 As Novel Extracellular Matrix Proteins In Aortic Stenosis

**Rihab Bouchareb,** CVRI, Mount Sinai, New York, NY; Sandra Guaque-Orlate, Univ Cooperativa de Colombia, Colombia, Colombia; Justin Snider, Stony Brook Univ Cancer Ctr, New York, NY; Devyn Zaminski, Dept of pathology, New York, NY; Anelechi Anyanwu, CVRI, New York, NY; Paul Stelzer, Surgery department, New York, NY; Djamel Lebeche, ICAHN SCHOOL OF MEDICINE MT SINAI, New York, NY

Calcified aortic valve disease (CAVD) affects over six million Americans and is associated with changes in valve leaflets' mechanical properties, resulting in impaired valvular blood flow. Currently, there is no viable pharmacological treatment to stop the disease's progression or activate mineral regression. The only effective therapy to treat CAVD is aortic valve replacement (AVR) or transcatheterization (TAVR). Therefore, it is imperative to understand the molecular mechanisms leading to aortic valve mineralization to identify new pharmacological targets. In this work, we examined the expression of extracellular matrix proteins (ECM) during valve calcification. Method: We used both RNAseq (n=18) and Proteomics (n=15) on explanted human valves of two different human cohorts to study the modulation of ECM proteins. Proteins were isolated from the fibrotic and the calcific side of each valve tissue. We next confirm our data in isolated human valve cells. Cells were treated with calcifying medium for one week and secreted ECM proteins were analyzed at different time points: Baseline, 3 days, and 7 days. Results: our network analysis revealed an interaction between ECM, metabolic, complement, and lipids transporters proteins. We identified SPP1, VTN, THSB2, MATN2, FNDC1, and MXRA5 as the common modulated ECM protein in both RNAseq and proteomics data set. Conclusion: This study yields new insight into ECM proteins expression during the aortic valve calcification process, and identified two new ECM proteins, MXRA5 and FNDC1, in aortic stenosis. The disruption of ECM proteins was more significant in the calcified stage and it was accompanied by a down-regulation of many metabolic enzymes.

**R.Bouchareb:** None. **S.Guaque-ortlate:** n/a. **J.Snider:** n/a. **D.Zaminski:** n/a. **A.Anyanwu:** n/a. **P.Stelzer:** n/a. **D.Lebeche:** None.

---

P114

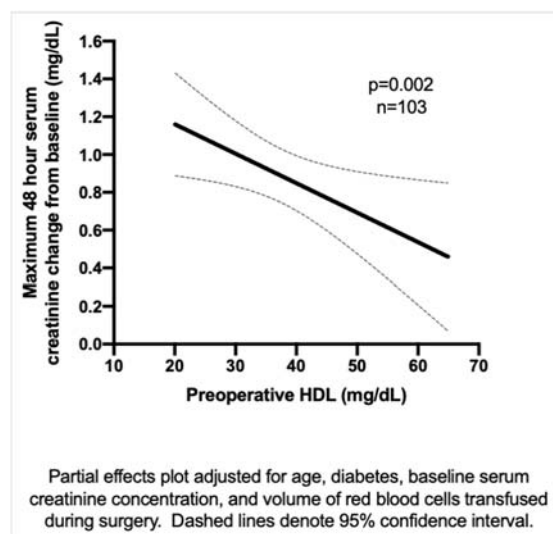
Statins, High-density Lipoprotein, And Acute Kidney Injury After Endovascular Aortic Repair

**Jordan T Patrick,** Meharry Medical Coll, Nashville, TN; Derek K Smith, Loren E Smith, Vanderbilt Univ Medical Ctr, Nashville, TN

Acute kidney injury (AKI) after endovascular aortic repair (EVAR) occurs in 20% of patients and is an independent predictor of death. Higher preoperative high-density lipoprotein (HDL) cholesterol concentration before revascularization of chronic limb ischemia is associated with a lower risk of AKI. Further, preoperative statin use has been shown to be associated with a decreased risk of AKI after EVAR. We hypothesized that both preoperative statin use and higher preoperative HDL are associated with a lower risk of AKI in patients undergoing EVAR. Charts from adult patients that underwent EVAR were selected using the ICD codes (n=251). Each chart was reviewed for demographic and medical information, preoperative and postoperative serum creatinine concentrations, and preoperative HDL concentration. One hundred and three patients had available statin

medication, serum creatinine, and HDL concentrations. The associations between statin dose, HDL concentration and maximum serum creatinine change from baseline in the first 48 postoperative hours was assessed using multivariable linear regression models, adjusted for AKI risk factors. Preoperative HDL concentration was not correlated with preoperative statin dose (Pearson's  $R=0.0515$ ,  $p=0.57$ ). Higher preoperative statin doses (atorvastatin equivalents) and higher preoperative HDL concentrations were associated with lower serum creatinine rise ( $p=0.042$  and  $0.002$  respectively, Figure). When both preoperative statin dose and preoperative HDL concentration were included in the model, both variables lost significance, suggesting HDL may mediate the relationship between preoperative statin dose and postoperative AKI.

Higher preoperative HDL concentrations and statin doses were associated with less postoperative AKI. Future work involves identifying the biological mechanism underlying these associations as a first step towards developing new therapies to prevent AKI following EVAR.



J.T.Patrick: None. D.K.Smith: n/a. L.E.Smith: n/a.

P115

## Building A Structurally Sound System To Understand SR-BI Function

**Hayley R Powers**, Shawn E Jenjak, Brian F Volkman, Daisy Sahoo, Medical Coll of Wisconsin, Milwaukee, WI

The interaction of scavenger receptor BI (SR-BI) and high density lipoproteins (HDL) is the key step for the bodily removal of cholesterol. The HDL/SR-BI interaction is one of the concluding steps of the reverse cholesterol transport (RCT) pathway. In RCT, cholesterol within atherosclerotic plaques is taken up by HDL particles, which then dock on SR-BI at the surface of the liver, where cholesterol can be delivered converted into bile for excretion. Humans with mutations in the gene encoding SR-BI display elevated HDL-cholesterol levels and an increased risk of cardiovascular disease (CVD). Therefore, understanding the interaction between HDL and SR-BI is crucial to discovering ways to lower plasma cholesterol and modulate CVD risk. Due to the importance of SR-BI, the goal of these studies is to resolve a structure of functional full-length human SR-BI. We have expressed and purified full-length SR-BI using an insect cell Sf9 system. In order to assess SR-BI's functions within this system, Sf9 cells were infected with baculovirus encoding empty vector or SR-BI, or left uninfected and plated into culture dishes. Expression of SR-BI significantly increased HDL cellular association and uptake of HDL-cholesteryl esters compared to empty vector and uninfected cells. Additionally, free cholesterol efflux was increased upon SR-BI expression. Lastly, SR-BI in Sf9 cells maintained its ability to form higher order oligomers in cells, which is crucial, as SR-BI oligomerization is important in cholesterol transport. Additionally, size exclusion chromatography shows that purified SR-BI is able to form oligomers in micelles. Lastly, using microscale thermophoresis, we demonstrated that purified SR-BI binds to its ligands (apolipoprotein A-I, holoparticle HDL, and oxidized LDL) with high affinity, regardless of the glycosylation state of SR-BI. Together, these assays represent the first steps in resolving a high-resolution structure of human full-length SR-BI and provide promise for delineating the ways in which the HDL/SR-BI relationship allows for efficient cholesterol clearance.

H.R.Powers: None. S.E.Jenjak: None. B.F.Volkman: n/a. D.Sahoo: None.

### Exercise And Quercetin Synergistic Effects On Omega 3 And 6 Fatty Acids In Mice Livers

Chinedu C Ochinn, UNIVERSITY OF MASSACHUSETTS, Lowell, MA; Emily Punch, N Chelmsford, MA; Halleh Mahini, **Mahdi O Garelnabi**, Univ of Massachusetts, Lowell, MA

**Synopsis:** omega 3 and omega 6 fatty acids are important precursors for the synthesis of other fatty acids and they play vital roles in many metabolic processes in health and diseases. **Objectives/Purpose:** Exercise and the use of antioxidants such as quercetin have been demonstrated to favorably modulate long chain fatty acid metabolism beneficial role in cardiovascular health. This study investigates the interactive effect of exercise and quercetin intake on hepatic omega-3 and omega-6 fatty acids. **Method:** Four groups of (10 each) C57BL6 LDLr -/- mice as follows; untreated control mice (NN), 100ug/day of Quercetin fed mice (NQ), exercise only mice (NE) and combined exercise with quercetin fed mice (EQ), were all fed an atherogenic diet for 30 days. The exercise groups were placed on an exercise regimen of 30 minute run for 5 days/week for 30 days. All animals were subsequently sacrificed, livers harvested and homogenized for lipid extraction and derivatization for GCMS analysis. The analysis was performed using a Shimadzu GCMS-QP2010 Plus instrument with an Agilent HP-5MS; 30m, 0.25mm, 0.25um column. Statistical analysis was performed using descriptive statistics, one-way and two-way ANOVA with statistical significance set at a  $p \leq 0.05$ . **Result:** There was statistically significant decrease of both omega 3 ( $p \leq 0.0002$ ) and omega 6 ( $p \leq 0.0001$ ) fatty acids in all groups when compared to the control. The interaction effect of exercise administration and quercetin supplementation (EQ) on the combined reduction of liver  $\omega$  3 and  $\omega$  6 fatty acids was also statistically significant ( $p \leq 0.009$ ). **Conclusion:** The results demonstrate that the use of quercetin antioxidant, exercise or the combination reduces both hepatic  $\omega$ 3 and  $\omega$ 6 fatty acids accumulation in LDLr deficient animal models fed atherogenic diet. This reduction was accompanied with a 78% drop in the atherosclerotic plaque development in exercising group compared to non-exercising mice and also accompanied with changes in plasma lipids and inflammatory markers.

**C.C.Ochinn:** n/a. **E.Punch:** None. **H.Mahini:** n/a. **M.O.Garelnabi:** None.

### The 15-lipoxygenase-derived Oxylipins 15-HETrE And 15-HETE Inhibit Platelet Activation In Part Through Activation Of PPARs

**Adriana Yamaguchi**, Benjamin E Tourdot, Jennifer Yeung, Univ of Michigan, Ann Arbor, MI; Theodore Holman, UC Santa Cruz, Santa Cruz, CA; Michael A Holnstat, Univ of Michigan, Ann Arbor, MI

Cardiovascular disease is the leading cause of mortality in the US annually. The underlying cause of mortality in cardiovascular disease is the formation of platelet-rich clots that occlude blood vessels due to aberrant platelet activation. While antiplatelet therapeutic intervention has significantly reduced the risk of an occlusive thrombotic event, many patients remain at risk for a myocardial infarction or stroke. The antiplatelet and antithrombotic effects of omega-6 polyunsaturated fatty acids are primarily attributed to its metabolism to bioactive metabolites by oxygenases such as lipoxygenases (LOX). LOXs are a group of lipid-peroxidizing enzymes named according to the specific position where they add an oxygen to arachidonic acid: 5-LOX, 12-LOX, and 15-LOX. Previous studies from our group have demonstrated that dihomo- $\gamma$ -linolenic acid and arachidonic acid regulate platelet function through their respective 12-LOX-derived oxylipins, 12(S)-hydroxyeicosatrienoic (12-HETrE) and 12(S)-hydroxyeicosatetraenoic acid (12-HETE). While the expression of 15-LOX in platelets is controversial, platelets have demonstrated the ability to generate the 15-LOX-derived bioactive metabolites. In this study we sought to elucidate the mechanistic effects of 15(S)-hydroxyeicosatrienoic acid (15-HETrE) and 15(S)-hydroxyeicosatetraenoic (15-HETE) on platelet reactivity. Washed human platelets were treated with 15-HETrE or 15-HETE and platelet aggregation, integrin  $\alpha$ IIb $\beta$ 3 activation, calcium mobilization, and granule secretion were quantified. Both 15-HETrE and 15-HETE were shown to inhibit platelet aggregation mediated by collagen. In comparison to vehicle-treated platelets, treatment with 15-HETrE or 15-HETE inhibited agonist-induced intracellular signalling events, including PKC activation, calcium mobilization, and granule secretion. Surprisingly, while 15-HETrE was shown to inhibit platelets through a signalling cascade involving the activation of PPAR $\beta$ , 15-HETE's inhibitory effect was shown to involve the activation of PPAR $\alpha$  and the inhibition of 12-HETE production. A better understanding of the effects of 15-LOX oxylipins in platelets could lead to the identification of novel antiplatelet therapies.

**A. Yamaguchi:** None. **B.E. Tourdot:** None. **J. Yeung:** None. **T. Holman:** None. **M.A. Holinstat:** Ownership Interest; Significant; Veralox Therapeutics. Research Grant; Significant; National Institutes of Health.

---

P120

Heparin-warfarin Therapy Could Be An Alternative Treatment For Diabetes Mellitus In Addition To Being A Standard Therapy For Pulmonary Vein Thrombi.

**Hidekazu Takeuchi,** Takeuchi Naika Clinic, Ogachi, Japan

**Background:** Our previous study showed that warfarin or direct oral anticoagulants (DOACs) dissolved pulmonary vein thrombi (PVTs). However, in some instances, warfarin or DOACs could not dissolve PVT. It is unclear whether heparin-warfarin therapy affects PVT and diabetes mellitus (DM). **Methods and Results:** Our patient was a 74 year-old male. The patient had cerebral infarction one year prior; at that time, he was not treated with any medications. The patient was examined, and it was found that he had diabetes mellitus, hypertension and dyslipidemia. His HbA1c was 9.5%. The patient was treated with medications including ipragliflozin L-proline (50 mg), sitagliptin (50 mg), repaglinide (0.25 mg) and clopidogrel (75 mg). One year after discharge, we detected PVTs in the patient's left lower pulmonary vein (LLPV) via cardiac CT and transesophageal echocardiography (TEE). He was treated with standard doses of heparin and warfarin after stopping clopidogrel. The patient's HbA1c was 6.2% at admission. After one month of treatment with heparin-warfarin, the PVTs were almost dissolved. The patient showed a tendency of hypoglycemia the day after admission, so the three glucose-lowering medications were discontinued within nine days. One month later, HbA1c was 6.1% without DM medications. After discharge, warfarin was continued, and blood glucose levels gradually increased. Three months later, HbA1c was 7.3%, and 4 months later, HbA1c was 7.8%, so DM medications were restarted. PVTs can release microclots, which can occlude the microvessels of all organs, leading to cell dysfunction. Heparin-warfarin can decrease microclots and reopen microvessels. Thus, blood glucose could be taken into cells, decreasing blood glucose levels. There is a possibility that DM could be prevented if we treat PVTs in their early stage. Compared to other similar cases, this patient showed hypoglycemia rather early, which might be caused by the interaction between repaglinide and clopidogrel. **Conclusion:** One month of heparin-warfarin therapy almost completely dissolved PVTs. During that course, DM medications were stopped in order to prevent hypoglycemia. During the next four months of warfarin therapy, the blood glucose levels gradually increased without DM medications.

**H.Takeuchi:** None.

---

P121

Combining Extracellular Matrix Biomarkers Using Cluster Analysis More Accurately Predicts The Development Of Systolic Dysfunction In Acute Myocardial Infarction Compared To Single Biomarker Analysis

**Morgane Brunton-O'Sullivan,** Ana Holley, Univ of Otago, Wellington, New Zealand; Bijia Shi, Scott Harding, Capital & Coast District Health Board, Wellington, New Zealand; Peter Larsen, Univ of Otago, Wellington, New Zealand

**Introduction.** The extracellular matrix (ECM) is central to cardiac repair following acute myocardial infarction (AMI), and pathological ECM activity may result in adverse ventricular remodeling. Systolic dysfunction is a manifestation of adverse remodeling, and the utility of combined biomarker analysis for prognosis remains undetermined. Cluster analysis is a statistical methodology that can combine biomarkers, while also accounting for collinearity. **Hypothesis.** In this study, we assessed the hypothesis that combining biomarkers using cluster analysis may more accurately predict the development of systolic dysfunction in AMI patients when compared to single biomarker analysis. **Methods.** In a cohort of 120 AMI patients, plasma levels of matrix metalloproteinase (MMP) -3, -8, -9 and tissue inhibitor of matrix metalloproteinase-1 (TIMP-1) were measured using ELISA and multiplexing assays during hospital admission. All patients had an echocardiogram within 1 year of AMI (median [IQR], 145 [89 - 252] days). Patients were divided into impaired (n=37, LVEF <50%) and preserved (n=83, LVEF ≥50%) systolic function. Hierarchical clustering was performed using Ward's method of minimum variance. Mann-Whitney U and Chi-Squared testing was performed for univariate analysis, and binary logistic regression was performed for multivariate analysis. **Results.** Upon univariate analysis, current smoking, prescription of ACE inhibitor

at discharge, peak Troponin T > 610 ng/L (median), and MMP-8 levels were predictive of impaired systolic function. Cluster analysis partitioned patients into two clusters (Cluster One, n=31; Cluster Two, n=89). Cluster One comprised a higher proportion of patients with impaired systolic function when compared to Cluster Two (15 out of 31 [48.4%] versus 22 out of 89 [24.7%]). Upon multivariate analysis, Cluster One assignment (odds ratio [95% CI], 2.74 [1.04-7.23], p=0.04) remained an independent predictor of systolic dysfunction in combination with clinical variables, while MMP-8 levels did not (3.43 [0.32-36.68], p=0.308). **Conclusion.** Findings from our study demonstrate a combined biomarker approach outperforms single biomarker analysis for predicting the development of systolic dysfunction following AMI.

**M.Brunton-osullivan:** None. **A.Holley:** None. **B.Shi:** None. **S.Harding:** None. **P.Larsen:** None.

---

P122

#### Leveraging Machine Learning Models For Dynamic Prediction Of Bleeding And Ischemic Risk After Drug-eluting Stent Implantation

**Fang Li**, Laila Bekhet, Univ of Texas Health Science Ctr at Houston, Houston, TX; Yang Xiang, Pengcheng Lab, Shenzhen, China; Jingna Feng, Jingcheng Du, Univ of Texas Health Science Ctr at Houston, Houston, TX; David Aguilar, Univ of Texas Health Science, Houston, TX; Abhijeet Dhoble, Univ of Texas Health Science, Houston, TX, houston, TX; Qing Wang, Shuteng Niu, Xinyue Hu, Yifang Dang, Degui Zhi, Univ of Texas Health Science Ctr at Houston, Houston, TX; Cui Tao, Univ of Texas Health Science, Houston, TX

**Background:** Contemporary risk scores for ischemic or bleeding endpoint prediction after drug-eluting stent (DES) implantation have limited predictive accuracy and fixed prediction windows.

**Objective:** This study aimed to dynamically predict the ischemic and bleeding risks in different follow-up windows for patients with DES leveraging cutting-edge machine learning models.

**Methods:** Using the Cerner Health Facts, we identified 98,236 adult patients who received DES with more than three months of follow-up after discharge. Three traditional machine learning models (LR, RF, and LGBM), three RNN-based deep learning models (GRU, LSTM, RETAIN), and one transformer-based model (Med-BERT) were applied for the risk stratification. The total follow-up window covered two years after discharge. ML models were tested in three types of prediction windows with varying lengths (i.e., one year, six months, and three months). Model performance was assessed according to a range of learning metrics including area under the receiver operating characteristic curve (AUC) and precision-recall curve.

**Results:** For bleeding event prediction, the best AUC for the three-month window was 77.02% (GRU), for the six-month window was 81.11% (BiGRU + MedBert), and for the one-year window is 71.86% (LGBM). For ischemic event prediction, the best AUC for the three-month window was 71.09% (GRU), for the six-month window was 68.97% (LGBM), for the one-year window was 69.41% (LSTM). The transformer-based model and RNN-based models generally performed better than the traditional ML in both bleeding and ischemic risk prediction.

**Conclusions:** Our machine learning model-based approaches for dynamically predicting the ischemic and bleeding risks after stenting is feasible and effective. The best-performing models show good discriminative capabilities in different prediction scenarios and have the potential to guide the clinical decision-making of the optimum DAPT duration in a personalized way.

**F.Li:** None. **X.Hu:** n/a. **Y.Dang:** n/a. **D.Zhi:** n/a. **C.Tao:** n/a. **L.Bekhet:** n/a. **Y.Xiang:** n/a. **J.Feng:** n/a. **J.Du:** n/a. **D.Aguilar:** None. **A.Dhoble:** None. **Q.Wang:** n/a. **S.Niu:** n/a.

---

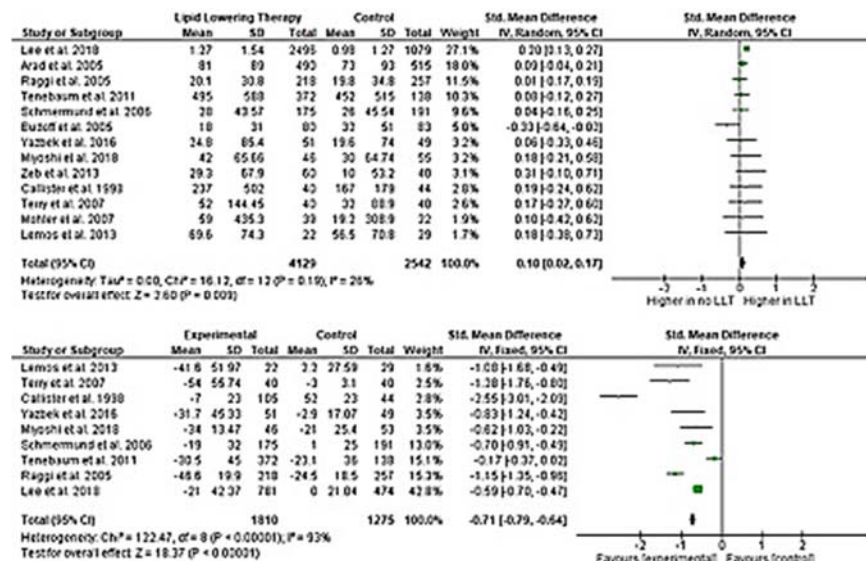
P123

#### Effects Of Lipid Control On Coronary Calcification

**Mustafa Alam**, Olga V Savinova, New York Inst of Technology, Old Westbury, NY

**Introduction:** Lipid lowering drugs are some of the most prescribed medications to control coronary artery disease (CAD). The long-term lipid lowering effects on coronary artery calcium (CAC) progression remain a subject of controversy with inconclusive results from multiple literature reviews. The purpose of this meta-analysis is to elucidate the relationship between lipid control and CAC progression. **Methods:** A computerized search of MEDLINE was conducted using the search terms "coronary", "calcification", "statin", and "lipid lowering." Search filters included studies in English performed on human subjects, clinical trials, and journal articles. Studies were included if they measured mean value changes from

baseline in coronary calcium using cardiac computed tomography. Data were extracted from the articles according to the Cochrane manual. RevMan 5.4 was used to aggregate the studies and report statistics. Results: A total of 13 studies were included with a total of 6671 patients. LDL reduction amongst the studies was significant as compared to placebo or lower dose lipid lowering therapy (standardized mean difference [SMD]: -0.71; 95% CI: -0.79, -0.64;  $p < 0.00001$ ). Study heterogeneity was not significant amongst the CAC progression studies ( $p = 0.19$ ). An increase in CAC was statistically significant (standardized mean difference [SMD]: 0.10; 95% CI: 0.02, 0.17;  $p = 0.009$ ). Conclusion: Lipid lowering therapy shows efficacy in LDL reduction however, it does not lead to coronary calcium reduction. Further studies are needed to elucidate the long-term effects of lipid lowering on CAC and the prognostic value of CAC in CAD patients receiving optimal therapy.



M.Alam: None. O.V.Savinova: None.

P124

Post Acute Infection Of Severe Acute Respiratory Syndrome Coronavirus 2 (SARS-CoV-2) Leads To Systemic Inflammation And Podocyte Injury.

**Seshagiri Nandula**, George Washington Univ, Washington, DC; Sabyasachi Sen, Veterans Affairs Medical Ctr, Bethesda, MD; Beda Brichacek, The George Washington Univ, Washington, DC; Rajesh Naidu Janapala, George Washington Univ, Washington, DC

Introduction: COVID-19 attributed to SARS-CoV2 infection is a world-wide pandemic. SARS-CoV2 has been associated with cardiovascular disease and diabetes. At a cellular level, the infection causes endothelial cell dysfunction (ECD), which is manifested by entities such as microvascular thrombosis. ECD is quite common in type 2 diabetes mellitus (T2DM) where the renal podocyte dysfunction is often an early manifestation of microvascular complication. In this study we explored whether presence of hyperglycemia predisposes to increased SARS-CoV2 infection and whether co-morbid presence of COVID-19 and hyperglycemia predisposes to cardio-metabolic complications such as diabetic kidney disease (DKD). To estimate kidney damage we evaluated albuminuria and podocyte markers in urine exosomes from SARS-CoV2 patients at 10 days, 6 months and 12 months post COVID-19 infection. Methods: Blood and Urine samples from SARS-CoV2 patients post acute phase of infection were procured from the core facility. Peripheral blood mononuclear cells (PBMCs) and urine exosomes were isolated and podocyte protein markers such as Nephron (Nep), Podocalyxin (PODXL) and Wilms' Tumour-1 (WT-1) were identified by western blot analysis. Results: Our results showed that human kidney cells on exposure to hyperglycemia (5 vs 25mM) upregulates expression of TMPRSS2 gene, a key receptor for SARS-CoV2, by 5 fold. Next we examined blood and urine samples from COVID-19, subjects (n=16). As all examined subjects had blood glucose levels above 400mg%, we used samples from T2DM subjects with no COVID-19 infection, as a comparator. COVID-MNCs showed persistent over-expression of IL-6 and TNF $\alpha$  (4-fold) even at 12 months post infection. Urine-exosomal-Nephron protein band expression was 10-fold higher than T2DM-No-COVID urine-exosomal-Nephron protein band Similar trend was noted on estimating PODXL and WT-1.



Conclusions: A persistent inflammatory marker over-expression at 12 months in COVID samples indicate possible long standing renal damage. Increased podocyte specific protein loss at 12 months compared to samples from T2DM subjects with similar GFR also indicates persistent kidney damage which may lead to renal failure and hypertension.

**S.Nandula:** None. **S.Sen:** None. **B.Brichacek:** None. **R.Janapala:** None.

P125

# IL-6-induced Signaling In PD-1<sup>+</sup> CD4 Effector Memory T Cells Is Associated With Human Coronary Pathology

**Hema Kothari**, UNIVERSITY OF VIRGINIA, Charlottesville, VA; Chantel McSkimming, Fabrizio Drago, Univ of Virginia, Charlottesville, VA; Corey Williams, Charlottesville, VA; Eli Zunder, Univ of Virginia, Charlottesville, VA; Coleen McNamara, UNIVERSITY OF VIRGINIA, Charlottesville, VA

**Objective:** Murine data, prospective epidemiological studies, and genetic association data support a potential causal role of IL-6 signaling in atherosclerosis development. IL-6 inhibitors have emerged as potential therapeutics for reducing events in both stable coronary artery disease (CAD) and acute coronary syndromes. IL-6-induced immune regulation plays an important role in atherosclerosis, however, a comprehensive map of IL-6 signaling in human immune cells is currently lacking. We developed a 32-antibody custom mass cytometry (CyTOF) panel to characterize IL-6 signaling across all major human immune cell subsets and applied it to identify IL-6-induced immune signatures linked with unstable atherosclerotic plaque. **Methods:** Peripheral blood mononuclear cells from healthy donors and subjects with CAD undergoing virtual histology-intravascular ultrasound imaging (IVUS-VH) were stimulated with vehicle and IL-6, stained, and ran in CyTOF. Unsupervised analysis algorithms (SPADE, UMAP, and Leiden clustering) were used to identify immune cell subsets and IL-6-induced intracellular phosphorylation status. **Results:** IL-6 induced STAT1 and STAT3 activation in CD4 and CD8 naïve T cell subsets and CD4 memory T subsets. Notably, we identified that IL-6 also activates STAT5 within the CD4 and CD8 naïve T subsets. IL-6 induced a much more robust activation of STAT1 as compared to STAT3 and STAT5. Other cell types such as CD14<sup>+</sup> monocytes, and CD11c<sup>+</sup>, and CD123<sup>+</sup> dendritic cells also showed IL-6-induced STAT activation. IL-6-induced phosphorylation of STAT1 and STAT3 in a novel PD-1<sup>+</sup>CD4<sup>+</sup> effector memory T cell subtype was associated with higher CAD burden and unstable plaque features. **Conclusions:** Findings are significant for mechanistic insights into IL-6-induced inflammation and may enable discovery of new approaches to reduce inflammation in CAD and other pathologies.

Fold Change Median		p-STAT1	p-STAT3	p-STAT5
Max. Stenosis (%)	R-value	0.64	0.78	0.12
	P-value	0.004	0.0001	0.64
Atheroburden (%)	R-value	0.76	0.73	0.16
	P-value	0.0002	0.0006	0.52
Fibrous (%)	R-value	-0.63	-0.7	-0.42
	P-value	0.005	0.001	0.08
Fatty (%)	R-value	0.68	0.49	0.08
	P-value	0.002	0.039	0.76
Necrotic (%)	R-value	0.5	0.63	0.43
	P-value	0.03	0.005	0.08
Calcium (%)	R-value	0.48	0.62	0.32
	P-value	0.04	0.006	0.19

Spearman correlation analysis between IVUS-VH characteristics and fold change in median expression of p-STATs (median in IL-6-stimulated samples/median in vehicle treated samples). N=18

**H.Kothari:** None. **C.McSkimming:** None. **F.Drago:** None. **C.Williams:** None. **E.Zunder:** None. **C.Mcnamara:** No ne.

## Pro-Inflammatory Macrophage Secretome Promotes Cardiac Fibroblast Activation

**Georgios Kremastiotis**, Raimondo Ascione, Jason L. Johnson, Sarah J. George, Univ of Bristol, Bristol, United Kingdom

### Introduction

Following myocardial infarction, an acute immune response occurs, and infiltrating monocytes and monocyte-derived macrophages migrate into the infarct. Under the influence of intricate pro- and anti-inflammatory stimuli, macrophages drive cardiac fibroblast (CF) activation. The interaction between macrophages and CFs regulates fibrosis-driven wound healing.

### Hypothesis

We hypothesised that pro- and anti-inflammatory macrophages divergently effect CF activation. We aimed to identify macrophage proteins that regulate CFs as potential intervention targets.

### Methods

Monocytes from healthy volunteers were differentiated towards pro- or anti-inflammatory macrophages using GM-CSF (20 ng/mL) and M-CSF (20 ng/mL) or M-CSF (40 ng/mL) alone, respectively. CF activation was characterised by  $\alpha$ -SMA expression, contraction, and migration. Proteomics were performed on macrophage secretome and subjected to bioinformatics (IPA, Qiagen). CFs were cultured with macrophage-conditioned medium (CM) in the presence of recombinant proteins or neutralising antibodies, as indicated.

**Results** Pro-inflammatory macrophage CM enhanced CF activation, as evidenced by elevated  $\alpha$ -SMA expression (1.6-fold change,  $p < 0.05$ ,  $n = 7$ ), contraction (1.3-fold change,  $p < 0.05$ ,  $n = 4$ ), and migration (1.2-fold change,  $p < 0.05$ ,  $n = 4$ ) in comparison to anti-inflammatory macrophage CM. Bioinformatics and validating Western blotting revealed that CTSZ and CXCL10 were significantly differentially expressed, and they were upregulated in the pro- and anti-inflammatory macrophage secretome, respectively.

Neutralisation of CTSZ or addition of recombinant CXCL10 to pro-inflammatory macrophage CM reduced CF  $\alpha$ -SMA expression, supporting a causal role for CTSZ and CXCL10 in CF activation. Finally, CTSZ cleaved CXCL10 *in vitro* (33% reduction in 2 hours, 37°C), which, subsequently, abrogated the suppression of  $\alpha$ -SMA expression by CXCL10 in CFs.

**Conclusions** Our findings indicate that macrophage phenotype exerts divergent effects on CF behaviour, with pro-inflammatory macrophages promoting CF activation, through enhanced CTSZ secretion and associated CXCL10 cleavage, revealing both proteins as potential targets for modulating fibrosis-driven wound healing.

**G. Kremastiotis:** None. **R. Ascione:** None. **J.L. Johnson:** None.

## Myeloid-specific PKM2 Deletion Reduces Atherosclerosis By Limiting Inflammation

**Prakash Doddapattar**, UNIVERSITY OF IOWA, Iowa City, IA; Rishabh Dev, Univ of Iowa, Iowa city, IA; Madankumar Ghatge, Univ of Iowa, Iowa City, IA; Manish Jain, university of Iowa, Iowa City, IA; Nirav Dhanesha, Steven R Lentz, UNIVERSITY OF IOWA, Iowa City, IA; Anil K Chauhan, UNIVERSITY IOWA, Iowa City, IA

**Introduction:** The underlying cause of coronary artery disease (CAD) is atherosclerosis, which is a pathological response to chronic inflammation and hyperlipidemia. The onset of atherogenesis is characterized by infiltration of myeloid cells, including monocytes followed by fatty streak formation and progressive accumulation of smooth muscle cells (SMCs). These microenvironmental changes dictate the balance between inflammatory and anti-inflammatory macrophages. Pyruvate kinase M2 (PKM2), a glycolytic enzyme, is highly expressed in activated proinflammatory macrophages. The mechanistic role of PKM2 in atherosclerosis remains unknown.

**Hypothesis:** We hypothesize that PKM2 promotes macrophage migration in response to MCP-1 and mediates atherosclerosis by increasing inflammation. **Methods and Results:** PKM2 was upregulated in macrophages of *Ldlr*<sup>-/-</sup> mice fed a high-fat "Western" diet compared with a control chow diet. We generated the novel myeloid cell-specific PKM2<sup>fl/fl</sup>LysMCre<sup>+/-</sup> on a *Ldlr*-deficient background (PKM2<sup>fl/fl</sup>LysMCre<sup>+/-</sup>*Ldlr*<sup>-/-</sup>) and evaluated atherosclerosis after 14 weeks high-fat "Western" diet feeding.

Controls were littermate PKM2<sup>fl/fl</sup>LysMCre<sup>-/-</sup>*Ldlr*<sup>-/-</sup> mice. Myeloid cell-specific deletion of PKM2 led to a significant reduction in lesions in the whole aorta and aortic sinus despite high cholesterol and triglyceride

levels. ( $P < 0.05$ ,  $n = 10-12$  mice/group). Furthermore, we found decreased macrophage content in the lesions of myeloid cell-specific PKM2<sup>-/-</sup> mice compared with control mice that was associated with decreased plasma levels of pro-inflammatory cytokines, including MCP-1, and reduced transmigration of macrophages in response to MCP-1. Macrophages isolated from myeloid-specific PKM2<sup>-/-</sup> mice fed a high-fat "Western" diet exhibited reduced expression of pro-inflammatory genes, including MCP-1, IL-1 $\beta$ , IL-12, and increased expression of the anti-inflammatory genes Arg1 and IL-10. Inhibiting PKM2 nuclear translocation in bone marrow-derived macrophages led to a significant reduction in MCP-1 and IL-1 $\beta$  levels and reduced transmigration of macrophages.

**Conclusion:** Genetic deletion of PKM2 in myeloid cells reduces atherosclerosis by limiting inflammation.

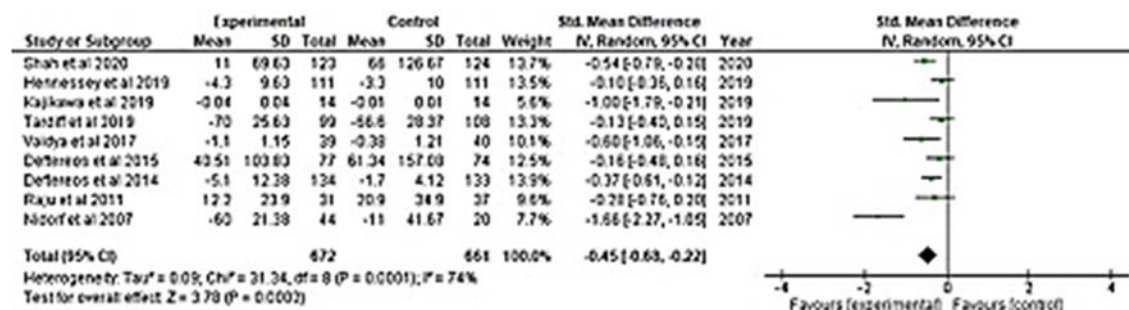
**P.Doddapattar:** n/a. **R.Dev:** n/a. **M.Ghatge:** None. **M.Jain:** None. **N.Dhanesha:** None. **S.R.Lentz:** Other; Modest; Opko, Other; Significant; Novo Nordisk, Research Grant; Significant; Novo Nordisk, Apellis. **A.K.Chauhan:** None.

P128

## Reducing Inflammation In Coronary Atherosclerosis: A Renewed Look At Colchicine

**Mustafa Alam,** Olga V Savinova, New York Inst of Technology, Old Westbury, NY; Sunny Jhamnani, CommonSpirit Health, Phoenix, AZ

**Introduction:** Atherosclerosis is an inflammatory disease. Randomized controlled trials (RCT) have demonstrated that targeting inflammation is important for the secondary prevention of major adverse cardiovascular events (MACE) in patients with acute coronary syndrome (ACS) and chronic coronary artery disease (CAD). Out of these trials, low-dose colchicine has emerged as an inexpensive therapy for coronary atherosclerosis. This meta-analysis focuses to understand colchicine's anti-inflammatory efficacy via reduction in high sensitivity C-Reactive Protein (hs-CRP) in patients with ACS and CAD. **Methods:** A computerized search of MEDLINE was conducted to retrieve journal articles reporting the results in human studies performed from January 1, 2005 to January 1, 2021 using the keywords: "Colchicine" AND "Coronary" OR "CRP" OR "Coronary Artery Disease." Studies were included if they measured hs-CRP changes from baseline and colchicine or placebo were given to patients with ACS or CAD. Studies were graded on quality via the Jadad scoring criteria. **Results:** A total of nine studies with a total population of 1502 patients and mean Jadad score of 4 were included in the meta-analysis. Five studies were RCT. The mean/median age ranged from 57 to 67 years while the duration of therapy ranged from one day to one year. Overall, colchicine treatment reduced hs-CRP levels compared with placebo (standardized mean difference [SMD]: -0.45; 95% CI: -0.68, -0.22;  $p = 0.0001$ ). **Conclusion:** Colchicine reduces hs-CRP in patients with ACS and CAD. This finding supports the role of colchicine in the reduction of inflammation associated with ACS or CAD. Further randomized control trials are needed to quantify long-term inflammatory control and subsequent MACE reduction.



**M.Alam:** None. **O.V.Savinova:** None. **S.Jhamnani:** n/a.

# Ablation Of TNAP (tissue-nonspecific Alkaline Phosphatase) In Macrophages Does Not Affect Atherosclerotic Plaque Calcification Or Cardiovascular Physiology

**Ethan Shamsian**, Sandy Than, Maria Canellos, New York Inst of Technology, Old Westbury, NY; Mohnish Singh, NYITCOM, Glen Head, NY; Olga V Savinova, New York Inst of Technology, Old Westbury, NY

**Introduction:** Increased expression of TNAP (tissue-nonspecific alkaline phosphatase) in macrophages exacerbates atherosclerotic calcification in a mouse model. However, whether or not TNAP is necessary in the progression of calcification, or for proper cardiac function has yet been studied. **Objective:** The purpose of this study was to test the effect of TNAP ablation in macrophages on atherosclerotic plaque calcification and cardiovascular physiology, and compare it to a wild type situation. **Methods:** Macrophage-specific WHC-mTNAP knockout (KO) mice were produced in our colony by intercrossing floxed *alpl* transgenic mice (*alpl* gene encodes TNAP) and macrophage-specific CRE recombinase mice, in which CRE was expressed under the control of the lysozyme gene promoter. The macrophage TNAP KO strain was developed on the background of homozygous WHC ("wicked high cholesterol") mutation in the low density lipoprotein receptor gene. WHC-TNAP KO (n=10) and their WHC littermates (n=9) were placed on an atherosclerosis inducing diet at 8 weeks of age. The mice were maintained on the diet for 44 weeks, or until they turned 52 weeks. Microcomputed tomography (microCT) analyses of calcification in the aortic roots and arches were performed *ex vivo*. Echocardiographic studies were performed to assess cardiac structure and function at 52 weeks of age. Data were analyzed via a 2-way ANOVA to calculate the effect of TNAP ablation on calcification and cardiovascular physiology while adjusting for sex. **Results:** CT data showed no significant difference in calcification levels between the two genotypes. Cardiac parameters such as left ventricular (LV) mass, LV diameter and wall thickness, ejection fraction, fractional shortening and cardiac output also showed no significant difference between the two genotypes. **Conclusion:** Our data suggest that, despite TNAP expression in macrophages being sufficient to induce calcification of atherosclerotic plaques, it is not necessary in the calcification process. To the extent of our study, the ablation of TNAP in macrophages does not appear to have any consequences in a mouse model of atherosclerosis.

**E.Shamsian:** None. **S.Than:** None. **M.Canellos:** None. **M.Singh:** None. **O.V.Savinova:** None.

# Inflammation-Mediated Modification Of Extracellular Matrix Generates A New Adhesive Substrate For Integrin $\alpha_D\beta_2$ -Dependent Macrophage Retention During Chronic Inflammation

Cady Forgey, William Bailey, Jared Casteel, Haley Scarbrough, East Tennessee State Univ, Johnson City, TN; Eugene A Podrez, CLEVELAND CLINIC FOUNDATION, Cleveland, OH; Tatiana V Byzova, CLEVELAND CLINIC, Cleveland, OH; **Valentin P Yakubenko**, East Tennessee State Univ, Johnson City, TN

The accumulation of pro-inflammatory macrophages in the inflamed vascular wall is a critical step in atherogenesis. The mechanism of macrophage retention within the site of inflammation is not understood yet. High adhesion that prevents macrophage migration is one of the potential mechanisms. We previously showed that integrin  $\alpha_D\beta_2$  is upregulated on pro-inflammatory macrophages, promotes macrophage retention, and contributes to atherogenesis. However, we have not identified a key ligand for  $\alpha_D\beta_2$  within the tissue, since  $\alpha_D\beta_2$  does not interact with major ECM proteins, collagens, and laminins. We recently found that during acute inflammation, the oxidation of docosahexaenoic acid (DHA) leads to the generation of end product carboxyethylpyrrole (CEP), which forms an adduct with fibrinogen and albumin via  $\epsilon$ -amino group of lysines. Moreover, we revealed that macrophages adhered to CEP-modified albumin in  $\alpha_D\beta_2$ -dependent manner. Now we are testing a hypothesis that DHA oxidation is a universal mechanism during chronic inflammatory diseases that promotes the generation of CEP adducts with different ECM proteins and forms  $\alpha_D\beta_2$ -mediated strong anchorage of macrophages, which is critical for macrophage retention during chronic inflammation. We detected CEP-modified proteins in digested atherosclerotic lesions by western blot. In vitro DHA oxidation leads to the formation of CEP adducts with collagen IV and laminin but not with collagen I. Using  $\alpha_D\beta_2$ -transfected HEK293 cells, WT and  $\alpha_D^{-/-}$  mouse macrophages, we revealed that CEP-modified proteins support stronger cell adhesion and spreading to compare with natural macrophage ligands. Using site-directed mutagenesis, we generated mutant  $\alpha_D$  I-domains and  $\alpha_D\beta_2$ -transfected cells with single amino acid substitutions. Applying protein-protein binding and adhesion assays we detected one amino acid within integrin  $\alpha_D$ , K<sup>246</sup>, which is critical for  $\alpha_D\beta_2$  binding to CEP-

modified proteins. In summary, we propose a new mechanism of macrophage retention, which is based on inflammatory modifications of ECM with DHA end-product, CEP. The identification of a binding site for CEP-modified proteins within  $\alpha_D\beta_2$  will help to develop a blocking reagent for the treatment of the inflammatory component of atherosclerosis.

**C.Forgey:** n/a. **W.Bailey:** n/a. **J.Casteel:** None. **H.Scarbrough:** None. **E.A.Podrez:** None. **T.V.Byzova:** None. **V.P.Yakubenko:** None.

---

P131

#### Na/k-atpase Is A Negative Regulator Of Lps-induced Macrophage Activation

**Jue Zhang,** Versiti blood research institute, Milwaukee, WI; **Wenxin Huang,** VERSITI BLOOD RESEARCH INSTITUTE, Milwaukee, WI; **Yiqiong Zhao,** Versiti blood research institute, Milwaukee, WI; **Roy L Silverstein,** MEDICAL COLLEGE WISCONSIN, Milwaukee, WI; **Yiliang Chen,** Medical Coll of Wisconsin, Milwaukee, WI

**Introduction and objective-** A strong association between atherosclerosis and infections has been suggested in several studies. Clarifying the mechanism of macrophage inflammatory activation is critical to reduce the risk of atherosclerotic cardiovascular disease. Recent studies indicate that the Na/K-ATPase (NKA) is a novel regulator of macrophage activation. Nevertheless, its role in bacterial lipopolysaccharide (LPS)-induced innate immune responses remains unclear. In this study, we aim to investigate how NKA regulates LPS signaling and macrophage inflammatory activation. **Methods and Results-** Using murine peritoneal macrophages isolated from genetically modified mice, we showed that macrophages partially deficient in NKA  $\alpha 1$  were hypersensitive to LPS. 100 ng/ml LPS triggered enhanced pro-inflammatory cytokine production such as IL-1 $\beta$ , IL-6, MCP-1 and TNF- $\alpha$  through RT-PCR and Elisa assay. Furthermore, intraperitoneal injection of LPS inducing septic shock in mice resulted in higher plasma pro-inflammatory cytokine levels and lower survival rate in NKA  $\alpha 1$  heterozygous null mice. Mechanistically, co-IP experiments showed that TLR4 assembles with NKA and phosphorylated-Lyn as a complex in response to LPS in WT macrophages and reduction in NKA  $\alpha 1$  led to more co-precipitated p-Lyn by LPS stimulation. Moreover, the Src-family kinases inhibitor PP2 blocked the production of pro-inflammatory cytokine from post culture medium of LPS treated WT macrophages. In addition, RNA sequencing and Gene Set Enrichment Analysis showed an upregulation of NF- $\kappa$ B target genes. The activation and nuclear translocation of NF- $\kappa$ B were also augmented. **Conclusions-** NKA is a novel negative regulator of LPS-mediated inflammatory activation by regulating NKA  $\alpha 1$ /TLR4/Lyn Complex and NF- $\kappa$ B signaling pathway in macrophages.

**J.Zhang:** None. **W.Huang:** n/a. **Y.Zhao:** None. **R.L.Silverstein:** None. **Y.Chen:** None.

---

P132

#### Heterogeneously Expressed Bcl6 Controls Endothelial Inflammatory Response

**Nicole M Valenzuela,** UCLA Immunogenetics Ctr, Los Angeles, CA

We recently reported that *BCL6*, a DNA binding protein important in germinal center responses and lymphonogenesis, was heterogeneously expressed across human endothelial cells (EC). Its expression correlated with more intense inflammatory responses. Here, we asked what role BCL6 might play in endothelial inflammation. We examined public expression and epigenomic data and tested BCL6 function *in vitro*. BCL6 was significantly enriched in cardiac microvascular and endocardial EC, associated with cardiovascular disease in GWAS studies, and was elevated in rejecting cardiac transplant biopsies. The chromatin landscape around BCL6 reflected that of a superenhancer in EC, with high H3K27ac and H3K4me3 signal indicative of active/poised transcription. EC treated with TNF $\alpha$ , IFN $\gamma$  or IL-1 $\beta$  upregulated BCL6 within 2-3hr, maintained through 24hr. The BCL6 gene had putative NF $\kappa$ B/REL transcription factor binding sequences, and p65/RelA binding to the BCL6 gene increased more than 8-fold under TNF $\alpha$  or IL-1 $\beta$  stimulation. BCL6 DNA binding sites were found in EC adhesion molecule and chemokine genes, including *VCAM1*, *CXCL2*, *CX3CL1*, *SELE*, *CCL5*; as well as NF $\kappa$ B genes themselves. Perturbation of BCL6 complexes with inhibitors (FX1, BI-3812) led to dramatic changes in the TNF $\alpha$ -induced transcriptome and at the protein level in endothelial cells. For example, FX1 and BI-3812 significantly blocked TNF $\alpha$ -induction of *VCAM1* and *CXCL2*/GRO $\beta$ , but upregulated *CCL5*/RANTES and *CXCL10*/IP-10. Interestingly, TNF $\alpha$ -induced expression of miR155, a pro-inflammatory microRNA important in atherosclerosis, was also suppressed. We

hypothesize that BCL6 is a novel NFκB-inducible regulator of vascular inflammation. Surprisingly, BCL6 corepressor antagonism both enhanced and suppressed TNFα mediated EC activation. Therefore BCL6 performs transcriptional modification that is context and cell-type dependent. Its role in vascular inflammation merits further investigation.

**N.M.Valenzuela:** None.

---

P133

#### Inflammatory Biomarkers As Predictors Of Adverse Outcome In Acute Myocardial Infarction

**Gisela A Kristono**, Ana S Holley, Univ of Otago, Wellington, New Zealand; Kathryn Hally, Univ of Otago, Wellington, Wellington; Morgane M Brunton-O'Sullivan, Univ of Otago, Wellington, Wellington, New Zealand; Scott Harding, Wellington Hosp, Wellington; Peter Larsen, UNIVERSITY OF OTAGO WELLINGTON, Wellington

**Introduction:** Inflammation contributes to the pathogenesis of major adverse cardiovascular events (MACE) after an acute myocardial infarction (AMI). However, the optimal way to characterise inflammation and predict risk is unclear. While various biomarkers have been used to examine the relationship between acute inflammation and MACE risk, results are inconsistent between studies. Using a range of inflammatory markers, we assessed their utility to predict MACE in AMI patients.

**Hypothesis:** A combined inflammatory biomarker approach is superior to individual biomarkers for predicting MACE risk in AMI patients.

**Methods:** We conducted a systematic review of multi-marker approaches to characterise inflammation following AMI. Through cohort studies, a case control study, and a time series, we also examined the relationship between inflammatory markers and MACE. The studies ranged in size from 23 to 860 patients, with an average MACE rate of 13 in 100 at one year follow up.

**Results:** Our systematic review found four studies that attempted various combined cytokine approaches. All found statistical associations with MACE, and performed better than single markers. In our studies, we first explored simple methods of combining biomarkers (ratios of leukocyte counts, and simple addition of C-reactive protein, IL-6 and TNF-α). We found no independent associations with MACE when biomarkers were combined via simple methods. We then examined a more sophisticated approach for combining cytokines. We chose to use a mathematical technique (principal component analysis, PCA) that could deal with co-linearity within individual cytokine measurements and combine individual cytokine measurements into a score. We selected six cytokines, and a PCA score derived from these markers was associated with MACE on univariate analysis. Individually, IL-6 and IL-8 levels were univariate predictors of MACE. Combining these two into a PCA-derived score resulted in a stronger, independent association with MACE (odds ratio 2.77,  $p < 0.05$ ) than seen with either marker alone.

**Conclusion:** Multi-marker inflammatory scores may produce more consistent associations with MACE than single biomarkers. We suggest that PCA is a useful mathematical method for creating this type of score.

**G.A.Kristono:** n/a. **A.S.Holley:** None. **K.Hally:** None. **M.M.Brunton-O'sullivan:** n/a. **S.Harding:** None. **P.Larsen:** None.

---

P134

#### Peg-arginase 1 Limits Vascular Complications Of Type 2 Diabetes

**Ammar A. Abdelrahman**, Katharine L. Bunch, Modesto Rojas, Ruth B Caldwell, Robert W. Caldwell, Medical Coll of Georgia, Augusta Univ, Augusta, GA

**Background:** Distinct from its role in the urea cycle, the function of arginase 1 (A1) in regulating inflammatory responses has been demonstrated to be an intriguing target for controlling chronic, neuroinflammatory disease. Arginase competes with nitric oxide synthase (NOS) isoforms for their common substrate, L-arginine. Inflammatory cytokines increase expression of inducible NOS (iNOS) resulting in oxidant stress. Our group has recently shown that the polyethylene glycol-linked arginase 1 (PEG-A1) formulation, which provides enzyme stability, is a promising treatment that can counteract the destructive effects of neuro-inflammation and oxidative stress in ischemic retinal disease. This study assessed the efficacy of systemic PEG-A1 treatment in protecting the retinal neurovascular system from the effects of chronic hyperglycemia in a well-established murine model of type 2 diabetes.

**Methods:** Studies were performed using 16-week-old obese, diabetic *db/db* mice to examine effects of chronic hyperglycemia and dyslipidemia on the retina. Lean *Db/db* littermates served as controls (n= 7/group). The *db/db* mice (n= 8/group) were treated with PEG-A1 (25 mg/kg IP) or PEG alone (control) 7 times over 2 weeks. Activation of the inflammasome pathway was examined by Western blots. Immuno-labeling of 4-HNE was used to quantify oxidative stress. Breakdown of the blood retinal barrier (BRB) was examined via albumin extravasation.

**Results:** Expression of inflammasome pathway proteins, iNOS, caspase 1, IL-1 $\beta$ , and TNF $\alpha$  were upregulated in conjunction with increased cell death and breakdown of the BRB in *db/db* mice compared to controls. PEG-A1 treatment of the *db/db* mice significantly decreased the expression of iNOS, IL-1 $\beta$ , and TNF $\alpha$ , while reducing oxidative stress and preserving the BRB, as evidenced by decreased albumin leakage compared to *db/db* mice treated with PEG.

**Conclusions:** Chronic diabetes increases retinal inflammation, oxidative stress and BRB disruption. We hypothesize that systemic PEG-A1 administration provides significant anti-inflammatory and anti-oxidant protection while inhibiting BRB breakdown in the *db/db* obese, diabetic mouse by decreasing L-arginine availability for iNOS and thereby inhibiting its expression/activity.

**A.A.Abdelrahman:** None. **K.L.Bunch:** None. **M.Rojas:** None. **R.B.Caldwell:** None. **R.W.Caldwell:** None.

P135

## Platelet Activation Is Present In Psoriasis And Associated With Psoriasis Severity And Endothelial Dysfunction

Kamelia Drenkova, New York, NY; Khrystyna Myndzar, Brooklyn, NY; Stuart D Katz, NEW YORK UNIVERSITY SCHOOL MED, New York, NY; James Krueger, Rockefeller Univ, New York City, NY; Jeffrey S Berger, NEW YORK UNIVERSITY SCHOOL MEDICINE, New York, NY; **Michael Garshick**, NYU Langone Health, New York City, NY

**Background:** Psoriasis is associated with impaired endothelial function and increased CV risk. P-selectin, a platelet transmembrane protein involved in binding leukocytes and endothelial cells, is implicated in CVD. **Objective:** To explore platelet P-selectin expression in psoriasis and its association with biomarkers of inflammation and endothelial dysfunction.

**Methods:** Patients with psoriasis (n=15, age 51  $\pm$  18 years, 73% male), percent body surface area (BSA) psoriasis 9  $\pm$  20, were compared to controls (Table 1A). The vascular endothelium was assessed via brachial artery flow-mediated dilatation (FMD), a metric of endothelial health and biomarker of CV risk. Platelet P-selectin expression was measured on freshly isolated platelets via flow cytometry in resting and stimulated (thrombin, ADP, arachidonic acid and epinephrine) conditions. High-sensitivity C-reactive protein (hs-CRP) was measured in a clinical laboratory.

**Results:** Psoriasis patients were matched for traditional CV risk factors (Table 1A) aside from diabetes, which trended higher in psoriasis. No difference in hs-CRP was noted, however BSA positively correlated with hs-CRP ( $r=0.65$ ,  $p=0.02$ ), while FMD trended higher in psoriasis vs. controls (5.7% vs. 2.7%,  $p=0.07$ ) even after accounting for diabetes status ( $\beta=-3.0$ ,  $p=0.08$ ). Platelet analysis revealed higher basal and stimulated P-selectin expression in psoriasis vs. controls (Table 1B). Positive correlations were noted between platelet activation, BSA and hs-CRP, while a negative association was noted between FMD and platelet activation (Table 1C).

**Conclusion:** We describe platelet P-selectin in resting and stimulated conditions as elevated in psoriasis, positively correlated with biomarkers of psoriatic activity, and negatively associated with endothelial health. These findings have important implications for future clinical trials of targeting platelet activity to reduce CV risk in psoriasis.

A Demographics	Control (n=9)	Psoriasis (n=15)	P-value	B Platelet markers	Control (n=9)	Psoriasis (n=15)	P-value
Age	45 $\pm$ 17	51 $\pm$ 18	0.47	P-selectin	5.56 (4.67 - 6.06)	6.41 (5.86 - 7.75)	0.003
Male, % (n)	55 (5)	73 (11)	0.37	P-selectin + Epi	6.50 (5.65 - 9.39)	9.51 (7.71 - 14.7)	0.03
Caucasian	66 (6)	80 (12)	0.54	P-selectin + Thrombin	12.75 (6.99 - 17.01)	21.70 (11.30 - 43.51)	0.11
Hispanic origin	33 (3)	20 (3)	0.47	P-selectin + ADP	9.45 (7.25 - 12.70)	12.15 (9.77 - 18.00)	0.07
Systolic blood pressure	114 $\pm$ 8	124 $\pm$ 12	0.13	P-selectin + AA	6.25 (5.46 - 6.83)	9.08 (6.92 - 10.34)	0.002
Diastolic blood pressure	64 $\pm$ 6	77 $\pm$ 12	0.08				
Diabetes, % (n)	0 (0)	27 (4)	0.09				
Hyperlipidemia, % (n)	11 (1)	20 (3)	0.57				
Body mass index kg/m <sup>2</sup>	27 $\pm$ 8	27 $\pm$ 4	0.91				
Body surface area psoriasis, %	-	9 $\pm$ 20					
Psoriasis disease duration, y	-	20 $\pm$ 19					
hs-CRP, mg/L	0.7 (0.5 - 1.5)	1.35 (0.5 - 5.7)	0.57				
Biologic therapy, % (n)	-	53 (8)					
Flow mediated dilatation, %	5.7 $\pm$ 4	2.7 $\pm$ 1.6	0.07				

Table 1. A - Demographic characteristics. B - Mean fluorescent intensity values of platelet P-selectin expression in basal and stimulated conditions (via flow cytometry). C - Pearson's correlation coefficient between platelet P-selectin expression, BSA, and hs-CRP. AA: arachidonic acid. ADP: adenosine diphosphate. BSA: body surface area. Epi: epinephrine. FMD: flow mediated dilatation. Hs-CRP: high sensitivity C-reactive protein.

C	BSA	hs-CRP	FMD
P-selectin	0.55	0.44	-0.32
P-selectin + Epi	0.49	0.62	-0.29
P-selectin + Thrombin	0.69	0.14	-0.30
P-selectin + ADP	0.48	0.62	-0.45
P-selectin + AA	0.28	0.35	-0.38

**K.Drenkova:** None. **K.Myndzar:** None. **S.D.Katz:** Research Grant; Modest; Amgen, Sanofi, BioCardia, Luitpold, AMAG Pharmaceuticals Inc., Applied Therapeutics, Inc., Pfizer, Inc.. **J.Krueger:** n/a. **J.S.Berger:** Honoraria; Modest; Amgen, Other Research Support; Significant; Jannssen, Research Grant; Significant; NIH, AHA, Astra Zeneca. **M.Garshick:** None.

---

P136

#### First Steps In Uncovering Mechanisms In Late Onset Preeclampsia

**Jakara Griffin,** Brian Lindemer, John G. Krolkowski, MED COLLEGE WISCONSIN, Milwaukee, WI; Nicole L Lohr, MEDICAL COLLEGE OF WISCONSIN, Milwaukee, WI; Dorothee Weihrauch, MED COLLEGE WISCONSIN, Milwaukee, WI

Preeclampsia is a leading cause of maternal morbidity and mortality worldwide, complicating 2-8% of pregnancies. The etiology of PE is poorly understood, the role of placental extracellular matrix (pECM) in PE is understudied. Extravillous trophoblasts (HTR8/svneo) and pECM are crucial in placental blood vessel formation, including spiral arteries. The objective is to identify changes in signaling mechanisms in late onset PE and how HTR8/svneo respond. Additionally, we explored a novel therapeutic to restore HTR8/svneo phenotype by phototherapy using a 670nm LED light. Western blot analysis shows eNOS, phospho-eNOS and Hsp90 expressions are unchanged in late onset PE placental samples despite previous reports in early onset of PE. The association of Hsp90 to eNOS and eNOS to phospho-eNOS is reduced in the PE sample. Soluble Flt, a diagnostic marker for PE, levels are increased in media from HTR8/svneo trophoblasts cultured on PE pECM. Endothelial function is significantly reduced in an isolated vessel as determined by acetylcholine stimulation. 670nm light reverses this impairment. Migration of HTR8/SVneo on PE pECM is reduced (control  $86.29 \pm 18.58$ , PE  $30.16 \pm 15.49$ ) but proliferation of HTR8/SVneo on PE pECM is unaffected in patients (control:  $59.125 \pm 6262.9$ , PE:  $67.125 \pm 7706.5$ ). Proliferation and migration are improved by 670nm light (proliferation control  $101.375 \pm 2075.4$ ; PE  $106.875 \pm 4870.7$ , migration control  $125 \pm 11.97$ , PE  $144.84 \pm 16.01$ ). An increase of apoptotic HTR8/SVneo cultured on PE pECM is observed compared to healthy pECM in patients control  $2.4 \pm 0.24$ , PE  $3 \pm 0.4$  samples. 670nm light treatment decreases the number of apoptotic cells, control  $1.2 \pm 0.58$ , PE  $1.4 \pm 0.5$ . Conclusion: In late onset preeclampsia, endothelial function is decreased, sFlt release is increased, the eNOS/Hsp90/p-eNOS axis is slightly reduced pointing to  $O_2^-$  synthesis. Migration is decreased likely due to impaired trophoblast invasion, but proliferation is unaffected. 670nm light treatment can reverse some of the effects of the preeclamptic microenvironment. Extracellular matrix is altered in late onset PE leading to an abnormal HTR8/SVneo phenotype. 670nm light restores the phenotype of HTR8/SVneo on PE pECM suggesting 670nm light as a therapeutic treatment.

**J.Griffin:** None. **B.Lindemer:** None. **J.G.Krolkowski:** None. **N.L.Lohr:** None. **D.Weihrauch:** None.

---

P137

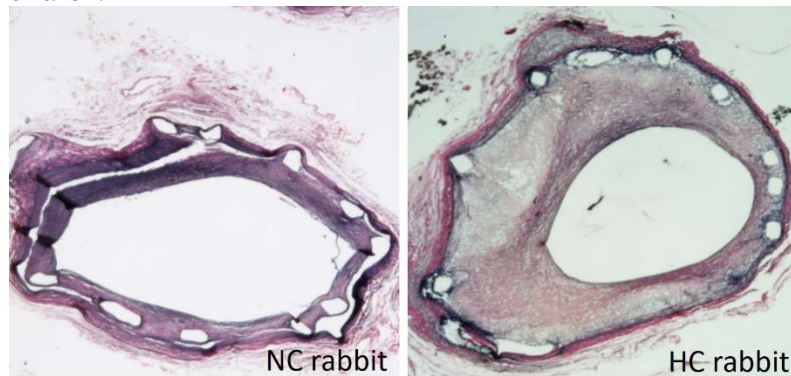
#### Hypercholesterolemia Aggravates In-stent Restenosis In Rabbits By Escalating Vascular Inflammation

**Vaishali Inamdar,** The Children's Hosp of Philadelphia, Philadelphia, PA; **Menekhem Zviman,** George Bratinov, Univ of Pennsylvania, Philadelphia, PA; **Emmett of Fitzpatrick,** The Children's Hosp of Philadelphia, Philadelphia, PA; **Kristin Gardiner,** Univ of Pennsylvania, Philadelphia, PA; **Ivan S Alferiev,** Robert J Levy, Stanley J Stachelek, **Ilia Fishbein,** The Children's Hosp of Philadelphia, Philadelphia, PA

**Background:** Hypercholesterolemia (HC) has previously been shown to augment restenotic response in several animal models. However, the mechanistic aspects of in-stent restenosis (ISR) on an HC background are not fully understood. **Methods:** HC was induced in 5 NZW rabbits by hypercholesterolemic diet (HCD) fed for 4 weeks prior to bilateral implantation of stainless steel stents in the iliac location. The diet was continued until sacrifice. In parallel, stents were deployed in the iliac arteries of 5 normocholesterolemic (NC) rabbits. All animals were euthanized 4 weeks after stenting. Harvested arteries were formalin-fixed. The stent struts were dissolved in a mixture of nitric and hydrofluoric acids. The destented arteries were paraffin-embedded, sectioned, stained according to the Verhoeff-vanGieson method, and the lumen area, neointimal thickness, neointimal area, neointima-to-media ratio, and percent of luminal stenosis were determined morphometrically. A semiquantitative scale was used to assess the intensity and spread of TNF $\alpha$  expression by immunohistochemistry (IHC). The prevalence of peri-strut macrophages (M $\Phi$ ) was determined by IHC as a percentage of a strut circumference infiltrated with M $\Phi$ . **Results:** HC diet drastically



increased severity of ISR (Fig). The corresponding values of the lumen area, neointimal thickness, neointimal area, neointima-to-media ratio and percent of luminal stenosis for the groups of NC and HC animals were  $1.86 \pm 0.44$  vs  $1.48 \pm 0.54$  ( $p < 0.05$ ),  $0.06 \pm 0.02$  vs  $0.31 \pm 0.14$  ( $p < 0.0001$ ),  $0.66 \pm 0.16$  vs  $2.07 \pm 0.56$  ( $p < 0.0001$ ),  $1.99 \pm 0.11$  vs  $4.57 \pm 0.76$  ( $p < 0.0001$ ), and  $26.35 \pm 4.78$  vs  $57.89 \pm 13.71$  ( $p < 0.0001$ ). Compared to NC animals, TNF $\alpha$  immunopositivity and M $\Phi$  infiltration of peri-stent areas increased in HC group animals 1.81- and 2.58-fold, respectively ( $p < 0.001$  for both). **Conclusions:** The inflammatory response to stent deployment is intensified in HC metabolic conditions, leading to the augmented neointimal expansion and ISR.



**V.Inamdar:** None. **M.Zviman:** None. **G.Bratinov:** None. **E.O.Fitzpatrick:** None. **K.Gardiner:** None. **I.S.Alferiev:** None. **R.J.Levy:** Other; Modest; WL Gore. **S.J.Stachelek:** None. **I.Fishbein:** None.

---

P138

#### *Schistosoma Mansoni*-Induced Shedding Of Extracellular Vesicles From Lung Microvascular Endothelial Cells

**Suellen D Oliveira,** Andrew Schwartz, Univ of Illinois at Chicago, Chicago, IL; David Williams, Rush Univ, Chicago, IL; Marcelo Bonini, Northwestern Univ, Chicago, IL; Claudia Lucia Martins Silva, Federal Univ of Rio de Janeiro, Rio de Janeiro, RJ, Brazil; Richard D Minshall, Univ of Illinois at Chicago, Chicago, IL

**Introduction:** Schistosomiasis-associated Pulmonary Arterial Hypertension (Sch-PAH) is a life-threatening complication of chronic *Schistosoma mansoni* infection. Sch-PAH is marked by obliteration and remodeling of the pulmonary vasculature in response to *S. mansoni* eggs. Remodeled and occluded vessels increase vascular resistance and can lead to heart failure and death. Currently, there are no target therapies for the treatment of Sch-PAH. **Hypothesis:** *S. mansoni* egg-derived antigens alter pulmonary endothelial cell (EC) Caveolin-1 (Cav-1) expression and phosphorylation contributing to the loading and shedding of extracellular vesicles (EVs), which in turn stimulates abnormal EC survival leading to Sch-PAH. **Methods/Results:** Immunohistology and western blot analysis of lungs from *S. mansoni*-infected mice revealed a significant decrease in Cav-1 expression in the egg-dependent granuloma area when compared to uninfected control animals, indicating that local *S. mansoni*-associated molecules and inflammatory mediators contribute to Cav-1 depletion. Previously we showed that upon vascular injury, Cav-1 deficiency leads to the survival of an abnormal EC phenotype through an unclear mechanism. Analysis of survival-associated genes in isolated lung ECs from Flk1<sup>+/GFP</sup>;Cav1<sup>-/-</sup> mice, revealed a high expression of the anti-apoptotic BIRC2 and BIRC5 (known as c-IAP2 and surviving, respectively) when compared to control ECs. Interestingly, in vitro exposure to the major *S. mansoni* egg antigen, Sm-p40 (1  $\mu$ g/mL), induced time-dependent phosphorylation of Cav-1 Tyr14 in human lung microvascular ECs (HMVEC-L;  $228.2 \pm 38.28\%$  of control;  $p < 0.05$ ;  $n=4$ ), which culminated in c-IAP2 expression. Furthermore, Sm-p40 treatment of HMVEC-L increased ERK1/2 phosphorylation, which in presence of pro-inflammatory mediators IL-6, TNF- $\alpha$ , and ATP, significantly increased the shedding of EVs implicating P-ERK1/2 in the mechanism of shedding of Cav-1-EVs. **Conclusions:** This work is uncovering the biological role and potential translational relevance of pathogen-induced EC-Cav-1 depletion via shedding of EVs during Sch-PAH.

**S.D.Oliveira:** None. **A.Schwartz:** None. **D.Williams:** n/a. **M.Bonini:** n/a. **C.Silva:** n/a. **R.D.Minshall:** n/a.

## Diet-induced Shifts In HDL Profiles Are Associated With Changes In Immune Parameters

Julia Greco, Christa Palancia Esposito, Dominika Mis, **Catherine J Andersen**, Fairfield Univ, Fairfield, CT

**Introduction:** Preclinical and population-based studies have demonstrated immunomodulatory and anti-inflammatory properties of HDL; however, it is unclear whether diet-induced changes in HDL profiles can directly impact markers of immune inflammation. **Hypothesis:** We hypothesized that daily consumption of different egg-based diets, which have been shown to differentially impact serum lipids and lipoprotein profiles, would induce changes in HDL parameters that correspond to shifts in clinical and molecular immune markers. **Methods:** Healthy men and women (18-35y, BMI < 30kg/m<sup>2</sup> or < 30% body fat for men and < 40% body fat for women, n = 26) participated in a 16-week randomized, crossover intervention trial (NCT03577223), in which they consumed an egg-free diet for 4 weeks, followed by a 4-week diet containing either 3 whole eggs or 3 egg whites per day. Participants then followed a 4-week egg-free diet washout period, before switching to the alternative whole egg or egg white diet treatment. Fasting lipoprotein profiles, complete blood cell counts, and gene expression in peripheral blood mononuclear cells (PBMCs) was measured at the end of each diet period. **Results:** While no changes in total HDL particles, average HDL particle diameter, or the concentration of small (7.4-8.0 nm) or medium (8.1-9.5 nm) HDL particles was observed, the concentration of large HDL particles (10.8nm) was increased by whole egg intake as compared to intake of egg whites. A trend toward increased apolipoprotein A1 during the whole egg diet period as compared to the egg-free diet period was additionally observed. In line with our hypothesis, changes in large HDL concentrations between whole egg vs. egg white periods were inversely correlated with total white blood cell counts and absolute lymphocyte counts. CD8A mRNA expression in PBMCs was inversely correlated with concentrations of total and large HDL particles. Importantly, while serum choline and betaine were increased by whole egg intake compared to the other diet periods, no differences in pro-atherogenic and inflammatory trimethylamine-N-oxide (TMAO) between diet periods was observed. **Conclusion:** These findings suggest that diet-induced changes in HDL profiles are directly associated with changes in immune parameters.

**J.Greco:** None. **C.Palancia esposito:** None. **D.Mis:** None. **C.J.Andersen:** Research Grant; Significant; USDA.

## Molecular Signatures Of The Delayed Healing Response To Arterial Injury In Diabetic Rats

**Sampath Narayanan**, Karolinska Instt, STOCKHOLM, Sweden; Samuel Rohl, Karolinska Inst, Stockholm, Sweden; Ljubica Matic, Karolinska Instt, STOCKHOLM, Sweden; Anton Razuvaev, Karolinska Instt, Stockholm, Sweden; Mariette Lengquist, Karolinska Instt, STOCKHOLM, Sweden

**Aim:** Atherosclerosis is a major complication of diabetes mellitus and a leading cause of mortality in diabetic patients. Vascular interventions in diabetic patients can lead to complications attributed to defective vascular remodeling and impaired healing response. In this study, we aim to elucidate the physiological and molecular differences in the vascular healing response over time using a rat model of arterial injury applied in healthy and diabetic conditions. **Methods:** Wistar (healthy) and Goto-Kakizaki (GK, diabetic) rats (n = 40 per strain) were subjected to left common carotid artery (CCA) balloon injury and euthanized at different timepoints: 0 and 24 hours, 5 days, 2, 4 and 6 weeks. Non-invasive morphological and physiological assessment, and microarray profiling of the CCA was performed for each timepoint. Bioinformatic analyses were conducted using R software, DAVID bioinformatic tool, online STRING database and Cytoscape software. **Results:** Significant increase in the neointimal thickness (p<0.01; 2-way ANOVA) was observed after 2 weeks of injury in diabetic compared to healthy rats, which was confirmed by histological analyses. Moreover, a decrease in the reendothelialization rate was also detected in the diabetic rats at 4 and 6 weeks after injury. Bioinformatic analyses showed that expression of early response genes related to inflammation and proliferation were delayed in diabetic rats, coupled with the dysregulation of key pathways related to vascular healing. Defective expression patterns were observed for endothelial, macrophage and lymphocyte markers indicating potential faults on cell regulation level. TF-PPI analysis provided mechanistic evidence wherein an array of transcription factors was dysregulated in diabetic rats specifically from 2 weeks after injury. **Conclusions:** In this study, we investigated the effect of diabetes on vessel wall healing. We demonstrate that diabetic rats exhibit impaired arterial remodelling characterised by a delayed healing response. These results further corroborate the higher prevalence of

restenosis in diabetic patients and provide vital molecular insights into the mechanisms contributing to the impaired arterial healing response in diabetes.

**S.Narayanan:** None. **S.Rohl:** None. **L.Matic:** None. **A.Razuvaev:** None. **M.Lengquist:** None.

---

P141

#### Downregulation Of Deletion Variants Of Telomerase Reverse Transcriptase (TERT) By Transforming Growth Factor- $\beta$ 1-silencing Decreases Mitochondrial ROS In Diabetic CD34<sup>+</sup> Cells

**Jesmin Jahan,** North Dakota State Univ, Fargo, ND; **Ildamaris Montes de Oca,** Ahmad Maghrabi, Christine Lopez-Yang, Museum District Eye Ctr, Houston, TX; **Andreas M Beyer,** MEDICAL COLLEGE WISCONSIN, Milwaukee, WI; **Charles Garcia,** Museum District Eye Ctr, Houston, TX; **Yagna P Jarajapu,** NDSU, Fargo, ND

Telomerase reverse transcriptase (TERT) modulates mitochondrial levels of reactive oxygen species (mitoROS). Deletion variants,  $\alpha$ -,  $\beta$ - and  $\alpha\beta$ , are negative regulators of TERT. Increased ROS levels in diabetic CD34<sup>+</sup> cells impair vasoreparative functions. Our recent studies showed that silencing of transforming growth factor- $\beta$ 1 (TGF- $\beta$ 1) decreased ROS levels and stimulated vasoreparative functions. This study tested the hypothesis that prevalence of TERT deletion variants is higher in diabetic CD34<sup>+</sup> cells and that TGF- $\beta$ 1-silencing decreases mitoROS by downregulation of the variants.

CD34<sup>+</sup> cells derived from either male or female nondiabetic (ND) (n=38) or diabetic (DB), both type 1 and type 2, (n=43) subjects were studied. Phosphorodiamidate morpholino oligomers (PMO) were used for TGF- $\beta$ 1-silencing. TERT variants were characterized by qPCR and agarose gel electrophoresis. MitoSOX-flow cytometry and ELISA were used for determining mitoROS levels and telomerase activity, respectively. TGF- $\beta$ 1-silencing decreased mitoROS levels in DB-CD34<sup>+</sup> cells ( $P < 0.01$  vs ND-cells, n=6). This effect was reversed by TERT inhibitor, BIBR1532 (1 $\mu$ M) (n=6) or mito-X-TERT, a decoy peptide that prevents mitochondrial translocation of TERT (n=5). TERT expression was higher in DB compared to ND cells ( $P < 0.05$ , n=18) but telomerase activity was lower ( $P < 0.05$  vs ND, n=10). Prevalence of TERT deletion variants was higher among DB cells compared to ND (DB - 8/10 vs ND - 2/10 subjects have one or more of  $\alpha$ ,  $\beta$ , or  $\alpha\beta$  variants). TGF- $\beta$ 1-silencing downregulated the expression of TERT variants and increased full-length TERT that was accompanied by increased telomerase activity in DB-CD34<sup>+</sup> cells ( $P < 0.05$  vs untreated, n=5). This study suggests that diabetes is associated with higher prevalence of TERT variants that would impede mitochondrial functions of TERT. TGF- $\beta$ 1-silencing decreases mitoROS levels at least in part by downregulation of TERT variants.

**J.Jahan:** None. **I.Montes de oca:** None. **A.Maghrabi:** None. **C.Lopez-yang:** None. **A.M.Beyer:** None. **C.Garcia:** None. **Y.P.Jarajapu:** None.

---

P142

#### B Cell Activating Factor Neutralization In High-Fat Diet-Induced Obese Mice Retains Adipose Tissue B Cells And Exacerbates Glucose Homeostasis

**Melissa D Lempicki,** Jake Gray, Saikat Paul, Debajit Bhowmick, Akshaya K Meher, East Carolina Univ, Greenville, NC

Adults with type 2 diabetes have a two-to-three-fold increased risk of cardiovascular diseases. B cell activating factor (BAFF), a tumor necrosis superfamily member, is implicated both in diabetes and cardiovascular diseases. BAFF deficiency in mice retains glucose homeostasis despite high-fat diet-induced obesity. We examined if neutralization of BAFF with an anti-BAFF antibody improves glucose utilization in high-fat diet-induced obese mice. Male C57BL/6J mice fed with a high-fat diet (60% calories from fat) for 12 weeks were segregated into two groups based on their glucose intolerance (GI) determined by a glucose tolerance test (GTT). Each group received a total of 4 injections of anti-BAFF or an isotype control antibody, and GTT was performed every two weeks. BAFF neutralization was confirmed by depletion of B2 B cells in the blood two weeks after the first anti-BAFF antibody injection. Although GI increased after continuous feeding of a high-fat diet, no differences in GI was observed between the groups till 18 weeks on diet. At 20 weeks, GI was significantly higher in the anti-BAFF treated group compared to the control group. Extensive cellular phenotyping using flow cytometry revealed that BAFF neutralization depleted mature B2 B cells in the spleen and blood but did not affect the CD4<sup>+</sup> T cells and CD8<sup>+</sup> T cells. No differences were found in fat accumulation in the liver, whole body fat content, visceral adipose tissue (VAT) weight, or in the number of

VAT-infiltrated M1 and M2 macrophages, eosinophils, natural killer T cells, CD4+ T cells, and CD8+ T cells. Unexpectedly, in the VAT of anti-BAFF antibody-treated mice, B2 cells were retained, whereas, the number of CD4+ T cells and dead adipocytes was higher. Real-time RT-PCR analysis of stromal vascular fraction from VAT revealed increased expression of both the M1 and M2 macrophage markers IL-1 $\beta$ , IL-6, IL-10, Arg1, and Mrc1 in the anti-BAFF treated mice. Altogether, these results suggest BAFF neutralization promotes inflammation in the VAT of obese mice and exacerbates systemic glucose intolerance. Furthermore, our results highlight the need for more studies on the use of anti-BAFF biologics for the treatment of systemic lupus erythematosus patients who are diabetic.

**M.D.Lempicki:** None. **J.Gray:** None. **S.Paul:** None. **D.Bhowmick:** None. **A.K.Meher:** None.

---

P143

#### Arterial Stiffness And Body Mass In Young Adults: Another Aspect Of The Obesity Paradox?

**Maria Evseyeva,** Michail Eremin, STAVROPOL STATE MEDICAL UNIVERSITY, Stavropol, Russian Federation; oxana sergeeva, MARIA ROSTOVTSEVA, Stavropol, Russian Federation; Evgeny Shchetinin, Stavropol State Medical Univ, Stavropol, Russian Federation; Victoria Kudrjavitseva, STAVROPOL STATE MEDICAL UNIVERSITY, Stavropol, Russian Federation

**Background.** The phenomenon of the "paradox" of obesity has been studied mainly in the elderly and even senile population in the presence of one or another obvious cardiovascular pathology, usually in combination with various complications. The study in this aspect of young people (YP), taking into account the surrogate endpoint in the form of vascular stiffness (VS), which is the basis for assessing vascular age, has not yet been conducted. **Aim** - to study VS in relation to metabolic status in YP with increase in body mass (BM), taking into account gender. **Methods.** 93 boys and 171 girls aged 18 to 25 years were screened for risk factors (RF), including determination of total cholesterol (TC), low-density lipoproteins (LDL), high-density lipoproteins (HDL), triglycerides (TG) and glucose. Angiological screening was performed using VaSera VS-1500 (Japan). VS type CAVI was evaluated on left (L) and right (R). Three groups were formed in accordance with criteria of reduced, normal and excessive BM. **Results.** With BM increase in these groups in YM, the TC was  $3.5 \pm 0.2$ ,  $3.5 \pm 0.1$ ,  $4.0 \pm 0.2$  ( $P_{2-3}=0.038$ ); LDL -  $1.9 \pm 0.3$ ,  $2.1 \pm 0.1$ ,  $2.32 \pm 0.14$ ; TG  $1.1 \pm 0.3$ ,  $1.04 \pm 0.1$ ,  $1.6 \pm 0.2$  ( $P_{2-3}=0.020$ ); HDL  $1.02 \pm 0.08$ ;  $0.99 \pm 0.04$ ;  $0.95 \pm 0.06$ . The girls have TC  $4.02 \pm 0.2$ ,  $3.94 \pm 0.08$ ,  $4.6 \pm 0.16$  ( $P_{2-3}=0.003$ ;  $P_{1-3}=0.033$ ); LDL  $2.1 \pm 0.2$ ,  $2.21 \pm 0.08$ ,  $2.8 \pm 0.2$  ( $P_{2-3}=0.006$ ;  $P_{1-3}=0.011$ ); TG  $0.7 \pm 0.04$ ,  $0.82 \pm 0.04$ ,  $1.35 \pm 0.2$  ( $P_{2-3}=0.000$ ;  $P_{1-3}=0.006$ ); HDL  $1.5 \pm 0.08$ ,  $1.35 \pm 0.03$ ,  $1.13 \pm 0.13$  ( $P_{1-2}=0.028$ ,  $P_{2-3}=0.014$ ,  $P_{1-3}=0.013$ ). Glucose increased slightly. Against background of BM growth with such negative shifts in metabolic parameters, the CAVI, on contrary, decreased. Its gender specificity was revealed - the difference between extreme weight categories for boys was 1.4 ( $P_{1-3}=0.000$ ) for both CAVI sides, while for girls it was only 0.3 for CAVI-R ( $P_{1-3}=0.091$ ) and 0.4 for CAVI-L ( $P_{1-3}=0.053$ ). **Conclusion.** We revealed another obesity "paradox" in form of improvement in elastic vascular status with BM increase in YP. It is also paradoxical that VS improvement takes place despite obvious deterioration of metabolic RF. Obtained results should be used when conducting preventive interventions among YP in order to control not only traditional RF, but also VS state, as another important RF.

**M.Evseyeva:** None. **M.Eremin:** n/a. **O.Sergeeva:** None. **M.Rostovtseva:** n/a. **E.Shchetinin:** None. **V.Kudrjavtseva:** n/a.

---

P144

#### Bariatric Surgery Normalizes Diabetes Risk Index By 1 Month Post-operation

**Vincent J. Sinatra,** BingXue Lin, Manish Parikh, Jeffrey S. Berger, Edward A. Fisher, Sean P. Heffron, NYU Grossman Sch of Med, New York, NY

The Diabetes Risk Index (DRI) is a composite of NMR-measured lipoproteins and branched chain amino acids shown to be predictive of diabetes in prospective cohorts. Bariatric surgery is indicated in patients with severe obesity, many of whom are at high-risk for developing diabetes. Substantial weight loss occurs after bariatric surgery and sustained weight loss likely contributes to lower risk of diabetes and cardiovascular disease. However, evidence suggests that bariatric surgical procedures themselves may contribute to reducing risk independent of weight loss. We aimed to investigate DRI and its association with weight loss over one year following bariatric surgery. We examined 51 severely obese premenopausal

women without diabetes, 25 of whom met criteria for metabolic syndrome. DRI, BMI, body weight and waist measurements were made before and at 1, 6 and 12 months after Roux-en-Y Gastric Bypass or Sleeve Gastrectomy. Values were compared to healthy women with normal BMI (18.5 - 24.9 kg/m<sup>2</sup>; n=15). Obese (BMI 44.7 ± 6.2 kg/m<sup>2</sup>) subjects had significantly elevated DRI scores prior to surgery (35 [26, 39] vs 12 [1, 20]; p < 0.0001). At 1 month after surgery, BMI had decreased 5.1 ± 1.1 kg/m<sup>2</sup>, but DRI decreased so that it no longer differed from that of normal BMI controls (Figure). Subjects continued to lose weight, whereas DRI remained similar, throughout 12 months. Changes in DRI did not correlate with changes in BMI, body weight or waist circumference at any time during follow-up (r = -0.16 - 0.16). There was no difference in response between surgeries or pre-operative metabolic syndrome status. Our analysis of DRI scores supports the capacity of bariatric surgery to reduce risk of developing diabetes in severely obese individuals with or without metabolic syndrome. The rapidity of normalization and the lack of associations with weight loss or anthropometric changes suggest that bariatric surgical techniques may have inherent effects that improve cardiometabolic risk.

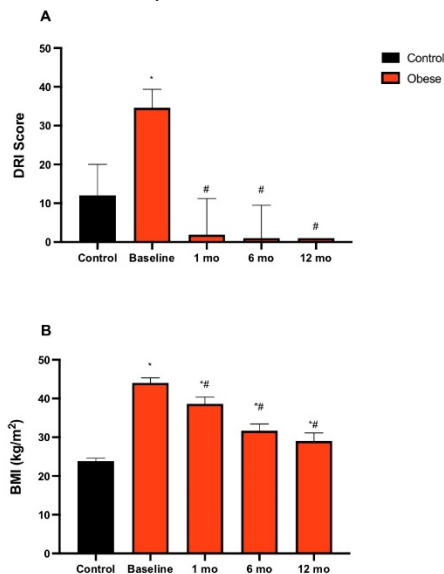


**Figure 1.** Diabetes Risk Index score (A) and Body Mass Index (B) from baseline to 12 months after bariatric surgery compared with control subjects. Each bar represents the median with error bars representing 95% confidence interval. \*P < 0.001; #P < 0.001

\* \* = indicates p-value for comparison between Control and Obese values  
 # = indicates p-value for comparison between Baseline and subsequent values

DRI = Diabetes Risk Index, BMI = Body Mass Index

**V.J.Sinatra:** None. **B.Lin:** None. **M.Parikh:** None. **J.S.Berger:** n/a. **E.A.Fisher:** n/a. **S.P.Heffron:** None.

P145

## Renal Proximal Tubule-specific Renin Deficiency Has No Effect On Atherosclerosis In Hypercholesterolemic Mice

**Dien Ye,** Chingling Liang, Deborah A. Howatt, Jessica J. Moorleghen, Univ of Kentucky, Lexington, KY; Jan A.H. Danser, Erasmus MC, Rotterdam, Netherlands; Alan Daugherty, UNIVERSITY OF KENTUCKY, Lexington, KY; Hong Lu, Univ of Kentucky, Lexington, KY

**Objective:** Renin cleaving angiotensinogen to release angiotensin I is the rate-limiting step to produce angiotensin II. Although juxtaglomerular cells are the predominant source of renin in circulation, renin protein is also present in proximal tubules. In this study, we investigated the effects of renin in proximal tubule cells (PTC) on development of atherosclerosis in hypercholesterolemic mice. **Approach and Result:** Inducible PTC-specific renin deficient (PTC-renin -/-) mice were developed by breeding renin floxed mice with mice expressing Cre under the control of the N-myc downstream regulated gene 1 (Ndr1-Cre ERT2). All study mice were in a low-density lipoprotein receptor (LDLR) deficient background, and both male and female littermates were studied. Littermates of renin floxed mice with or without Ndr1-Cre ERT2 transgene were injected intraperitoneally with tamoxifen (150 mg/kg/day) for 5 consecutive days when they were 4-6 weeks old. Cre genotypes were determined after weaning (~ 3-4 weeks old) and deletion of renin gene in kidney was verified by PCR of DNA extracted from kidney after termination (~18-20 weeks old). Two weeks after the last injection of tamoxifen, mice were fed a Western diet for 12 weeks, which led

to plasma total cholesterol concentrations above 1000 mg/dl ( $P = 0.893$  in male and  $P = 0.192$  in female between PTC-renin  $+/+$  and  $-/-$  mice). PTC-specific renin deficiency did not affect blood pressure (PTC-renin  $+/+$  vs  $-/-$ :  $110 \pm 1$  mmHg vs  $112 \pm 1$  mmHg in male,  $P = 0.452$ ; and  $105 \pm 3$  mmHg vs  $106 \pm 2$  mmHg in female,  $P = 0.875$ ), as measured by a tail-cuff system. Atherosclerosis in the ascending and aortic arch regions was measured with an *en face* method. No differences on percent lesion area between the two genotypes in both male and female mice (PTC-renin  $+/+$  vs  $-/-$ :  $18.1 \pm 1.4\%$  vs  $18.9 \pm 1.5\%$  in male,  $P = 0.315$ ; and  $16.2 \pm 1.5\%$  vs  $16.2 \pm 1.2\%$  in female,  $P = 0.648$ ). **Conclusion:** Renal proximal tubule-specific renin deficiency does not affect blood pressure and atherosclerosis in hypercholesterolemic mice.

**D.Ye:** None. **C.Liang:** n/a. **D.A.Howatt:** None. **J.J.Moorlegghen:** None. **J.A.Danser:** Research Grant; Significant; Alnylam Pharmaceuticals. **A.Daugherty:** None. **H.Lu:** None.

---

P147

Dietary Protein Elicits A Leucine-mediated Threshold Effect On Monocyte/macrophage Mtorc1-autophagy Signaling Resulting In Elevated Cardiovascular Risk

**Xiangyu Zhang,** WASHINGTON UNIVERSITY, Saint Louis, MO; Divya Kapoor, Washington Univ, St Louis, MO; Se-jin Jeong, Washington Univ, Saint Louis, St Louis, MO; Jeremiah Stitham, Washington Univ at St. Louis, St Louis, MO; Alan Fappi, Eman Yousif, Astrid Rodríguez-Vélez, WASHINGTON UNIVERSITY, Saint Louis, MO; Yu-sheng Yeh, Washington Univ in St. Louis, Saint Louis, MO; Arick Park, WASHINGTON UNIVERSITY IN ST LOUIS, St Louis, MO; Bettina Mittendorfer, Washington Univ, Saint Louis, MO; Babak Razani, WASHINGTON UNIVERSITY SCHOOL MED, Saint Louis, MO

High-protein intake is common in Western societies and generally considered healthy. However, results from some epidemiological studies suggest elevated protein intake is associated with increased risk for ischemic cardiovascular diseases. In addition, results from studies conducted in mice show that a high protein, compared with a standard Western diet, increases atherosclerosis burden and lesion complexity. The adverse effect of protein ingestion on plaque biology in mice is mediated by amino acid-mammalian target of rapamycin (mTOR)-dependent inhibition of autophagy in macrophages. Here, we evaluate the effect of graded amounts of protein ingestion on this amino acid-mTORC1-autophagy mechanism in human monocytes/macrophages and identify leucine as the key amino acid responsible for activating mTORC1 in macrophages. We describe the presence of a threshold effect of high protein intake on this deleterious signaling pathway wherein protein content greater than about 22% of total energy, which is consumed by nearly 1/4<sup>th</sup> of the population in Western societies, acutely activates mTORC1 signaling in monocytes/macrophages. Furthermore, we identify leucine as the critical amino acid modulator and threshold indicator, capable of the dose-dependent mTORC1 activation and downstream functional effects. Finally, by designing specific mouse diets with protein contents mimicking graded levels of protein ingestion in our study participants, we demonstrate the presence of a dietary protein threshold effect in driving atherosclerosis in mouse models. These data demonstrate the potential deleterious impact of excessive protein intake on macrophages and atherosclerotic plaque progression.

**X.Zhang:** None. **B.Mittendorfer:** n/a. **B.Razani:** None. **D.Kapoor:** None. **S.Jeong:** None. **J.Stitham:** None. **A.Fappi:** n/a. **E.Yousif:** None. **A.Rodríguez-vélez:** n/a. **Y.Yeh:** n/a. **A.Park:** None.

---

P148

Angiotensin II Type 1a Receptor Deletion In Renal Proximal Tubular Cells Does Not Attenuate Atherosclerosis In Hypercholesterolemic Mice

**Masayoshi Kukida,** Dien Ye, Deborah Howatt, Yuriko Katsumata, Ching Ling Liang, Hisashi Sawada, Jessica J Moorlegghen, Alan Daugherty, Hong S Lu, UNIVERSITY OF KENTUCKY, Lexington, KY

**Objective:** AngII (Angiotensin II) acts through AT1aR (AngII type 1a receptor) to promote atherosclerosis. Despite the consistency that global inhibition of AT1aR markedly attenuates atherosclerosis, it remains undefined in which cell types that AT1aR contributes to atherosclerosis formation. Since renal AngII is associated with increased atherosclerosis in hypercholesterolemic mice, and AT1aR is abundant on PTCs (proximal tubular cells), the present study investigated the effects of AT1aR deletion in PTCs on atherosclerosis in hypercholesterolemic mice. **Approach and Results:** First, both male and female LDL receptor  $-/-$  mice were fed a Western diet and infused with either vehicle or losartan for 12 weeks. Losartan

led to more profound increases of plasma renin concentrations and greater reduction of systolic blood pressure in female than in male mice, whereas atherosclerosis was attenuated by losartan equivalently in both sexes. Secondary, we determined whether the effects of losartan were attributed to inhibition of AT1aR on PTCs. To generate PTC-specific AT1aR  $-/-$  mice, AT1aR floxed mice were bred with mice expressing Cre under the control of the N-myc downstream regulated gene 1. These mice were injected with 150 mg/kg/day of tamoxifen for 5 days to activate Cre at the age of 4 - 6 weeks. RNAscope detected AT1aR mRNA in both PTCs and glomeruli; mRNA of AT1aR was absent in PTCs, but not glomeruli, of PTC-specific AT1aR  $-/-$  mice. Two weeks after completion of tamoxifen injection, these mice in LDL receptor  $-/-$  background were fed Western diet for 12 weeks. Deletion of AT1aR in PTCs did not affect plasma renin concentrations, blood pressure and atherosclerosis in either sex. Finally, to investigate the impacts of PTC-specific AT1aR deletion under the conditions with enhanced AngII stimulation, AngII was infused subcutaneously for 12 weeks. There were no differences in both blood pressure and atherosclerosis between genotypes. **Conclusion:** Although pharmacological inhibition of AT1aR reduced atherosclerosis profoundly in both sexes, PTC-specific AT1aR deletion did not affect atherosclerosis in hypercholesterolemic mice. Our future study will determine whether the presence of AT1aR in both PTCs and glomeruli are needed to promote atherosclerosis.

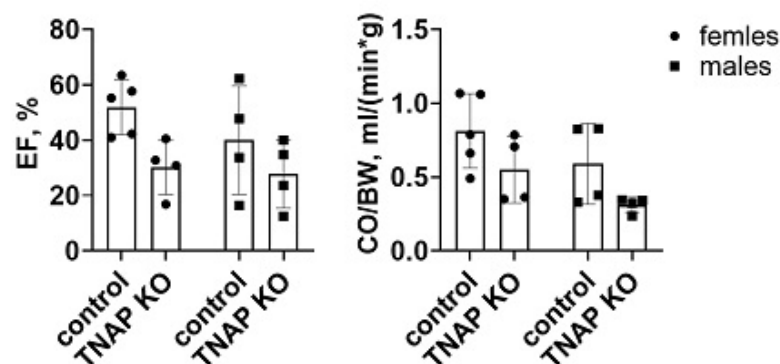
**M.Kukida:** None. **D.Ye:** None. **D.Howatt:** None. **Y.Katsumata:** None. **C.L.Liang:** None. **H.Sawada:** None. **J.J.Moorlegghen:** None. **A.Daugherty:** None. **H.S.Lu:** None.

P152

#### Downregulation Of Tissue-nonspecific Alkaline Phosphatase In Endothelial Cells Does Not Affect Calcification But Reduces Cardiac Function In Mice With Atherosclerosis

**Sandy Than,** Maria Canellos, Ethan Shamsian, New York Inst of Technology, Old Westbury, NY; Mohnish Singh, NYITCOM, Glen Head, NY; Olga V Savinova, New York Inst of Technology, Old Westbury, NY

**Introduction:** We have previously demonstrated that overexpression of tissue-nonspecific alkaline phosphatase (TNAP) in endothelial cells increases vascular calcification and accelerates atherosclerosis. Whether TNAP activity in vascular endothelium is essential for intimal calcification and the progression of atherosclerosis is unknown. **Hypothesis:** We hypothesized that elimination of TNAP expression in endothelial cells would be sufficient to reduce intimal calcification associated with atherosclerosis. **Methods:** Endothelial TNAP knockout (KO) mice were developed on the background of the low density lipoprotein receptor mutation. Endothelial TNAP KO (n = 8) and control (n = 9) mice were fed a Western diet starting from 8 weeks and until 52 weeks of age. Cardiac structure and function were assessed by echocardiography. Calcium volume was measured in the aortic root and aortic arch area by microcomputed tomography (microCT). Data were analyzed using a 2-way ANOVA to calculate the effects of the genotype adjusted for sex. **Results:** MicroCT data did not show any statistically significant decrease in calcification in endothelial TNAP KO mice compared to controls; however, other cardiac parameters were affected by genotype. The physiological examination of the mice demonstrated that ablation of TNAP expression in the endothelium resulted in significant reduction in ejection fraction, stroke volume, and cardiac output in the absence of cardiac hypertrophy. **Conclusion:** Contrary to our hypothesis, TNAP has no effect on natural progression of calcified atherosclerosis; however, our data indicate that TNAP is required for protection of cardiac function under conditions of atherosclerosis in mice



**S.Than:** None. **M.Canellos:** None. **E.Shamsian:** None. **M.Singh:** None. **O.V.Savinova:** None.

# Upregulation Of Thrombospondin-1 Associates With Accelerated Atherosclerosis And Reduced Smooth Muscle Cell Differentiation In Metabolic Syndrome

**Shreya Gupta**, Saugat Khanal, Kent State Univ, Kent, OH; Amy Mathias, Jason Lallo, Northeast Ohio Medical Univ, Rootstown, OH; Jessica Ferrell, Priya Raman, Kent State Univ, Kent, OH

Hyperglycemia and obesity, characteristic of metabolic syndrome (MetS), are important risk-factors for atherosclerosis. MetS patients manifest increased vascular smooth muscle cell (VSMC) migration and proliferation, hallmark of VSMC phenotypic transition, critical for evolution of atherosclerosis. We previously reported that high glucose and high leptin independently upregulate a potent proatherogenic extracellular matrix protein, Thrombospondin-1 (TSP-1), expression in VSMC. The goal of the present study was to interrogate the role of TSP-1 in SMC de-differentiation and development of atherosclerosis in MetS. We utilized a mouse model of combined MetS and atherosclerosis (KKAY<sup>+/+</sup>/ApoE<sup>-/-</sup>) generated by crossing obese hyperglycemic agouti KKAY<sup>+/+</sup> mice with atherosclerotic ApoE<sup>-/-</sup>. Upon weaning (4 wks age), male yellow KKAY<sup>+/+</sup>/ApoE<sup>-/-</sup> and age-matched black KKAY<sup>-/-</sup>/ApoE<sup>-/-</sup> littermates on standard lab diet were monitored monthly for body weight and blood glucose. At 24 wks age, mice were harvested after overnight fasting; plasma, aorta and heart were collected for biochemical, molecular and lesion studies. Prior to harvest, mice were subjected to treadmill exercise test at an incline with progressively increasing speed until exhaustion. At 16 wks age, yellow KKAY<sup>+/+</sup>/ApoE<sup>-/-</sup> mice showed significant increase in body weight and random blood glucose levels (<0.0001) vs. black KKAY<sup>-/-</sup>/ApoE<sup>-/-</sup> littermates, validating the MetS phenotype. Peak oxygen consumption (VO<sub>2max</sub>), maximum running speed and total run time until exhaustion were significantly reduced in MetS KKAY<sup>+/+</sup>/ApoE<sup>-/-</sup> mice (p<0.003 vs. non-MetS KKAY<sup>-/-</sup>/ApoE<sup>-/-</sup>), suggesting impaired cardiovascular fitness. Aortic root morphometry revealed 4-fold increase in lesion lipid burden in MetS vs non-MetS mice. This was accompanied with reduced LMOD (SM contractile marker) and SRF (transcriptional activator of SM contractile genes) expression in aortic vessels of MetS mice (p<0.04 vs. non-MetS mice). Notably, lesion abundance and reduced SMC differentiation associated with increased TSP-1 expression in the aortic vasculature of MetS mice. Together, our data suggest a putative role of TSP-1 in SMC de-differentiation and atherosclerotic lesion formation in metabolic syndrome.

**S.Gupta:** None. **S.Khanal:** None. **A.Mathias:** None. **J.Lallo:** None. **J.Ferrell:** None. **P.Raman:** None.

# Pgc1a Regulates The Endothelial Response To Fluid Shear Stress Via Telomerase Reverse Transcriptase Control Of Heme Oxygenase-1

**Shashi Kant**, Brigham Women's Hosp, Boston, MA

Fluid shear stress (FSS) is known to mediate multiple phenotypic changes in the endothelium. Laminar FSS (undisturbed flow) is known to promote endothelial alignment to flow that is key to stabilizing the endothelium and rendering it resistant to atherosclerosis and thrombosis. The molecular pathways responsible for endothelial responses to FSS are only partially understood. Here we have identified peroxisome proliferator gamma coactivator-1α (PGC-1α) as a flow-responsive gene required for endothelial flow alignment *in vitro* and *in vivo*. Compared to oscillatory FSS (disturbed flow) or static conditions, laminar FSS (undisturbed flow) increased PGC-1α expression and its transcriptional co-activation. PGC-1α was required for laminar FSS-induced expression of telomerase reverse transcriptase (TERT) *in vitro* and *in vivo* via its association with ERRα and KLF4 on the TERT promoter. We found that TERT inhibition attenuated endothelial flow alignment, elongation, and nuclear polarization in response to laminar FSS *in vitro* and *in vivo*. Among the flow-responsive genes sensitive to TERT status was heme oxygenase-1 (HMOX1), a gene required for endothelial alignment to laminar FSS. Thus, these data suggest an important role for a PGC-1α-TERT-HMOX1 axis in the endothelial stabilization response to laminar FSS.

**S.Kant:** None.



## Intimal And Medial Calcification Underlie Differential Molecular Mechanisms

**Marina Augusto Heuschkel**, Jonas Heyn, Dept of Internal Med I – Cardiology, Medical Faculty, RWTH Aachen Univ, Aachen, Germany; Emiel van der Vorst, Interdisciplinary Ctr for Clinical Res (IZKF), Inst for Molecular Cardiovascular Res (IMCAR), RWTH Aachen Univ, Aachen, Germany; Nikolaus Marx, Claudia Goettsch, Dept of Internal Med I – Cardiology, Medical Faculty, RWTH Aachen Univ, Aachen, Germany

**Introduction:** Vascular calcification (VC) is a significant risk factor for cardiovascular morbidity and mortality. Based on the mineral deposition site in the arterial wall, VC classifies into intimal and medial calcification. We hypothesize that distinct in vitro mineralization methods promote specific intracellular signalling pathways in vascular smooth muscle cells (SMC), reflecting both VC types. **Methods and results:** Human coronary artery SMCs were cultured in osteogenic medium (OM) or high calcium-phosphate medium (CaP) to induce calcification. OM resembles SMCs differentiation in intimal calcification – a key process in atherosclerotic plaque remodeling. CaP is associated with chronic kidney disease – a risk factor for medial calcification. Transcriptomics revealed a distinct gene expression profile of OM and CaP-calcifying SMCs, that share 6.9% and 11.3% of their genes, respectively. The 109 shared dysregulated genes between OM and CaP-calcifying SMCs highlighted enriched pathways related to SMC contraction and metabolism. Real-time extracellular efflux analysis demonstrated a different metabolic profile in OM and CaP-calcifying SMCs. We observed decreased mitochondrial respiration and glycolysis (-57,3%  $p=0.029$ ) by CaP and increased mitochondrial respiration without altered glycolysis by OM. Subsequent kinome and in silico drug repurposing analysis (Connectivity Map) revealed a distinct role of protein kinase C (PKC). Validation using prostratin, a specific PKC activator, demonstrated differential effects on matrix mineralization that was decreased by OM (-69,3%,  $p<0.001$ ) and increased by CaP (+69,6%,  $p=0.044$ ). **Conclusions:** In conclusion, OM and CaP-induced SMC calcification underlies differential mechanisms in vitro. Therefore, research should distinguish between the two aspects of VC and increased knowledge about the underlying pathophysiological mechanisms may open the possibility for preventing intimal and medial calcification.

**M.Augusto heuschkel:** None. **J.Heyn:** None. **E.Van der vorst:** None. **N.Marx:** None. **C.Goettsch:** None.

## Loss Of Nicotinamide Nucleotide Transhydrogenase Promotes Endothelial Activation In Atherosclerosis

**Shashanka Rao**, Nicole Gautier, LSU HEALTH SCIENCES CENTER, Shreveport, LA; Robert Schilke, LSU Health Science Ctr – Shrevep, Shreveport, LA; Matthew D Woolard, LSUHSC, Shreveport, LA; David M Krzywanski, LSU HEALTH SCIENCES CENTER, Shreveport, LA

Heart disease is the leading cause of death in the United States and atherosclerosis accounts for nearly 75% of all deaths from heart disease. Atherosclerosis is a chronic inflammatory disease and mitochondrial reactive oxygen species (mtROS) are critical contributors to disease development. Nicotinamide nucleotide transhydrogenase (NNT) is a mitochondrial protein that maintains mitochondrial NADPH pools and supports the enzymatic degradation of mtROS. Preliminary data indicates that NNT expression is decreased in the endothelium of human atherosclerotic plaques and we sought to test the hypothesis that the loss of NNT increases mtROS and promotes atherosclerosis by enhancing endothelial and vascular dysfunction. Previous we have demonstrated that the loss of NNT was associated with increased vascular ROS production, plaque formation, and plaque size in response to treatment with PCSK9 and high fat diet (HFD). We now show that the loss of NNT in endothelial specific NNT knockout mice promotes enhanced endothelial VCAM-1 expression in response to HFD and disturbed flow. Similarly, *in vitro*, the loss of NNT promoted both VCAM-1 and ICAM-1 expression in response to oxLDL. Increased adhesion molecule expression associated with the loss of NNT also augmented monocyte adhesion in response to oxLDL consistent with vascular inflammation observed in early atherosclerosis. Additionally, macrophages isolated from NNT knockout mice display enhanced M1 polarization, decreased lipid uptake, and impaired lipid utilization. Co-treatment with the mitochondria targeted antioxidant MitoEbselen is able to normalize both endothelial and macrophage function, underscoring a critical role for mtROS in promoting an inflammatory phenotype in these cells. In both global and endothelial cell specific NNT knockout mice the loss of NNT was associated with increased necrotic core formation in response to PCSK9 treatment and 16 weeks of high fat diet. Taken together, these data indicate that decreased NNT expression promotes

endothelial activation, increased inflammatory cell trafficking, macrophage metabolic dysfunction and M1 polarization that could contribute to an acceleration of necrotic core development and severe atherosclerotic disease.

**S.Rao:** None. **N.Gautier:** n/a. **R.Schilke:** None. **M.D.Woolard:** Research Grant; Significant; NIH NHLBI. **D.M.Krzywanski:** None.

---

P158

Hepatic Trib1 Induces Proteasome-dependent Degradation Of C/ebp $\alpha$  In A Cop1- And Stk40- Dependent Manner

**Caio V Matias,** Kavita S Jadhav, Elizabeth H Ha, Columbia Univ, New York, NY; Marek Nagiec, Broad Inst, Cambridge, MA; Adam P Skepner, Broad Inst of MIT and Harvard, Cambridge, MA; Rajesh K Soni, Columbia Univ, New York, NY; Robert C Bauer, COLUMBIA UNIVERSITY, New York, NY

The gene tribbles pseudokinase 1 (*TRIB1*) has been repeatedly linked to multiple human cardiometabolic traits through genome-wide association studies, including coronary artery disease, plasma cholesterol and triglycerides, and circulating liver transaminases, signaling that *TRIB1* is a key regulator of liver metabolism and health. Studies in liver specific *Trib1* KO mice have shown that hepatic TRIB1 regulates de novo lipogenesis and steatosis through the regulation of protein levels of the transcription factor C/EBP $\alpha$ , yet the mechanism governing this relationship in hepatocytes has not been investigated. We demonstrate here that human TRIB1 promotes the degradation of C/EBP $\alpha$  in both a COP1- and proteasome-dependent manner in human hepatoma cells. We also observe rapid degradation of TRIB1 protein in hepatoma cells, and find that this is also COP1- and proteasome-dependent. To identify hepatocyte-specific interacting partners of TRIB1 that regulate these processes, we performed tandem-affinity purification of TRIB1 in Huh7 cells and subsequent mass-spec analysis, and identified multiple novel TRIB1 binding partners including the pseudokinases serine/threonine kinase 38 (STK38) and 40 (STK40). We confirmed these interactions in vitro and found that STK40, but not STK38, is required for TRIB1-mediated proteasomal degradation of C/EBP $\alpha$ . Together, our results reveal that TRIB1 induces proteasomal degradation of CEBP/ $\alpha$  in a COP1- and proteasome-dependent manner in human hepatocytes. Further, we identify the pseudokinase STK40 as a novel regulator of hepatic TRIB1 function, and ongoing work aims to investigate the role of STK40 in hepatic lipid metabolism. Finally, we show that TRIB1 is itself degraded by the proteasome in a COP1-dependent manner. As increased hepatic Trib1 confers a beneficial metabolic profile in mice, these findings could provide a novel avenue for therapeutic targeting of TRIB1 in the treatment of cardiometabolic disease. Overall, our findings add greater detail to the molecular mechanisms governing the regulation of metabolism by hepatic TRIB1, a gene which human genetics highlights as a crucial regulator of cardiometabolic traits in humans.

**C.V.Matias:** None. **K.S.Jadhav:** None. **E.H.Ha:** None. **M.Nagiec:** Stock Shareholder; Modest; Pfizer. **A.P.Skepner:** None. **R.K.Soni:** None. **R.C.Bauer:** None.

---

P159

Induction Of Human Angiotensinogen In Hepatocytes And Human Renin In Renal Proximal Tubule Cells Does Not Accelerate Atherosclerosis In Mice

**Naofumi Amioka,** Univ of Kentucky, Saha Cardiovascular Res Ctr, Lexington, KY; Masayoshi Kukida, Lexington, KY; Dien Ye, Univ of Kentucky, Lexington, KY; Deborah A Howatt, UNIVERSITY OF KENTUCKY, KY; Jessica J Moorlegghen, Alan Daugherty, UNIVERSITY OF KENTUCKY, Lexington, KY; Hong Lu, Univ of Kentucky, Lexington, KY

**Objective:** Hepatocyte-produced angiotensinogen (AGT) can be filtered by glomeruli and retained in renal proximal tubules. Renin protein has also been detected in proximal tubules (PTC) of kidney. However, it is unknown whether AGT and renin in proximal tubules contribute to atherosclerosis. This study aimed to determine whether hepatocyte-derived AGT interacts with renin in proximal tubules to promote atherosclerosis. **Approach and Results:** Transgenic mice expressing human renin driven by a kidney androgen-related protein promoter (KAP-hREN) in an LDLR  $-/-$  background were administered subcutaneously with testosterone (15 mg/mouse, constant release for 60 days) to activate the human renin transgene in PTCs. To induce synthesis of human AGT in hepatocytes, adeno-associated viral (AAV; 3

x 10<sup>10</sup> genomic copies/mouse) vector containing human AGT with a liver-specific promoter was injected intraperitoneally. Three groups of male littermates were administered testosterone: (1) wild type mice administered null AAV (n=11), (2) KAP-hREN transgenic mice administered null AAV (n=7), and (3) KAP-hREN transgenic mice (n=8) administered AAV containing human AGT. Two weeks after administration of testosterone and AAVs (either null or human AGT), all mice were fed a Western diet for 6 weeks. Induction of human renin was confirmed by mRNA abundance of human renin in kidney of KAP-hREN transgenic mice. In mice administered human AGT AAV, presence of human AGT was detected in plasma with a human AGT ELISA kit. Induction of both human AGT in liver and human renin in proximal tubules did not affect plasma cholesterol concentrations or systolic blood pressure. Atherosclerotic lesion sizes, as quantified by percent lesion area using an *en face* method, were not different among the 3 groups (Group 1 vs 2 vs 3: 3.7 ± 0.4% vs 3.3 ± 0.9% vs 2.3 ± 0.3%; P = 0.19). **Conclusions:** Induction of human AGT in hepatocytes and human renin in proximal tubules does not augment atherosclerosis in hypercholesterolemic mice.

**N.Amioka:** None. **M.Kukida:** None. **D.Ye:** None. **D.A.Howatt:** None. **J.J.Moorlegghen:** None. **A.Daugherty:** None. **H.Lu:** n/a.

---

P160

#### Deficiency Of Angiotensin-converting Enzyme In Renal Proximal Convolved Tubules Does Not Attenuate Atherosclerosis In Mice

**Hui Chen,** Kukida Masayoshi, Dien Ye, Univ of Kentucky, Lexington, KY; Deborah A Howatt, UNIVERSITY OF KENTUCKY, KY; Jessica J Moorlegghen, UNIVERSITY OF KENTUCKY, Lexington, KY; Hisashi Sawada, Univ of Kentucky, Lexington, KY; Alan Daugherty, UNIVERSITY OF KENTUCKY, Lexington, KY; Hong S Lu, UNIVERSITY KENTUCKY, Lexington, KY

**Objective:** Angiotensin-converting enzyme (ACE) is the enzyme to generate Angiotensin II (AngII), an important contributor to atherosclerosis. ACE is present in all 3 segments (S1, S2, and S3) of proximal tubular cells (PTCs), and AngII concentrations are higher in kidney than in plasma. The purpose of this study was to determine whether ACE in PTCs contributes to atherosclerosis in mice. **Approach and Results:** Female ACE floxed mice and male Ndr1-Cre ERT2<sup>+/+</sup> transgenic mice were bred to generate ACE f/f x Ndr1-Cre ERT2<sup>-/-</sup> (PTC-ACE<sup>+/+</sup>) and ACE f/f x Ndr1-Cre ERT2<sup>-/-</sup> (PTC-ACE<sup>-/-</sup>) littermates. Male PTC-ACE<sup>+/+</sup> (n=7) and PTC-ACE<sup>-/-</sup> (n=10) littermates in an LDL receptor<sup>-/-</sup> background were used for atherosclerosis study. After Cre genotyping using tail DNA, mice (both Cre ERT2<sup>-/-</sup> and Cre ERT2<sup>+/+</sup>) were injected with 150 mg/kg/day of tamoxifen for 5 consecutive days at the age of 4-6 weeks. Two weeks after the last injection of tamoxifen, mice were fed a Western diet (Envigo, Diet #TD.88137) for 12 weeks to induce hypercholesterolemia. Blood pressure was measured using a tail-cuff system. No difference of blood pressure was detected between the two genotypes (PTC-ACE<sup>+/+</sup> vs. PTC-ACE<sup>-/-</sup>: 126 ± 4 vs. 125 ± 3 mmHg; P = 0.763). All study mice were hypercholesterolemic, but plasma cholesterol concentrations were not different between the two genotypes (PTC-ACE<sup>+/+</sup> vs. PTC-ACE<sup>-/-</sup>: 1376 ± 119 vs. 1543 ± 93 mg/dl; P = 0.28). PTC-specific deletion of ACE was confirmed after termination using immunostaining of ACE. In mice with Ndr1-Cre ERT2 transgene, immunostaining of ACE in kidney section showed an absence of ACE in S1 and S2 of PTCs, but ACE protein in S3 remained. Deletion of ACE in S1 and S2 of PTCs did not change hypercholesterolemia-induced atherosclerosis in the ascending and aortic arch regions (PTC-ACE<sup>+/+</sup> vs. PTC-ACE<sup>-/-</sup>: 9.6 ± 0.9% vs. 7.0 ± 1.9%; P = 0.13 by Mann-Whitney Rank Sum Test), as measured using an *en face* method. **Conclusion:** ACE deficiency in S1 and S2 of renal proximal tubular cells had no effect on atherosclerosis in hypercholesterolemic mice. Since ACE is more abundant in S3 than in S1 and S2 of PTCs, it would be important to determine the role of ACE in the S3 segment.

**H.Chen:** None. **K.Masayoshi:** n/a. **D.Ye:** None. **D.A.Howatt:** None. **J.J.Moorlegghen:** None. **H.Sawada:** None. **A.Daugherty:** None. **H.S.Lu:** None.

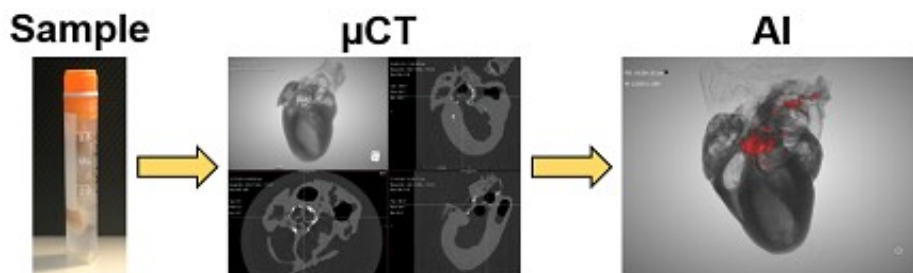
---

P161

#### Novel Micro-CT Method To Assess Atherosclerotic Calcification In Mice

**Jashandeep Kaur,** Beatrice Carpo, Nina D. Kosciuszke, Mohnish Singh, Olga V Savinova, New York Inst of Technology Coll of Osteopathic Med, Old Westbury, NY

**Introduction:** Animal models are used to study mechanisms and consequences of calcification in atherosclerosis. As a standard practice, vascular calcification in a mouse model is measured by laborious histological preparation and calcium staining. In this study, we developed an ex-vivo micro-CT ( $\mu$ CT) method to quantify calcium volume in the aortic roots and arches in mice with atherosclerosis. **Objective:** The purpose of this study was to evaluate feasibility and compare calcium measurements between the  $\mu$ CT and histological methods. **Methods:** We used a mouse model of increased atherosclerotic calcification due to overexpression of tissue nonspecific alkaline phosphatase (TNAP) in macrophages. Formalin-fixed tissues were dissected and slowly immersed in mineral oil. Samples were assembled in cryogenic vials pre-filled with mineral oil. Cotton was used to immobilize and space the samples.  $\mu$ CT images of whole hearts and aortic arches were collected at a 7.1 micron resolution. Multiple Deep Learning models, implemented in Dragonfly 2020.1 (ORS), were trained on one sample for image segmentation. Histological analysis was performed according to standard protocols. **Results:** Multiple preparations of hearts and aortic roots can be scanned in a single overnight experiment. A Deep Learning model of the U-Net5 architecture was most successful in the segmentation of soft tissues and calcifications, while excluding  $\mu$ CT artifacts. The data showed a good correlation between detection of calcium by  $\mu$ CT and histology.  $\mu$ CT analysis of samples from 1-year-old TNAP transgenic mice demonstrated a 4-fold increase in calcification volume compared to control mice. **Conclusion:** Our  $\mu$ CT method is feasible and, in some aspects, superior to the traditional histological analysis because it is less time-consuming and less prone to artifacts.  $\mu$ CT approach is non-destructive thus permitting analyses of samples by multiple analytical methods after removal of mineral oil.



J.Kaur: None. B.Carpo: None. N.D.Kosciuszek: None. M.Singh: None. O.V.Savinova: None.

---

P162

## Leveraging Lysosomal Calcium Flux As A Strategy To Induce Autophagy-lysosomal Biogenesis In Macrophages

**Se-Jin Jeong**, Washington Univ, Saint Louis, St Louis, MO; Xiangyu Zhang, WASHINGTON UNIVERSITY, Saint Louis, MO; Yu-sheng Yeh, Washington Univ in St. Louis, Saint Louis, MO; Astrid Rodríguez-Vélez, Washington Univ, Saint Louis, St Louis, MO; Babak Razani, WASHINGTON UNIVERSITY SCHOOL MED, Saint Louis, MO

Dysfunction in macrophage lysosomes leading to poor handling of atherogenic lipids, apoptotic cells, and other cytotoxic debris leads to progression of atherosclerotic plaque size and complexity. Stimulation of TFEB, the master transcriptional regulator of autophagy-lysosomal biogenesis, in macrophages has been shown to promote the degradative capacity of plaque macrophages with reductions in atherosclerosis. Thus, there is interest in harnessing this pathway for cardiovascular therapeutics. One of the mechanisms by which TFEB is activated and triggered to translocate to the nucleus is the release of calcium from the lysosomal lumen to the cytosol via specialized channels located at the lysosomal membrane including mucolipin 1, also known as the transient receptor potential cation channel mucolipin 1 (TRPML1). We find that TRPML1 is highly expressed in macrophages and is involved in a feedback loop by which TFEB positively regulates TRPML1 mRNA expression to further support long-term autophagy-lysosomal biogenesis. Utilizing a mammalian TRPML1 agonist, mucolipin synthetic agonist 1 (ML-SA1), we show that induction of lysosomal calcium release can robustly trigger TFEB nuclear translocation in macrophages. In turn, numerous downstream TFEB transcriptional targets mediating autophagy-lysosomal biogenesis are upregulated resulting in salutary effects including enhanced aggrephagy and clearance of cytotoxic p62-enriched protein aggregates, blunting of inflammasome activation and proinflammatory IL-1 $\beta$  production, and reductions in macrophage apoptosis. Taken together, our data support that stimulation of lysosomal

calcium flux can be a novel strategy of enhancing TFEB and macrophage degradative capacity in atherosclerosis.

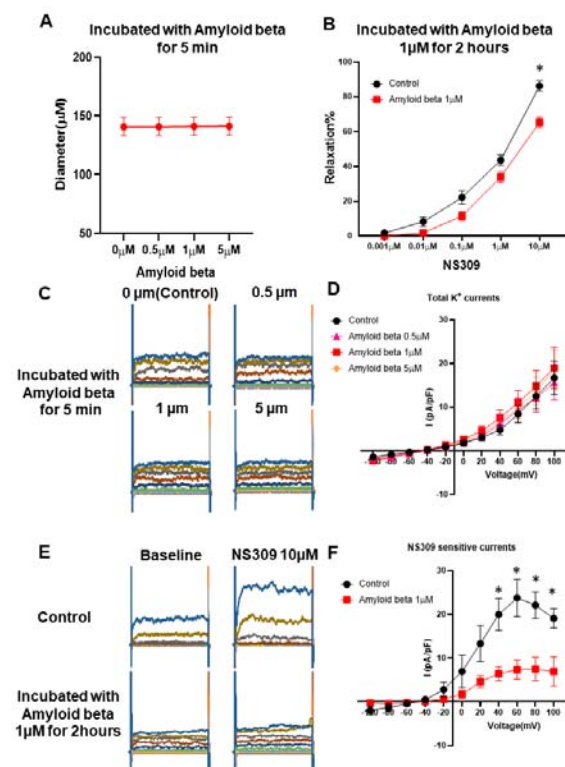
**S.Jeong:** None. **X.Zhang:** None. **Y.Yeh:** n/a. **A.Rodríguez-vélez:** n/a. **B.Razani:** None.

P163

## Acute Treatment With Amyloid Beta Impaired Cerebral Artery Reactivity And Endothelial Sk Channel Activity

**Hang Xing**, Zhiqi Zhang, Jun Feng, Rhode Island Hosp, Providence, RI

**Introduction** The accumulation/aggregation of amyloid-beta(A $\beta$ ) has been recognized to play a key role in the progression of Alzheimer's disease (AD) and the neurovascular dysfunction induced by A $\beta$  may contribute to cognitive impairment and dementia during AD. A $\beta$  deposition in cerebrovasculature exerts direct toxicity to smooth muscle cells and impairs nitric oxide signaling in the endothelium. Endothelium-dependent hyperpolarization and vascular relaxation are partially mediated by small-conductance calcium-activated potassium (SK) channels, and the inhibition of SK channels plays an important role in endothelial dysfunction. However, there has been limited investigation into the acute effect of A $\beta$  on the endothelial SK channel function and related cerebrovascular reactivity. **Hypothesis** We hypothesized that acute treatment with A $\beta$  downregulates SK channel activity and impaired cerebrovascular reactivity. **Methods** A $\beta$  and SK channel activator NS309 were used in measuring *in-vitro* relaxation response of pre-contracted mouse cerebral arteries, and the SK channel currents of human cerebral artery endothelial cells by the whole-cell patch-clamp. **Results** Mouse cerebral artery diameter was no significantly changed in incubation with A $\beta$  (0.5–5 $\mu$ M) for 5 minutes (Fig. A, n=6, respectively). However, cerebral artery dilation with NS309 (10 $\mu$ M) was significantly decreased after incubation with A $\beta$  (1 $\mu$ M) for 2 hours (Fig. B, n=6, respectively). The patch clamp recording showed that total potassium currents were no significantly changed in the incubation with A $\beta$  (0.5–5 $\mu$ M) for 5 minutes (Fig. C&D, n=6, respectively). In contrast, the currents of SK channels in cerebral artery endothelial cells were significantly impaired after incubation with A $\beta$  (1 $\mu$ M) for 2 hours (Fig. E&F, n=5–7, respectively). **Conclusions** Acute treatment with A $\beta$  dysregulated of cerebrovascular endothelial SK channels and impaired the cerebrovascular reactivity.



**H.Xing:** None. **Z.Zhang:** None. **J.Feng:** None.

### Pronethalol Reduces Sox2 To Ameliorate Vascular Calcification

**Daoqin Zhang**, Xiaojing Qiao, Jiayi Yao, UCLA, Los Angeles, CA; Xiuju Wu, Los Angeles, CA; Xinjiang Cai, Uni. of California, Los Angeles, Los Angeles, CA; Jocelyn A. Ma, Kristina I Bostrom, Yucheng Yao, UCLA, Los Angeles, CA

Vascular calcification is present in most people over 60 years of age and results in severe complications that increase all-cause mortality of cardiovascular disease, diabetes mellitus and chronic kidney disease. Previous studies demonstrated that endothelial induction of SRY (sex determining region Y)-box 2 (Sox2) triggered endothelial-mesenchymal transitions (EndMTs) and drove endothelial cells (ECs) towards osteoblastic differentiation. The excess Sox2 induced mesenchymal markers and promoted ECs to acquire mesenchymal potential and undergo osteogenic differentiation. Recently, we reported that beta-adrenergic receptor antagonists (beta-blockers) decreased Sox2 expression in cerebrovascular endothelium and limited arteriovenous malformations. In this study, we hypothesize that the beta-blockers suppress Sox2 also in arterial endothelium to limit vascular calcification. To test this hypothesis, we used the *Mgp*<sup>-/-</sup> mouse model, where the elastic arteries start to calcify at 1-2 weeks of age and exhibit severe calcification at 4 weeks of age. We treated *Mgp*<sup>-/-</sup> mice with pronethalol for two weeks starting at 2 weeks of age and revealed that the pronethalol treatment significantly ameliorated the aortic calcification in *Mgp*<sup>-/-</sup> aortas. To examine the time-course of the pronethalol effect on calcification, we started the pronethalol treatment at three different time points, at 1, 2 and 3 weeks of age. The treatments all ended at 5 weeks of age. The results showed that the total aortic calcium was immediately reduced if the pronethalol was started at 1 or 2 weeks of age and was maintained at low levels as the treatment continued. When the treatment was started at 3 weeks of age, it still reduced the aortic calcium but to a lesser degree. To determine if pronethalol limits vascular calcification also in atherosclerosis and diabetes, we treated *Apoe*<sup>-/-</sup> mice and *Ins2*<sup>Akita/+</sup> mice with pronethalol. Aortic calcium and histology showed that pronethalol reduced the atherosclerotic lesion calcification and decreased the calcification in *Ins2*<sup>Akita/+</sup> mice. Together, the results suggest that the beta-blocker pronethalol reduces Sox2 expression in the arterial endothelium, thereby limiting EndMTs and vascular calcification.

**D.Zhang:** n/a. **X.Qiao:** n/a. **J.Yao:** n/a. **X.Wu:** None. **X.Cai:** None. **J.A.Ma:** None. **K.I.Bostrom:** None. **Y.Yao:** No ne.

### Cardiac Capillary Pericytes Constriction Mediates Sleep Deprivation Induced Coronary Microcirculation Dysfunction

**Chao Wu**, Ziyu Guo, Peking Univ China-Japan Friendship Sch of Clinical Med, Beijing, China; Yimin Tu, Chinese Acad of Medical Sciences and Peking Union Medical Coll, Beijing, China; Yaxin Wu, Qing Li, Peking Univ China-Japan Friendship Sch of Clinical Med, Beijing, China; Xiaozhai Yu, Yike Li, Chinese Acad of Medical Sciences and Peking Union Medical Coll, Beijing, China; Changan Yu, China-Japan Friendship Hosp, Beijing, China; Yi Fu, Peking Univ, Beijing, China; Yanxiang Gao, China-Japan Friendship Hosp, Beijing, China; Wei Kong, Peking Univ, Beijing, China; Jingang Zheng, China-Japan Friendship Hosp, Beijing, China

**Background:** Lack of sleep can lead to a variety of adverse cardiovascular events and even sudden death. In most cases, there is no obstructive coronary artery. Coronary microcirculation dysfunction (CMD) is thereby thought to play an important role in cardiovascular events caused by sleep loss. Pericytes regulate blood flow and mediate neurovascular signaling in brain. Here, we hypothesized that cardiac capillary pericytes mediate sleep loss related CMD.

**Methods and results:** Eight-week-old male C57BL/6J mice were deprived sleep for 6 hours or 72 hours. Cardiac function was detected by transthoracic echocardiography before and after sleep deprivation (SD). Vascular endothelial dyes were perfusion before tissue harvest to evaluate cardiac perfusion. By whole heart clearing, 3D immunolabeling and imaging, the effect of pericytes on cardiac capillary was accessed. Acute 6-hours total sleep deprivation or 72-hours severe sleep deprivation led to decreased cardiac systolic and diastolic dysfunction. Left ventricular end diastolic diameter and left ventricular end systolic diameter increased by 10.12% (0.32 mm of 3.14 mm) and 19.00% (0.31 mm of 1.63 mm). Although coronary flow velocity reserve showed no differences between sleep deprivation and control groups, the basal and

maximum coronary blood velocity were increased in acute and severe total sleep deprivation mice, which illustrated CMD. Compared with mice in the control group, the area of cardiac perfusion in the sleep deprivation group was significantly reduced ( $33.42 \pm 4.30\%$  vs.  $53.81 \pm 7.42\%$ ,  $P < 0.05$ ; SD group,  $n=7$ ; control group,  $n=6$ ). Whole mount heart imaging showed pericytes were widely distributed around the microvascular, without difference in regional distribution in the heart. In the area of cardiac perfusion defect, capillary blockages colocalized with pericytes, and the capillary diameter at the pericyte body was significantly reduced in sleep deprived mice ( $2.01 \pm 0.12 \mu\text{m}$  vs.  $2.92 \pm 0.07 \mu\text{m}$ ,  $P < 0.05$ ; SD group,  $n=10$ ; control group,  $n=10$ ).

Conclusion: Sleep restriction led to cardiac dysfunction and CMD, that pericytes mediated contraction of capillaries might contribute to the process. Cardiac pericytes would be a novel therapeutic target in sleep loss associated heart disease.

**C.Wu:** Research Grant; Significant; National Natural Science Foundation of China, National Key Clinical Specialty Discipline Construction Program, Natural Science Foundation of Beijing Municipality. **Y.Gao:** None. **W.Kong:** None. **J.Zheng:** None. **Z.Guo:** None. **Y.Tu:** None. **Y.Wu:** None. **Q.Li:** None. **X.Yu:** None. **Y.Li:** None. **C.Yu:** None. **Y.Fu:** None.

---

P166

Gsk3beta Shifts Osteoblast To Endothelial Differentiation To Reduce Osteogenesis

**Yucheng Yao,** Jiayi Yao, UCLA, Los Angeles, CA; Xiuju Wu, Xiaojing Qiao, Los Angeles, CA; Li Zhang, Jocelyn Ma, UCLA, Los Angeles, CA; Xinjiang Cai, Uni. of California, Los Angeles, Los Angeles, CA; Kristina I Bostrom, Yucheng Yao, UCLA, Los Angeles, CA

Transitions between cell fates commonly occur in development and disease. However, reversing an unwanted cell transition in order to treat disease remains an unexplored area. Here, we report a successful process of guiding ill-fated transitions toward normalization in vascular calcification. Vascular calcification is a severe complication that increases all-cause mortality of cardiovascular disease but lacks medical therapy. The vascular endothelium is a contributor of osteoprogenitor cells to vascular calcification through endothelial-mesenchymal transitions, in which endothelial cells (ECs) gain plasticity and ability to differentiate into osteoblast-like cells. We created a high throughput screening and identified SB216763, an inhibitor of glycogen synthase kinase 3 (GSK3), as an inducer of osteoblastic-endothelial transition. We demonstrated that SB216763 limits osteogenic differentiation in ECs at an early stage of vascular calcification. Lineage tracing showed that SB216763 redirected osteoblast-like cells to the endothelial lineage and reduced late-stage calcification. We also find that deletion of GSK3 $\beta$  in osteoblasts recapitulated osteoblastic-endothelial transition and reduced vascular calcification. Overall, inhibition of GSK3 $\beta$  promoted the transition of cells with osteoblastic characteristic to endothelial differentiation thereby ameliorating vascular calcification.

**D.Zhang:** n/a. **J.Yao:** n/a. **X.Wu:** None. **X.Qiao:** n/a. **L.Zhang:** None. **J.Ma:** None. **X.Cai:** None. **K.I.Bostrom:** None. **Y.Yao:** None.

---

P167

Utilization Of A Novel Artery-on-a-chip For Target Discovery And Drug Testing In Experimental Vascular Medicine

**Nora Margaux Hummel,** TECHNICAL UNIVERSITY MUNICH, Munich, Germany; Valentina Paloschi, TECHNICAL UNIVERSITY MUNICH, Munich; Nadiya Glukha, TECHNICAL UNIVERSITY MUNICH, Munich, Germany; Lars Maegdefessel, TECHNICAL UNIVERSITY MUNICH, Munich, Germany, Munich

The aorta-on-a-chip (AoOC) is a micro-engineered 3D in vitro model which aims to mimic the *in vivo* complexity of a human aorta in terms of cell-cell interaction, tissue architecture and hemodynamic conditions, i.e., the wall shear stress (WSS) force that the blood exerts on the vessel luminal surface in the direction of blood flow. The device used to generate the AoOC consists of a resealable glass chip with an intermediate semi-permeable membrane dividing the chip into two distinct chambers. This enables the flow of different fluids under varying dynamic conditions through the respective chambers. Primary aortic endothelial cells are cultivated on a thin layer of collagen on the flat-side of the membrane, whereas primary aortic smooth muscle cells are cultured on a fibronectin layer on the well-side of the same

membrane. Once cells are confluent, the glass chip is assembled and sealed due to the slight pressure applied by the chip holder which is ultimately connected to a microfluidic pressure controller. The chamber containing the endothelial cells is subjected to a high flow rate of 1.2 ml/min, equivalent to 10 dynes/cm<sup>2</sup>, mimicking the shear stress of the aortic wall. In contrast, the smooth muscle cells are exposed to a slow flow rate of 20 µl/min, corresponding to 0.0042 dynes/cm<sup>2</sup>, that simulates the physiological diffusion rate between the intima and the media layer (of the aorta), ensuring an adequate supply of nutrients to the cells. The quality of the co-culture system is assessed by immunofluorescence staining using CD31 and SM22 antibody which specifically mark ECs and SMCs attached at opposite sides of the membrane. To evaluate transcriptomic changes under different flow conditions (static vs 10dyne/cm<sup>2</sup>) cells were carefully collected at opposite site of the membrane and subjected to RNA sequencing analysis.

**N.M.Hummel:** None. **V.Paloschi:** None. **N.Glukha:** n/a. **L.Maegdefessel:** None.

---

P168

#### Promising Diagnostic Biomarkers For Congenital Vascular Malformations

**Jeries Abu-Hanna,** Calver Pang, Alexander Valnarov-Boulter, Univ Coll London, London, United Kingdom; Ruhaid Khurram, Anthie Papadopoulou, Royal Free Hosp, London, United Kingdom; Chung Sim Lim, Univ Coll London, London, United Kingdom; Jocelyn Brookes, Royal Free Hosp, London, United Kingdom; George Hamilton, Janice Tsui, Univ Coll London, London, United Kingdom

**Background:** Congenital vascular malformations (CVMs) are vascular lesions that result from developmental errors during embryogenesis. They can occur anywhere in the body, causing pain, bleeding, ulcers, disfiguration, organ failure or limb loss. Depending on intralesional blood flow dynamics, CVMs can be broadly classified into low-flow (LF), which involve veins, lymphatics, capillaries or a mixture, and high-flow (HF), which involve arteries and veins. Accurate diagnosis and monitoring of LF and HF CVMs remains challenging and requires a wide range of imaging modalities. **Aim:** We sought to identify potential diagnostic serum biomarkers, particularly those pertaining to the processes of inflammation and angiogenesis. **Methods:** Sera were isolated from the peripheral bloods of consented healthy controls ( $n = 10$ ) and patients diagnosed as having either LF ( $n = 10$ ) or HF ( $n = 10$ ) CVMs. Various mediators of inflammation and angiogenesis were analysed in the sera using the Inflammation 20-Plex and Angiogenesis 18-Plex Human ProcartaPlex™ Panels. The levels of these mediators in patients with LF or HF CVMs were compared with those in healthy controls using the Kruskal-Wallis test and correlated with lesion volumes and visual analogue scores for pain using the Spearman rank correlation test. **Results:** Compared to healthy controls, the inflammatory mediators E-selectin, IFN $\alpha$ , IFN $\gamma$ , IL1 $\beta$ , IL4, IL12, IL17, MIP1 $\alpha$ , MIP1 $\beta$  and TNF $\alpha$  were elevated in the sera of LF CVM patients, whereas only MIP1 $\alpha$  was raised in the sera of HF CVM patients. None of the angiogenic mediators were altered in the sera of patients with LF or HF CVMs. Serum IFN $\alpha$ , IFN $\gamma$ , IL4, IL12, TNF $\alpha$ , VEGFA, VEGFD and syndecan correlated positively with pain scores in patients with LF CVMs, whereas only IP10 did in patients with HF CVMs. Serum Ang1 and leptin correlated negatively with lesion volumes in patients with LF or HF CVMs, respectively. **Conclusion:** Serum inflammatory mediators could be used as biomarkers to distinguish LF from HF CVMs and their expression seemed to be associated with pain severity in patients with LF CVMs. The angiogenic mediators Ang1 and leptin were associated with lesion volumes in patients with LF or HF CVMs, respectively.

**J.Abu-hanna:** None. **C.Pang:** n/a. **A.Valnarov-boulter:** n/a. **R.Khurram:** n/a. **A.Papadopoulou:** n/a. **C.Lim:** n/a. **J.Brookes:** n/a. **G.Hamilton:** n/a. **J.Tsui:** n/a.

---

P169

#### $\beta$ -catenin C-terminal Domain/Sphingosine-1-Phosphate Receptor 1 Axis Drives Neointima Formation After Carotid Injury

**Gustavo H Oliveira De Paula,** Vanessa Almonte, Albert Einstein Coll of Med, Bronx, NY; Tomas Valenta, Konrad Basler, Univ of Zurich, Zurich, Switzerland; Dario Riascos-Bernal, Nicholas Sibinga, Albert Einstein Coll of Med, Bronx, NY

**Introduction:** The  $\beta$ -catenin C-terminal domain (CTD) is required for artery formation during embryogenesis, but its role in vascular remodeling in adulthood is unknown. Inhibitors targeting



specifically the CTD of  $\beta$ -catenin have been developed, but their use in obstructive vascular disease is not yet justified because of this gap of knowledge. Loss of  $\beta$ -catenin in mouse aortic smooth muscle cells (MASMCs) decreases the transcript levels of sphingosine-1-phosphate receptor 1 (S1PR1). However, no studies have evaluated the crosstalk between these proteins in vascular remodeling. **Hypothesis:** We hypothesized that the CTD of  $\beta$ -catenin promotes neointima formation after vascular injury, and that it acts by inducing S1PR1 expression. **Methods:** We studied mice bearing a knockin mutant  $\beta$ -catenin allele ( $\Delta$ C) that lacks  $\beta$ -catenin CTD transcriptional activity. Mice expressing the SMC-specific SMA-CreERT2 and bearing one floxed and one mutant  $\beta$ -catenin allele were treated with tamoxifen to inactivate the floxed allele, leaving the mutant allele as the only source of  $\beta$ -catenin in SMC (SM $\beta$ C $\Delta$ C mice). Carotid artery ligation was performed to induce vascular injury. MASMCs were isolated from SM $\beta$ C $\Delta$ C mice ( $\beta$ C $\Delta$ C cells). **Results:** We found reduced neointima formation after injury in SM $\beta$ C $\Delta$ C male (SM $\beta$ CWT/-:  $0.52 \pm 0.09$  vs SM $\beta$ C $\Delta$ C:  $0.16 \pm 0.05$ ;  $n=10$ ;  $P<0.05$ ) and female (SM $\beta$ CWT/-:  $0.56 \pm 0.11$  vs SM $\beta$ C $\Delta$ C:  $0.17 \pm 0.04$ ;  $n=10$ ;  $P<0.05$ ) mice. These findings were associated with reduced SMC proliferation, increased SMC apoptosis, and prevention of loss of SMC markers. In vitro,  $\beta$ C $\Delta$ C MASMCs showed reduced growth compared to control cells ( $n=6$ ;  $P<0.05$ ).  $\beta$ C $\Delta$ C MASMCs also showed reduced S1PR1 expression and decreased *S1pr1* promoter activity, which were both rescued by the transfection of a constitutively active form of  $\beta$ -catenin. Interestingly, overexpression of S1PR1 restored  $\beta$ C $\Delta$ C MASMC growth towards control levels ( $n=6$ ;  $P<0.05$ ). In vivo, we found reduced S1PR1 expression in SMCs of injured arteries from SM $\beta$ C $\Delta$ C mice. **Conclusion:** Our results define an essential SMC  $\beta$ -catenin CTD-S1PR1 axis that drives neointima formation after arterial injury, and point to multiple points for potential therapeutic intervention to control vascular remodeling in disease.

**G.H.Oliveira de paula:** None. **V.Almonte:** None. **T.Valenta:** n/a. **K.Basler:** n/a. **D.Riascos-bernal:** n/a. **N.Sibinga:** None.

---

P170

Targeting Angiotensin II-induced Endoplasmic Reticulum Stress In Vsmcs To Reduce Pathological Vascular Amyloid Burden And Remodeling

**Stephanie M Cicalese,** Keisuke Okuno, Kyle Preston, Satoru Eguchi, Temple Univ, Philadelphia, PA

Hypertension is a complex disorder and risk factor for cardiovascular disease, ultimately contributing to premature death. The societal burden of hypertension is enormous, therefore better understanding of molecular mechanisms underlying hypertension and associated pathological vascular remodeling is needed for mechanism-targeted therapy development. Endoplasmic reticulum (ER) stress occurs in cells under increased protein synthesis,  $\text{Ca}^{2+}$  flux, or ROS generating environments- all of which are induced by Angiotensin II signaling in vascular cells. ER stress leads to the accumulation of misfolded proteins, and mediates cell death, fibrotic, and hypertrophic responses. The aim of this study was to target ER stress via chemical chaperone 3-hydroxy-2-naphthoic acid (3HNA) or genetic overexpression of chaperone glucose-regulated protein 78 (GRP78) to reduce protein aggregation and pathological response in VSMCs. Rat primary VSMCs were treated with 500  $\mu\text{M}$  3HNA or 30 MOI lacZ-GRP78 prior to stimulation with Ang II (100 nM). Protein synthesis assessed via puromycin incorporation revealed ER stress inhibition blocked Ang II associated protein synthesis in VSMCs, fold change relative to control of 1.7 (saline + Ang II) to 1.2 (3-HNA + Ang II) treated cells ( $P<0.05$ ). GRP78 overexpression attenuated Ang II induction pre-amyloid oligomers ( $P<0.01$ ) from 2.1 aggregates/cell to 0.9 aggregates/cell. Proteomic assessment of aggregates revealed Ang II induced crystallin AB (1.3 fold rel to control), HSP70 (1.716 fold rel to control) and annexin a2 (1.3 fold increase) enrichment in detergent insoluble fractions, which was attenuated by GRP78 overexpression ( $P=0.03$ , 0.03, and 0.024, respectively). In a 2 week Ang II infusion model, 3HNA was injected in C57/Bl6 mice. Ang II-induced medial thickness and cardiac vessel fibrosis was significantly reduced by 3-HNA ( $P<0.05$ ). SM22 $\alpha$  Cre GRP78 mice were generated and found protective against Ang II induced cardiac hypertrophy via HW/BW ratio (Cre- vs Cre+ Ang II  $P<0.05$ ), and a trend in reduction of aortic medial thickness ( $P=0.098$ ). Overall, GRP78 chaperone expression reduced protein aggregation and subsequent vascular remodeling induced by hypertensive stimulus and may elude novel therapeutic targets.

**S.M.Cicalese:** None. **K.Okuno:** n/a. **K.Preston:** n/a. **S.Eguchi:** None.

## Glucose Consumption Of Vascular Cell Types In Culture; Toward Optimization Of Experimental Conditions

**Keiichi Torimoto**, Lewis Latz Sch of Med at Temple Univ, Philadelphia, PA; **Keisuke Okuno**, Ryohei Kuroda, Philadelphia, PA; **Stephanie M Cicalese**, Kunie Eguchi, Temple Univ, Philadelphia, PA; **Katherine Elliott**, Tatsuo Kawai, Lewis Latz Sch of Med at Temple Univ, Philadelphia, PA; **Satoru Eguchi**, TEMPLE UNIVERSITY SCHOOL OF MEDICIN, Philadelphia, PA

Any experimental outcomes are potentially influenced by extracellular glucose availability and its cellular metabolism. However, there is a lack of attention paid to the supply and utilization of glucose in many cultured experiments. Surveillance of vascular related journals for the past 5 years demonstrated that less than 20% of published articles declared the medium glucose concentration. The present studies were designed to seek ideal medium glucose concentration(s) in various cell types with particular attention paid to changes in glucose consumption. By using distinct glucose concentrations in Dulbecco's Modified Eagle's medium (DMEM), we identified ideal glucose media for stimulation experiments. We have compared glucose consumption in three vascular cell types, endothelial cells (EC), vascular smooth muscle cells (VSMC) and adventitial fibroblasts (AF) with or without angiotensin II (All) stimulation. In all cell types after a 48h incubation in relatively low glucose media (1 g/L), medium glucose concentration was reduced to almost 0 (EC  $0.01 \pm 0.01$  g/L, VSMC  $0.13 \pm 0.05$  g/L, AF  $0.02 \pm 0.01$  g/L). Whereas medium glucose concentration remained significantly higher (EC  $2.77 \pm 0.05$  g/L, VSMC  $3.87 \pm 0.05$  g/L, AF  $3.32 \pm 0.01$  g/L) when cells were incubated for 48h in high glucose (4.5 g/L) media. In middle glucose (2.75 g/L) media, medium glucose concentration remained in physiological ranges (EC  $0.62 \pm 0.18$  g/L, VSMC  $1.98 \pm 0.07$  g/L, AF  $1.17 \pm 0.17$  g/L). All treatment enhanced glucose consumption in AF and low passage VSMC but not in EC. In AF, All induction of target proteins varied depending on the glucose concentration used. In low glucose media induction of Grp78 or hexokinase II was highest, whereas induction of VCAM1 was lowest. Utilization of specific inhibitors further suggest essential roles of AT1 receptor and glycolysis in All-induced fibroblast activation. Overall, the present study demonstrates a high risk of hypo- or hyperglycemic conditions when standard low or high glucose media is used with vascular cells. Moreover, these conditions may significantly alter experimental outcomes. Medium glucose concentration should be monitored during any culture experiments and utilization of middle glucose media is recommended for all vascular cell types.

**K.Torimoto:** None. **K.Okuno:** n/a. **R.Kuroda:** n/a. **S.M.Cicalese:** None. **K.Eguchi:** n/a. **K.Elliott:** n/a. **T.Kawai:** n/a. **S.Eguchi:** None.

## Pulmonary Valve Papillary Fibroelastoma In A Patient With Chronic Chest Pain

**Davood Karimi Hosseini**, Noreen Ahmed, Hackensack Univ Medical Ctr, Hackensack, NJ; **Elina Shkolnik**, Rutgers Robert Wood Johnson Medical Sch, New Brunswick, NJ; **Lesley Philip**, Hackensack Univ Medical Ctr, Hackensack, NJ; **Prabhjeet Sandhu**, St. George Univ, Grenada, Grenada; **Ali Yildiz**, **Rajiv Patel**, **Dennis Villegas**, Hackensack Univ Medical Ctr, Hackensack, NJ

Primary cardiac tumors are rare entity, and the most common benign cardiac neoplasms include myxomas, lipomas and papillary fibroelastomas (PFE) with PFE accounting for 8% of the tumors. A 53-year-old female presented with chronic chest pain and exertional shortness of breath. She first sought evaluation four years ago, when her pulmonologist referred her to thoracic surgery after an incidental finding of a 3.9 cm anterior mediastinal mass on CT-scan (Figure 1A-B). The patient described the pain as a constant pressure and squeezing sensation in her chest and worsening shortness of breath while laying on her sides, relieved only when a pillow was propped up under her chest. The pain did not significantly reduce her mobility or capacity to work. Initial evaluation, including transthoracic echocardiogram, stress testing, carotid ultrasound, and pulmonary function testing - was performed and found to be unremarkable. Further evaluations revealed a hiatal hernia, leading her symptoms to be attributed to GERD as causing her persistent non-exertional chest pain. The patient remained in good health despite her symptoms persisting. She later re-sought attention for chest pain on exertion and hoarseness three years later. She again underwent a full cardiopulmonary workup, yielding benign findings on EKG, troponins, and echocardiogram. Due to no alarming symptoms at the time, she was subsequently discharged. The patient continued to endorse chest pain and a follow-up MRI revealed a now 5 cm anterior mediastinal mass, thought to be a thymic cyst. Over the next few months, the patient continued to endorse worsening

chest pain and exertional shortness of breath. She followed up with her cardiologist and a subsequent TEE was significant for a pulmonic valvular mass. She was admitted to the hospital for further investigation. During her hospital stay, the patient underwent surgery to resect the anterior mediastinal mass likely to be a thymic cyst and the pulmonary artery mass which was determined to be a pulmonary valve papillary fibroelastoma in the histopathology exam (Figure 2). The surgery was successful with no complications postoperatively. The patient was discharged with no further chest pain and with improvement of the exertional shortness of breath.

**D.Karimi**

**hosseini:** None. **N.Ahmed:** None. **E.Shkolnik:** n/a. **L.Philip:** n/a. **P.Sandhu:** n/a. **A.Yildiz:** n/a. **R.Patel:** n/a. **D.Vi  
llegas:** n/a.

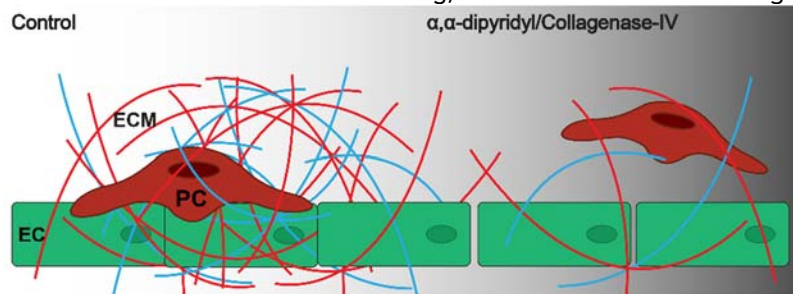
---

P173

#### Collagen-iii, An Index Of Vascular Maintenance

**Maruf M Hoque**, Virginia Tech, Roanoke, VA; John Chappell, Fralin Biomedical Res Inst, Roanoke, VA

Brain capillary integrity is compromised during stroke (Hu 2017). Re-establishing the blood-brain barrier (BBB) post-stroke requires integration of cues from endothelial cells (EC), pericytes (PC), and the extracellular matrix (ECM) to promote vessel remodeling. Two ECM components, Types III and IV Collagen (Col-III and Col-IV, respectively), support vascular growth and maintenance. Here, we utilized a murine embryonic stem cell (ESC) model to investigate how ECM mis-regulation impacts PC and EC collagen synthesis. ECM stability was targeted by administering  $\alpha,\alpha$ -dipyridyl (iron chelator) (Ikeda 1992) or Type IV Collagenase to ESC-derived vessels. Our aim was to establish potential mechanistic roles of both Col-III and Col-IV in promoting vascular maintenance. We observed by qRT-PCR that  $\alpha,\alpha$ -dipyridyl administration decreased Col3a1 expression, but not Col4a1, in a dose-dependent manner. Analysis by immunostaining and confocal microscopy revealed increases in vascular-associated and interstitial Col-IV with the lower doses of  $\alpha,\alpha$ -dipyridyl, but decreases in both Col-IV regions at higher doses. Preliminary imaging data for Col-III, however, suggested **decreases in both vascular-associated and interstitial Col-III with lower doses, but increases in these Col-III regions with the highest  $\alpha,\alpha$ -dipyridyl dose**. In separate experiments, Type IV Collagenase exposure reduced both vascular and interstitial Col-IV despite apparent increases in Col3a1 and Col4a1 gene expression. Taken together, these data suggest that perturbations to the ECM microenvironment surrounding developing blood vessels can elicit various compensatory responses depending on the severity and specificity of the ECM component targeted. These observations, support the idea that dynamic remodeling of the microvessel wall, and specifically the surrounding ECM, may contribute to microvascular instability, as seen in the BBB following acute ischemic stroke.



**M.M.Hoque:** None. **J.Chappell:** n/a.

---

P174

#### Nuclear Smooth Muscle $\alpha$ -actin Is Critical For Smooth Muscle Cell Differentiation And To Prevent Cerebrovascular Disease

**Callie Kwartler**, Xue-yan Duan, UTHSC-HOUSTON, Houston, TX; Shuangtao Ma, Michigan State Univ, East Lansing, MI; Anita Kaw, Michigan State Univ, East Lansing, MI, Houston, TX; Caroline Kernell, UTHHealth, Houston, TX; Charis Wang, UTHSC-HOUSTON, Houston, TX; Jiyuan Chen, UTHHealth, Houston, TX; Xuetong Shen, MD Anderson Cancer Ctr, Houston, TX; Dianna M Milewicz, Univ of Texas Health Science, Houston, TX

Missense mutations in ACTA2, encoding  $\alpha$ -smooth muscle actin ( $\alpha$ -SMA), predispose to thoracic aortic aneurysms. A subset of these ACTA2 mutations also predispose to childhood onset cerebrovascular disease characterized by occlusion of the distal internal carotid arteries and small vessel disease. In our studies to identify how specific ACTA2 mutations predispose to cerebrovascular disease, we confirmed that  $\alpha$ -SMA translocates to the nucleus in wildtype (WT) smooth muscle cells (SMCs), is enriched in the nucleus over  $\beta$ -actin with differentiation of SMCs, associates with the INO80 chromatin remodeling complex, and selectively binds to the promoters of SMC contractile genes. Expression of individual mutant  $\alpha$ -SMAs in 293 cells determined that missense mutations associated with cerebrovascular disease inhibit this nuclear translocation. To further examine the effects of reduced nuclear  $\alpha$ -SMA with ACTA2 mutations, we used two model systems: pluripotent stem cell-derived SMCs from patients with ACTA2-associated cerebrovascular disease (ACTA2 R179C) as well as SMCs explanted from a knockin mouse model (Acta2SMC-R179C/+). Both mouse and human cells harboring the R179C mutation proliferate and migrate more than WT SMCs, are less differentiated than WT SMCs, and have increased expression of pluripotency-associated genes. Although the mutation is heterozygous, these cells show a dominant negative impact on nuclear  $\alpha$ -SMA function through dramatically reduced levels of  $\alpha$ -SMA in the nucleus, in the INO80 chromatin remodeling complex, and on the promoters of SMC-specific genes. Finally, forced nuclear localization of  $\alpha$ -SMA in WT SMCs increases levels of SMC contractile proteins. Taken together, we have identified a novel role for  $\alpha$ -SMA in driving differentiation of SMCs, and our data supports that defects in this nuclear role drive cellular phenotypes consistent with the cerebrovascular disease seen in patients with ACTA2 R179 mutations.

**C.Kwartler:** None. **X.Duan:** n/a. **S.Ma:** None. **A.Kaw:** n/a. **C.Kernell:** None. **C.Wang:** n/a. **J.Chen:** None. **X.She n:** n/a. **D.M.Milewicz:** Other; Modest; Doris Duke Foundation, Sarnoff Foundation, Other; Significant; Genetic Aortic Disease Association of Canada, Research Grant; Significant; NIH, AHA, John Ritter Foundation, Marfan Foundation, Texas Heart Institute.

---

P175

#### *In Vitro Cholesterol Treatment Does Not Reproduce Smooth Muscle Cell Phenotypic Plasticity Observed In Vivo*

**Austin Conklin,** Univ of Arizona, Tucson, AZ; **Florencia Schlamp,** Tiit Ord, Minna U Kaikkonen, Univ of Eastern Finland, Kuopio, Finland; **Edward Fisher,** Casey E Romanoski, Univ of Arizona, Tucson, AZ

Vascular Smooth Muscle Cells (SMCs) exhibit a significant degree of phenotypic plasticity in atherosclerotic lesions. Previously, this phenotypic plasticity, and specifically the re-differentiation of SMCs into macrophages, has been modeled in vitro using cholesterol treatment. We performed a meta-analysis of five different murine SMC lineage tracing single-cell RNA sequencing (scRNA-seq) experiments performed by four different research groups; we identified 24 different cell types and find considerable differences in the proportion of recovered normal 'contractile' SMCs and SMC-derived macrophages between experiments.

In addition, we performed bulk RNA-seq on cultured murine SMCs with and without cholesterol treatment for 0, 24, or 48 hours. We find that cholesterol treatment regulates transcripts associated with the induction of the unfolded protein response, reduction of cholesterol biosynthesis, and reduction in cell proliferation.

Additionally, chromatin immunoprecipitation followed by high-throughput sequencing for H3K27ac performed on in vitro SMCs treated and untreated for 0, 24, or 48 hours reveals that AP-1 and ATF4 binding motifs are found more frequently at cholesterol treatment specific H3K27ac chromatin sites.

Finally, we compared transcriptomic data between in vivo vascular cell types identified in our meta-analysis and in vitro SMCs. We additionally included scRNA-seq data and microarray data collected for in vitro SMCs and bulk RNA-seq data collected for M1, M2, and oxLDL treated macrophages. We find that compared to the phenotypic plasticity observed in vivo, cholesterol exhibits modest effects on the transcriptomes of in vitro SMCs and does not reproduce the changes observed in vivo, while in vitro macrophages, especially oxLDL treated macrophages, more closely approximate their in vivo counterparts.

We conclude that differences between SMC lineage-tracing scRNA-seq experiments obscures the degree to which SMC-derived macrophages are present in murine atherosclerotic plaques, that cholesterol has modest effects on in vitro SMC transcriptomes, and that the effects of cholesterol do not reproduce the phenotypic plasticity observed in vivo.

**A.Conklin:** None. **F.Schlamp:** n/a. **T.Ord:** None. **M.Kaikkonen:** None. **E.Fisher:** n/a. **C.E.Romanoski:** None.

## Pharmacological Inhibition Of Drp1 Dependent Mitochondrial Fission Alleviates Mitochondrial Dysfunction-associated Cell Death In Vascular Smooth Muscle Cells

Anshul Jadli, Univ of Calgary, Calgary, AB, Canada; Karina Gomes, Vaibhav B Patel, Univ of Calgary, Calgary, AB, Canada

**Background:** Vascular smooth muscle cell (VSMC) death has been linked to the pathogenesis of various vascular diseases. Excessive mitochondrial fission in response to pathological stimuli contributes to apoptosis, thus inhibition of mitochondrial fission appears to be a promising therapeutic target in vascular disease. Mitochondrial division inhibitor 1 (mDivi-1) inhibits Drp1 dependent fission by attenuation of its GTPase activity. The limited literature on mDivi-1-mediated attenuation of VSMCs apoptosis and its effect on the pathogenesis of vascular disease warrants further investigation.

**Methods and results:** Staurosporine (STS)-induced apoptosis and attenuated cell proliferation were observed in VSMCs. The treatment with mDivi-1 ameliorated these detrimental effects of STS and led to reduced apoptosis, and increased cell proliferation. The mitochondrial fission was evaluated using Mitotracker Red staining which showed reduced mitochondrial fragmentation with significantly higher mitochondrial networks, mean branch length, and mitochondrial footprint upon treatment with mDivi-1. Drp1 levels were increased in STS-treated cells with localization in the mitochondria. Cellular and mitochondrial stress response assessed by DHE and mitoxox staining. mDivi-1 treatment attenuated STS-induced ROS generation in VSMCs. Mitochondrial function via evaluation of Mitochondrial permeability transition pore (mPTP) opening, mitochondrial membrane potential, and bioenergetic profile showed significantly reduced mPTP opening and higher metabolic potential represented by OCR and ECAR in mDivi-1-treated cells compared to STS group. The autophagy marker LAMP1 showed increased colocalization in mitochondria of STS-treated VSMCs. The apoptotic proteins were assessed using a protein array. The mDivi-1 treated VSMCs showed significantly reduced autophagy and apoptosis-related proteins. This suggested attenuation of apoptosis-mediated mitochondrial damage upon treatment with mDivi-1. **Conclusion:** Pharmacological inhibition of mitochondrial fission provides a potential therapeutic target in VSMCs death-associated vascular diseases.

A.Jadli: None. K.Gomes: None. V.B.Patel: None.

## Pronethalol Decreases Rbpjk To Reduce Sox2 In Cerebral Arteriovenous Malformation

Xiaojing Qiao, Univ of California, Los Angeles, Los Angeles, CA; Daoqin Zhang, Li Zhang, Jiayi Yao, UCLA, Los Angeles, CA; Xiuju Wu, Los Angeles, CA; Xinjiang Cai, Uni. of California, Los Angeles, Los Angeles, CA; Kristina I Bostrom, Yucheng Yao, UCLA, Los Angeles, CA

Cerebral arteriovenous malformations (AVMs) are the common vascular malformations that tend to rupture and cause hemorrhagic strokes. Disruptions in the integrity of vascular endothelium and endothelial cell (EC) differentiation give rise to the formation of cerebral AVMs. In previous studies, we reported that endothelial-mesenchymal transitions (EndMTs) contributed to cerebral AVMs in that ECs lost their identity and gained mesenchymal plasticity to cause lumen disorder. We have shown that unwanted induction of Sry-box 2 (Sox2) signaling was responsible for the EndMTs in cerebral AVMs, and identified the beta-adrenergic antagonist pronethalol as an inhibitor of Sox2 expression that stabilized EC differentiation and lumen formation, thereby limiting the cerebral AVMs. We also showed that the depletion of beta-adrenergic receptors had no effect on the Sox2 expression, which suggested that the beta antagonists exerted their effect through other pathways. However, the nature of these pathways remains unclear. Here, we hypothesize that beta-adrenergic antagonist directly inhibits notch-associated transcription factor recombination signal binding protein for immunoglobulin kappa J (RBPJk), a key component of Notch signaling, to limit induction of Sox2 so as to improve cerebral AVMs. We treated MGP CRISPR cells, in which matrix Gla protein (Mgp) was depleted by using gene-editing tool of clustered regularly interspaced short palindromic repeats and its associated protein 9, with BMP6. We found that BMP6 induced Sox2, Notch1 and Jagged1 and 2. We further performed gene knockdown to reduce RBPJk and found that the knockdown of RBPJk abolished the Sox2 induction. We revealed that pronethalol significantly reduced the expression of RBPJk but did not affect Notch1, Jagged1 or 2. We showed more enriched DNA-binding around the RBPJk binding site in the Sox2 promoter of the MGP CRISPR cells than

control cells. Excess RBPJ $\kappa$  DNA-binding was abolished by treatment of pronethalol in MGP CRISPR cells. Together, the results suggest that the beta antagonists reduce RBPJ $\kappa$ , thereby preventing excess BMP/Notch signaling from inducing Sox2.

**X.Qiao:** n/a. **D.Zhang:** n/a. **L.Zhang:** None. **J.Yao:** n/a. **X.Wu:** None. **X.Cai:** None. **K.I.Bostrom:** None. **Y.Yao:** None.

---

P178

#### A Novel Subset Of Adventitial Vascular Stem Cells Paracrine Control Media Smooth Muscle Cell Dedifferentiation Leading To Intimal Hyperplasia In Vein Grafts

Weiwei Wu, UNIVERSITY OF SOUTH CAROLINA, Columbia, SC; Rong Yin, Wenbin Tan, Univ of South Carolina, Columbia, SC; Mitzi Nagarkatti, Univ of South Carolina SOM, Columbia, SC; Prakash Nagarkatti, Univ of South Carolina, Columbia, NC; Isidro Sanz-Garcia, Insto de Biología Molecular y Celular del Cáncer, Consejo Superior de Investigaciones Científicas/Univ de Salamanca, Salamanca, Spain; Guoshuai Cai, Igor B. Robinson, Univ of South Carolina, Columbia, SC; **Taixing Cui**, UNIVERSITY OF SOUTH CAROLINA, Columbia, SC

Vein graft failure (VGF) is associated with vein graft (VG) intimal hyperplasia, which is characterized by abnormal accumulation of vascular smooth muscle cells (SMCs). The majority of neointimal SMCs are derived from pre-existing vascular SMCs via a process of vascular SMC dedifferentiation; however, the underlying mechanisms remain poorly understood. Here, we tracked down the fate of vascular stem cells (VSCs) expressing stem cell antigen 1 (SCA1) in VG remodeling. After transplantation, most of the donor venous cells including endothelial cells, SMCs, and VSCs died within 3 days, and the recipient arterial SCA1+ VSCs were recruited to repopulate the adventitia and the intima but did not differentiate into neointimal SMCs in VGs. However, ablation of the SCA1+ VSCs ameliorated intimal hyperplasia in VGs. Single-Cell RNA sequencing (scRNA-seq) analysis revealed a unique subset of VSCs expressing Sca1 and cyclin-dependent kinase 8 (Cdk8) in the artery. Notably, the number of SCA1+CDK8+ cells was increased in the adventitia prior to dramatic proliferation of SMCs in the media and neointima in VGs. Inactivation of CDK8 intensified SCA1+ VSC naïve stemness but suppressed SCA1+ VSC proliferation, migration, and exosome release for paracrine enforcement of vascular SMC dedifferentiation. A short-time perivascular delivery of CDK8 inhibitors ameliorated adventitial SCA1+ VSC accumulation associated with a long-term efficacy in suppressing intimal hyperplasia in VGs. These findings uncover that a novel subset of adventitial VSCs paracrine control media SMC dedifferentiation for intimal hyperplasia in VGs toward VGF.

**W. Wu:** None. **M. Nagarkatti:** None. **T. Cui:** None.

---

P179

#### A Text Processing Tool To Identify And Characterize Carotid Artery Stenosis In Radiology Reports

**Syedmohammad Saadatagah**, Omar Elsekaily, Lubna Alhalabi, Mayo Clinic, Rochester, MN; Iftikhar J Kullo, MAYO CLINIC, Rochester, MN

**Introduction.** We aimed to identify and characterize carotid artery stenosis (CAS), defined as  $\geq 40\%$  stenosis in the internal carotid artery (ICA) or the common carotid artery (CCA), among participants of the Mayo Vascular Disease Biorepository (VDB, n = 11,814). **Hypothesis.** A string-based text processing (TP) tool coded in R can analyze radiology text reports to ascertain and characterize CAS. **Methods.** After importing a radiology report into R, it was segmented for analysis and each segment was tested for 22 unique features. The TP tool was able to i) identify stenosis in the ICA or the CCA while excluding stenosis of vertebral arteries, subclavian arteries, or external carotid arteries, ii) recognize both quantitative and qualitative descriptions of CAS, iii) interpret numerical expressions by considering the surrounding text, iv) detect negations, and v) ascertain previous revascularization procedures if mentioned in the text. We manually ascertained CAS and characterized it in 800 randomly selected radiology reports to assess the performance of the TP tool in terms of precision, recall, and F-score. **Results.** We retrieved 21,651 imaging reports for 6,342 unique patients including 20,461 ultrasonography reports, 812 magnetic resonance imaging reports, 357 computed tomography scan reports, and 21 interventional radiology reports. The performance of TP is outlined in **Table 1**. **Conclusion.** We demonstrate that a string-based TP tool coded in R is efficient and accurate in identifying and characterizing CAS from carotid radiology reports. The tool

does not require natural language processing and could be used in a wide range of settings for genetic and biomarker studies.

**Table 1.** Performance of the TP tool (based on manual review of 800 radiology reports)

	Precision	Recall	F-score	Accuracy
Carotid artery stenosis				99.63%
Negative for carotid artery stenosis	100.00%	99.27%	99.63%	
Positive for carotid artery stenosis	99.24%	100.00%	99.62%	
Carotid artery stenosis subtypes				98.88%
No carotid artery stenosis	100.00%	92.31%	96.00%	
<40% stenosis of ICA or CCA	100.00%	99.72%	99.86%	
40% stenosis of ICA or CCA	95.56%	97.73%	96.63%	
41 - 69% stenosis of ICA or CCA	99.03%	97.14%	98.08%	
70 - 99% stenosis of ICA or CCA or history of carotid revascularization	98.09%	99.51%	98.80%	
Occlusion of ICA or CCA	97.22%	100.00%	98.59%	
Non-atherosclerotic stenosis	94.44%	100.00%	97.14%	

**S.Saadatagah:** None. **O.Elsekaily:** n/a. **L.Alhalabi:** None. **I.J.Kullo:** None.

P180

## Tunable Elastin-like Protein-based Hydrogels For Cell Transplantation In Vascular Repair

**Mahdis Shayan,** Riley Suhar, Stanford Univ, Palo Alto, CA; Ngan F Huang, STANFORD UNIVERSITY, Stanford, CA; Sarah Christine Heilshorn, Stanford Univ, Palo Alto, CA

**Introduction:** Endothelial cells can improve blood perfusion in diseased blood vessels; however, direct injection of cells significantly decreases their survival and functionality for angiogenesis. To address these limitations, we study a family of engineered extracellular matrices with tunable biochemical and biomechanical cues for enhanced survival and improved angiogenic behavior of ECs. **Materials & Methods:** Engineered hydrogels, termed ELP-PEG, consists of two components of a hydrazine-modified elastin-like protein (ELP-HYD) and an aldehyde- or benzaldehyde-modified, polyethylene glycol (PEG-ALD or PEG-BZA), which interact with each other through hydrazone dynamic covalent chemistry (DCC) bonds to form ELP-PEG hydrogels. Stiffness is controlled by altering the number of PEG-ALD or PEG-BZA crosslinks, and the stress relaxation rate is tuned by varying the PEG-ALD crosslinks vs. PEG-BZA. Stiffness and stress relaxation rates of the hydrogels were assessed by dynamic oscillatory rheology. Afterward, human umbilical vein endothelial cells (HUVECs) were encapsulated within gels to assess cell viability and spreading using a Live/Dead Cytotoxicity assay and confocal fluorescence imaging. **Results and Discussion:** Stress relaxation rate in ELP/PEG-ALD is much slower compared with a similar combination in ELP/PEG-BZA. Rheology measurements of the RGD-ELP/PEG (2%/2%) hydrogels demonstrated a storage modulus of 800Pa. It confirms the tunability of the stress relaxation rate with constant stiffness. Cell viability assay demonstrated that both hydrogels could support high cell viability (>90%) for 7 days. After 7 days, cell spreading increased in RGD-ELP/PEG-BZA hydrogels, however, cells did not form elongated morphology in RGD-ELP/PEG-ALD hydrogels, suggesting that stress relaxation rate and mechanical stiffness are key characteristics in modulating endothelial cell behavior. **Conclusions:** ELP/PEG-ALD/BZA promotes the angiogenic behavior of endothelial cells and is a promising candidate for cell delivery in vascular diseases.

**M.Shayan:** None. **R.Suhar:** None. **N.F.Huang:** None. **S.C.Heilshorn:** None.

## Machine Learning Methods For Predicting 30-day All Cause Readmission Following Carotid Endarterectomy Among Acute Ischemic Stroke Cases: A Nsqip Study (2014 - 2017)

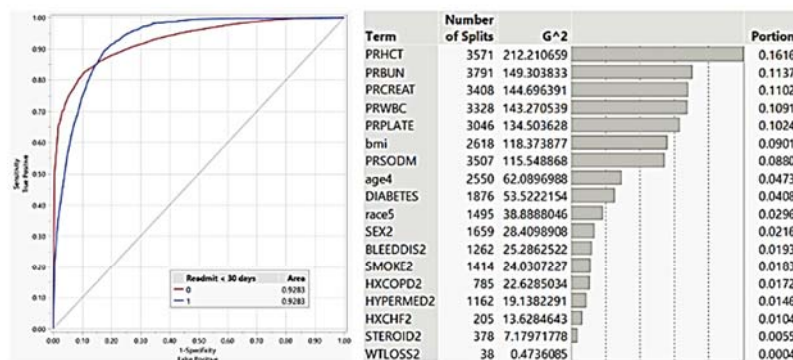
**Anshul Saxena**, Muni Rubens, Venkataraghavan Ramamoorthy, Baptist Health South Florida, Coral Gables, FL; Mariana Suarez, Massachusetts Inst of Technology, Coral Gables, FL; Sandeep Appunni, Calicut Medical Coll, Calicut, India; Peter McGranaghan, Emir Veledar, Baptist Health South Florida, Coral Gables, FL; Mahdi O Garelnabi, UMass Lowell, Lowell, MA

**Background:** Carotid endarterectomy (CEA) is associated with improved overall clinical outcomes in patients with acute ischemic stroke (AIS). However, studies on rates and factors associated with readmission following CEA for AIS are scarce. In this study, we used machine learning (ML) methods to identify the factors associated with readmission using a large-scale national database.

**Methods:** We used National Surgical Quality Improvement Program (NSQIP) registry (2014-2017) and included patients 18 years or older, who underwent CEA for AIS. AIS and CEA were identified using ICD-9 and ICD-10 diagnosis and CPT procedure codes, respectively. We used Naïve Bayes, Boosted Decision Trees, and Bootstrapped Random Forest classification techniques to explore the predictors of 30-day readmission using demographics, past medical history, and preoperative variables.

**Results:** There were a total of 22,373 AIS patients who underwent CEA. Mean (SD) age of the patients was 70.7 (9.4) years, and 61% were men. Majority were non-Hispanic White (80%), followed by non-Hispanic Black (4.6%). During the study period, 1 in 15 AIS patients who underwent CEA experienced 30-day readmission. Bootstrapped Random Forest classification performed best and Naïve Bayes worst with an AUROC of 92% and 59% respectively. The top 5 predictors of 30-day readmission after CEA were Hematocrit, BUN, Creatinine, WBC count, and Platelet count, all collected pre-operatively.

**Conclusion:** Our study showed that ML techniques could accurately predict 30-day readmission using pre-operative risk factors. This ML model could be incorporated in EMR as a potential clinical decision support system. Implementing this system could help in early identification of patients who are at high risk for readmission following CEA. This could help physicians to plan and intervene effectively and prevent short-term readmissions; thereby improving quality of care and saving healthcare costs.



PRHCT: Pre-operative hematocrit; PRBUN: Pre-operative BUN; PRCREAT: Pre-operative serum creatinine; PRWBC: Pre-operative WBC; PRPLATE: Pre-operative platelet count; PRSODM: Pre-operative serum sodium  
 Medical Hx: Diabetes mellitus with oral agents or insulin; Bleeding disorders; Current smoker; History of severe COPD; Hypertension requiring medication; Congestive heart failure (CHF) in 30 days before surgery; Steroid use for chronic condition; >10% loss body weight in last 6 months  
 Demographics: Age categories; Race categories; Female sex; BMI

**A.Saxena:** None. **M.Rubens:** n/a. **V.Ramamoorthy:** n/a. **M.Suarez:** None. **S.Appunni:** n/a. **P.Mcgranaghan:** None. **E.Veledar:** None. **M.O.Garelnabi:** None.

## Recombinant Human Lecithin-cholesterol Acyltransferase Treatment In Patients With ASCVD Increases HDL Through Increases In Cholesterol Ester Content.

**Gisette Reyes-soffer**, Anastasiya Matveyenko, James Lignos, Nelsa Matienzo, Leinys Santos Baez, Lau Y Yung, Rajasekhar Ramakrishnan, Columbia Univ Medical Ctr, Coll of Physicians and Surgeons, New York,



NY; Richard T. George, AstraZeneca, Gaithersburg, MD; Henry N Ginsberg, Columbia Univ Medical Ctr, Coll of Physicians and Surgeons, New York, NY

Lecithin-cholesterol acyltransferase (LCAT) mediates the esterification of free cholesterol (FC) to cholesteryl ester (CE) in HDL and, therefore, plays a critical role in reverse cholesterol transport. MEDI6012, a recombinant human LCAT (rhLCAT) increases HDL-C. Our goal was to interrogate the pathways regulating the increase in HDL-C and effects of rhLCAT on apoB metabolism. **Methods:** We enrolled five subjects (4 Man, mean age 67) with stable ASCVD into a Phase II, placebo controlled, double-blind, randomized cross-over study to determine the effects of two IV doses of MEDI6012, administered 48-hrs apart, versus placebo, on plasma lipids and lipoproteins. Stable isotope kinetic studies with D2-Leu, 13C-Phe, D2-Glycerol were performed to examine the metabolism of apoB100, ApoA1, ApoA2 and triglyceride. **Results:** As expected two doses of IV MEDI6012 increased total cholesterol and HDL-C levels significantly (Table1). We did not observe significant changes in other measured lipids or lipoproteins. The significant increase in HDL-C was  $34.9 \pm 10.3$  ( $p=0.002$ ) and due to an increase in the amount of CE ( $33 \pm 8.9$   $p=0.001$ ); there was no change in free cholesterol ( $1.9 \pm 1.9$ ). We found no changes in levels of sterols (i.e. Lathosterol) between the two periods. Preliminary in vivo kinetic studies of HDL metabolism in 3 subjects, showed no changes in the mean fractional clearance rate (FCR) or production rate (PR) of apoA1 between placebo ( $0.3 \pm 0.2$  pool/day,  $1.3 \pm 0.5$  mg/kg/day) and rhLCAT treatment ( $0.28 \pm 0.1$  pools/day,  $1.3 \pm 0.3$ ). There were no changes in ApoA2 FCR and PR after rhLCAT administration. Complete data for ApoA1, ApoA2 and ApoB100 and TG kinetics will be presented. **Conclusions:** In subjects with ASCVD, treatment with rhLCAT increased HDL-C mainly by increasing HDL CE; there were no changes in the FCR or PR of HDL ApoA1 or ApoA2. Together, these results suggest that rhLCAT treatment is associated with increased steady-state transport of CE by HDL.

**Table 1. Lipid and Lipoprotein Levels During Placebo and After 2-doses of rhLCAT Treatment**

	Placebo	rhLCAT Treatment	p-value
Total Cholesterol mg/dl	103.2(16)	136.7(39)	0.004
Triglycerides mg/dl	87.3(12)	78.5(39)	0.64
HDL mg/dl	33.8(10)	73.4(21)	0.005
LDL mg/dl	44.1(16)	47.8(17)	0.7
Plasma ApoB100 mg/dl	68.2(16)	50.9(8)	0.06
VLDL-apoB mg/dl	6.0(3)	4.5(4)	0.6
IDL-apoB mg/dl	0.7(0.7)	0.8(0.8)	0.9
LDL-apoB mg/dl	46.5(19)	42.6(12)	0.7
Plasma ApoA1 mg/dl	106.2(22)	122.2(7)	0.4
Plasma ApoA2 mg/dl	31.1(6)	31.8(7)	0.9
Plasma ApoC3 ug/ml	101.1(20)	114.2(7)	0.49
Plasma ApoE ug/ml	114(24)	136.2(7)	0.28

•All values presented as means(Standard Deviation).

Data analyzed with R-software using unpaired T-test.

•FCR: fractional clearance rate, PR: Production Rate,

Apo: Apolipoproteins.

**G.Reyes-soffer:** Other; Modest; Amgen, Inc, Pfizer. **A.Matveyenko:** None. **J.Lignos:** None. **N.Matienzo:** None. **L.Santos baez:** Other Research Support; Significant; Columbia University Medical Center. **L.Y.Yung:** None. **R.Ramakrishnan:** n/a. **R.T.George:** Employment; Significant; MedImmune/AstraZeneca, Stock Shareholder; Significant; AstraZeneca. **H.N.Ginsberg:** Other; Modest; Merck, Silence Therapeutics, AstraZeneca, Janssen, Sanofi, Resverlogix, Other; Significant; Kowa, Research Grant; Significant; Pfizer, Amgen.

P183

FFAR4: A Novel Target In Preventing Atherosclerosis?

**Gage Stutgen,** Medical Coll of Wisconsin, Milwaukee, WI; Daisy Sahoo, MEDICAL COLLEGE OF WISCONSIN, Milwaukee, WI

Free fatty acid receptor 4 (FFAR4), also known as G-protein coupled receptor 120 (GPR120), is a long-chain unsaturated fatty acid receptor expressed in adipocytes, endothelial cells, and macrophages. Activation of FFAR4 helps maintain metabolic homeostasis by regulating adipogenesis, insulin sensitivity, and inflammation. While FFAR4 is best known for its role its role in preventing obesity and diabetes, recent studies have demonstrated that FFAR4 may also play an important role in the development of

atherosclerosis and cardiovascular disease (CVD). Given FFAR4's importance in anti-inflammatory signaling and high expression levels in macrophages, we designed experiments to test the hypothesis that FFAR4 prevents the development of atherosclerosis by reversing macrophage foam cell formation, a hallmark of early atherogenesis. In these studies, we isolated peritoneal macrophages from wild-type C57/BL6 mice and incubated them with 20 µg/ml oxidized low-density lipoprotein (oxLDL) to generate foam cells. We then investigated the effects of FFAR4 activation on lipid accumulation, cytokine secretion, and cholesterol efflux. We found that activation of FFAR4 with synthetic agonist GW9508 reduced lipid accumulation as observed by decreased Oil Red O staining and reduced cellular cholesterol content. Activation of FFAR4 by GW9508 also decreased macrophage secretion of pro-inflammatory cytokines interleukin 1 beta (IL-1β) by 5.3-fold, interleukin 6 (IL-6) by 2.4-fold, monocyte chemoattractant protein-1 (MCP-1) by 44.1-fold, and tumor necrosis factor alpha (TNFα) by 2.4-fold. Additionally, activation of FFAR4 by GW9508 significantly increased [<sup>3</sup>H] cholesterol efflux to high-density lipoprotein (HDL) from peritoneal macrophages. Taken together, our results support an exciting and novel protective role for FFAR4 in the reversal of foam cell formation and could emerge this receptor as a new target for treating CVD by preventing accumulation of atherosclerotic plaque.

**G.Stuttgen:** None. **D.Sahoo:** None.

---

P184

Novel Model Of Ionizing Radiation-induced Mouse Coronary Arteriosclerosis, Which Was Attenuated By Precise Time Treatment Of Poly (adp-ribose) Polymerase (parp) Inhibitor

**Kyung ae Ko,** Jun-ichi Abe, MD Anderson Cancer Ctr, Houston, TX; Sivareddy Kotla, Houston, TX; YOUNG JIN GI, MD ANDERSON CANCER CENTER, HOUSTON, TX; Masaki Imanishi, MD Anderson Cancer Ctr, Houston, TX; Keigi Fujiwara, U. of Texas MD Anderson Cancer Cent, Houston, TX

**Background:** It is well known that radiation therapy (RT) induces coronary artery disease (CAD). However, since we don't have an adequate mouse model to evaluate CAD after RT, it has been difficult to perform pre-clinical study to detect the effective treatment. The inhibition of PARPs can prevent apoptosis and inflammation. Although PARP inhibitors have already been used as anti-tumor agents, their long-term use in CAD is not recommended because the inhibition of DNA damage response can cause DNA instability and eventually cancer. In this study, we restricted the use of PARP inhibitors to the time of IR exposure only and detected IR-induced atherosclerosis (AS). **Methods and Results:** Marino et al. reported that thoracic aortic constriction (TAC) can exacerbate coronary artery stenosis and myocardial infarction in ApoE<sup>-/-</sup> mice. We tested this model in LDLR<sup>-/-</sup> mice that were fed a high fat (HFD) with or without IR (3, 5, and 10 Gy). We observed cardiac hypertrophy and dose-dependent reduction of fractional shortening (FS) after 4-5 weeks of TAC (FS%, 33.74 ± 7.35 (Non-IR, n=9), 26.59 ± 9.19 (3Gy, n=6), 28.49 ± 2.49 (5Gy, n=5), 22.62 ± 6.16 (10Gy, n=6), mean ± SD, p <0.05). Most importantly, we observed localized cardiac dysfunction and infarct only in mice exposed to 10 Gy (n = 2 out of 6), detected by transmural strain analysis with echocardiography. Next, the whole heart was sectioned, with sets of 11 consecutive sections of 5 µm collected every 450 µm interval. We also found the diffuse increase of vascular wall thickness at left anterior descending coronary artery in mice exposed to IR. We fed a HFD on LDLR<sup>-/-</sup> mice with Olaparib (10 mg/kg/day) or vehicle one day before & after, and the day of IR (5 Gy twice, total 6 days only), then performed TAC. The reduction of FS induced by IR (10 Gy) was significantly improved by the precise time treatment of Olaparib against IR. **Conclusion:** These data suggested the usefulness of TAC-induced coronary AS mouse model to develop medical countermeasures against RT-induced CAD as pre-clinical study.

**K.Ko:** None. **J.Abe:** n/a. **S.Kotla:** None. **Y.Gi:** None. **M.Imanishi:** None. **K.Fujiwara:** None.

## Abstract Author Index

MP = moderated poster; P = ePoster

**Bolded** presentation number denotes presenting author

Abdelrahman, Ammar A. .... **P134**  
 Abdullah, Chowdhury S. .... 118  
 Abe, Junichi ..... MP45, P184  
 Abe, Masanori ..... 114  
 Abu-Hanna, Jeries ..... **P168**  
 A Fisher, Edward A. .... 105  
 Aggarwal, Anu ..... 127  
 Aguilar, David ..... P122  
 Ahmed, Noreen ..... P172  
 Aikawa, Elena ..... 112  
 Aikawa, Masanori ..... 112  
 Ait-Aissa, Karima ..... **119**  
 Alam, Mustafa ..... **P123, P128**  
 Alarabi, Ahmed ..... 126  
 Albinsson, Sebastian ..... MP27  
 Alfaidi, Mabruka ..... **MP06**  
 Alferiev, Ivan S. .... P137  
 Alhalabi, Lubna ..... P179  
 Almonte, Vanessa ..... P169  
 Alshbool, Fatima Z. .... **126**  
 Amioka, Naofumi ..... **P159**  
 Amrute, Junedh M. .... **MP07**  
 Anandh Babu, Pon Velayutham  
 ..... MP26  
 Anaya-Ayala, Javier E. .... **P103**  
 Andersen, Catherine J. .... **P139**  
 Anyanwu, Anelechi ..... P113  
 Appunni, Sandeep ..... P181  
 Archer, David R. .... MP17  
 Arditi, Moshe ..... 114  
 Asano, Takaharu ..... 112  
 Ascione, Raimondo ..... P126  
 Ashley, Euan A. .... 113  
 Aslan, Joseph ..... **108**  
 Aslan, Joseph E. .... 127  
 Ason, Brandon ..... MP07  
 Assimes, Themistocles L. .... MP16  
 Assini, Julia ..... **MP47**  
 Atzler, Dorothee ..... 101  
 Auguste, Gaelle E. .... 113  
 Augusto Heuschkel, Marina ..... **P156**  
 Ayala, Claudia ..... 123  
 Baban, Babak ..... MP37  
 Babur, Ozgun ..... 108  
 Bailey, William ..... P130

Ballasy, Noura ..... P109  
 Barbosa Lorenzi, Valeria ..... MP49  
 Barrett, Tessa J. .... **105, 109**  
 Bashline, Michael ..... MP08  
 Basler, Konrad ..... P169  
 Bauer, Robert C. 103, 120, MP35, P158  
 Baxi, Adir ..... MP09  
 Becari Ribeiro, Christiane ..... P108  
 Behrmann, Abraham S. .... 130  
 Bekhet, Laila ..... P122  
 Bellomo, Tiffany ..... MP16  
 Berger, Jeffrey S. .... 105, 109, P135,  
 ..... P144  
 Beyer, Andreas M. .... P141  
 Bhandari, Prajwal ..... MP22  
 Bhandari, Rohan ..... **127**  
 Bhavnani, Neha ..... MP48  
 Bhowmick, Debajit ..... P142  
 Bhuiyan, Shenuarin ..... 118  
 Bick, Alexander G. .... 125  
 Biebuyck, Antoine ..... 109  
 Billaud, Marie ..... MP08  
 Binder, Christoph J. .... 101  
 Bischoff, Lukas ..... **MP18**  
 Bjorkegren, Johan L. .... 113, MP39  
 Bledsoe, Amber ..... MP26  
 Blick-Nitko, Sara K. .... **124**  
 Boffa, Michael B. .... MP47, **P110**  
 Bone, William P. .... **MP16**  
 Bonini, Marcelo ..... P138  
 Bostrom, Kristina I. ... P164, P166, P177  
 Botts, Steven R. .... **P104**  
 Bouchareb, Rihab ..... **P113**  
 Boudina, Sihem ..... MP26  
 Boufford, Camille ..... MP08  
 Bozal, Fazli ..... 105  
 Braekkan, Sigrid ..... 110  
 Bramel, Emily E. .... **131**  
 Bratinov, George ..... P137  
 Bravo-Reyna, Carlos ..... P103  
 Bredemeyer, Andrea ..... MP07  
 Brichacek, Beda ..... P124  
 Broadhurst, Kimberly ..... 119  
 Brookes, Jocelyn ..... P168  
 Brown, Emily J. .... 105

Bruemmer, Dennis ..... MP08  
 Brunton-O'Sullivan, Morgane .... **P121**,  
 ..... P133  
 Bunch, Katharine L. .... P134  
 Burgess, Hannah ..... 109  
 Byzova, Tatiana V. .... P130  
 Cai, Xinjiang ..... P164, P166, P177  
 Caldwell, Robert W. .... P134  
 Caldwell, Ruth B. .... P134  
 CAMERON, Scott J. .... 127  
 Campbell, Robert A. .... 116  
 Campos, Lgia C. B. .... P108  
 Canellos, Maria ..... P129, P152  
 Cannon, Allison L. .... 118  
 Carpo, Beatrice ..... P161  
 Cassim Bawa, Fathima Nafrisha **MP01**  
 Casteel, Jared ..... P130  
 Cavallero, Susana ..... MP43  
 Cavašin, Maria A. .... MP28  
 Cerbie, James ..... MP26  
 Chakraborty, Raja ..... MP11  
 Chambliss, Ken ..... MP40  
 Chang, Hyun-kyung ..... 103, **MP35**  
 Chang, Kyong-Mi ..... MP16  
 Chang, Ziyi ..... 129, MP42  
 Chappell, John ..... P173  
 Chatterjee, Payel ..... **MP11**  
 Chauhan, Anil K. .... 107, P127  
 Chaurasiya, Birendra ..... 106  
 Chelvanambi, Sarvesh ..... 112  
 Chemaly, Melody ..... **MP02**  
 Chen, Brian Y. .... MP16  
 Chen, Eugene ..... 129, MP42  
 Chen, Hui ..... **P160**  
 Chen, Jiyuan ..... P174  
 Chen, Shuang ..... 114  
 Chen, Sing-Young ..... 122  
 Chen, Yiliang ..... MP33, P131  
 Chesler, Naomi C. .... MP15  
 Cho, Jae ..... **MP26**  
 Cho, Kelly ..... MP16  
 Chu, Claire ..... MP08  
 Chu, Haiyan ..... MP40  
 Chuecos, Marcel ..... 123  
 Chung, Allen ..... **103**

Cicalese, Stephanie M. .... **P170**, P171  
 Civelek, Mete ..... MP39  
 Clark, Justin ..... MP47  
 Cochran, Blake J. .... 122  
 Cody, Mark J. .... 116  
 Conklin, Austin ..... **P175**  
 Connor, John H. .... 111  
 Cooke, John P. .... 111  
 Cornwell, MacIntosh ..... 109  
 Corr, Emma ..... 105  
 Corsi, Carlos A. C. .... P108  
 Cotzia, Paolo ..... 109  
 Couto, Ariel E. C. .... P108  
 Crane, Alexander ..... MP08  
 Creamer, Tyler J. .... 131  
 Crother, Timothy R. .... 114  
 Cuevas, Rolando A. .... **MP08**  
 Cui, Taixing ..... **P178**  
 Cui, Yaru ..... MP27  
 Cynn, Esther ..... MP38  
 Daichendt, Luke G. .... P110  
 Damrauer, Scott ..... 125, MP16  
 Dang, Tan ..... MP10  
 Dang, Yifang ..... P122  
 Danser, Jan A. .... P145  
 Da Silva Lopes Salle, Evila ..... **MP37**  
 Daugherty, Alan ..... MP21, P105,  
 ..... P106, P145, P148,  
 ..... P159, P160  
 David, Larry ..... 108  
 Dayal, Sanjana ..... MP03  
 DEBEER, Frederick C. .... P101  
 Decano, Julius ..... **112**  
 De Giorgi, Marco ..... 123  
 De Guzman, Hazel C ..... P112  
 De Jong, Annika ..... 105  
 Demir, Emek ..... 108  
 Dennison, Taylor ..... MP09  
 Denorme, Frederik ..... **116**  
 Deshpande, Nandan ..... 122  
 DeSilva, Gayan ..... MP25  
 Dev, Rishabh ..... P127  
 Devkota, Laxman ..... **MP22**  
 Dhanesha, Nirav ..... **107**, P127  
 Dhoble, Abhijeet ..... P122

Dinh, Huy .....	MP04	Fujiwara, Keigi .....	MP45, P184	Guaque-Orlate, Sandra .....	P113	Huang, Ngan F. ....	P180
Doddapattar, Prakash .....	107, <b>P127</b>	Furtado, Milena B. ....	MP07	Gulati, Rishab .....	MP04	Huang, Wenxin .....	P131
Doerfler, Alexandria M. ....	<b>123</b>	Furuie, Yoshito .....	P111	Guo, Zhenheng .....	MP20	Huang, Xiaojia .....	106
Domingo, Liezl .....	MP37	Gallo MacFarlane, Elena .....	131	Guo, Ziyu .....	P165	Huffman, Jennifer .....	125
Dominic, Paari .....	118	Gao, Yanxiang .....	P165	Gupta, Shreya .....	MP48, <b>P153</b>	Hummel, Nora M. ....	<b>P167</b>
Dong, Daoyin .....	106	Gao, Yuan .....	MP27	Gurkar, Aditi .....	MP08	Hurley, Ayrea .....	123
Dong, Nianguo .....	MP41	Garcia, Charles .....	P141	Ha, Elizabeth E. ....	120	Hurtado, Julian .....	<b>MP17</b>
Dou, Kefei .....	MP19	Gardiner, Kristin .....	P137	Ha, Elizabeth H. ....	P158	Hussain, M .....	P112
Drago, Fabrizio .....	MP04, P125	Garelnabi, Mahdi O. MP05, <b>P116</b> , P181		Haag, Elisabeth .....	<b>MP10</b>	Hussain, M M. ....	MP31
Drenkova, Kamelia .....	105, 109, P135	Garshick, Michael .....	<b>P135</b>	Hadi, Tarik .....	115	Hwa, John .....	MP11
D'Souza, Edwin .....	112	Gautier, Nicole .....	P157	Hally, Kathryn .....	P133	Imanishi, Masaki .....	<b>MP45</b> , P184
Du, Jingcheng .....	P122	Gawronski, Katerina A. B. ....	MP16	Hamilton, George .....	P168	Inamdar, Vaishali .....	P137
Du, Mingyuan .....	<b>MP13</b>	Gaziano, Michael .....	MP16	Han, Jun .....	123	Ito, Sohei .....	<b>P105</b> , P106
Duan, Xue-yan .....	P174	Geoffrion, Michele .....	100, MP09	Han, Yan .....	117	Jackson, Simon .....	MP07
Dubner, Allison ....	MP12, MP14, MP28	George, Richard T. ....	P182	Hand, Nicholas J. ....	121	Jadhav, Kavita .....	120, P158, MP01
Dugaich, Vinícius F. D. ....	P108	George, Sarah J. ....	P126	Hansen, John-bjarne .....	110	Jadli, Anshul .....	<b>P109, P176</b>
Dugan, Adam .....	P101	Gepner, Adam .....	MP15	Hansen, Laura M. ....	<b>MP29</b>	Jahan, Jesmin .....	<b>P141</b>
Durant, Chirstopher .....	MP04	Gerdes, Norbert .....	101	Harding, Scott .....	P121, P133	Jain, Abhishek .....	<b>111</b>
Eguchi, Kunie .....	P171	Ghaghada, Ketan .....	MP22	Harroun, Nikolai .....	MP25	Jain, Manish .....	107, P127
Eguchi, Satoru .....	P170, P171	Gharibeh, Lara .....	P155	Hazen, Stanley L. ....	127	Janapala, Rajesh Naidu .....	P124
Elbadawi, Ayman .....	127	Ghatge, Madankumar .....	P127	Hedin, Ulf .....	MP39	Jarajapu, Yagna P. ....	P141
Elliott, Katherine .....	P171	Ghosh, Saikat .....	113	Hedrick, Catherine C. ....	MP04	Jarrett, Kelsey E. ....	123
Elsekaily, Omar .....	P179	Ghosheh, Yanal .....	MP04	Heffron, Sean P. ....	P144	Javidan, Aida .....	<b>P107</b>
Emerton, Christina .....	P155	GI, YOUNG JIN .....	MP45, P184	Hegge, Louise .....	MP10	Jenjak, Shawn E. ....	P115
Engel, Connor .....	<b>MP25</b>	Gillard, Baiba K. ....	<b>MP30</b>	Heilshorn, Sarah C. ....	P180	Jensen, Melissa .....	MP03
Englander, S. Walter .....	121	Ginsberg, Henry N. ....	P182	Heo, Kyung-Sun .....	MP45	Jeong, Se-jin .....	P147, <b>P162</b>
Eremin, Michail .....	P143	Glaros, Elias .....	122	Hernandaz, Rebecca .....	<b>MP43</b>	Jhamnani, Sunny .....	P128
Espinosa-Diez, Cristina .....	MP13	Glawe, John D. ....	118	Heyn, Jonas .....	P156	Ji, Ailing .....	P101
Eustes, Alicia S. ....	<b>MP03</b>	Gleason, Thomas G. ....	MP08	Hindberg, Kristian .....	110	Jiang, Weihua .....	P107
Évora, Paulo Roberto B. ....	P108	Glukha, Nadiya .....	P167	Hinojosa, Carlos A. ....	P103	Jiang, Zhihua .....	<b>MP24</b>
Evseyeva, Maria .....	<b>P143</b>	Godwin, Matthew .....	127	Hochman, Judith .....	109	Jin, Hong .....	MP02
Faber, James E. ....	MP27	Goeders, Nicholas E. ....	118	Hochman, Judith S. ....	105	Jin, Hua .....	106
Fappi, Alan .....	P147	Goettsch, Claudia .....	P156	Hodonsky, Chani J. ....	113	Jin, Xiaohua .....	MP25
Farber, Emily .....	113	Goldberg, Ira J .....	P112	Hoehne, Carolin .....	MP10	Jo, Hanjoong .....	MP41
Fendrikova-Mahlay, Natalia .....	127	Gomes, Karina .....	P109, P176	Holinstat, Michael A. ....	P119	Johnson, Jason L. ....	P126
Feng, Jingna .....	P122	Gomez, Angela .....	114	Holley, Ana .....	P121	Jolly, Austin .....	<b>MP12</b> , MP14, MP28
Feng, Jun .....	P163	Gomez, Delphine .....	MP13	Holley, Ana S. ....	P133	Jones, Cameran .....	MP07
Fermoyle, Caitlin C. ....	MP26	Gonen, Ayelet .....	MP04	Holman, Theodore .....	P119	Jordani, Maria Cecilia .....	P108
Fernandez, Timothy F. ....	<b>MP23</b>	Gong, Ming C. ....	MP20	Hoque, Maruf M. ....	<b>P173</b>	Joseph, Giji .....	MP29
Ferrell, Jessica .....	P153	Goodarzi, Mohammad .....	130	Hortells, Luis .....	MP08	Joviliano, Edwaldo E. ....	P108
Fields, Alexander .....	109	Goodlett, David R. ....	123	Howatt, Deborah A. ....	P105, P106, P145, P148, P159, P160	Junop, Murray S. ....	P110
Finn, Alope .....	113	Gopoju, Raja .....	MP01	Howe, Kathryn L. ....	P104	Kaikkonen, Minna U .....	104, P175
Fish, Jason E. ....	P104	Gotto, Antonio M. ....	MP30	Hsiai, Tzung K. ....	MP43	Kant, Shashi .....	<b>P154</b>
Fishbein, Ilia .....	<b>P137</b>	Gray, Jake .....	P142	Hu, Krista Y. ....	<b>120</b>	Kapoor, Divya .....	P147
Fisher, Edward A. ....	P144, P175	Greco, Julia .....	P139	Hu, Sheng-en .....	113	Karim, Zubair .....	126
Fitzpatrick, Emmett o. ....	P137	Griffin, Jakara .....	<b>P136</b>	hu, shuwei .....	MP01	Karimi Hosseini, Davood .....	<b>P172</b>
Forgey, Cady .....	P130	Gros, Robert .....	MP47	Hu, Xingue .....	P122	Kasabali, Ahmad .....	118
Franklin, Michael .....	P105, P106	Grover, Steven P. ....	<b>110</b>	Huang, Linzhang .....	102	Katsumata, Yuriko .....	MP21, P148
Fu, Yi .....	P165	Grumbach, Isabella M. ....	119			Katz, Stuart D. ....	P135

Kaur, Jashandeep ..... **P161**  
 Kaw, Anita ..... P174  
 Kawai, Tatsuo ..... P171  
 Kernell, Caroline ..... P174  
 Kessler, Thorsten ..... MP10  
 Kevil, Chris ..... 118  
 Khabaz, Kameel ..... **P102**  
 Khacho, Mireille ..... 100  
 Khan, Mohammad Daud ..... MP39  
 Khanal, Saugat ..... **MP48**, P153  
 Khasawneh, Fadi T. .... 126  
 Khodadadi, Hesam ..... MP37  
 Khurram, Ruhaid ..... P168  
 Khyzha, Nadiya ..... P104  
 Kim, Anne ..... P155  
 Kim, Eunyoung ..... MP35  
 Kishore, Bellamkonda K. .... MP26  
 Klarin, Derek ..... MP16  
 Klimek, John ..... 108  
 Knaack, Darcy A. .... **MP33**  
 Ko, Kyung ae ..... MP45, **P184**  
 Kockx, Maaïke ..... 122  
 KOELWYN, Graeme J. .... 105  
 Koenig, Andrew ..... MP07  
 Kolluru, Gopi Krishna K. .... **118**  
 Kong, Wei ..... P165  
 Korcarz, Claudia E. .... MP15  
 Kornblith, Lucy ..... 109  
 Koschinsky, Marlys L. .... MP47, P110  
 Kosciuszek, Nina D. .... P161  
 Kothari, Hema ..... **P125**  
 Kotla, Sivareddy ..... MP45, P184  
 Kovacic, Jason C. .... 113, MP39  
 Koval, Olha ..... 119  
 Kremastiotis, Georgios ..... **P126**  
 Kristono, Gisela A. .... **P133**  
 Krolikowski, John G. .... P136  
 Krueger, James ..... P135  
 Krzywanski, David M. .... P157  
 Kudchadkar, Shibani M. .... MP03  
 Kudrjavitseva, Victoria ..... P143  
 Kukida, Masayoshi ..... **P148**, P159  
 Kullo, Iftikhar J. .... P179  
 Kumamoto, Natsuko ..... P111  
 Kumar, Sandeep ..... MP41  
 Kumaragurubaran, Rathnakumar P104  
 Kumskova, Mariia ..... 107  
 Kunapuli, Satya P. .... MP26  
 Kundaje, Anshul B. .... 113

Kundu, Soumya ..... 113  
 kuppusamy, maniselvan ..... MP39  
 Kuroda, Ryohei ..... P171  
 Kwartler, Callie ..... **P174**  
 Kwon, Oh Sung ..... MP26  
 Lagor, William R. .... 123  
 Lallo, Jason ..... MP48, P153  
 Larsen, Peter ..... P121, P133  
 La Salle, D. Taylor ..... MP26  
 Lassegue, Bernard P. .... MP23  
 Lavine, Kory J. .... MP07  
 Le, Nhat T. .... MP45  
 Lebeche, Djamel ..... P113  
 Lee, Angela ..... 105, MP08  
 Lee, Richard ..... MP09  
 Lee, Wan-Ru ..... MP40  
 Lee, Youngho ..... 114  
 Leeper, Nick J. .... 113  
 Leira, Enrique C. C. .... 107  
 Lemaire, Scott A. .... MP21, MP22  
 Lemoff, Andrew ..... 130  
 Lempicki, Melissa D. .... **P142**  
 Lengquist, Mariette ..... P140  
 Lentz, Steven R. .... MP03, P127  
 Levin, Michael ..... **125**, MP16  
 Levy, Robert J. .... P137  
 Ley, Klaus F. .... MP04  
 Li, Ang ..... 123  
 Li, Chi-Ming ..... MP07  
 Li, Fang ..... **P122**  
 Li, Li ..... 130  
 Li, Qing ..... P165  
 Li, Yanming ..... MP21  
 Li, Yike ..... P165  
 Liang, Ching L. .... P148  
 Liang, Chingling ..... P145  
 Lignos, James ..... P182  
 Lim, Chung Sim ..... P168  
 Lin, BingXue ..... P144  
 Lin, Zhiyong ..... MP41  
 Lindemer, Brian ..... P136  
 Lindsey, Nathaniel R. .... 119  
 Liu, Jing ..... MP30  
 Liu, Mingjun ..... MP13  
 Liu, Shu ..... MP20  
 Liu, Wen ..... MP38  
 Liu, Yuhao ..... MP42  
 Livada, Alison C. .... 124  
 Lohr, Nicole L. .... P136

Lopez, Nicolas G. .... 113  
 Lopez-Yang, Christine ..... P141  
 Lozano, Patricia ..... 126  
 Lu, Haocheng ..... 129, MP42  
 Lu, Hong S. .... MP21, P105, P106,  
 ..... P145, P148, P159, P160  
 Lu, Sizhao ..... MP12, **MP14**, MP28  
 Lucitti, Jennifer ..... MP27  
 Luo, Xin ..... MP07  
 Lutgens, Esther ..... 101  
 Luttrell-Williams, Elliot ..... 109  
 Lynch, Julie ..... MP16  
 Ma, Cheng-I Jonathan J. .... **MP49**  
 Ma, Jocelyn A. .... P164, P166  
 Ma, Lijiang ..... 113, MP39  
 Ma, Shuangtao ..... P174  
 Ma, Wei Feng ..... 113  
 Mackman, Nigel ..... 110  
 Madduri, Ravi ..... 125  
 Maegdefessel, Lars ..... MP10, MP18,  
 ..... P167  
 Maghrabi, Ahmad ..... P141  
 Mahan, Sidney ..... MP13  
 Mahini, Halleh ..... P116  
 Maiorino, Enrico ..... 112  
 Majersik, Jennifer J. .... 116  
 Mak, Esther ..... P155  
 Malarstig, Anders ..... MP02  
 Maldonado, Thomas ..... 115  
 Malin, Stephen G. .... 101  
 Manandhar, Bikash ..... **122**  
 Marshall, Melissa ..... MP04  
 Martin, James F. .... 123  
 Martin, Kathleen A. .... MP11  
 Martinez-Martinez, Ricardo ..... P103  
 Marx, Nikolaus ..... P156  
 Masayoshi, Kukida ..... P160  
 Matamalas, Joan T. .... 112  
 Mathias, Amy ..... MP48, P153  
 Matias, Caio V. .... **P158**  
 Matic, Ljubica ..... MP02, MP39, P140  
 Matienzo, Nelsa ..... P182  
 Matveyenko, Anastasiya ..... P182  
 Maurya, Preeti ..... 124  
 Mavris, Sophia ..... MP29  
 Maxfield, Frederick R. .... MP49  
 McCarty, Owen J. .... 108  
 McClintock, Timothy ..... MP20  
 McGranaghan, Peter ..... MP05, P181

McKinsey, Timothy A. .... MP14, MP28  
 McNamara, Coleen ..... P125  
 McNamara, Coleen A. .... 101, MP04  
 McSkimming, Chantel ..... MP04, P125  
 Meade, Rodrigo ..... MP25  
 Medina, Luis A. .... P103  
 Meher, Akshaya K. .... P142  
 Melrose, Alexander ..... 108  
 Meng, Zhaojie ..... MP43  
 Mesquita, Carolina D. M. .... P108  
 Mestriner, Fabiola L. M. .... P108  
 Michelin Barbosa, Jessyca ..... **P108**  
 Milewicz, Dianna M. .... P174  
 Miller, Clint L. .... **113**, MP39  
 Miller, Francis J. .... MP03  
 Miller, Yury I. .... MP04  
 Milner, Ross ..... P102  
 Mineo, Chieko ..... 102, MP40  
 Minnier, Jessica ..... 108  
 Minshall, Richard D. .... P138  
 Mis, Dominika ..... P139  
 Mittendorfer, Bettina ..... P147  
 Mohammadmoradi, Shayan ..... **P106**  
 Mohr, Ian ..... 109  
 Monroe, Jacob ..... 117  
 Montes de Oca, Ildamaris ..... P141  
 Mookherjee, Sohom ..... MP26  
 Moore, Kathryn J. .... 105  
 Moorhead, William ..... MP08  
 Moorlegghen, Jessica J. .... P105, P145,  
 ..... P148, P159, P160  
 Morand, Pauline ..... 123  
 Morgan, David ..... MP26  
 Morrell, Craig ..... 124  
 Motaganahalli, Raghunandan .... 117  
 Moulton, Karen ..... MP12, MP14  
 Mu, Xufang ..... **MP20**  
 Mukai, Shin ..... 112  
 Mullick, Adam E. .... P101, P106  
 Mulorz, Joscha U. .... 128  
 Mulorz, Pireyatharsheny ..... 128  
 Munger, Joshua ..... 124  
 Murata, Takahisa ..... MP27  
 Mutryn, Marie ..... MP12, MP14, MP28  
 Myndzar, Khrystyna ..... 109, P135  
 Nagarkatti, Mitzi ..... P178  
 Nagiec, Marek ..... P158  
 Nahrendorf, Matthias ..... 105  
 Nandula, Seshagiri ..... **P124**

Narayanan, Sampath ..... **P140**  
 Nayak, Manasa ..... 107  
 Neal, MD, Matthew D. .... 109, 116  
 Nelson, Ashley ..... MP26  
 Nemenoff, Raphael A. .... MP12, MP14  
 ..... MP128  
 Newman, Alexandra ..... 105  
 Nguyen, Anh ..... MP04  
 Nguyen, David ..... 121  
 Nguyen, My Anh ..... 100, MP09, P155  
 Niu, Shuteng ..... P122  
 Noffsinger, Victoria ..... P101  
 Noval Rivas, Magali ..... 114  
 Ochín, Chinedu C. .... P116  
 O'Donnell, Chris J. .... MP16  
 Ohno, Satoko ..... P105  
 Okuno, Keisuke ..... P170, P171  
 Olalde, Heena M. .... 107  
 Oliveira, Suellen D. .... **P138**  
 Oliveira De Paula, Gustavo H. ... **P169**  
 Onengut-Gumuscu, Suna ..... 113  
 Ong, Kwok Leung ..... 122  
 Ord, Tiit ..... 104, P175  
 Oreilly, Marcella E. .... **MP38**  
 Orr, Wayne W. .... 118, MP06  
 Ottolini, Matteo ..... MP39  
 Ou, Caiwen ..... MP41  
 Ouimet, Mireille I. .... MP09, **P155**  
 Palaia, Thomas ..... P112  
 Palancia Esposito, Christa ..... P139  
 Palmore, Meredith ..... MP39  
 Paloschi, Valentina ..... MP18, P167  
 Palos-Jasso, Andrea ..... MP27  
 Pan, Xiaoyue ..... **MP31**  
 Pandzic, Elvis ..... 122  
 Pang, Calver ..... P168  
 Pang, Jiaqing ..... 108  
 Papadopoulou, Anthie ..... P168  
 Pardue, Sibile ..... 118  
 Parikh, Manish ..... P144  
 Park, Arick ..... P147  
 Park, Joseph ..... 121, MP16  
 Park, Seul-Ki ..... MP26  
 Parra-Izquierdo, Iván ..... 108  
 Pascual, Crystal ..... 127  
 Patel, Rajiv ..... P172  
 Patel, Rakeshkumar ..... 107  
 Patel, Vaibhav B. .... P109, P176  
 Patrick, Jordan T. .... **P114**

Pattarabajinard, Oom ..... 101  
 Pattarabanjird, Tanyaporn ..... **MP04**  
 Paul, Saikat ..... P142  
 Pauli, Jessica ..... MP18  
 P Bharath, Leena ..... MP26  
 Penrose, Amanda ..... MP25  
 Perepu, Usha ..... MP03  
 Perkins, Susan ..... 117  
 Perry, Noah ..... MP39  
 Pewowaruk, Ryan ..... **MP15**  
 Philip, Lesley ..... P172  
 Phillips, Michael C. .... 121  
 Pietrangelo, Antonietta ..... P155  
 Pittaluga, Stefania ..... 109  
 Pocivavsek, Luka ..... P102  
 Podrez, Eugene A. .... P130  
 Poels, Kikkie ..... 101  
 Polonis, Katarzyna ..... P108  
 Porritt, Rebecca A. .... **114**  
 Portier, Irina ..... 116  
 Powers, Hayley R. .... **P115**  
 Pownall, Henry J. .... MP30  
 Prajapati, Kamalben ..... P104  
 Preston, Kyle ..... P170  
 Punch, Emily ..... P116  
 Qiao, Xiaojing ..... P164, P166, **P177**  
 Quartuccia, Gabriella ..... 120  
 Quettermous, Thomas ..... 113  
 Rader, Daniel J. .... 121, MP16  
 Rajan, Sujith ..... **P112**  
 Rajeeva Pandian, Navaneeth Krishna  
 ..... 111  
 RAJENDRAN, Saranya ..... 118  
 Raju, Sneha ..... P104  
 Ramakrishnan, Rajasekhar ..... P182  
 Ramamoorthy, Venkataraghavan  
 ..... MP05, P181  
 Raman, Priya ..... MP48, P153  
 Ramkhelawon, Bhama ..... **115**  
 Rao, Shashanka ..... **P157**  
 Rapkiewicz, Amy ..... 109  
 Rasheed, Adil ..... **MP09**, P155  
 Rayner, Katey J. .... 100, MP09, P155  
 Razani, Babak ..... P147, P162  
 Razuvaev, Anton ..... P140  
 Reddick, Milla ..... MP06  
 Reddy, Ashok ..... 108  
 Regan, Cailyn ..... MP08  
 Reiche, Myrthe E. .... **101**

Reilly, Muredach P. .... 103, MP35,  
 ..... MP38  
 Reitsma, Stephanie ..... 108  
 Reyes-Soffer, Gisette ..... **P182**  
 Reynolds, Harmony ..... 105  
 Reza, Tasnim ..... MP47  
 Rhamkhelawon, Bhama ..... 105  
 Rhee, YaeHyun ..... 128  
 Riascos-Bernal, Dario ..... P169  
 Ribeiro, Maurício S. .... P108  
 Richardson, Russ ..... MP26  
 Ritchie, Marylyn ..... MP16  
 Rivera, Cristobal F. .... 115  
 Robichaud, Sabrina ..... MP09, P155  
 Rodriguez, Alexis ..... 125  
 Rodríguez-Vélez, Astrid .... P147, P162  
 Rohl, Samuel ..... P140  
 Rojas, Mauricio ..... MP08  
 Rojas, Modesto ..... P134  
 Rolling, Christina ..... 109  
 Romanoski, Casey E. .... 104, P175  
 Rondina, Matthew T. .... 116  
 Rosales, Corina ..... MP30  
 Roseguini, Bruno ..... **117**  
 Rostovtseva, Maria ..... P143  
 Rubens, Muni ..... MP05, P181  
 Ruggles, Kelly ..... 109  
 Ruiz, Henry H. .... **MP32**  
 Rye, Kerry Anne ..... 122  
 Saadatagah, Seyedmohammad **P179**  
 Sabaeifard, Parastoo ..... 130  
 Sacharidou, Anastasia ..... **102, MP40**  
 Sahoo, Daisy ..... MP33, P115, P183  
 Saigusa, Ryosuke ..... MP04  
 Sandhu, Prabhjeet ..... P172  
 Sankary, Seth ..... P102  
 Santos Baez, Leinys ..... P182  
 Saqib, Muzna ..... 131  
 Satta, Sandro ..... MP43  
 Savinova, Olga V. .... P123, P128,  
 ..... P129, P152, P161  
 Sawada, Hisashi .... **MP21**, P105, P106,  
 ..... P148, P160  
 Saxena, Anshul ..... MP05, **P181**  
 Scarbrough, Haley ..... P130  
 Schafer, Xenia ..... 124  
 Schilke, Robert ..... P157  
 Schlamp, Florencia ..... 105, P175  
 Schmidt, Ann Marie ..... MP32

Schunkert, Heribert ..... MP10  
 Schwartz, Andrew ..... P138  
 Sellak, Hassan ..... MP17, MP23  
 Semenkovich, Clay F. .... MP25  
 Sen, Sabyasachi ..... P124  
 sergeeva, oxana ..... P143  
 Sessa, William C. .... MP27  
 Shackelford, Rodney ..... 118  
 Shafqat, Mehreen ..... MP25  
 Shamsian, Ethan ..... **P129**, P152  
 Shanley, Lianne ..... 105  
 Sharma, Amitabh ..... 112  
 Shaul, Philip W. .... 102, MP40  
 Shayan, Mahdis ..... **P180**  
 Shchetinin, Evgeny ..... P143  
 Shen, Xingguo ..... MP06  
 Shen, Xuetong ..... P174  
 Shen, Ying H. .... MP21, MP22  
 Shi, Bijia ..... P121  
 Shi, Sally ..... MP07  
 Shim, Sharon ..... 127  
 Shimada, Kenichi ..... 114  
 Shkolnik, Elina ..... P172  
 Shridas, Preetha ..... **P101**  
 Shroyer, Noah ..... 123  
 Sibinga, Nicholas ..... P169  
 Silva, Claudia Lucia Martins ..... P138  
 Silverstein, Roy L. .... P131  
 Silvestro, Michele ..... 105, 115  
 Sinatra, Vincent J. .... **P144**  
 Singh, Mohnish ..... P129, P152, P161  
 Singh, Sasha A. .... 112  
 Sizer, Ashley ..... MP11  
 Skepner, Adam P. .... P158  
 Smith, Derek K. .... P114  
 Smith, Grace ..... 109  
 Smith, Loren E. .... P114  
 Snider, Justin ..... P113  
 Sol-Church, Katia ..... 113  
 Solingen, Coen ..... 105  
 Soni, Rajesh ..... 103  
 Soni, Rajesh K. .... P158  
 Sonkusare, Swapnil K. .... MP39  
 Sorci Thomas, Mary G. .... MP33  
 Spin, Joshua M. .... **128**  
 Spruill, Tanya ..... 105  
 Stachelek, Stanley J. .... P137  
 Stankov, Sylvia ..... **121**  
 Stapleford, Kenneth ..... 109

Starosolski, Zbigniew ..... MP22  
 Stein, James H. .... MP15  
 Stelzer, Paul ..... P113  
 St Hilaire, Cynthia ..... MP08  
 Stitham, Jeremiah ..... P147  
 Stitzel\*, Nathan O. .... MP07  
 Stolze, Lindsey K. .... **104**  
 Strand, Keith ..... MP12, MP14, **MP28**  
 Stromberg, Arnold ..... MP20  
 Stuttgarten, Gage ..... **P183**  
 Suarez, Mariana ..... P181  
 Suarez, Mariana M. .... **MP05**  
 Subramanian, Venkateswaran .. P107  
 Suhar, Riley ..... P180  
 Sultan, Ibrahim ..... MP08  
 Susser, Leah I. .... **100**  
 Suur, Bianca E. .... MP02  
 Swamy, Jagadish ..... MP03  
 Swirski, Filip K. .... 105  
 Symons, J David D. .... MP26  
 Szabla, Robert ..... P110  
 Takase, Hiroshi ..... P111  
 Takeuchi, Hidekazu ..... **P120**  
 Tandar, Megan ..... MP26  
 Tang, Li ..... 123  
 Tanigaki, Keiji ..... 102  
 Tannock, Lisa R. .... P101  
 Tao, Cui ..... P122  
 Tattersall, Matthew C. .... MP15  
 Tawil, Michael ..... 109  
 Taylor, Angela ..... MP04  
 Taylor, W. Robert R. .... MP17, MP29  
 Taylor, William R. .... MP23  
 Tedla, Jacob ..... MP15  
 Than, Sandy ..... P129, **P152**  
 Thedens, Daniel ..... 107  
 the VA Million Veteran Program, MP16  
 Thomas, Michael J. .... MP33  
 Thomas, Shane ..... 122  
 Thomas, Tamlyn ..... MP45  
 Tiemeijer, Bart ..... 112  
 Torimoto, Keiichi ..... **P171**  
 Toropainen, Anu ..... 104  
 Tourdot, Benjamin E. .... P119  
 Towler, Dwight A. .... **130**  
 Traylor, James G. .... 118

Trinity, Joel D ..... MP26  
 Trumbauer, Andrea ..... P101  
 Tsao, Noah ..... MP16  
 Tsao, Philip S. .... 128, MP16  
 Tsimikas, Sotirios ..... MP04  
 Tsubaki, Motonari ..... P111  
 Tsui, Janice ..... P168  
 Tsujita, Maki ..... **P111**  
 Tu, Peinan ..... **MP41**  
 Tu, Yimin ..... P165  
 Ture, Sara ..... 124  
 Turner, Adam W. .... 113, MP39  
 Ugawa, Shinya ..... P111  
 Upadhye, Aditi ..... 101  
 Upchurch, Gilbert R. .... MP24  
 Valenta, Tomas ..... P169  
 Valenzuela, Nicole M. .... **P132**  
 Vallejo, Jenifer ..... MP04  
 Vallim, Thomas A. .... 123  
 Valnarov-Boulter, Alexander .... P168  
 van der Vorst, Emiel ..... P156  
 van Tiel, Claudia ..... 101  
 Velatooru, Loka ..... MP45  
 Veledar, Emir ..... MP05, P181  
 Verdezoto Mosquera, Jose E. .... 113  
 Verduzco-Vazquez, Ana T. .... P103  
 Verma, Anurag ..... 125  
 Vijithakumar, Vigashini ..... P155  
 Villa-roel, Nicolas ..... MP41  
 Villasante-Tezanos, Alejandro . MP20  
 Villegas, Dennis ..... P172  
 Vitali, Cecilia ..... 121  
 Voight, Benjamin F. .... MP16  
 Volkman, Brian F. .... P115  
 Voora, Deepak ..... 109  
 Vujkovic, Marijana ..... MP16  
 Wagenhaeuser, Markus ..... 128  
 Walsh, Noel M. .... 120  
 Wang, Charis ..... P174  
 Wang, Fei ..... MP26  
 Wang, Fen ..... MP24  
 Wang, Haoyu ..... **MP19**  
 Wang, Qing ..... P122  
 Wang, Ziyi ..... MP30  
 Wasinger, Valerie C. .... 122  
 Webb, Nancy R. .... P101

Weber, Christian ..... 101  
 Weihrauch, Dorothee ..... P136  
 Weiser Evans, Mary C. ... MP12, MP14,  
 ..... MP28  
 Whalen, Michael B. .... 104  
 Whan, Renee ..... 122  
 Whelan, Mary ..... 112  
 Wilkins, Marc ..... 122  
 Williams, Corey ..... P125  
 Williams, David ..... P138  
 Wilmarth, Phillip ..... 108  
 Wilson, Katina M. .... MP03  
 Wilson, Peter ..... MP16  
 Winter, Hanna ..... MP10  
 Wirka, Robert ..... P155  
 Wobst, Jana ..... MP10  
 Wolberg, Alisa S. .... 110  
 Wong, Doris ..... 113, **MP39**  
 Wong, Ryan ..... MP08  
 Woolard, Matthew D. .... 118, P157  
 Wu, Chao ..... **P165**  
 Wu, Ruilin ..... P104  
 Wu, Weiwei ..... P178  
 Wu, Xiuju ..... P164, P166, P177  
 Wu, Yaxin ..... P165  
 Wyatt, Hailey ..... MP09  
 Xia, Yuhe ..... 109  
 Xiang, Yang ..... P122  
 Xie, Yi ..... MP11  
 Xing, Chuce ..... MP47  
 Xing, Hang ..... **P163**  
 Xu, Lin ..... MP40  
 Xu, Yanyong ..... MP01  
 Xue, Chao ..... MP42  
 Xue, Chengyi ..... MP38  
 Yakubenko, Valentin P. .... **P130**  
 Yamaguchi, Adriana ..... **P119**  
 Yamawaki, Tracy ..... MP07  
 Yanagihara, Yoshihiro ..... 112  
 Yang, Lihua ..... P107  
 Yang, Tianxin ..... MP26  
 Yao, Jiayi ..... P164, P166, P177  
 Yao, Yucheng ..... P164, P166, P177  
 Ye, Dien ..... P106, **P145**, P148,  
 ..... P159, P160  
 Yeh, Yu-sheng ..... P147, P162

Yelamanchili, Dedipya ..... MP30  
 Yeung, Jennifer ..... P119  
 Yildiz, Ali ..... P172  
 Yost, Christian C. .... 116  
 Yousif, Eman ..... P147  
 Yu, Changan ..... P165  
 Yu, Jack ..... MP37  
 Yu, Jun ..... **MP27**  
 Yu, Tao ..... MP29  
 Yu, Xiaozhai ..... P165  
 Yung, Lau Y. .... P182  
 Yuriditsky, Eugene ..... 109  
 Zaminski, Devyn ..... P113  
 Zang, Chongzhi ..... 113  
 Zavan, Bruno ..... MP37  
 Zayed, Mohamed ..... MP25  
 Zemmour, David ..... 114  
 Zhang, Chen ..... MP21, MP22  
 Zhang, Cheng ..... MP27  
 Zhang, Daoqin ..... **P164, P166**, P177  
 Zhang, David ..... MP16  
 Zhang, Jifeng ..... 129, MP42  
 Zhang, Jue ..... **P131**  
 Zhang, Li ..... P166, P177  
 Zhang, Xiangyu ..... **P147**, P162  
 Zhang, Xianming ..... 106  
 Zhang, Yanqiao ..... MP01  
 Zhang, Yuanyuan ..... MP27  
 Zhang, Zhiqi ..... P163  
 Zhao, Guizhen ..... **129**, MP42  
 Zhao, Yang ..... 129, **MP42**  
 Zhao, Yiqiong ..... P131  
 Zhao, Youyang ..... **106**  
 Zheng, jingang ..... P165  
 Zheng, Tony ..... 108  
 Zhi, Degui ..... P122  
 Zhong, Dalian ..... 130  
 Zhou, Changcheng ..... MP43  
 Zhou, Tong ..... MP43  
 zhou, xianming ..... MP41  
 Zhu, Lucie ..... MP38  
 Zhu, Tianqing ..... 129  
 Zhu, Yingdong ..... MP01  
 Zunder, Eli ..... P125  
 Zviman, Menekhem ..... P137